Deoxyribose Oxidation Chemistry and Endogenous DNA Adducts

by
Xinfeng Zhou

M.S. in Chemistry, University of Washington, 2001

Submitted to the Biological Engineering Division in Partial Fulfillment of the Requirements for the Degree of

PhD in Applied Biosciences
At the
MASSACHUSETTS INSTITUTE OF TECHNOLOGY

June 2006

Signature of Author .....

Biological Engineering Division
May 2006

Certified by .....

Peter C. Dedon
Professor of Biological Engineering and Toxicology
Thesis Supervisor

Accepted by .....

Ram Sasisekharan
Chairman, Committee on Graduate Students
Professor of Biological Engineering

This doctoral thesis has been examined by a committee of the Biological Engineering Division as follows:

Professor Bevin P. Engelward.....

Chairman

Professor Peter C. Dedon.....

Supervisor

Professor John M. Essigmann .....

Professor Steven R. Tannenbaum .....

Deoxyribose Oxidation Chemistry and Endogenous DNA Adducts

by
Xinfeng Zhou

Submitted to the Biological Engineering Division on May 8th, 2006 in Partial Fulfillment of the Requirements for the Degree of PhD in Applied Biosciences

ABSTRACT

Endogenous and exogenous oxidants react with cellular macromolecules to generate a variety of electrophiles that react with DNA produce cytotoxic and mutagenic adducts. One source of such electrophiles is deoxyribose in DNA itself. Oxidation of each position in deoxyribose generates a unique spectrum of products, many of which are highly reactive with DNA bases and lead to formation of adducts. The objective of this thesis was to clarify the chemistry of deoxyribose oxidation, with a focus on C4'-oxidation that gives rise to 3'-phosphoglycolate residues on the DNA backbone and releases base propenal or malondialdehyde, and to investigate the role of base propenals in the formation of an important endogenous DNA adduct, M_1dG.

First, an index of total deoxyribose oxidation was developed, one that provides a means to compare different oxidizing agents. This method exploits the reaction of aldehyde- and ketone-containing deoxyribose oxidation products with ^{14}C-methoxyamine to form stable oxime derivatives that are quantified by accelerator mass spectrometry. Sensitive GC/MS methods were developed to quantify 3′-phosphoglycolate residues from deoxyribose C4'-oxidation and HPLC/post-column derivatization methods were developed to quantify the corresponding base propenal or malondialdehyde. Combined with the quantification of total deoxyribose oxidation and the alternative product of C4'-oxidation, the 4′-ketoaldehyde abasic site, under the same conditions, these results offered direct insights into the partitioning of C4'-oxidation and the chemical mechanisms of deoxyribose oxidation in DNA.

With a foundation of deoxyribose oxidation chemistry and analytical methods, the *in vitro* DNA oxidative damage induced by γ-irradiation, Fe^{2+}/EDTA, bleomycin and peroxynitrite was explored. The results revealed that malondialdehyde was neither sufficient nor necessary for the formation of M_1dG, while base propenal was effective in generating M_1dG. These observations were extended to an *E. coli* cell model in which the membrane content of polyunsaturated fatty acids was controlled. The results revealed that lipid peroxidation caused by γ-irradiation was insufficient to produce M_1dG in cells and the level of M_1dG adducts was inversely correlated with the quantity of membrane polyunsaturated fatty acids when cells were treated with peroxynitrite. Finally, M_1dG showed a moderate (~50%) increase in tissues from a mouse model of inflammation, while etheno-adducts induced by lipid peroxidation increased ~3-fold. These results are again consistent with lipid peroxidation as a minor source of M_1dG.

Thesis Supervisor: Peter C. Dedon
Title: Professor of Biological Engineering and Toxicology

Acknowledgements

Many people have contributed to my thesis, to my education, and to my life, and it is now my great pleasure to take this opportunity to thank them.

First and foremost, I want to thank my thesis supervisor, Professor Peter Dedon, for his endless guidance and support in the last five years. Peter has given me enormous freedom to pursue my research while at the same time providing guidance to ensure that my efforts contribute to the mainstream of research. Peter has carefully read, over the years, many drafts of this thesis. I am grateful for his valuable comments, encouragement and thoughts for further development of my ideas. I will always be thankful for being given the opportunity to work in his laboratory. It gives me great pleasure to thank Professor Bevin Engelward, Professor John Essigmann, and Professor Steven Tannenbaum, the faculty members who have served on my thesis committee. Thank you all for having been so encouraging, giving so generously of your time and expertise, and contributing valuable insights to my thesis work.

I am deeply indebted to many current and former members of Dedon lab for their support and their contribution to my thesis. The group has been a source of friendships as well as good advice and collaboration. Many thanks to Dr. Min Dong and Dr. Mohammed Awada for getting me started in the lab. I was privileged to collaborate with Dr. Bo Pang, Dr. Bingzi Chen and Yelena Margolin for part of my thesis work. They have been a continuous source of inspiration and support. Special thanks to Dr. Eric Elmquist and Dr. Michael DeMott for the time and effort they devoted to proofreading my manuscripts and thesis. Thanks to Dr. Tao Jiang, Dr. Shivashnkar Kalinga, Ms. Marita Barth, Ms. Debra Dederich, and Mr. Vasileios Dendroulakis for all the stimulating discussions. My thanks also go to Ms. Olga Parkin and Jackie Goodluck for all their help.

I am also very grateful to colleagues from other research groups for significant contributions to this thesis. Dr. Koli Taghizadeh from the Center for Environmental Health Sciences (CEHS) at MIT helped me develop a variety of GC/MS, LC/MS and LC/MS-MS analysis methods. Dr. Rosa Liberman and Dr. Paul Skipper from the research group of Prof. Steven Tannenbaum developed the AMS instrument at MIT and performed all the analyses for the ^{14}C-labeled samples. Dr. Hogbin Yu developed the LC-MS/MS method to quantify nucleobase oxidation. Dr. Pete Wishnok and Ms. Elaine Plummer-Turano provided generous help in using mass spectrometry and other equipments. Ms. Laura Trudel from the research group of Prof. Gerald Wogan provided the SJL/RcsX mice for our study. I thank Professor Lawrence Marnett (Vanderbilt University) for the gift of M_1dG-containing DNA standard and Elaine Plummer for expert assistance with GC/MS analyses.

Lastly, I would like to thank my family for all their love and encouragement.

Table of Contents

Chapter 1 Background and Literature Review

Chapter 2 Quantification of DNA strand breaks and abasic sites

Chapter 3 Quantification of C4′ deoxyribose lesions 3'-Phosphoglycolate and 4′-ketoaldehyde abasic sites

Chapter 4 Chemical and biological evidence for base propenals as the major source of M_1dG adducts in cellular DNA

Chapter 5 A survey of DNA biomarkers from a SJL mouse model of nitric oxide overproduction

Chapter 6 Conclusions and Future Studies

List of Abbreviations

BER	base excision repair
bp	base pair
BSTFA	bisstrifluoroacetamide
EDTA	ethelenediaminedetraacetic acid
EI	electron impact ionization
GC	gas chromatography
HNE	4-hydroxy-2-nonenal
H_2O_2	hydrogen peroxide
HPLC	high pressure liquid chromatography
MDA	malondialdehyde
M_1G	pyrimido[1]purin-10sone
M_1dG	pyrimidoppurin-10(3H)one-2'-deoxyribose
MRM	multiple reaction monitoring
MS	mass spectrometry
NO•	nitric oxide
nt	deoxynucleotide
$O_2^{\cdot}$	superoxide anion radical
•OH	hydroxyl radical
$ONOO^-$	peroxynitrite
$ONOOCO_2^-$	nitrosoperoxycarbonate
8-oxodG	8-oxo-7,8-dihydro-2'-deoxyguanosine
PGA	phosphoglycoladehyde
PGL	pohsophoglycolate

PUFA	polyunsaturated fatty acids
RHS	reactive halogen species
RNS	reactive nitrogen species
ROS	reactive oxygen species
SIM	selective ion monitoring
TBA	thiobarbituric acid

List of Figures

Figure 5-6. Formation of 8-oxodG in spleen and liver DNA of SJL mice bearing the RcsX tumor

Figure 5-7. Formation of εdA and εdG and M_1dG in spleen and liver DNA of SJL mice bearing the RcsX tumor

Figure 6-1. $^{13}C_3$-M_1dG formed from peroxidation of uniform-[^{13}C]-labeled lipids vs. unlabled M_1dG formed from deoxyribose oxidation product base propenal.

List of Tables

Chapter 1

Background and Literature Review

1.1. Introduction

There is now substantial evidence linking reactive oxygen and nitrogen species to aging and chronic diseases [2], as illustrated by the epidemiological evidence associating chronic inflammation and increased cancer risk [3-5]. Many of these effects have been associated with reactions of endogenous and exogenous oxidants with DNA bases to produce mutagenic lesions such as 8-oxo-dG and thymine glycol. The oxidants also react with lipids, carbohydrates and proteins to generate electrophilic species capable of reacting with DNA bases to form secondary adducts. This is illustrated by the reaction of a metabolite of hydroxynonenal, a product of peroxidation of polyunsaturated fatty acids (PUFA), with dG, dA, and dC to form etheno adducts [6]. A similar argument has been made for the PUFA peroxidation product, malondialdehyde (MDA), which reacts *in vitro* with dG to form M_1dG, the exocyclic pyrimido[1,2-α]purin-10-(3H)-one adduct of dG (Figure 1-1).

In recent years, evidence has emerged that deoxyribose oxidation also plays a critical role in the genetic toxicology of oxidative stress, including involvement in complex DNA lesions, cross-linking with DNA repair proteins and the formation of endogenous DNA adducts. For example, as part of a complex DNA lesion, closely opposed strand breaks and oxidized abasic sites are resistant to repair by endonucleases and other enzymes [7, 8]. Studies also suggest that deoxyribose oxidation may be an alternative to lipid peroxidation as a source of DNA-reactive electrophiles. Oxidation of deoxyribose in DNA produces a variety of oxidized abasic sites and strand breaks with different sugar residues, many of which are electrophilic and thus capable of reacting with local nucleophiles to form adducts [9-13]. For example, the β-elimination product of the 5'-(2-phosphoryl-1,4-dioxobutane) residue arising from 5'-oxidation of deoxyribose (*trans*-1,4-dioxo-2-butene) reacts with dG, dA and dC to form stable bicyclic adducts [9, 10]. Research

in Dedon laboratory has also shown the reaction of 3'-phosphoglycolaldehyde residues, which are products of 3'-oxidation of deoxyribose in DNA to form the glyoxal adducts of guanine [11]. Similarly, we demonstrated that the base propenal products of deoxyribose 4'-oxidation, structural analogs of the enol tautomer of MDA Figure 1-1), also react with DNA to form M_1dG [12], though with significantly greater efficiency than MDA [12, 13]. This may explain the 30- to 60-fold greater mutagenicity of base propenals than MDA [13].

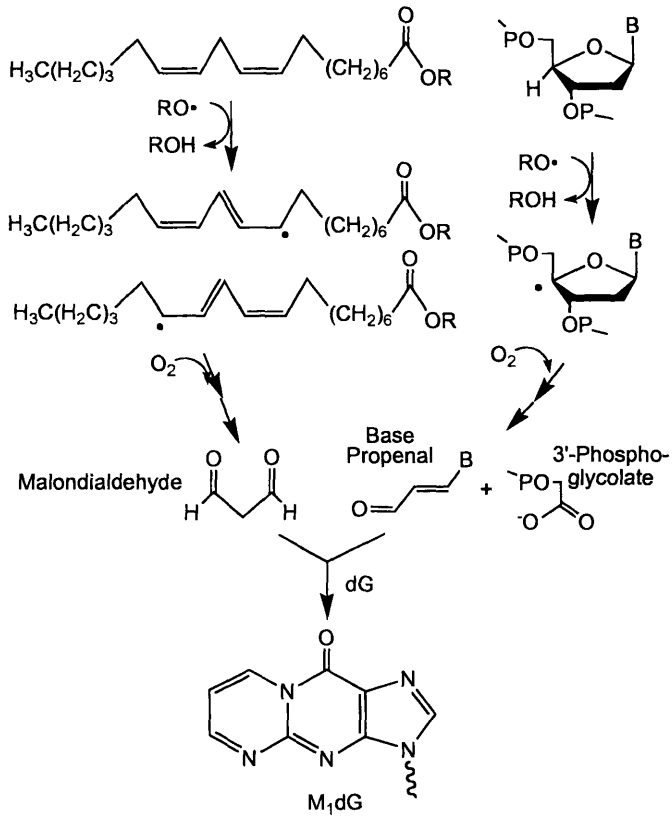

Figure 1-1. Malondialdehyde from lipid peroxidation and base propenals from deoxyribose oxidation react with dG to form M_1dG. B represents a base.

The goal of these studies undertaken in this thesis was to define chemical basis for the formation of M_1dG as a product of either lipid peroxidation-derived MDA or deoxyribose

oxidation-derived base propenals. This work entailed characterization of the chemistry of 4'-oxidation of deoxyribose in DNA, development of analytical methods for quantification of DNA and lipid oxidation products, and application of analytical methods to quantify M_1dG *in vitro*, in cells and in tissues from a mouse model of inflammation.

The thesis is organized as 6 chapters. In Chapter 1, we first present a comprehensive review of DNA base and sugar damage with an emphasis on deoxyribose oxidation pathways and products, especially 4'-oxidation products due to the relevance to our research. The chapter then discusses lipid peroxidation and secondary DNA adduct from lipid peroxidation. Finally it covers the mechanisms protecting cells/organisms against DNA damage. As a foundation for subsequent studies, the studies presented in Chapter 2 address the development of analytical methods to quantify strand breaks and abasic sites, which could serve as an index of total deoxyribose oxidation for comparing different oxidizing agents. In Chapter 3, we present the results of efforts to quantify 3'-phosphoglycolate residues and to define the spectrum of deoxyribose 4'-oxidation products associated with different oxidizing agents. These methods are applied in Chapter 4 to define the roles of base propenals and malondialdehyde in the formation of M_1dG *in vitro* and in cultured cells. Chapter 5 extends these studies to DNA adducts in tissues from a mouse model of inflammation, with development of analytical methods to quantify etheno adducts derived from lipid peroxidation and to investigate the relationship between etheno adducts and M_1dG formation. Finally, in Chapter 6 we conclude this thesis by summarizing our contributions to DNA damage study and offer directions for future research.

1.2. Sources of reactive oxidants

Cellular DNA is constantly subjected to reactions with a plethora of reactive oxidants. These reactions are triggered by exposure of cells to exogenous chemicals (e.g., environmental agents, food constituents, *etc.*) or they can result from endogenous metabolic processes, such as oxidants generated by oxidative phosphorylation, P450 metabolism, peroxisomes, and inflammatory cell activation. Oxidative damages can also be induced by exogenous sources, such as radiation, metal ions, chlorinated compounds, barbiturates, phorbol esters and some peroxisome proliferating compounds, all of which have been shown to induce oxidant formation *in vitro* and *in vivo* [14, 15]. Endogenous and exogenous oxidants can either directly damage DNA or they can induce DNA adduct formation indirectly by activation of otherwise inert molecules by generation of reactive electrophiles by oxidation of lipids, proteins, carbohydrates and even DNA itself. The former mechanism is illustrated by polycyclic aromatic hydrocarbon benzo[α]-pyrene and aflatoxin B1, both of which have been connected to bladder cancer and liver cancer respectively due to an adduct formed between their epoxide metabolite and DNA bases [16, 17]. This thesis focuses on the latter to study secondary DNA adducts formed by electrophiles from oxidation of lipids and DNA deoxyribose.

While reactive oxidants are often important components of the immune defense system, oxidative stress occurs when there is an imbalance between the oxidants and endogenous antioxidant systems in favor of the former due to an excess of free radicals, a decrease in antioxidant levels, or both [18]. For example, sustained production of reactive oxidants by phagocytes during chronic inflammation induces collateral damage in adjacent normal tissues,

which contributes to a range of diseases. In this section we will review the chemistry and biology of the formation of these oxidative species.

1.2.1 Reactive oxygen species

Reactive oxygen species (ROS) is the term used to describe a variety of species, which not only includes oxidizing radicals such as superoxide ($O_2^{\bullet-}$), hydroxyl (•OH), peroxyl (ROO•), and alkoxyl (RO•) radicals but also includes nonradicals such as hydrogen peroxide (H_2O_2), ozone (O_3), and singlet oxygen ($^1O_2$)—that are oxidizing agents or are easily converted into oxidizing radicals. During mitochondrial oxidative metabolism, a small fraction (0.2-0.6%) of molecular oxygen is converted to reactive oxygen species, primarily superoxide anion radical $O_2^{\bullet-}$, through one-electron reduction [19]. $O_2^{\bullet-}$ is then converted to hydrogen peroxide (H_2O_2) spontaneously or in reactions catalyzed by superoxide dimutase (SOD). The resulting H_2O_2 is further converted to hydroxyl radical (•OH) by Fenton chemistry involving Fe^{2+}, Cu^+, or other metal ions. The process is summarized in Figure 1-2. ROS are also released from neutrophils and macrophages through a process known as respiratory burst [20]. During the respiratory burst, membrane-bound NAD(P)H oxidase is activated and reduces oxygen to $O_2^{\bullet-}$, which is then converted to other reactive oxygen species as described above.

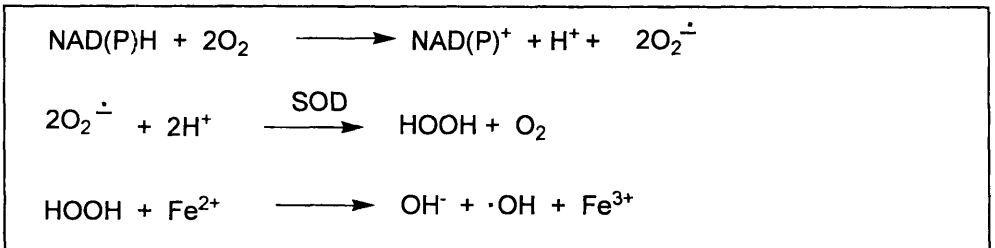

Figure 1-2. Formation of reactive oxygen species

Molecular oxygen itself is a relatively weak univalent electron acceptor that cannot efficiently oxidize biomolecules. In contrast, $O_2^{\bullet-}$, H_2O_2, and •OH are much stronger univalent oxidants. However, the anionic charge of $O_2^{\bullet-}$ inhibits its effectiveness as a direct oxidant of electron-rich molecules, while the reactivity of H_2O_2 is diminished by the stability of its oxygen-oxygen bond [19]. Of these species, •OH is considered to be the major reactive oxygen species contributing to endogenous oxidation of cellular molecules. Since the rate of reactions of •OH is controlled by diffusion, the reactions are non-specific and occur close to the site of its formation. A wide variety of •OH-induced damages, including oxidized bases and deoxyribose, DNA-protein and DNA-DNA cross-links have been identified and will be discussed in detail in the subsequent sections of Chapter 1.

Singlet oxygen $^1O_2$ is an excited form of dioxygen in which the π antibonding electrons are spin-paired. $^1O_2$ can be formed endogenously by energy transfer to oxygen by excited chromophores in stimulated phagocytes during the respiratory burst. $^1O_2$ also reacts with biomolecules and exerts genotoxic, virucidal and cytotoxic effects [21, 22]. In contrast to •OH, which reacts almost indifferently with all nucleobases and the sugar moiety of DNA, the reaction of $^1O_2$ with DNA is highly specific with guanine base as the exclusive target and 8-oxodG as the main oxidation product [23].

Besides endogenous sources, ROS can also be generated by a variety of exogenous sources. Ionizing radiation can induce the homolysis of H_2O to form •OH and •H. It can also directly deposit energy into covalent bonds to cause damage to biolmolecules. The non-ionizing UVA component of solar radiation has been shown to produce $^1O_2$ in its lowest excited state [21]. Tobacco smoke contains a variety of free radicals, which generate free radicals in exposed

tissues [24]. In addition, drugs such as Phenobarbital and carcinogens such as benzo(a)pyrene have also been shown to induce the formation of ROS [25].

1.2.2 Reactive nitrogen species

The class of reactive nitrogen species (RNS) includes, among other species, nitric oxide (NO•), nitrous anhydride N_2O_3, peroxynitrite ($ONOO^-$), and nitrosoperoxycarbonate ($ONOOCO_2^-$). NO• is produced from L-arginine by nitric oxide synthase, with NADPH as an electron donor and HEM, FMN, FAD and tetrahydrobiopterin as cofactors. Three distinct isoforms of NOS have been identified: endothelial NOS (eNOS), inducible NOS (iNOS) and neuronal NOS (nNOS) [26]. Both eNOS and nNOS are constitutively expressed and are activated by calcium and calmodulin, while iNOS is induced in macrophages, endothelium, hepatocytes and mast cells by bacterial endotoxin and cytokines IL-1 and tumor necrosis factor (TNF) [27]. NO• can also be produced nonenzymatically from nitrite at low pH under reducing conditions [28].

One important reaction of NO• is oxidation by molecular oxygen to form the powerful nitrosating agent N_2O_3, as shown in Figure 1-3. Current evidence suggests that N_2O_3 is the predominant species in aqueous media [29]. Based on these equations, the half-life of NO• is inversely proportional to its concentration, with competition between hydrolysis to form nitrite [30] and reactions with amines, thiols, or hydroxyl groups to form NO• adducts through nitrosation.

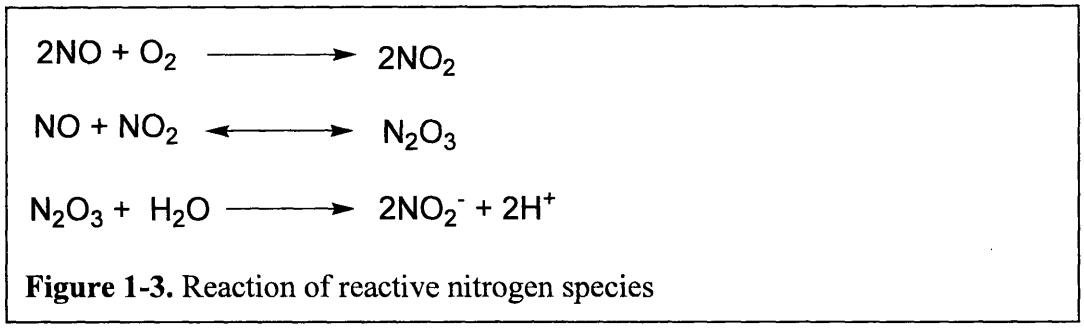

Figure 1-3. Reaction of reactive nitrogen species

Macrophage activation induces both $O_2^{\bullet}$ and NO• production, both of which can react together at a diffusion-controlled rate ($k = 6.6\text{-}19 \times 10^9\ M^{-1}S^{-1}$) to yield $ONOO^-$ [31, 32]. While approximately equal rates of $O_2^{\bullet}$ and NO• generation produces the maximal amount of $ONOO^-$-induced damage, widely differing amounts of either $O_2^{\bullet}$ or NO• lead to side reactions with $ONOO^-$ to form NO_2, and thus inhibiting $ONOO^-$-induced oxidation [33]. Individually, $O_2^{\bullet}$ and NO• are both relatively unreactive. However $ONOO^-$ is very reactive and rapidly decomposes in the absence of CO_2 via a proton-catalyzed homolysis with $k = 1.3\ s^{-1}$, with ~67% of caged radicals reacting to form NO_3^- and the reaming ~33% escape the cage and become free •OH and $•NO_2$ as shown in Figure 1-4. Under biological conditions, $ONOO^-$ reacts rapidly ($t_{1/2} < 0.1\ \mu S$) with CO_2 to form nitrosoperoxycarbonate $ONOOCO_2^-$. Homolysis of the O-O bond produces carbonate ($CO_3^{\bullet}$) and $•NO_2$. The concentration of CO_2 *in vivo* is relatively high (1-2 mM) due to the high levels (12 mM) of bicarbonate in intracellular fluids [34]. This suggests that the reaction of $ONOO^-$ with CO_2 is a major pathway for $ONOO^-$ consumption *in vivo*. Since the intrinsic life time of $ONOOCO_2^-$ is considerably shorter than $ONOO^-$ ($t_{1/2} \approx 0.7s$) [35], the cellular targets for $ONOO^-$ are likely restricted to the location of its formation .

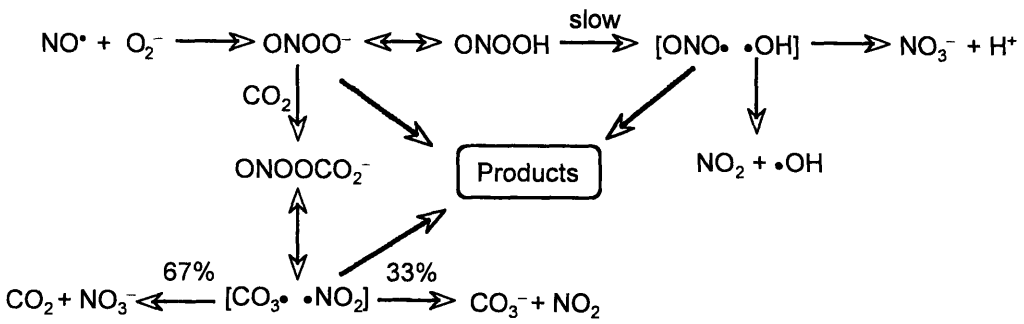

Figure 1-4. Reactive species produced during peroxynitrite decomposition

RNS contribute to direct genotoxicity through reaction with DNA and indirect genotoxicity due to activation of nitrosamines, lipidoxidation-induced DNA damage and inhibition of DNA repair enzymes. For example, RNS have been shown to inhibit formamidopyrimidine-DNA glycosylase (Fpg) and 3-methyladenine-DNA glycoxylase (Alka) by a nitrosation reaction at RNS concentrations 100-fold less than those required to deaminate DNA [36].

1.2.3 Reactive halogen species

Reactive halogen species (RHS) include hypochlorous acid (HOCl), hypobromous acid (HOBr), and hypoiodous acid (HOI). The lysosomal enzyme myeloperoxidase in the granules of neutrophils catalyses the H_2O_2-mediated oxidation of halides to form RHS, as shown in Figure 1-5.

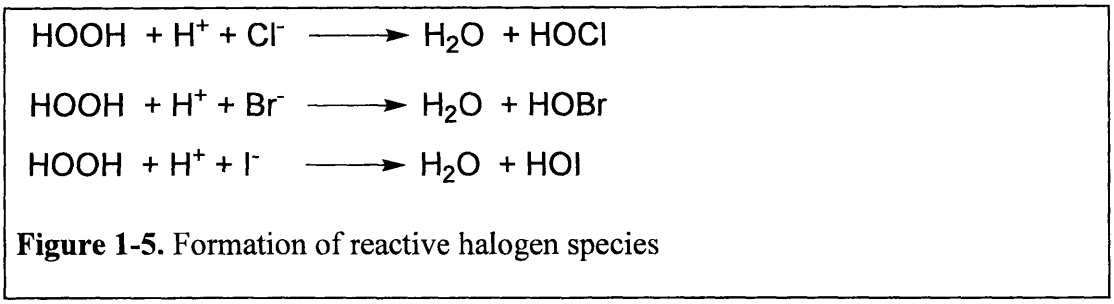

Figure 1-5. Formation of reactive halogen species

Similar to ROS and RNS, RHS are strongly oxidizing and halogenating species that can induce lipid peroxidation [37], halogenation of DNA bases (*e.g.*, 5-chlorouracil) [38], and cross-linking of DNA and protein [39], all of which may play a rose in tissue damage during inflammation [40].

In summary, these reactive oxidants can alter cell function by directly damaging cellular molecules as well as by generating electrophilic species capable of causing further damage. The following sections address the reactions of ROS, RNS and RHS with biomolecules and the resulting primary and secondary DNA adducts.

1.3. DNA base damage

Free radicals can adversely alter DNA and have been implicated in aging and a number of human diseases [41, 42]. In a given human cell, an estimated 10^4 oxidative DNA lesions per day are formed [43]. DNA damage, if not repaired, can lead to mutations and cell death. The magnitude of oxidative DNA damage has led many research groups to study the mechanisms of DNA oxidative damage, to identify the damage products and to define their biological significance.

ROS/RNS/RHS can oxidize both nucleobases and deoxyribose moieties by addition or H atom abstraction. For example, •OH can add to double bonds of DNA bases and abstract H atoms from the C-H bonds of deoxyribose. Given the prominence of nucleobase lesions and their potential to cause DNA mutation, carcinogenesis and aging [44], this section of the background and literature review will address the base damages in detail.

1.3.1 Hydroxyl radical induced base damage

•OH is often considered to be the major ROS responsible for endogenous oxidation of DNA and it serves as an illustration for the types of damage products generated by ROS and RNS. As noted earlier, •OH arises from a variety of sources and rapidly reacts at its site of formation either by H atom abstraction or addition to C=C. Given its low oxidation potential relative to other DNA bases, guanine is the most reactive toward a variety of oxidants including •OH. •OH can add to the C4 (~60%), C5 (~15%) and C8 (~25%) positions of guanine, with subsequent dehydration of C4-OH- and C5-OH-adduct radicals yielding a guanine(-•H) radical. The radical can either be reduced back to guanine or further oxidized to 2-amino-5-[(2-deoxy-β-D-*erythro*-pentofuranosyl)amino]-4*H*-imidazol-4-one and 2,2-diamino-4-[(2-deoxy-β-D-*erythro*-pentofuranosyl)amino]-5(2*H*)-oxazolone as shown in Figure 1-6. The C8-OH-adduct radicals can be oxidized to form final product 8-oxoG or reduced to form the formamidopyrimidine, 2,6-diamino-4-hydroxy-5-formamidopyrimidine (FapyGua) [45].

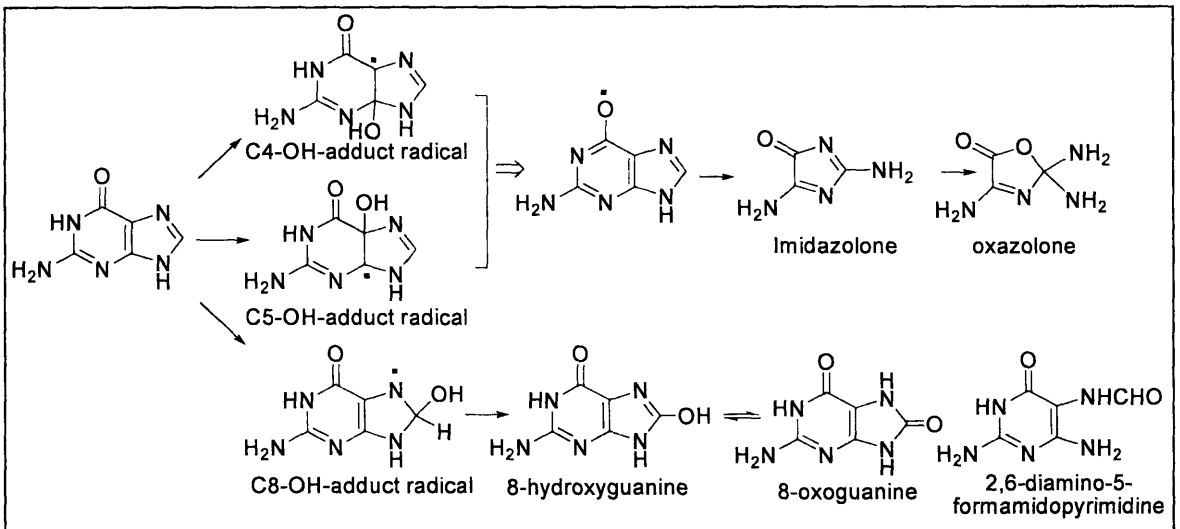

Figure 1-6. Product formation from guanine oxidation

Adenine undergoes reactions analogous to guanine, yielding C2-OH-, C4-OH- and C8-OH-adduct radicals that further react to form 2-hydroxyadenine, 8-hydroxyadenine and 4, 6-diamino-5-formamidopyrimidine (FapyAde) [46], as shown in Figure 1-7.

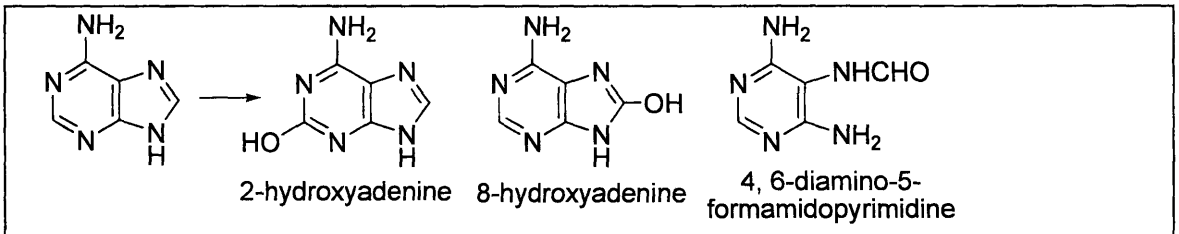

Figure 1-7. Product formation from adenine oxidation

For cytosine, •OH adds at the C5 position to the extent of ~87%, whereas ~10% of •OH adds to the C6 [47] (Figure 1-8) . Molecular O_2 then adds to the C5-OH-adduct radical generating C5-OH-6-peroxyl radicals that subsequently eliminate $O_2^{\cdot-}$ followed by reaction with water to yield cytosine glycol. Deamination and dehydration of cytosine glycol yields uracil glycol, 5-hydroxyuracil and 5-hydroxycytosine. In the absence of oxygen, the C5-OH-adduct

radical can be reduced to 5-hydroxy-6-hydrocytosine, which can be further converted to 5-hydroxy-6-hydrouracil through deamination [42]. Other reactions of C5-OH-6-peroxyl and C6-OH-5-peroxyl radical result in the formation of the intermediates, 5-OH-6-hydroperoxide and 6-OH-5- hydroperoxide that then decompose to 4-amino-5-hydroxy-2, 6(1H, 5H)-pyrimidinedione and 4-amino-6-hydroxy-2, 5(1H, 6H)-pyrimidinedione [48], respectively. The former deaminates to give dialuric acid, which is readily oxidised to yield alloxan, while the latter deaminates to isodialuric acid [49] (Figure 1-8).

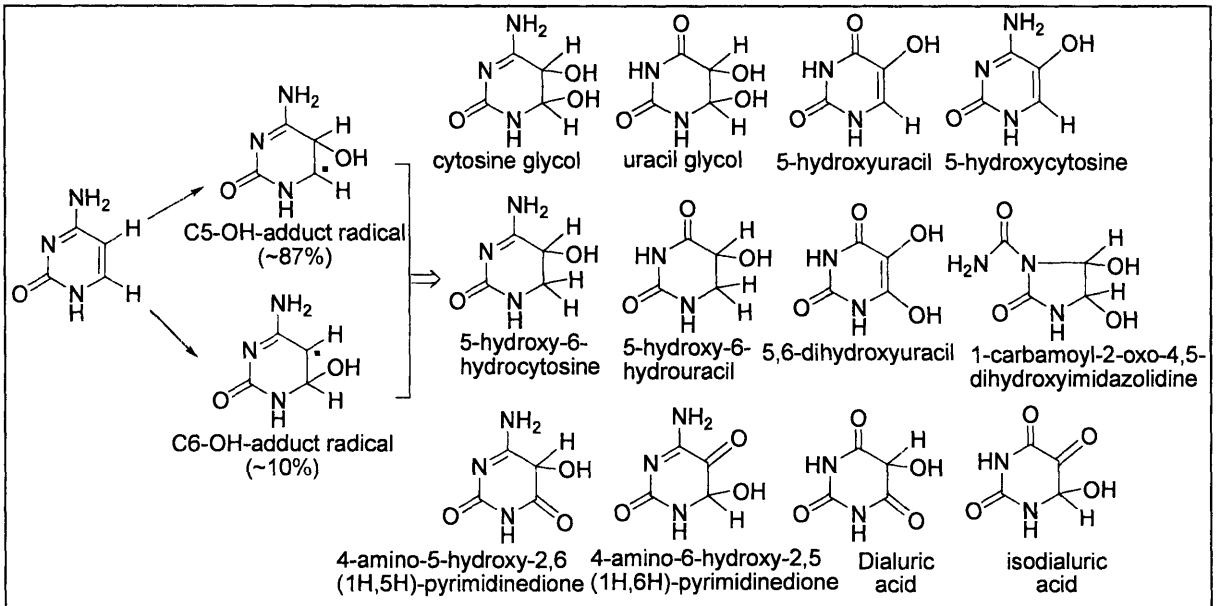

Figure 1-8. Product formation from cytosine oxidation

•OH adds preferentially to the C-5 of thymine, whereas approximately 10-15% of •OH adds to C-6 and 5 – 10% abstracts a H atom from the 5'-methyl group to form an allyl radical (Figure 1-9). Similar to cytosine, the C5-OH-adduct radical can be oxidized to thymine glycol or reduced to 5-hydroxy-6-hydrothymine and 6-hydroxy-5-hydrothymine, as shown in Figure 1-9. Reaction with molecular oxygen yields peroxyl radicals that decompose to 5-hydroxy-5-

methylhydantoin [50]. The oxidation of the allyl radical of thymine yields 5-hydroxymethyluracil and 5-formyluracil.

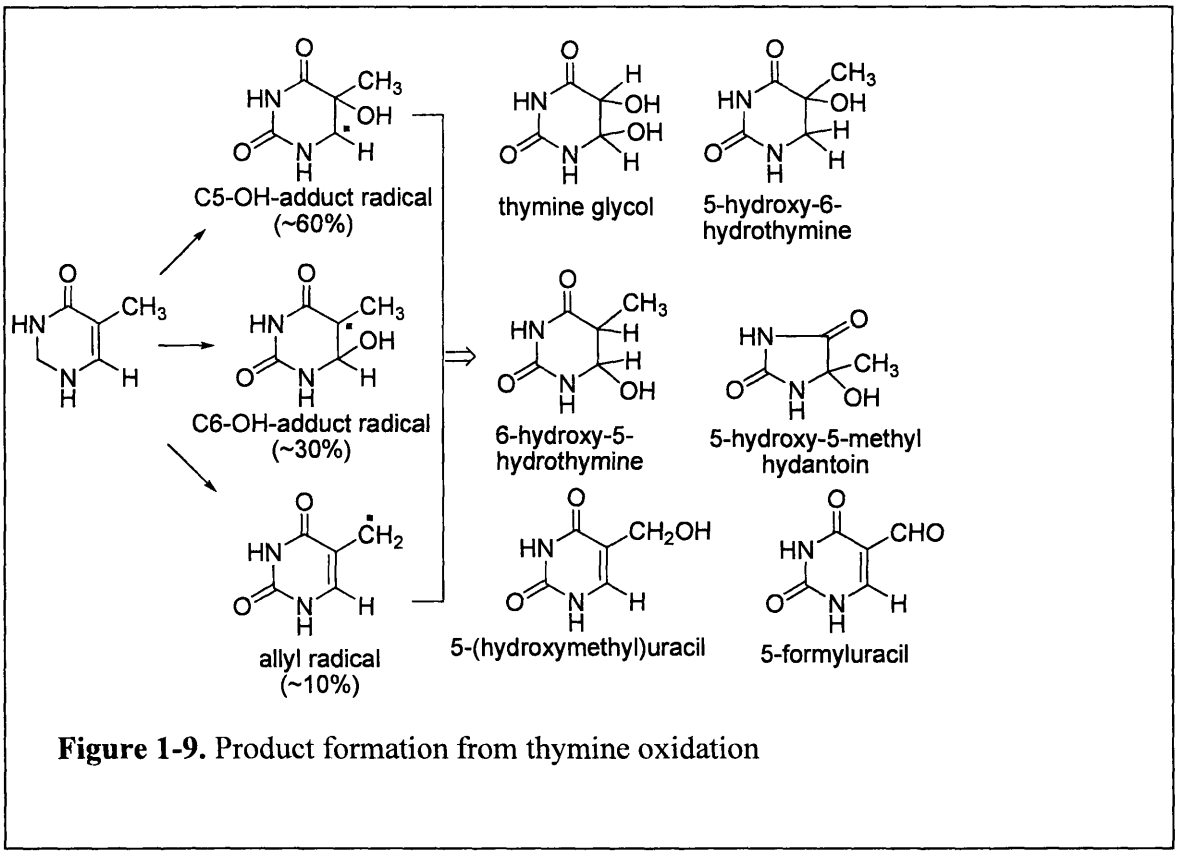

Figure 1-9. Product formation from thymine oxidation

1.3.2 $ONOO^-$ and $ONOOCO_2^-$ induced base damage

As we have discussed in Section 1.2, $ONOO^-$ is among the most reactive species of RNS. $ONOO^-$ induced damage is influenced by CO_2. In the absence of CO_2, the majority of $ONOO^-$ induced DNA damage is deoxyribose oxidation. The presence of CO_2 results in the formation of $ONOOCO_2^-$ and cause a shift from deoxyribose oxidation to base oxidation and nitration with little change in the total number of lesions [51, 52]. $ONOOCO_2^-$ primarily reacts with dG to form 5-guanidino-4-nitroimidazole (NitroIm), 2,2-diamino-4-{(2-deoxypentofuranosyl) amino}-

5(2H)-oxazolone (oxazolone; OZ), and 8-nitro-dG as shown in Figure 1-10 [53]. 8-NitrodG rapidly depurinates ($t_{1/2}$ ~ 1-4h) at neutral pH and ambient temperature to yield the measurable 8-nitroGua [54]. More recent evidence from the Tannenbaum group also revealed that 8-nitrodG can further react with $ONOOCO_2^-$ to yield additional 8-oxodG [55].

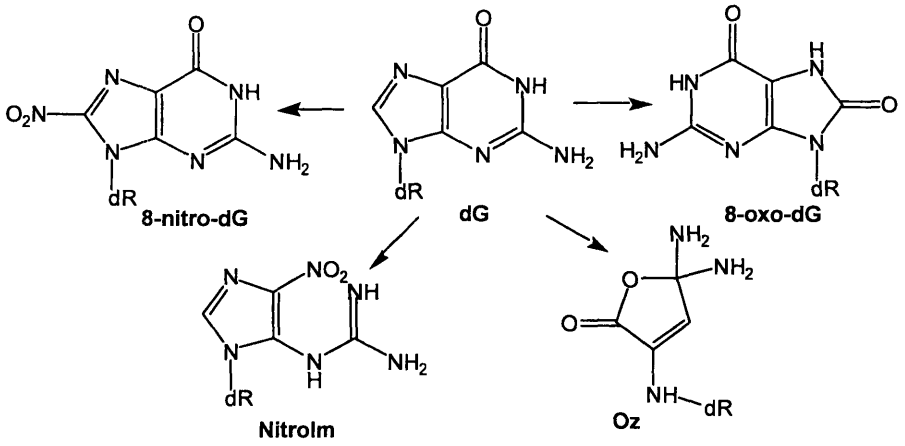

Figure 1-10. Oxidation products from the reaction of dG with $ONOOCO_2^-$

As a result of the lower oxidation potential of 8-oxodG compared to dG (0.74V vs. 1.29V), it is not surprising that 8-oxodG has been shown to be at least 1000-times more susceptible to further oxidation by $ONOOCO_2^-$ than dG and forms a variety of secondary lesions as shown in Figure 1-11 [53].

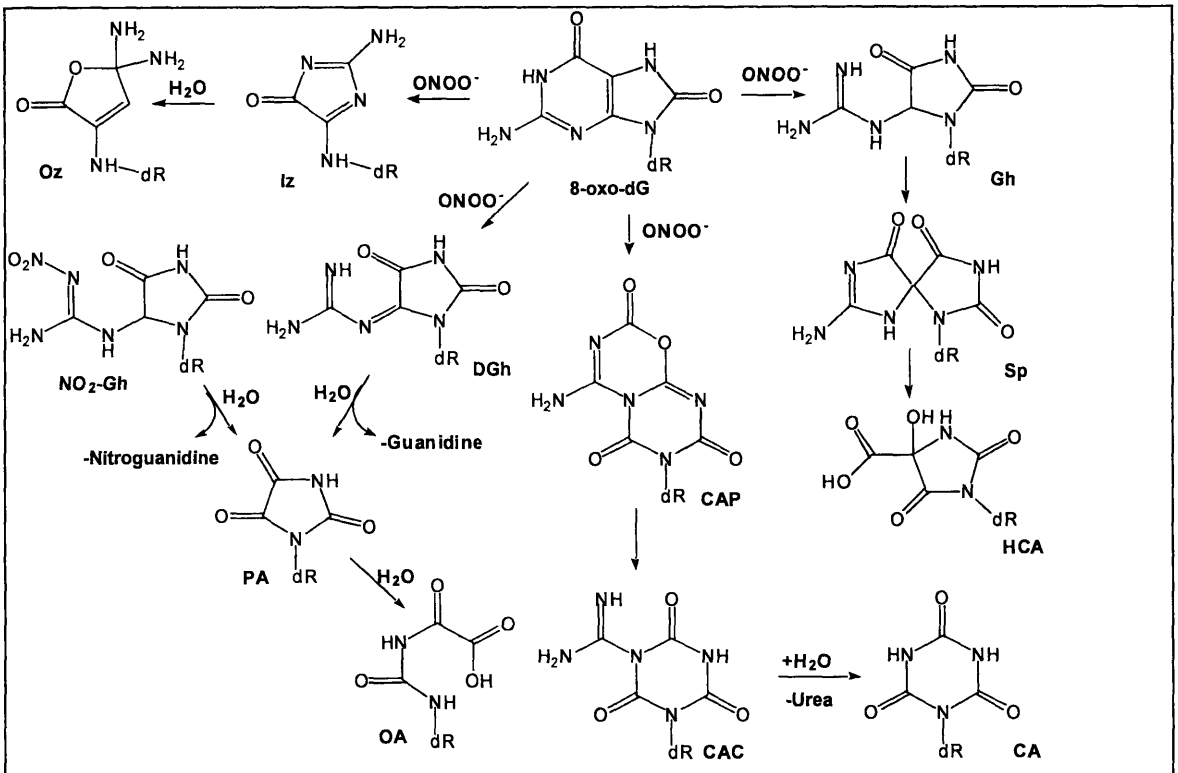

Figure 1-11. Oxidation products of dG reaction with $ONOO^-$ (Secondary oxidation products; adapted from ref. [56].

1.3.3 N_2O_3-induced base damage

Autooxidation of NO• yields N_2O_3, a potent nitrosating agent that induces the deamination of DNA bases. N-Nitrosation of a primary amine initially produces a nitrosamine that is quickly followed by the replacement of $-NH_2$ group bye H_2O. As shown in Figure 1-12, nitrosation by N_2O_3 (and NO_2^- in acidified solutions) converts adenine to hypoxanthine (2'-deoxyinonsine, dI), cytosine to uracil (dU in nucleoside form), 5-methylcytosine to thymine, and guanine to both xanthine (2'-deoxyxanthosine, dX) and oxanosine (2-deoxyoxanine, dO:

observed only at low pH), as well as abasic sites and inter- or intra-strand G-G cross-links [56, 57].

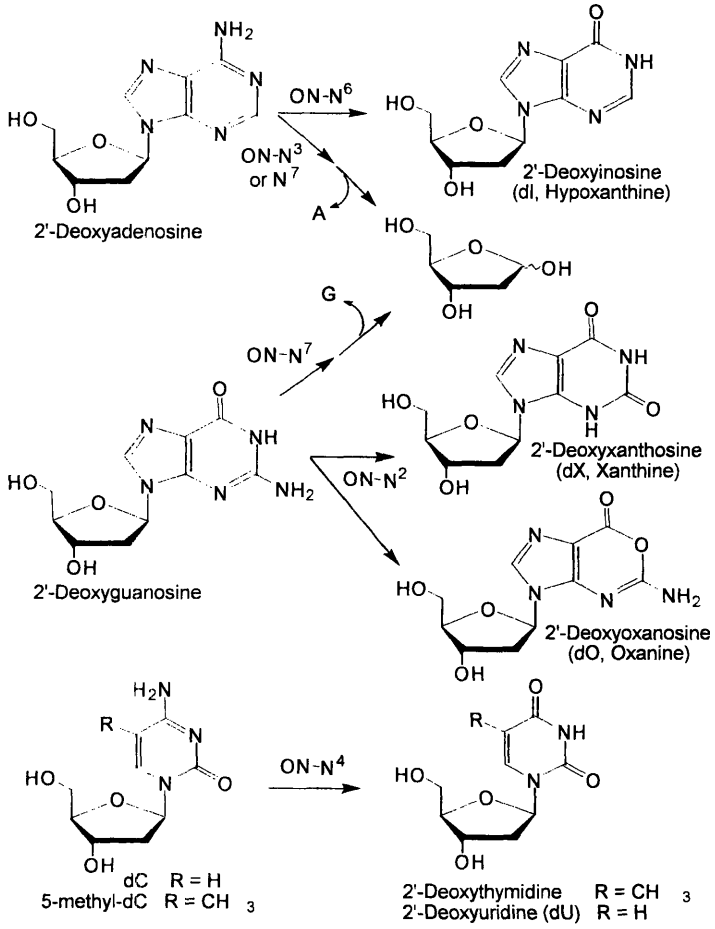

Figure 1-12. Products of N-nitrosative nucleobase deamination

1.3.4 Summary

Aforementioned pyrimidine and purine adducts are far from complete. More than 100 base lesions have been identified using different oxidants. Many of these products have been identified in mammalian cells and tissues as well, suggesting their importance *in vivo*.

It is worth noting that the sites of initial oxidation and terminal damage sites are not necessarily identical in DNA because of a phenomenon called long distance electron transfer. So bases with lower redox potential, dG, is more likely to be oxidized than other bases. Electrons were shown to transferred within the DNA duplex from guanine to the electron-deficient centers created by radiation [58], chemical oxidants and laser-induced photoionization [47, 59]. Further evidence showed that dG-repeats had lower redox potential than isolated dG, with 5'-dG having the lowest potential, and as a result was a more likely target. The oxidation product of dG, 8-oxodG has even lower redox potential than dG. Considering the persistent existence of 8-oxodG *in vivo*, it might be an important target for DNA damage as well.

1.4. DNA deoxyrobise oxidation

Although significant attention has been paid to nucleobase lesions given their role in toxicity and mutagenesis associated with oxidative species, there is growing evidence that deoxyribose oxidation plays a major role in the biological response to oxidative stress. Oxidation of each carbon in deoxyribose yields a unique spectrum of sugar residues or oxidized abasic sites, as shown in Figure 1-13 [60]. Among these products are several reactive electrophiles capable of forming mutagenic adducts with DNA bases [11, 12].

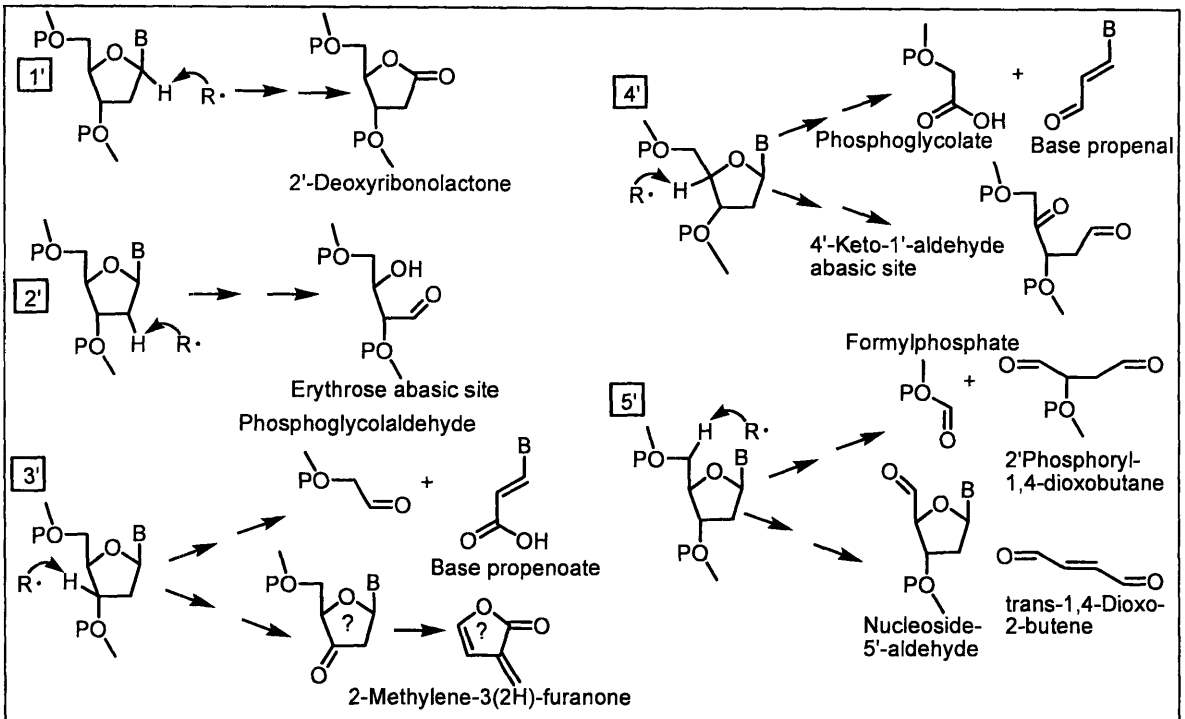

Figure 1-13. Overview of deoxyribose oxidation products

The deoxyribose in DNA has seven carbon-bound hydrogen atoms that are available for abstraction by radicals and other one-electron oxidants that are designated as H-1', H-2', H-2'', H-3', H-4', H-5', and H'5'', as shown in Figure 1-14 [61]. Mechanistic information on the reaction of the •OH with nucleic acids has been extensively studied using ionizing radiation as a source of •OH. Because of the high reactivity of •OH, a wide spectrum of products has been detected in irradiated DNA. For biologically relevant duplex DNA, besides the difference in reactivity due to carbon-hydrogen bond energies, the shape of the double helix has been proposed to influence the accessibility of the various C-H bonds to •OH. Using Fe(II)/EDTA/H_2O_2/ ascorbate system as a source of putative hydroxyl radicals, Balasubramanian *et al.* proposed that solvent accessibility dictates the relative reactivity of deoxyribose carbon atoms in duplex DNA with •OH [62]. They exploited deuterium isotope effects to demonstrate

that Fe-EDTA-induced oxidation exhibits a preference in the following order: 5' > 4' > 2' ≈ 3' > 1'. An atomistic stochastic model of •OH radical reactions with DNA was developed to compute relative •OH attack probabilities at individual deoxyribose hydrogen atoms [63]. Results from this computational model show that •OH radicals exhibit preferential attack at different deoxyribose hydrogens, as suggested by their corresponding percentage solvent-accessible surface areas. The percentage OH attack probabilities for the deoxyribose hydrogens [1H(5')+2H(5'), H(4'), H(3'), 1H(2')+2H(2'), H(1')] were calculated as approximately 54.6%, 20.6%, 15.0%, 8.5% and 1.3%, respectively, averaged across the sequence. These results are in good agreement with the latest experimental site-specific DNA strand break data of Balasubramanian *et al.* [62]

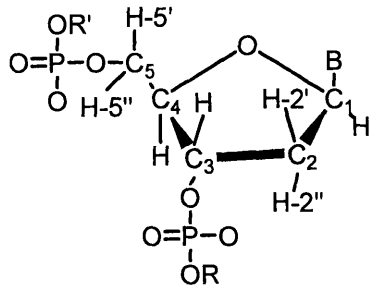

Figure 1-14. The seven abstractable hydrogen atoms in deoxyribose

Studies have shown the oxidation of each deoxyribose carbon position produces a unique spectrum of products. The chemical mechanism, as well as the products of these oxidation reactions, has been a major focus of the Dedon research group. So in this section, we will discuss DNA deoxyribose oxidation (proposed) pathways and products in detail.

1.4.1 C1'-oxidation

The H-1' is buried in the minor groove of B-DNA and is believed to be relatively inaccessible to solvent [64]. Hence, the importance of H-1' as a reactive site is thought to be limited primarily to minor groove binding molecules, where the oxidant is generated in the groove in close proximity to H-1'. One of the well-studied DNA cleavage reactions resulting from H-1' is that promoted by bis(1,10-phenanthroline)copper(I) [65, 66]. Hence, reactive copper-bound oxidants (*e.g.*, $[CuO]^+$, $[CuOH]^{2+}$ and CuO_2H) are believed to be the oxidizing species rather than •OH. Two products, 2'-Deoxyribonolactone and 5-methylene-2(5H)-furanone, were identified as the major products species resulting from H-1' oxidation, as shown in Figure 1-15 [67].

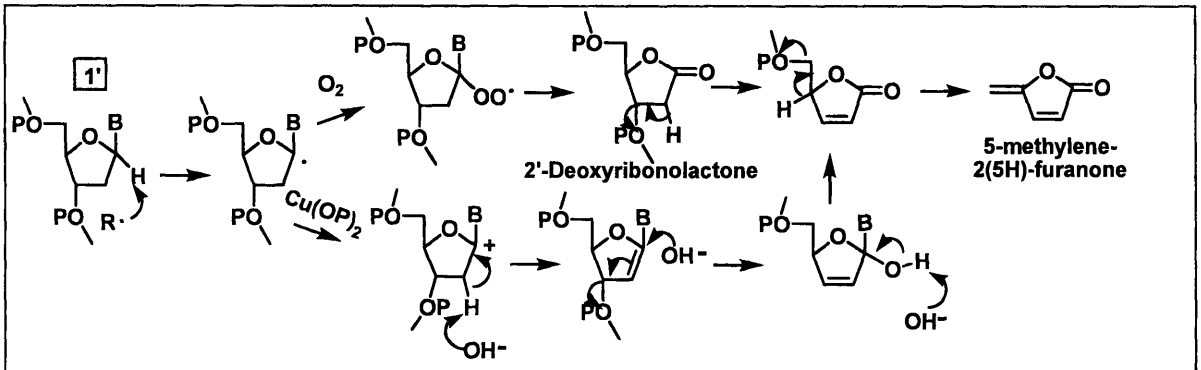

Figure 1-15. Proposed H-1' abstraction pathway and products

Another class of DNA-cleaving agents that reacts at the C1' position is the enediyne antibiotic family. These natural products from the eubacteria Actinomycetales include neocarzinostatin (NCS), calicheamicin, esperamicin and dynemicin A, *etc.* As shown in Figure 1-16, enediynes produce oxidative DNA damage by a common mechanism involving reductive activation to form a diradical species that, when positioned in the minor groove of one DNA

strand, may abstract hydrogen atoms from deoxyribose on each DNA strand. For neocarzinostatin, the lesions occur predominantly at AGC•GCT and AGT•ACT sequences and involves mainly 1' chemistry at C of AGC, 4' chemistry at the T of AGT, and 5' chemistry at the other T residues on the complementary strands [62, 68, 69].

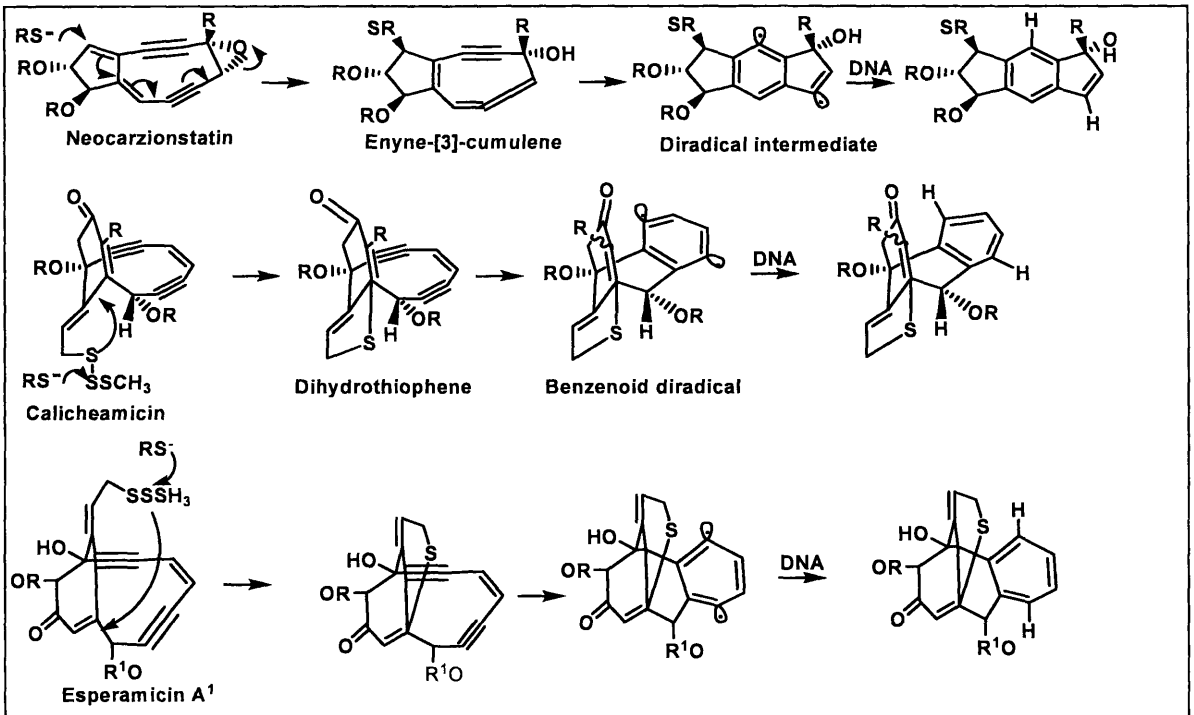

Figure 1-16. Activation of neocarzinostatin, Calicheamicin and Esperamicin

1.4.2 C2'-oxidation

Due to the low solvent accessibility of H-2' and H-2'', as well as the low reactivity of these C-H bonds because of the instability of C2' radical [64], these positions are believed to play a small role in deoxyribose oxidation. Dizdaroglu *et al.* proposed that a major product of C2'-oxidation is erythrose abasic site (Figure 1-17) and characterized erythrose abasic site in γ-

irradiated DNA using GC/MS [70]. Since the hydroxyl group next to the phosphate ester causes the site to be unstable, the erythrose abasic site has been shown to undergo retroaldol reaction to yield 3'-phosphoglycolaldehyde residues under heating or alkaline conditions [71]. In addition to ionizing radiation, photo-activation of 5-bromouracil has also been observed to induce C2' oxidation [72].

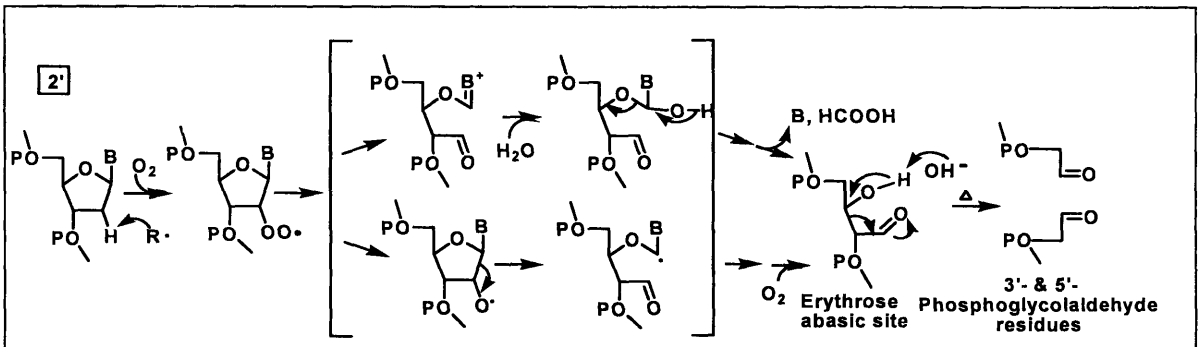

Figure 1-17. Proposed H-2' abstraction pathway and products

1.4.3 C3'-oxidation

The C3'-hydrogen atom is located in the major groove of DNA. Since the majority of the known oxidative cleavage agents bind in the minor groove rather than the major groove, C3'-oxidation was not well studied. C3'-oxidation is considered to be minor in •OH-induced deoxyribose oxidation due to limited accessibility of H-3' and the reduced stability of a 3'-deoxyribosyl radical. Major groove binding photoactive Rhodium(III) complexes were shown to induce C3'-oxidation efficiently [73]. The proposed products of C3'-oxidation includes phosphoglycoladehyde (PGA) residue and base propenoate in an oxygen-dependent mechanism and 2-Methylene-3(2H)-furanone under anaerobic conditions as shown in Figure 1-18 [61].

Using sequencing gel technique, Sitlani et al. tentatively identified PGA termini attached to the 3'-end of the strand breaks arising from deoxyribose oxidation by using Rhodium(III) complexes. They further showed that the molar ratio between PGA and based propenoates was indeed 1:1, which is consistent with the proposed pathway.

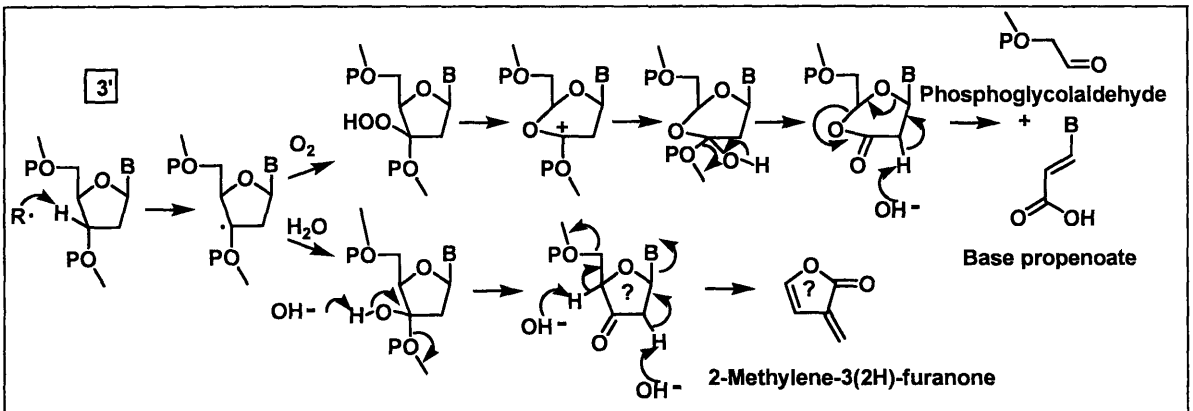

Figure 1-18. Proposed H-3' abstraction pathway and products

1.4.4 C4'-oxidation

The C4'-hydrogen atom is located on the outer edge of minor groove of DNA and is relatively solvent accessible. This C4' carbon-hydrogen bond also has relatively low bond dissociation energy, which makes the C4'-hydrogen atom a major target for •OH and other minor groove-binding oxidants. DNA damage initiated from 4'-hydrogen abstraction has been observed for ionizing radiation, Fe^{2+}/EDTA, Fenton-generated •OH, bleomycin, and enediyne antibiotics.

One of the best-characterized pathways of C4'-oxidation is the H-4' abstraction by bleomycin•Fe(II) [74, 75]. The bleomycin antibiotics represent a family of glycopetide-derived antitumor antibiotics widely used in clinical setting to treat cancer [76]. The attack of DNA by

Bleoymcin•Fe(II) complex requires a sequence of preliminary steps, including "activation". The drug binds to DNA in the minor groove and is "activated" either by molecular oxygen and two electrons, or by hydrogen peroxide (Figure 1-19). Although the exact identity of the oxidizing species in activated bleomycin is not settled, it is generally believed that a peroxide-Fe(III) • bleomycin is likely to be the activated form [77].

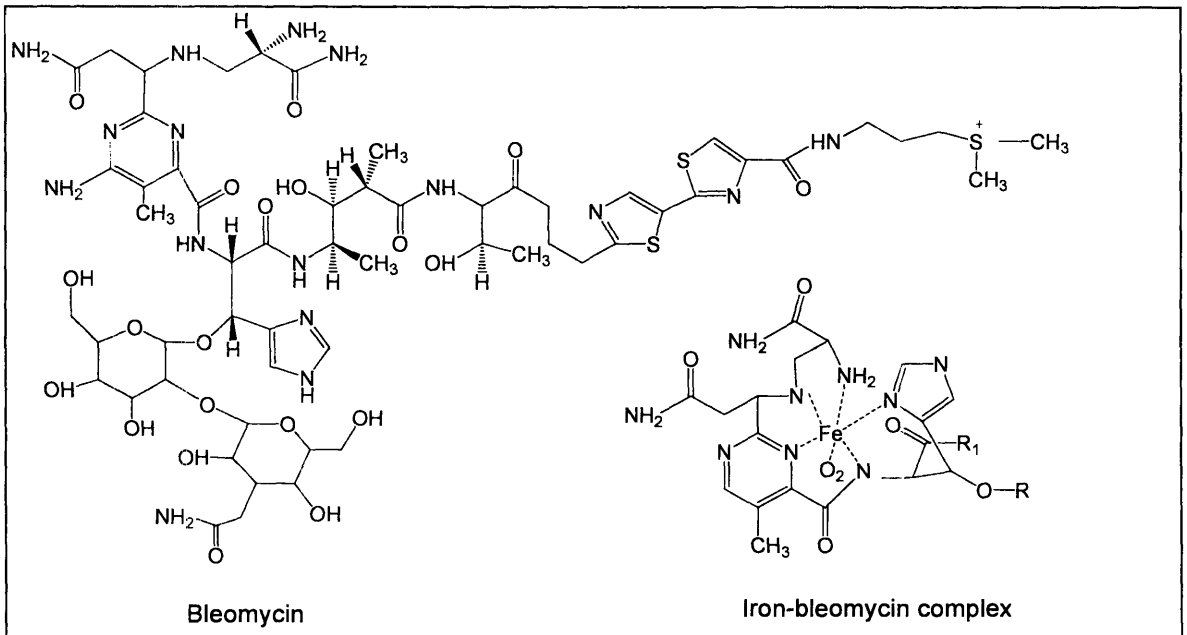

Figure 1-19. Structure of bleomycin and iron-bleomycin complex

Using deuterium-labeled deoxyribose, Stubbe *et al.* showed that the abstraction of H-4' by activated belomycin was the rate-limiting step in bleomycin-induced DNA degradation [75, 78]. Degradation of 4'-deoxyribosyl radical has two outcomes associated with two sets of products (Figure 1-20). One set of products includes strand breaks terminated by 5'-phosphate and 3'-phosphoglycolate moieties. The remainder of the cleaved nucleoside is released as base propenal. The other set of degradation products includes free nucleobase and an abasic sugar, 2-deoxypentos-4-ulose (4′-keto-1′-aldehyde). Under neutral pH conditions and high oxygen

tension, molecular oxygen reacts with the carbon radical to form a peroxy radical that may be reduced to a peroxide. This intermediate further degrades to base propenal and 3'-phosphoglycolate. At low oxygen tension, the carbon radical is further oxidized to a carbocation that adds water to yield a 4'-hydroxyl species. This product is proposed to give rise to a putative hemiketal species that is expected to eliminate the nucleobase while rearranging to yield 4′-keto-1′-aldehyde abasic site [79]. It was shown that bleomycin causes the formation of cytosine-, thymine-, and adenine-propenals accompanied by 3'-phosphoglycolate [80], while the 4′-keto-1′-aldehyde accounted for ~40% of bleomycin-induced DNA oxidation products [79].

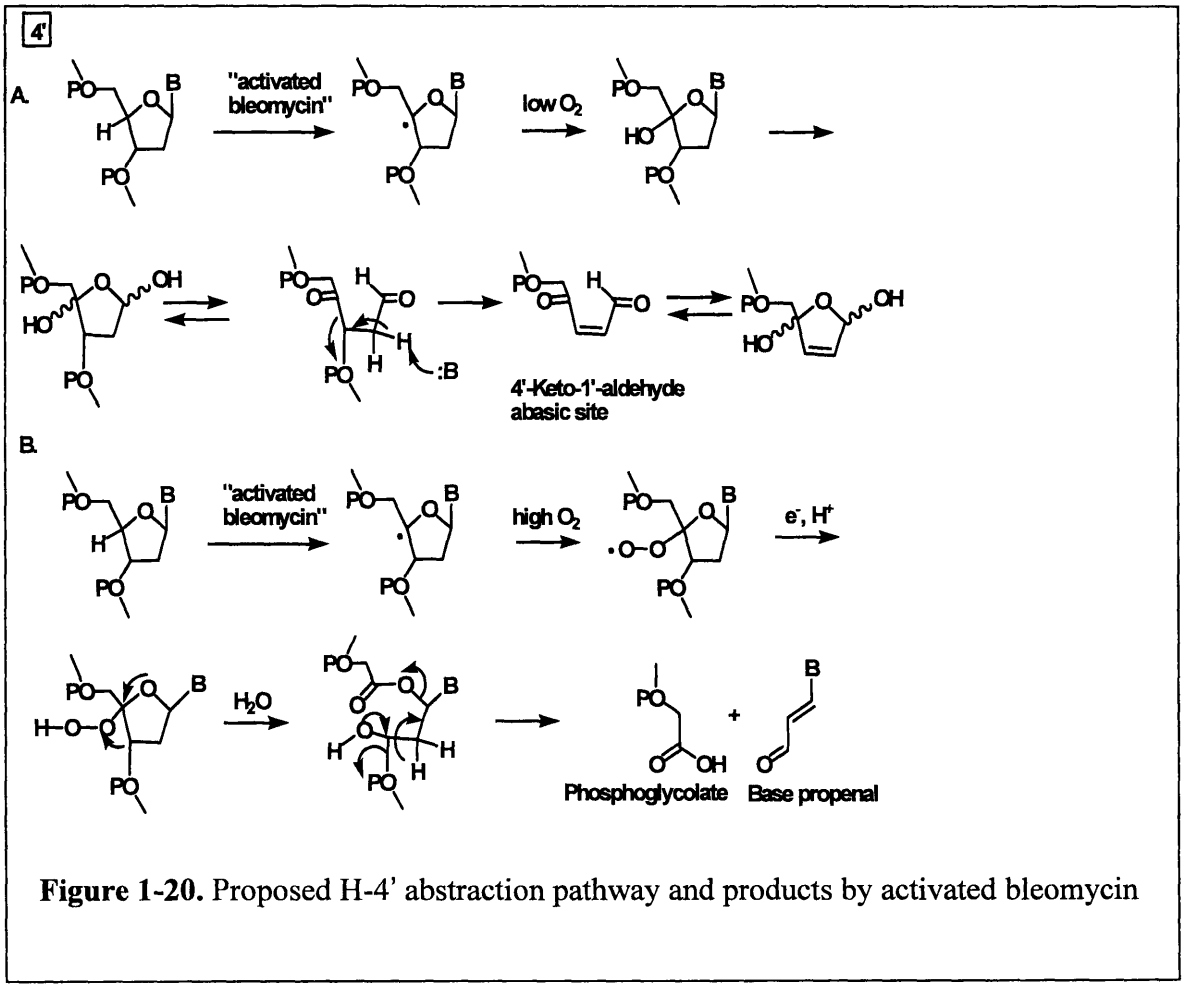

Figure 1-20. Proposed H-4' abstraction pathway and products by activated bleomycin

Unlike bleomycin, γ-radiation induces deoxyribose C4'-oxidation to form malondialdehyde and a free base instead of base propenal [80], a difference that indicates different reaction mechanisms. It is believed that bleomycin remains bound to DNA near the C4' radical after hydrogen atom abstraction and influences the formation of final products. The formation of malondialdehyde in irradiated DNA follows a linear dose-dependence and is accompanied by the formation of 3'-phosphoglycolate residues [80, 81].

Enediynes such as NCS and calicheamicin were also shown to induce C4'-oxidation [82]. DNA deoxyribose oxidation induced by activated NCS has been extensively studied [83]. It has been demonstrated that at least 80% of the DNA cleavage involves 5'-oxidation, which leads to the 5'-aldehyde of dA and dT selectively [84], while less than 20% of the strand breaks resulted from hydrogen atom abstraction at C4' and C1' positions [85, 86]. The C6 radical of activated NCS abstracts a H atom from the C5' of deoxyribose and the remaining NCS C2 radical reacts across the minor groove with the opposite strand at the C4' (or C1') position in the case of suitable special DNA sequences that promote double-strand breaks. Although NCS yields the same products from C4'-oxidation as bleomycin, the mechanism is believed to be different [86-88]. Bleomycin-induced abasic site formation is oxygen-independent, while both abasic site formation and 3'-phosphoglycolate formation are oxygen-dependent for NCS [89]. Similarly, calicheamicin and esperamincins C-E also induce DNA cleavage by C4'-hydrogen abstraction on one strand and C5'-hydrogen abstraction on the other strand. With calicheamicin, bistranded lesions represent >95% of the DNA damage and the 4'-chemistry on one strand is accompanied by products of 5'-hydrogen atom abstraction on the complementary strand [90].

There is also evidence for participation of thiols in reactions of the deoxyribose carbon radicals after their formation. Neutral and positively charged thiols cause a reduction in the level

of double-stranded DNA lesions induced by NCS and esperamincins relative to that of negatively charged thiols [91]. For calicheamicin, no such quenching effect was observed. Yet, neutral and, to an even greater extent, positively charged thiols inhibit the formation of 3-phosphoglycolate residues with a proportional increases in the formation of the alternative abasic sites, which may be due to concentration of the positive thiols on or around the negatively charged backbone of DNA [82].

1.4.5 C5'-Oxidation

In the minor groove of the B-DNA helix, both H5' and H5'' have been estimated to be the most solvent accessible deoxyribose hydrogen atoms [61]. C5'-oxidation has been observed by γ-radiation, Fenton-generated •OH, enediyne antibiotics, cationic metal porphyrins, and the perhydroxyl radical [92, 93]. As shown in Figure 1-21, the reaction partitions to form either a nucleoside 5'-aldehyde residue attached to the 5'-end of the DNA strand, or a 5'-formylphosphate residue attached to the 3'-end of the DNA strand that is accompanied by a four-carbon fragment on the 5'-end, which was identified as 5'-(2-phosphoryl-1,4-dioxobutane) [94]. Formation of a hydroxyl group at the C5' carbon radical gives rise to a C5' aldehyde at one strand terminus and a 3'-phosphate at the other at ambient temperature [95]. Upon heating, consecutive β- and δ-elimination result in the formation of furfural, free base, and a 5'-phosphate terminus. Pratviel *et al.* developed a GC/MS method to quantify furfural and showed that furfural can be used as a convenient marker of C5' hydroxylation of deoxyribose [95]. Alternatively, the deoxyribose 5'-peroxide may form an oxygen radical intermediate with subsequent β-scission of the 4'-5' bond (Creigee-type rearrangement) to generate the 3'-formylphosphate and 5'-(2-phosphoryl-1, 4-

dioxobutane) residue. The Dedon group has shown that the *trans*-5'-(2-phosphoryl-1,4-dioxobutane) residue has the potential to undergo β-elimination to form 1,4-dioxo-2-butene, a highly reactive α, β-unsaturated dicarbonyl species [94].

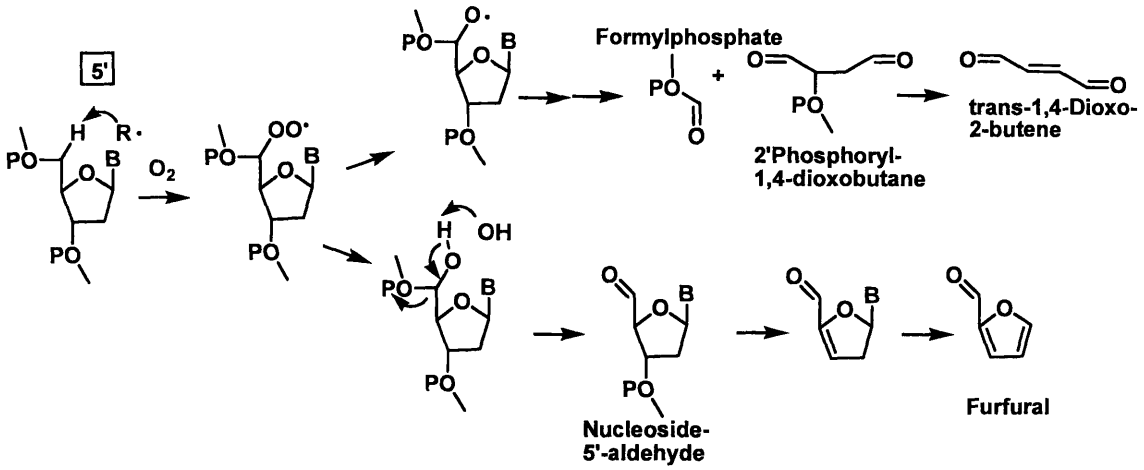

Figure 1-21. Proposed H-5' abstraction pathway and products

As discussed in Section 4.5, the activated enediynes abstract a H atom from the C5' of deoxyribose. The resulting nucleoside 5'-aldhyde accounts for a majority of the damage produced by C5'-hydrogen abstraction, while 3'-formylphosphate and 2'-phosphoryl-1,4-dioxobutane products are often the minor lesions [90, 96].

1.5. Complex DNA lesions

A special type of oxidative DNA damage, termed a complex lesion, has been associated with ionizing radiation. This type of damage consists of two or more lesions—single-strand breaks or modified bases—located within one to two helical turns on the same strand or on opposite strands. Radiation, especially high LET radiation, produces dense ionization in the

vicinity of the DNA helix and induces multiple oxidation events. The best known example of complex lesion is double strand break (DSB), which is generated when the two complementary stands of the DNA double helix are broken simultaneously at sites that are sufficiently close to one another to allow the dissociation of the helix [97]. As potent inducer of mutation and cell death, a DSB is probably the most toxic DNA lesions with a single DSB capable of killing a metazoan cell if it leads to the inactivation of an essential gene or, more commonly, triggers apoptosis [98]. Evidence also showed a causal link between the generation of DSBs and the induction of mutations and chromosomal translocations with tumorigenic potential [99, 100].

Another example of complex lesion, termed tandem lesion (Figure 1-22), involves two vicinal modifications on the same DNA strand and is generated by one initial radical hit that leads to cyclization [101]. These cyclo-lesions are formed through a covalent linkage between the bases of adjacent nucleotides or linkage between the base and deoxyribose moeities of the same nucleotide. A well-studied example, 5',8-Cycolpurine (g and h in Figure 1-22) nucleosides were first identified more than 20 years ago [102] and have been observed in γ-irradiated isolated DNA [103] and in DNA from mammalian tissues [104]. 5', 8-cycolpurine nucleosides arise from the attack of the C-5' centered radical of the sugar moiety at the C-8 of the purine within the same nucleoside leading to intramolecular cyclization followed by oxidation of the thus formed N-7 centered radical. These compounds represent a concomitant damage to both sugar and base moieties of the same nucleoside and thus can be considered complex lesions. Because of thc presence of a covalent bond between the sugar and purine moieties, these tandem lesions are not repaired by base excision repair but instead by nucleotide excision repair. Thus, they may play a role in diseases with defective nucleotide excision repair.

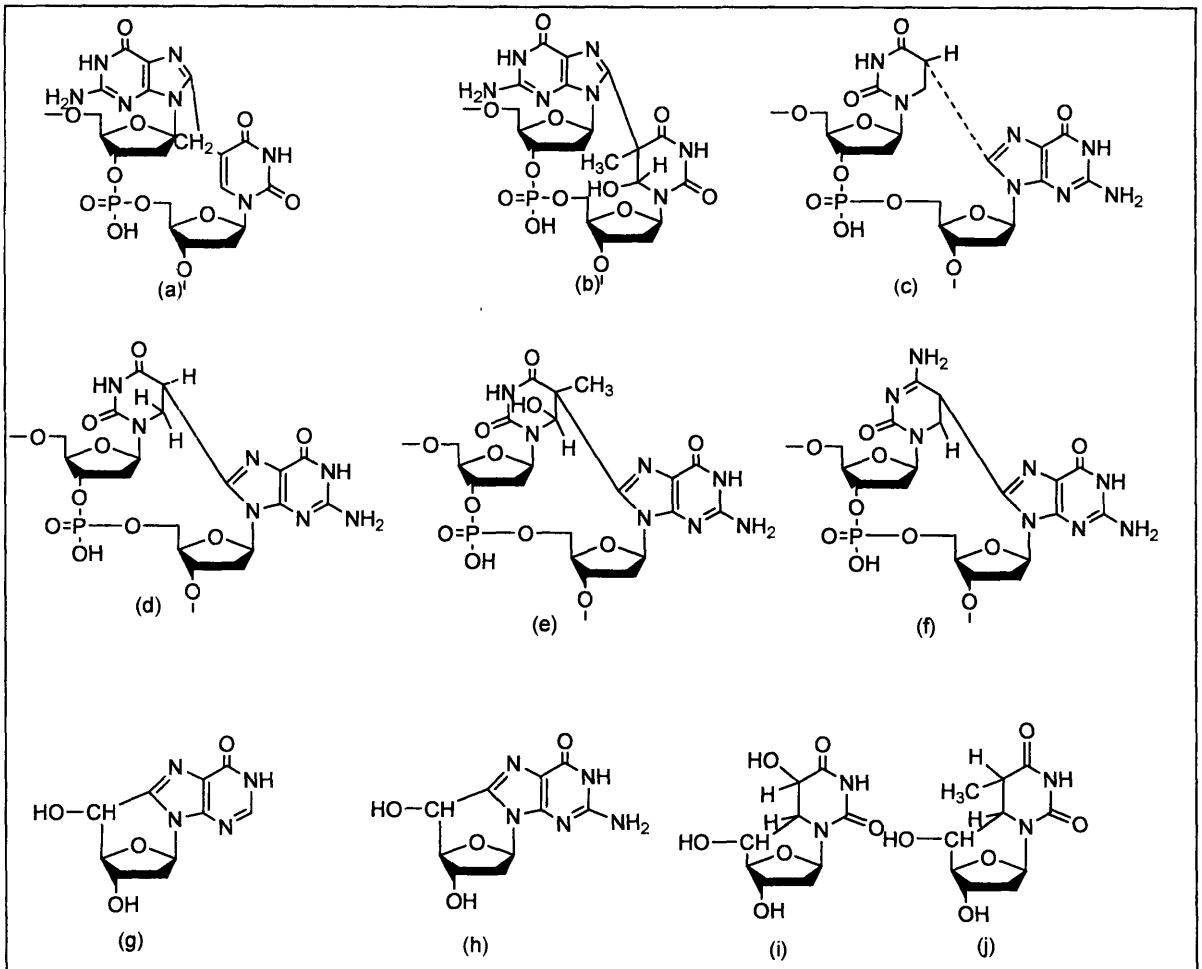

Figure 1-22. Free radical-induced double lesions

1.6. Biological consequences of DNA deoxyribose oxidation

Oxidation of deoxyribose in DNA results in the formation of a variety of electrophilic products, many of which have the potential to further react with nucleobases or protein to form adducts and cross-links. For example, C1'-oxidation product, 2'-deoxyribonolactone (dL) represents a conservative structural change from an AP site. However it cannot be incised by AP lyases such as EndoIII, Fpg, end VIII, NTH1, NEIL1, NEIL2, yOGG1, hOGG1 and NTG2 [105]

and it was shown to inversibly inhibits *E. coli* endonuclease III by cross linking to Lys120 [105, 106] (Figure 1-23). Although dL residues are efficiently incised by the main human abasic endonuclease enzyme Ape1, DeMott *et al.* have shown that dL forms a stable protein-DNA cross-link with DNA polymerase β that resists further processing and is consequently highly toxic in cells [107]. Considering that the half-life of 2'-deoxyribonolactone in double helix DNA under physiological conditions (pH 7.4, 37°C) is 32-54 hours [108], dL may exert significant effects on the repair of normal abasic sites and oxidative base lesions in cells by reducing the cellular activity of these BER enzymes either via cross-linking or competition with binding to the BER enzymes [105].

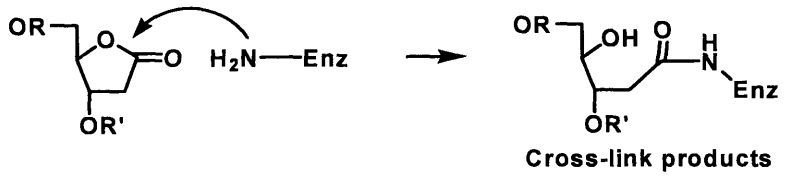

Figure 1-23. Covalent trapping of DNA repair enzyme by 2'-deoxyribonolactone

A second example of adduct formation by products of deoxyribose oxidation involves 3'-phosphoglycoladehyde residue (PGA). Our laboratory has shown that PGA form glyoxal by a novel radical-independent pathway, and the glyoxal subsequently reacts with dG in DNA to form 1,N^2-glyoxal adduct (Figure 1-24) [11].

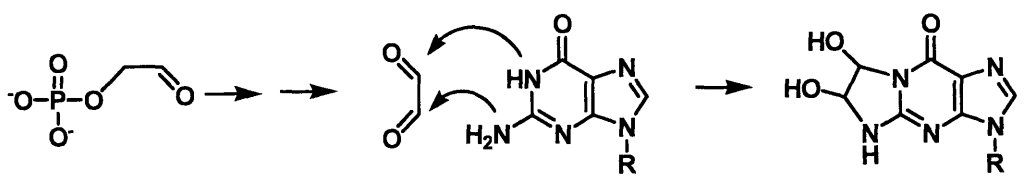

Figure 1-24. Formation of 1,N^2-glyoxal adducts of dG from phosphoglycolaldehyde

The β-elimination product of the 5'-(2-phosphoryl-1,4-dioxobutane) residue arising from 5'-oxidation of deoxyribose (*trans*-1,4-dioxo-2-butene) can react with dG, dA and dC to form stable bicyclic adducts [9, 10]. The reaction between *trans*-1,4-dioxo-2-butene and dC was shown to be nearly quantitative and produced two interchanging diastereomer adducts with a second-order rate constant of $3.66 \times 10^{-2}\ M^{-1}\ s^{-1}$, which is nearly 10-fold faster than the reaction with the *cis*-isomer ($3.74 \times 10^{-3}\ M^{-1}\ s^{-1}$), a metabolite of furan [109]. HPLC analyses of reactions of 1,4-dioxo-2-butene with both dA and 9-methyladenine revealed multiple products including a novel pair of closely eluting fluorescent species, which were also tentatively identified as diastereomeric oxadiazabicyclo(3.3.0) octaimine adducts [109].

The final example of adduct formation involves deoxyribose 4'-oxidation product base propenal. Base propoenal, structural analogs of the enol tautomer of MDA , reacts with DNA to form M_1dG as shown in Figure 1-1 [12], though with significantly greater efficiency than MDA [12, 13]. Marnett et al. confirmed that base propenals were significantly more reactive (30 – 150 times) than MDA toward DNA to form M_1G a product and are 30 to 60 times more mutagenic than MDA [13].

In addition to adduct formation, the deoxyribose oxidation products can block DNA repair activities. PGA and PGL can block DNA synthesis [110] and the removal of 3'-terminal blocking groups, such as 3'-phosphates, and 3'-(2,3-didehydro-2,3-dideoxyribose phosphates), has been shown to be rate-limiting during DNA repair [111, 112]. PGL was shown to be relatively a poor substrate for Ape1 excision [113]. The 4'-keto-1'-aldehyde abasic site was shown to be a blocking lesion for Klenow exo^+/exo^- fragments and the bypass polymerases pol II, pol IV and polV were compromised in their ability to extend past the lesion with preferential thymidine incorporation by polymerase II exo^- [114, 115].

1.7. Lipid peroxidation products

Besides DNA, RNS and ROS can damage all types of cellular molecules including lipids and proteins. These reactions often lead to generation of reactive electrophilic species that are also capable of modifying DNA. Polyunsaturated fatty acids (PUFA) in phospholipids, cholesterol esters, and triglycerides are prone to peroxidation by RNS/ROS, which is usually called lipid peroxidation. Lipid peroxidation proceeds by a classic chain reaction that includes three discrete phases: initiation, propagation, and termination. Fundamental steps occurring during lipid peroxidation are shown in Figure 1-25 [116].

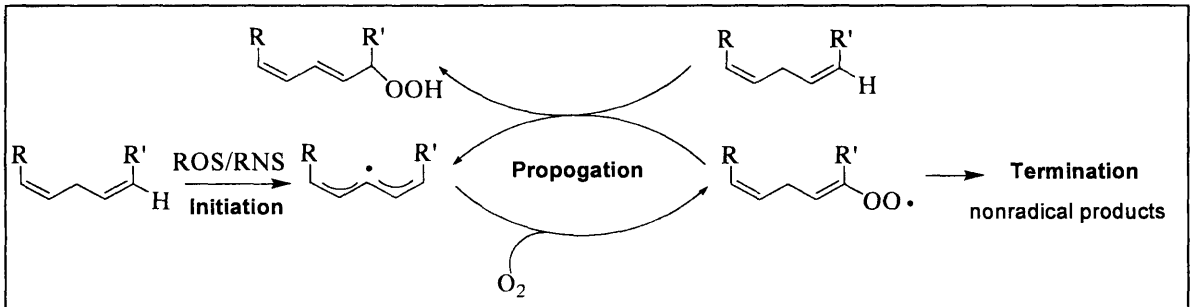

Figure 1-25. Chemical transformations of the three phases of lipid

Initiation occurs by H atom abstraction from the highly reactive methylene groups between the double bonds in PUFA by RNS/ROS to form carbon-centered radicals [116]. Reaction of molecular oxygen with a carbon-centered radical to form a peroxyl radical occurs at a diffusion-limited rate. A peroxyl radical can then be reduced to a hydroperoxide by oxidation of another PUFA molecule. This propagation step can be cycled many rounds to generate new peroxyl radicals (after O_2 addition), which results in the net conversion of lipids to lipid hydroperoxides. Through propagation, one ROS/RNS molecule can induce peroxidation of many

PUFA molecules. It is estimated that one free-radical initiation can induce the oxidation of approximately 60 linoleic acid molecules and 200 arachidonic acid molecules [117]. The termination step often involves the reaction of a peroxyl radical with vitamin E (α-tocopherol). Furthermore, any kind of alkyl radicals (lipid free radicals) can react with a lipid peroxide to give non-initiating and non-propagating species such as the relatively stable dimers or two peroxide molecules combining to form hydroxylated derivatives [118]. As a result, vitamin E concentration in the lipid bylayer is a major factor determining the free-radical reaction chain length *in vivo* [119].

After the initiation, transformation of peroxyl radicals depends on their positions in the carbon chain of PUFA [120]. If the peroxyl radical exists at the end of a double bond system (*e.g.* **3** in Figure 1-26), it is often directly reduced to a hydroperoxide **4** by another PUFA molecule or vitamin E. If the peroxyl radical is located within a double bond system (*e.g.* **2**), cyclization to an adjacent double bond will compete with reduction to a hydroperoxide. This cyclization product **5** can undergo further transformation. It can bind an oxygen molecule, yielding a peroxyl radical which is reduced to a hydroperoxide **6,** as described above. Alternatively, it can undergo another cyclization, yielding a bicyclic peroxide that, after coupling to O_2 and reduction, yields a compound **7** which is structurally analogous to the prostaglandin endoperoxide, PGG_2. Compound **7** can then be converted to a range of compounds including isoprostanes and malondialdehyde (MDA) [120, 121]. MDA has long been used as a biomarker for lipid peroxidation. Nevertheless it was constrained by issues such as its instability *in vivo* and nonspecificity of thiobarbituric acid derivitization methodology. In recent years, measurement of F2-isoprostanes has been developed as a more reliable alternative for assessment of lipid peroxidation *in vivo* [122].

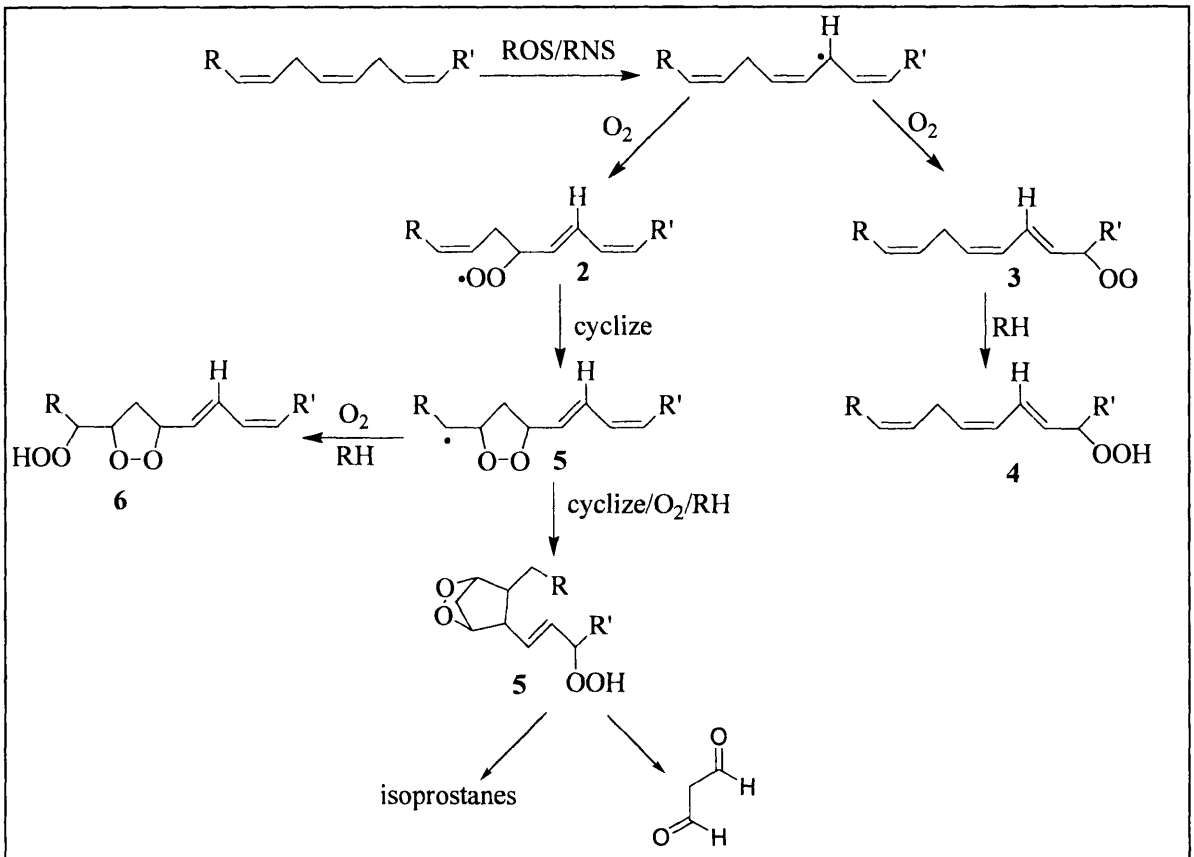

Figure 1-26. The pathways and products of lipid peroxidation

All of the hydroperoxides described in Figure 1-26, as well as their regioisomers and steroisomers, can be reduced by transition metal ions to alkoxyl radicals that can undergo β-cleavage to yield a wide range of products [116], including saturated and α, β-unsaturated aldehydes (*e.g.* 4-hydroxy-2-nonenal, acrolein, crotonaldehyde, 2,4-nonadienal) and epoxy compounds (*e.g.* 2,3-epoxybutanal, 2,3-epoxy-4-hydroxynonanal) [123]. It is believed that 4-hydroxy-2-nonenal is formed by the transformation of ω-6-polyunsaturated fatty acids (18:2, 20:4 *etc.*), while 4-hydroxyhexenals and propanals are formed from ω-3-polyunsaturated fatty acids [124]. Crotonaldehyde is mainly formed from α-linoleic acid and linoleate and in small amounts from cis-5,8,11,14,17-eicosapentaenoic and cis-4,7,10,13,16,19-docosahexaenoic acid [125].

Saturated and α, β-unsaturated aldehydes from lipid peroxidation are strong electrophiles that can readily react with small antioxidant molecules such as glutathione, a variety of nucleophilic amino acids in proteins [125-127] and with DNA bases. For proteins, the main targets include the sulfhydryl group of cysteine, the imidazole group of histidine, and the ε-amino group of lysine [125-128]. In this section, we will focus on the exocyclic base adducts formed by major lipid perxodation products in DNA and RNA.

1.7.1 Malondialdehyde

Malondialdehyde (MDA) is a well-studied lipid peroxidations products that mainly exists as its tautomeric form, β-hydroxyacrolein in aqueous solution. β-Hydroxyacrolein has a pKa of 4.6 (Figure 1-27) and as the neutral species it is both a good electrophile and a good nucleophile. As an electrophile, MDA reacts with DNA nucleobases to form multiple adducts as shown in Figure 1-28 [129-133]. *In vitro* studies indicate that the major adduct formed in the reaction of MDA with DNA is the pyrimido[1,2-α]purin-10(3H)one (M_1dG), adduct of dG. Both of MDA's carbonyl equivalents react with N^2 and N^1 of dG with the loss of two water molecules to form M_1G, a planar aromatic molecule that is moderately fluorescent (~3% quantum yield) [120]. MDA also reacts with dA to form a minor product N^6-(3-oxo-propenyl)deoxyadenosine (M_1dA), which occurs at 1/5 to the level of M_1dG, and trace amounts of N^4-(3-oxopropenyl)deoxycytidine (M_1dC). Both M_1dA and M_1dC are formed by a single addition step with no observed cyclization of these oxopropenyl derivatives. Since MDA is both an electrophile and a nucleophile, MDA oligomerization can happen, although at a slow rate in neutral medium, to form dimers and trimers that also react with DNA to form adducts such as M_2dG, M_3dA and M_3dC [132, 133].

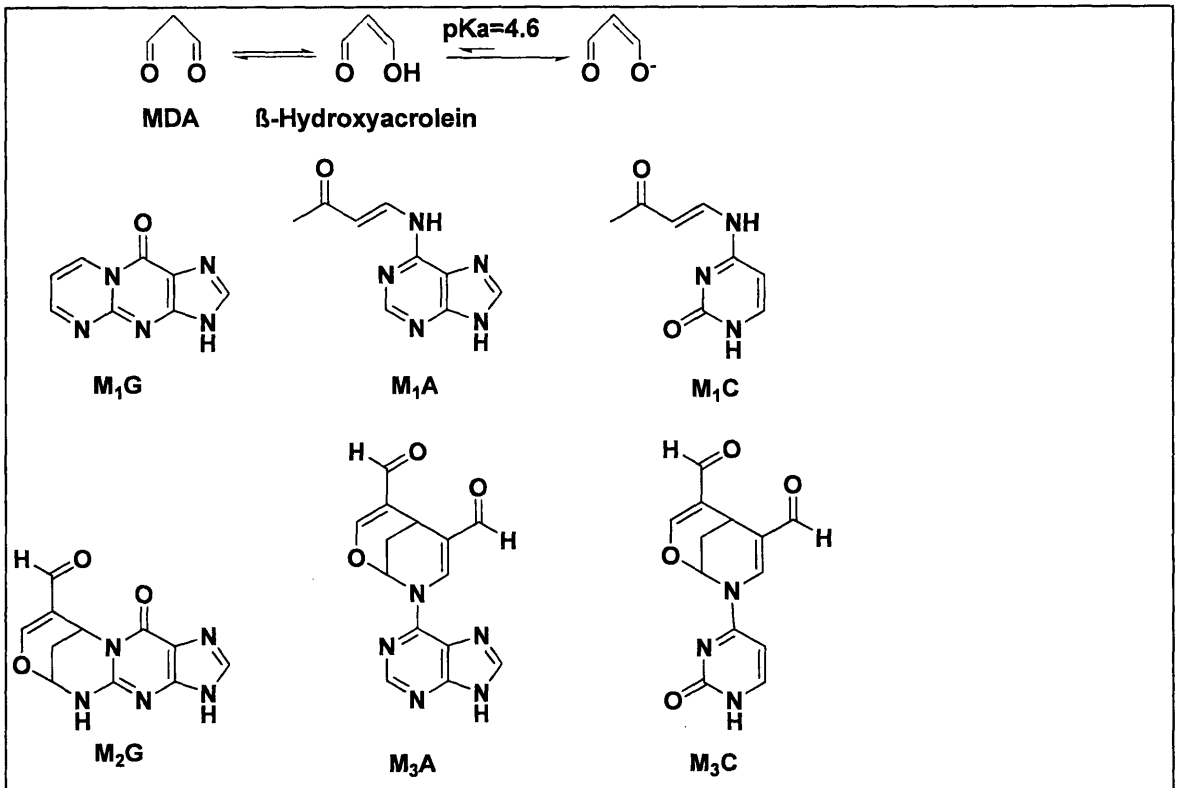

Figure 1-27. MDA structure and formation of MDA-DNA adduct

1.7.2 4-Hydroxy-2-nonenal

4-Hydroxy-2-nonenal (HNE) was shown to be a major product of lipid peroxidation that accumulates in membranes to concentrations of up to 10 to 50 μM in response to oxidative insults [128]. Enals such as HNE yield propanobases with DNA as the major products. For example, propano-guanosine is proposed to be formed by nucleophilic Michael addition of the exocyclic nitrogen atom of dG amino group to the aldehyde double bond followed by cyclization in position N^1 of the dG as shown in Figure 1-28. HNE and other α, β-unsaturated aldehydes can be further oxidized by hydrogen peroxide or fatty acid hydroperoxides to epoxy-aldehydes, *e.g.*

4-hydroxy-2,3-epoxynonanal. 4-Hydroxy-2,3-epoxynonanal is more reactive towards DNA bases than HNE and reacts with DNA to form etheno adducts, mainly 1,N^6-etheno-2'-deoxyadenosine (1,N^6-εdA), 3,N^4-etheno-2'-deoxycytidine (3,N^4--εdC), 1,N^2-etheno-2'-deoxyguanosine (1,N^2-εdG), and N^2,3-etheno-2'-deoxyguanosine (N^2,3-εdG) as shown in Figure 1-28.

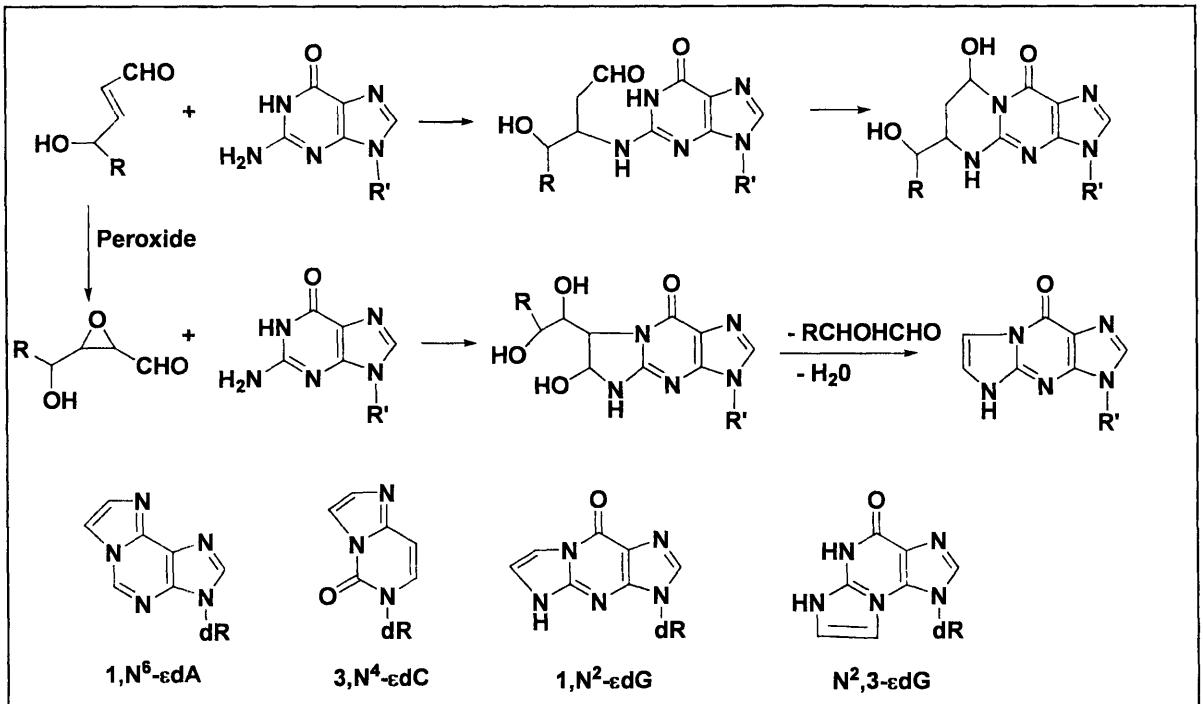

Figure 1-28. Formation of propano and etheno adducts from 4-hydroxy-2-nonenal

1.7.3 Acrolein

Acrolein is one of the most electrophilic α, β-unsaturated aldehydes. For example, it reacts with GSH 110- to 150- times faster than HNE or crotonaldehyde [134]. Similar to HNE and crotonaldehyde, acrolein can react with dA, dC and dG to form exocyclic DNA adducts as shown in Figure 1-29. Yet there is a significant difference. When the γ-hydrogen in α, β-unsaturated aldehyde is replaced by an alkyl group, as in HNE and crotonaldehyde, the steric

hindrance generated by the alkyl group and the oxygen atom at the C-6 carbon atom in dG prevents the Michael addition between the nitrogen N-1 and the carbon double bond of the substituted aldehyde. So only acrolein can form steroisomers AdG2 and AdG3, as shown in Figure 1-29. Immunochemical studies have established the formation of 1,N^2-propanodeoxyguanosine adduct in DNA from *Salmonella typhimurium* exposed to acrolein [135]. Acrolein can also be oxidized to acrolein epoxide, which reacts with DNA to form etheno adducts.

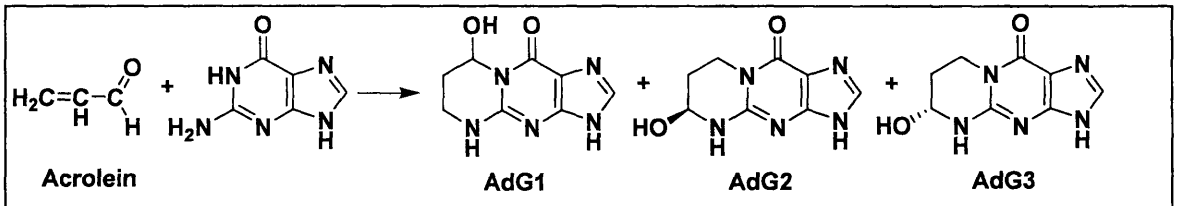

Figure 1-29. Formation of propano adducts from acrolein

1.7.4 4-oxo-2-nonenal

In addition to well-investigated genotoxic aldehdyes such as 4-hydroxy-2-nonenal, acrolein and crotonaldehyde, 4-oxo-2-nonenal (ONE) has been characterized as a novel principal breakdown product of linoleic acid hydroperoxide [136]. When free nucleobases were incubated with oxidized linoleate, dC and dG were significantly modified among the four 2′-deoxynucleosides [136]. In contrast to the similar reactivity of ONE toward free nucleobases (dC and dG), ONE preferentially reacted with dC in double-stranded DNA to yield 2-oxo-heptyl–substituted 3,N^4-etheno-dC as the major product (through mechanism shown in Figure 1-30)

[137, 138]. These results suggest that ONE and other 4-oxo-2-alkenals may play an important role in DNA damage as major endogenous genotoxins formed during lipid peroxidation.

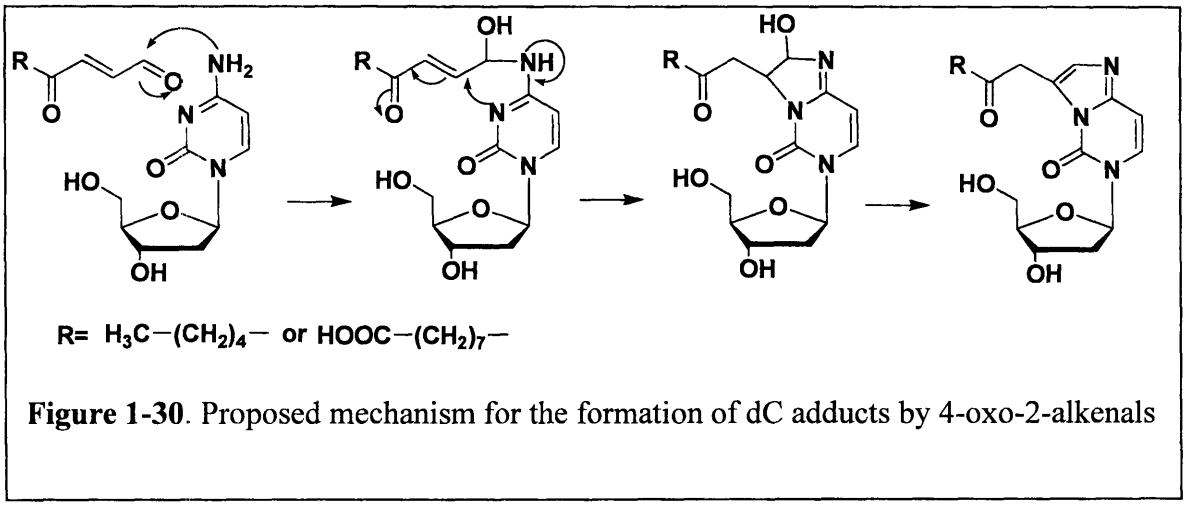

Figure 1-30. Proposed mechanism for the formation of dC adducts by 4-oxo-2-alkenals

1.7.5 Other lipid peroxidation products

Besides these well-studied electrophiles produced by lipid peroxidation, studies have revealed more complicated intermediates and DNA/protein adducts derived from these intermediates using LC-MS or LC-MS/MS analysis [139, 140]. For example, *trans, trans*-2, 4-decadienal was shown to be one of the most toxic breakdown products of lipid peroxidation. It inhibits cell growth, causes cell death, changes cellular glutathione levels and is involved in DNA fragmentation [141]. Similar to HNE, it reacts with DNA to form propano and etheno adducts [142]. Compared to free radicals, reactive electrophiles from peroxidation of PUFA are relatively stable and can diffuse within cells or even escape from cells to attack targets at some distance from the site of the original event. Therefore, they are not only end products, but also act as "second cytotoxic messengers" for the primary reactions. Because of their importance, the Dedon lab has initialized a new project to study endogenous adduct formation from lipid

peroxidation products using ^{14}C-labeled PUFA. These systematic studies begin with a quantitative survey of proportions of lipid peroxidation-derived adducts in total DNA, RNA and proteins. Then the project will extend to fractionate the various classes of macromolecules and try to identify the structures as well as amounts of different adducts. These studies will provide critical insights into the chemical basis for the endogenous adducts that may play a role in the pathophysiology of cancer and other human diseases, as well as providing the mechanistic insights to the development of rigorous biomarkers.

1.8. Protein oxidation

Proteins cannot be overlooked as major targets for radicals and electrophiles in cells. Reactions of a variety of ROS, RNS and RHS with proteins can lead to formation of protein hydroperoxides; hydroxylation of aromatic groups and aliphatic amino acid side chains; nitration of aromatic amino acid residues; oxidation of sulfhydryl groups, oxidation of methionines, conversion of some amino acid residues into carbonyl groups; cleavage of the polypeptide chain and formation of cross-links [143-146]. Such modifications of proteins have been observed to lead to loss of their function, their accumulation and inhibition of their degradation in several human diseases, aging, cell differentiation and apoptosis. Formation of specific protein oxidation products may be useful as biomarkers of oxidative stress. It is notable that when •OH oxidizes proteins, the amino acid radicals that they generate can be propagated to secondary sites, potentially causing the latter amino acids to be disproportionately modified [147-150].

1.9. Maintenance of DNA integrity

1.9.1 Defense against ROS/RNS/RHS

Due to the extremely short half-life (10^{-9}s) of •OH, there is no enzyme that specifically eliminates •OH. Instead the cellular antioxidant defenses effectively eliminate its precursors and products. Superoxide dismutases (SOD) located in the cytosol (Cu, Zn-SOD) and mitochondria (Mn-SOD) convert two superoxide anions into H_2O_2 and O_2. Subsequently, H_2O_2 is reduced to water by glutathione peroxidases in the cytosol and mitochondria or by catalase in peroxisomes [151, 152]. Nonenzymatic antioxidants such as glutathione, vitamin E, vitamin C, β-carotene can quench •OH-induced peroxyl radicals by providing a hydrogen atom to the radical [153].

1.9.2 Repair of DNA damage

As detailed in the previous sections, a large array of nucleobase and deoxyribose lesions are produced during DNA oxidation. Failure to repair these lesions could result in mutation, cytotoxicity and cell death. So under normal physiological conditions, cells are capable of removing these lesions through a variety of pathways. A detailed review of different DNA repair pathways is beyond the scope of this thesis [154-157]. However, a brief discussion of the general repair pathways is warranted, with a focus on base excision repair (Figure 1-31) given its direct importance to the work described in this thesis.

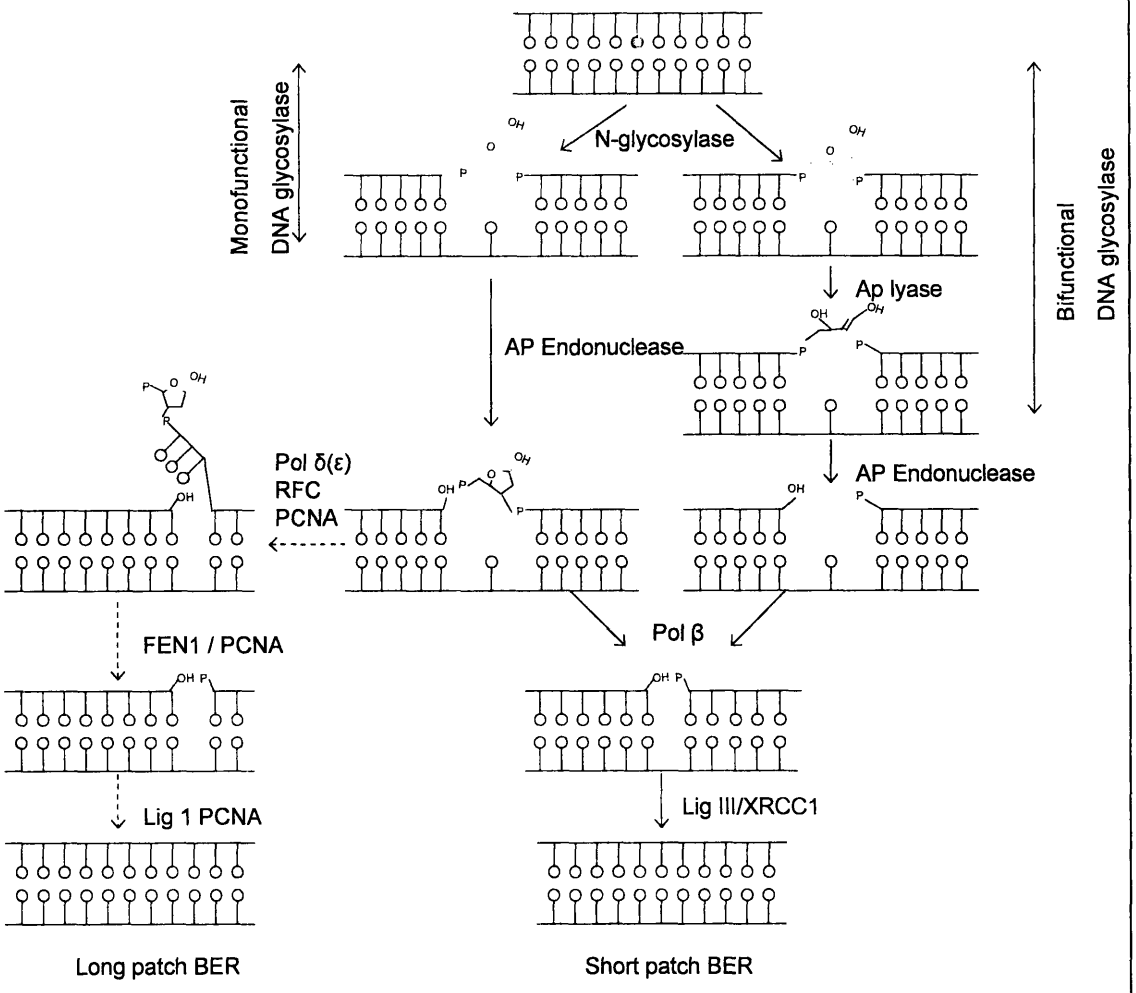

Figure 1-31. Pathways of Human base excision

Simple base lesions and some of tandem base lesions are often removed by base-excision repair [154, 158]. For base excision repair, the modified base is first recognized and removed by a specific glycosylase to leave an apurinic/apyrimidinic (AP) site. Some of the bifunctional glycosylases have an associated apurinic/apyrimidinic (AP) lyase activity that, via a β-elimination reaction, produces a 3'-α, β-unsaturated aldehyde and 5'-phosphate products. Several glycosylases also cleave the 3'-α, β-unsaturated aldehyde to produce a 3'-phosphate through δ–elimination. Alternatively, the AP site is processed by AP endonucleases that cleave the

phosphodiester bond either 5' or 3' to the AP site. As shown in Figure 1-32, monofunctional DNA glycosylases cleave the glycosidic bond by a hydrolytic mechanism that involves activating a water molecule to attack the C1' of the modified base. In contrast, bifunctional glycosylases such as fapy glycosylase and hOGG1 directly attack C1' position as nucleophiles. The imino intermediate is then hydrolyzed to release the enzyme and produces 3'-α, β-unsaturated aldehyde. The site is processed further to generate a 3'-OH suitable for polymerization and ligation. The resulting single nucleotide gap with a 3'-OH terminus is filled by DNA polymerase and finally the nick is sealed by DNA ligase (*e.g.* DNA ligase III, XRCC1). The net reaction in these BER process is the replacement of a single nucleotide and is called short patch BER. A different subpathway is called long patch BER, where a DNA polymerase (*e.g.* pol δ, RFC, PCNA) synthesizes several nucleotides by displacing the downstream strand containing 5'-dRP. The resulting flap structure containing the 5'-dRP is then incised by flap endonuclease and the nick is sealed by DNA ligase (*e.g.* DNA ligase I).

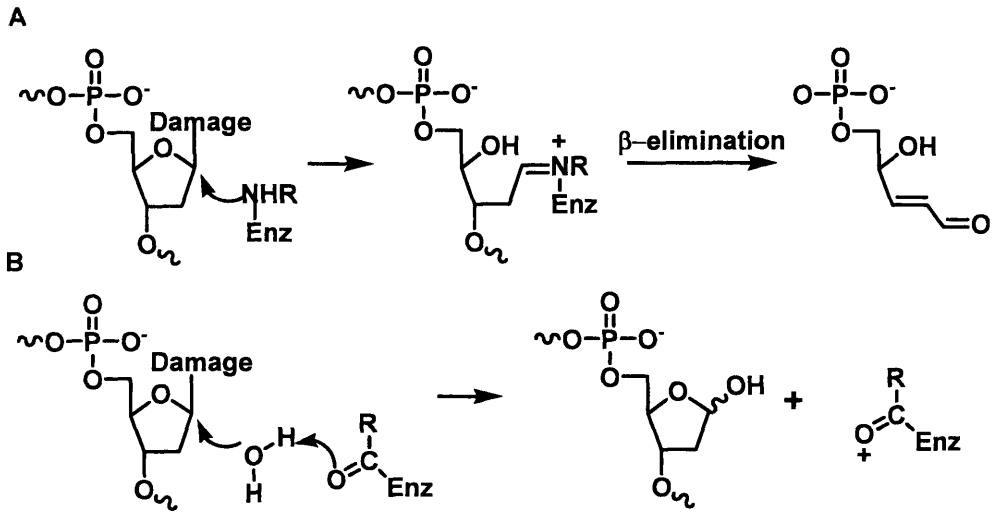

Figure 1-32. Catalytic mechanisms of (A) bifunctional and (B) monofunctional glycosylases.

Because of the importance of BER, extensive studies have been conducted to investigate the diversity of DNA glycosylases in prokaryotic and eukaryotic cells. Some of the identified glycosylases for *E. coli* and human cells and their substrates are summarized in the following tables:

Table I-1. E. *coli* DNA Glycosylases for Oxidative Base Damage

Glycosylase	Major substrates	AP Lyase	Reference
Fpg glycosylase	Fapy, 8oxoG, hoC, hoU	β, δ	[159]
Endo III	Tg, hoU, hoC, hoR, Ug	β	[49, 160]
Endo VIII	Tg, hoC, hoU	β	[161, 162]
UDG	U	None	[163]
AlkA	MeA, MeG, HX, εG, εA, fU	None	[164, 165]
MUG	εC, 1,N^2-εG, U in G:U pair	None	[166, 167]
MutY	A in A:G, A:C A:8oxoG	None	[168, 169]

Fapy: 2,6-diamino-4-hydroxy-5-formamidopyrimidine; 8oxoG: 7,8-dihydro-8-oxo-2'-deoxyguanosine; 5-hydroxy-2'-deoxycitidine; hoU: 5-hydroxyuracil; hoC: 5-hydroxy-2'-deoxycytidine; Tg: thymine glycol; dHT: 5,6-dihydrothymine; Ug: uracil glycol; U: uracil; fU: 5-formyluracil; hmU: 5-hydroxymethyluracil. hoR: 5-hydroxy-2'deoxyridine; HX: hypoxanthine; MeA: 3-methyladenine; MeG 7-methylguanine

Table I-2. Human DNA Glycosylases for Oxidative Base Damage

Glycosylase	Major substrates	AP Lyase	Reference
hOGG1	Fapy, 8oxoG	β	[170, 171]
hNTH	Tg, , hoU, hoC, urea, FapyG	β	[172, 173]
hNEIL	Tg, hoU, hoC, urea, FapyG, FapyA	β, δ	[174, 175]
hSMUG	U, hoU, hmU, fU	None	[176, 177]
ANPG	MeA, MeG, HX, εG, εA, fU	None	[164, 178]

Several alternatives to BER repair pathways have also been identified. Helix distorting, bulky lesions such as cis,syn-cycolbutane thymine dimer, formed by UV irradiation of DNA, are commonly repaired through nucleotide excision repair instead BER [179, 180]. NER was shown to repair non-bulky lesions such as 8-oxoG and thymine glycol. However it is generally less efficient than BER in removing these lesions and is believed to be a backup repair pathway for these lesions instead of a major one [181]. DSBs can be repaired by two distinct and complementary mechanisms - homologous recombination (HR) and non-homologous end-joining (NHEJ), both of which have been extensively review elsewhere [99, 182, 183].

Since failure to repair certain DNA lesions can induce cell death and can be detrimental to the biological function of a whole organism, many of the lesions can be removed by more than one enzymes or pathways. This built-in redundancy avoids the problem that the inhibition or elimination of one repair activity makes a particular lesion unrepairable.

1.10. Summary

A growing body of evidence from human and animal studies supports the role of DNA damage in diseases, including cancer. Lipids appear to be a main target for ROS/RNS and the peroxidation of PUFA yields a variety of intermediate electrophiles that can react with DNA bases to form exocyclic adducts. So lipid peroxidation is believed to be a major source of endogenous DNA damage in humans that may contribute significantly to cancer and other genetic diseases linked to oxidative stress and inflammation. Another source of electrophilic intermediates is from the oxidation of the deoxyribose moiety in DNA. All seven hydrogen atoms of deoxyribose have been found to be abstracted by oxidizing agents and oxidation at each position generates a unique spectrum of deoxyribose oxidation products, including many reactive electrophiles. Evidence has shown that both MDA, which is mainly a lipid peroxidation product and base propenal, which is a product of DNA deoxyribose oxidation, can react with DNA to form exocyclic nucleobase adduct M_1dG, though the latter has significantly greater efficiency. In the following chapters, the thesis first discusses methods developed to quantify DNA strand breaks and abasic sites that serve as an index for total DNA deoxyribose oxidation events. These methods have also been extended to quantify total DNA sugar and base damages, as well. To address the relative contribution of MDA and base propenal in M_1dG formation, the thesis then discusses quantification of deoxyribose C4'-oxidation products: 3'-phosphoglycolate, 4′-keto-1′-aldehyde and base propenals (or malondialdehyde). Finally, the thesis applies these quantification methods to investigate relative role of base propenals and malondialdehyde in the formation of M_1dG *in vitro*, cultured cells and in tissues from a mouse model of inflammation. These results reveal that base propenals from deoxyribose C4'-oxidation is the major source of M_1dG, while lipid peroxidation is likely to be the major sources of etheno adducts in DNA.

References

1. Cline, S.D., et al., *Malondialdehyde adducts in DNA arrest transcription by T7 RNA polymerase and mammalian RNA polymerase II.* Proceedings of the National Academy of Sciences of the United States of America, 2004. **101**(19): p. 7275-7280.
2. Klaunig, J.E. and L.M. Kamendulis, *The role of oxidative stress in carcinogenesis.* Annu Rev Pharmacol Toxicol, 2004. **44**: p. 239-67.
3. Yermilov, V., et al., *Effects of carbon dioxide/bicarbonate on induction of DNA single-strand breaks and formation of 8-nitroguanine, 8-oxoguanine and base-propenal mediated by peroxynitrite.* Febs Letters, 1996. **399**(1-2): p. 67-70.
4. Balkwill, F. and A. Mantovani, *Inflammation and cancer: back to Virchow?* Lancet, 2001. **357**(9255): p. 539-45.
5. Shacter, E. and S.A. Weitzman, *Chronic inflammation and cancer.* Oncology (Huntingt), 2002. **16**(2): p. 217-26, 229; discussion 230-2.
6. Chung, F.-L., H.-J.C. Chen, and R.G. Nath, *Lipid peroxidation as a potential endogenous source for the formation of exocyclic DNA adducts.* Carcinogenesis, 1996. **17**(10): p. 2105-2111.
7. Povirk, L.F. and I.H. Goldberg, *Endonuclease-resistant apyrimidinic sites formed by neocarzinostatin at cytosine residues in DNA: evidence for a possible role in mutagenesis.* Proc Natl Acad Sci U S A, 1985. **82**(10): p. 3182-6.
8. Weinfeld, M., et al., *Response of base excision repair enzymes to complex DNA lesions.* Radiat Res, 2001. **156**(5 Pt 2): p. 584-9.
9. Gingipalli, L. and P.C. Dedon, *Reaction of cis- and trans-2-butene-1,4-dial with 2 '-deoxycytidine to form stable oxadiazabicyclooctaimine adducts.* Journal of the American Chemical Society, 2001. **123**(11): p. 2664-2665.
10. Byrns, M.C., D.P. Predecki, and L.A. Peterson, *Characterization of nucleoside adducts of cis-2-butene-1,4-dial, a reactive metabolite of furan.* Chemical Research in Toxicology, 2002. **15**(3): p. 373-379.
11. Awada, M. and P.C. Dedon, *Formation of the 1,N2-glyoxal adduct of deoxyguanosine by phosphoglycolaldehyde, a product of 3'-deoxyribose oxidation in DNA.* Chem Res Toxicol, 2001. **14**(9): p. 1247-53.
12. Dedon, P.C., et al., *Indirect mutagenesis by oxidative DNA damage: formation of the pyrimidopurinone adduct of deoxyguanosine by base propenal.* Proc Natl Acad Sci U S A, 1998. **95**(19): p. 11113-6.
13. Plastaras, J.P., et al., *Reactivity and mutagenicity of endogenous DNA oxopropenylating agents: base propenals, malondialdehyde, and N(epsilon)-oxopropenyllysine.* Chem Res Toxicol, 2000. **13**(12): p. 1235-42.
14. Klaunig, J.E., et al., *The role of oxidative stress in chemical carcinogenesis.* Environmental Health Perspectives, 1998. **106**: p. 289-295.

15. Parke, D.V., *The Cytochromes P450 and Mechanisms of Chemical Carcinogenesis.* Environmental Health Perspectives, 1994. **102**(10): p. 852-853.

16. Day, B.W., et al., *Molecular dosimetry of polycyclic aromatic hydrocarbon epoxides and diol epoxides via hemoglobin adducts.* Cancer Res, 1990. **50**(15): p. 4611-8.

17. Smela, M.E., et al., *The chemistry and biology of aflatoxin B(1): from mutational spectrometry to carcinogenesis.* Carcinogenesis, 2001. **22**(4): p. 535-45.

18. Sies, H., *Oxidative Stress - from Basic Research to Clinical-Application.* American Journal of Medicine, 1991. **91**: p. S31-S38.

19. Imlay, J.A., *Pathways of oxidative damage.* Annu Rev Microbiol, 2003. **57**: p. 395-418.

20. Peterhans, E., *Oxidants and antioxidants in viral diseases: Disease mechanisms and metabolic regulation.* Journal of Nutrition, 1997. **127**: p. S962-S965.

21. Tyrrell, R.M., *Role for singlet oxygen in biological effects of ultraviolet A radiation.* Singlet Oxygen, Uv-a, and Ozone, 2000. **319**: p. 290-296.

22. Klotz, L.O., K. Briviba, and H. Sies, *Singlet oxygen mediates the activation of JNK by UVA radiation in human skin fibroblasts.* Febs Letters, 1997. **408**(3): p. 289-291.

23. Ravanat, J.L., et al., *Singlet oxygen induces oxidation of cellular DNA.* Journal of Biological Chemistry, 2000. **275**(51): p. 40601-40604.

24. Nishizawa, M., et al., *Presence of peroxyradicals in cigarette smoke and the scavenging effect of shikonin, a naphthoquinone pigment.* Chem Pharm Bull (Tokyo), 2005. **53**(7): p. 796-9.

25. Mattia, C.J., J.D. Adams, Jr., and S.C. Bondy, *Free radical induction in the brain and liver by products of toluene catabolism.* Biochem Pharmacol, 1993. **46**(1): p. 103-10.

26. Bredt, D.S., *Endogenous nitric oxide synthesis: Biological functions and pathophysiology.* Free Radical Research, 1999. **31**(6): p. 577-596.

27. Alderton, W.K., C.E. Cooper, and R.G. Knowles, *Nitric oxide synthases: structure, function and inhibition.* Biochemical Journal, 2001. **357**: p. 593-615.

28. Samouilov, A., P. Kuppusamy, and J.L. Zweier, *Evaluation of the magnitude and rate of nitric oxide production from nitrite in biological systems.* Archives of Biochemistry and Biophysics, 1998. **357**(1): p. 1-7.

29. Espey, M.G., et al., *Distinction between nitrosating mechanisms within human cells and aqueous solution.* J Biol Chem, 2001. **276**(32): p. 30085-91.

30. Lewis, R.S., et al., *Kinetic analysis of the fate of nitric oxide synthesized by macrophages in vitro.* J Biol Chem, 1995. **270**(49): p. 29350-5.

31. Kissner, R., et al., *Formation and properties of peroxynitrite as studied by laser flash photolysis, high-pressure stopped-flow technique, and pulse radiolysis.* Chem Res Toxicol, 1997. **10**(11): p. 1285-92.

32. Kissner, R., et al., *Formation and properties of peroxynitrite as studied by laser flash photolysis, high-pressure stopped-flow technique, and pulse radiolysis volume 10, number 11, november 1997, pp 1285-1292.* Chem Res Toxicol, 1998. **11**(5): p. 557.

33. Miles, A.M., et al., *Modulation of superoxide-dependent oxidation and hydroxylation reactions by nitric oxide.* J Biol Chem, 1996. **271**(1): p. 40-7.

34. Goldstein, S., J. Lind, and G. Merenyi, *Chemistry of peroxynitrites as compared to peroxynitrates.* Chemical Reviews, 2005. **105**(6): p. 2457-2470.

35. Alfassi, Z.B., et al., *On the reactions of CO3 center dot- radicals with NOx radicals.* Radiation Physics and Chemistry, 1999. **56**(4): p. 475-482.

36. Jaiswal, M., et al., *Inflammatory cytokines induce DNA damage and inhibit DNA repair in cholangiocarcinoma cells by a nitric oxide-dependent mechanism.* Cancer Research, 2000. **60**(1): p. 184-190.

37. Spickett, C.M. and G. Dever, *Studies of phospholipid oxidation by electrospray mass spectrometry: From analysis in cells to biological effects.* Biofactors, 2005. **24**(1-4): p. 17-31.

38. Jiang, Q., B.C. Blount, and B.N. Ames, *5-chlorouracil, a marker of DNA damage from hypochlorous acid during inflammation - A gas chromatography-mass spectrometry assay.* Journal of Biological Chemistry, 2003. **278**(35): p. 32834-32840.

39. Kulcharyk, P.A. and J.W. Heinecke, *Hypochlorous acid produced by the myeloperoxidase system of human phagocytes induces covalent cross-links between DNA and protein.* Biochemistry, 2001. **40**(12): p. 3648-3656.

40. Sugiyama, S., et al., *Hypochlorous acid, a macrophage product, induces endothelial apoptosis and tissue factor expression - Involvement of myeloperoxidase-mediated oxidant in plaque erosion and thrombogenesis.* Arteriosclerosis Thrombosis and Vascular Biology, 2004. **24**(7): p. 1309-1314.

41. Barja, G., *Free radicals and aging.* Trends in Neurosciences, 2004. **27**(10): p. 595-600.

42. Evans, M.D., M. Dizdaroglu, and M.S. Cooke, *Oxidative DNA damage and disease: induction, repair and significance.* Mutation Research-Reviews in Mutation Research, 2004. **567**(1): p. 1-61.

43. Cathcart, R., et al., *Thymine Glycol and Thymidine Glycol in Human and Rat Urine - a Possible Assay for Oxidative DNA Damage.* Proceedings of the National Academy of Sciences of the United States of America-Biological Sciences, 1984. **81**(18): p. 5633-5637.

44. Ames, B.N., L.S. Gold, and W.C. Willett, *The Causes and Prevention of Cancer.* Proceedings of the National Academy of Sciences of the United States of America, 1995. **92**(12): p. 5258-5265.

45. Cadet, J., et al., *Hydroxyl radicals and DNA base damage.* Mutation Research-Fundamental and Molecular Mechanisms of Mutagenesis, 1999. **424**(1-2): p. 9-21.

46. Breen, A.P. and J.A. Murphy, *Reactions of Oxyl Radicals with DNA.* Free Radical Biology and Medicine, 1995. **18**(6): p. 1033-1077.

47. Candeias, L.P. and S. Steenken, *Electron-Transfer in Di(Deoxy)Nucleoside Phosphates in Aqueous-Solution - Rapid Migration of Oxidative Damage (Via Adenine) to Guanine.* Journal of the American Chemical Society, 1993. **115**(6): p. 2437-2440.

48. Wagner, J.R., et al., *Hydroxyl-radical-induced decomposition of 2 '-deoxycytidine in aerated aqueous solutions.* Journal of the American Chemical Society, 1999. **121**(17): p. 4101-4110.

49. Dizdaroglu, M., J. Laval, and S. Boiteux, *Substrate specificity of the Escherichia coli endonuclease III: excision of thymine- and cytosine-derived lesions in DNA produced by radiation-generated free radicals.* Biochemistry, 1993. **32**(45): p. 12105-11.

50. Wagner, J.R., et al., *Thymidine Hydroperoxides - Structural Assignment, Conformational Features, and Thermal-Decomposition in Water.* Journal of the American Chemical Society, 1994. **116**(6): p. 2235-2242.

51. Kennedy, L.J., et al., *Quantitation of 8-oxoguanine and strand breaks produced by four oxidizing agents.* Chem Res Toxicol, 1997. **10**(4): p. 386-92.

52. Burney, S., et al., *DNA damage in deoxynucleosides and oligonucleotides treated with peroxynitrite.* Chem Res Toxicol, 1999. **12**(6): p. 513-20.

53. Yu, H., et al., *Quantitation of four Guanine oxidation products from reaction of DNA with varying doses of peroxynitrite.* Chem Res Toxicol, 2005. **18**(12): p. 1849-57.

54. Tretyakova, N.Y., et al., *Peroxynitrite-induced DNA damage in the supF gene: correlation with the mutational spectrum.* Mutat Res, 2000. **447**(2): p. 287-303.

55. Lee, J.M., et al., *Peroxynitrite reacts with 8-nitropurines to yield 8-oxopurines.* Chem Res Toxicol, 2002. **15**(1): p. 7-14.

56. Lucas, L.T., D. Gatehouse, and D.E.G. Shuker, *Efficient nitroso group transfer from N-nitrosoindoles to nucleotides and 2 '-deoxyguanosine at physiological pH - A new pathway for N-nitrosocompounds to exert genotoxicity.* Journal of Biological Chemistry, 1999. **274**(26): p. 18319-18326.

57. Lucas, L.T., D. Gatehouse, and D.E.G. Shuker, *Modification of nucleotides and 2 '-deoxyguanosine by nitrosated indoles results in deamination, depurination and the formation of a novel product oxanine via a transnitrosation mechanism.* British Journal of Cancer, 1999. **81**(4): p. 578-578.

58. Bamatraf, M.M.M., P. O'Neill, and B.S.M. Rao, *OH radical-induced charge migration in oligodeoxynucleotides.* Journal of Physical Chemistry B, 2000. **104**(3): p. 636-642.

59. Meggers, E., M.E. Michel-Beyerle, and B. Giese, *Sequence dependent long range hole transport in DNA.* Journal of the American Chemical Society, 1998. **120**(49): p. 12950-12955.

60. Pratviel, G., J. Bernadou, and B. Meunier, *Carbon-Hydrogen Bonds of DNA Sugar Units as Targets for Chemical Nucleases and Drugs.* Angewandte Chemie-International Edition in English, 1995. **34**(7): p. 746-769.

61. Pogozelski, W.K. and T.D. Tullius, *Oxidative Strand Scission of Nucleic Acids: Routes Initiated by Hydrogen Abstraction from the Sugar Moiety.* Chem Rev, 1998. **98**(3): p. 1089-1108.

62. Balasubramanian, B., W.K. Pogozelski, and T.D. Tullius, *DNA strand breaking by the hydroxyl radical is governed by the accessible surface areas of the hydrogen atoms of the DNA backbone.* Proc Natl Acad Sci U S A, 1998. **95**(17): p. 9738-43.

63. Aydogan, B., et al., *Site-specific OH attack to the sugar moiety of DNA: a comparison of experimental data and computational simulation.* Radiat Res, 2002. **157**(1): p. 38-44.

64. Miaskiewicz, K. and R. Osman, *Theoretical-Study on the Deoxyribose Radicals Formed by Hydrogen Abstraction.* Journal of the American Chemical Society, 1994. **116**(1): p. 232-238.

65. Johnson, G.R.A. and N.B. Nazhat, *Kinetics and Mechanism of the Reaction of the Bis(1,10-Phenanthroline)Copper(I) Ion with Hydrogen-Peroxide in Aqueous-Solution.* Journal of the American Chemical Society, 1987. **109**(7): p. 1990-1994.

66. Yamamoto, K. and S. Kawanishi, *Hydroxyl free radical is not the main active species in site-specific DNA damage induced by copper (II) ion and hydrogen peroxide.* J Biol Chem, 1989. **264**(26): p. 15435-40.

67. Goyne, T.E. and D.S. Sigman, *Nuclease Activity of 1,10-Phenanthroline Copper-Ion - Chemistry of Deoxyribose Oxidation.* Journal of the American Chemical Society, 1987. **109**(9): p. 2846-2848.

68. Kappen, L.S. and I.H. Goldberg, *Neocarzinostatin acts as a sensitive probe of DNA microheterogeneity: switching of chemistry from C-1' to C-4' by a G.T mismatch 5' to the site of DNA damage.* Proc Natl Acad Sci U S A, 1992. **89**(15): p. 6706-10.

69. Kappen, L.S., et al., *Isotope Effects on the Sequence-Specific Cleavage of Dc in D(Agc) Sequences by Neocarzinostatin - Elucidation of Chemistry of Minor Lesions.* Journal of the American Chemical Society, 1990. **112**(7): p. 2797-2798.

70. Dizdaroglu, M., et al., *Radiation-Chemistry of Carbohydrates .10. Gamma-Radiolysis of Crystalline D-Glucose and D-Fructose.* Zeitschrift Fur Naturforschung Section B-a Journal of Chemical Sciences, 1977. **32**(2): p. 213-224.

71. Sugiyama, H., et al., *Photoinduced Deoxyribose-C2' Oxidation in DNA - Alkali-Dependent Cleavage of Erythrose-Containing Sites Via a Retroaldol Reaction.* Journal of the American Chemical Society, 1993. **115**(11): p. 4443-4448.

72. Sugiyama, H., K. Fujimoto, and I. Saito, *Evidence for intrastrand C2' hydrogen abstraction in photoirradiation of 5-halouracil-containing oligonucleotides by using stereospecifically C2'-deuterated deoxyadenosine.* Tetrahedron Letters, 1996. **37**(11): p. 1805-1808.

73. Sitlani, A., et al., *DNA Photocleavage by Phenanthrenequinone Diimine Complexes of Rhodium(Iii) - Shape-Selective Recognition and Reaction.* Journal of the American Chemical Society, 1992. **114**(7): p. 2303-2312.

74. Burger, R.M., *Cleavage of Nucleic Acids by Bleomycin.* Chem Rev, 1998. **98**(3): p. 1153-1170.

75. Wu, W., et al., *Bleomycins: Structure and function.* Abstracts of Papers of the American Chemical Society, 1996. **212**: p. 111-ORGN.

76. Huang, L.R., Y. Xie, and J.W. Lown, *Bleomycin antibiotics and their role in cancer chemotherapy.* Expert Opinion on Therapeutic Patents, 1996. **6**(9): p. 893-899.

77. Wu, Y.D., et al., *Is Intramolecular Hydrogen-Bonding Important for Bleomycin Reactivity - a Molecular Mechanics Study.* Inorganic Chemistry, 1992. **31**(5): p. 718-&.

78. Wu, W., et al., *Interaction of Co-Center-Dot-Bleomycin a2 (Green) with D(Ccaggcctgg)(2) - Evidence for Intercalation Using 2D Nmr.* Journal of the American Chemical Society, 1994. **116**(23): p. 10843-10844.

79. Wu, J.C., J. Stubbe, and J.W. Kozarich, *Mechanism of Bleomycin - Evidence for 4'-Ketone Formation in Poly(Da-Du) Associated Exclusively with Free Base Release.* Biochemistry, 1985. **24**(26): p. 7569-7573.

80. Rashid, R., et al., *Bleomycin versus OH-radical-induced malonaldehydic-product formation in DNA.* Int J Radiat Biol, 1999. **75**(1): p. 101-9.

81. Henner, W.D., et al., *Gamma-Ray Induced Deoxyribonucleic-Acid Strand Breaks - 3' Glycolate Termini.* Journal of Biological Chemistry, 1983. **258**(2): p. 711-713.

82. Lopez-Larraza, D.M., K. Moore, and P.C. Dedon, *Thiols alter the partitioning of calicheamicin-induced deoxyribose 4 '-oxidation reactions in the absence of DNA radical repair.* Chemical Research in Toxicology, 2001. **14**(5): p. 528-535.

83. Chin, D.H. and I.H. Goldberg, *Sources of Hydrogen Abstraction by Activated Neocarzinostatin Chromophore.* Biochemistry, 1993. **32**(14): p. 3611-3616.

84. Kappen, L.S. and I.H. Goldberg, *Deoxyribonucleic-Acid Damage by Neocarzinostatin Chromophore - Strand Breaks Generated by Selective Oxidation of C-5' of Deoxyribose.* Biochemistry, 1983. **22**(21): p. 4872-4878.

85. Chin, D.H., L.S. Kappen, and I.H. Goldberg, *3'-Formyl Phosphate-Ended DNA - High-Energy Intermediate in Antibiotic-Induced DNA Sugar Damage.* Proceedings of the National Academy of Sciences of the United States of America, 1987. **84**(20): p. 7070-7074.

86. Kappen, L.S., et al., *Neocarzinostatin-Induced Hydrogen-Atom Abstraction from C-4' and C-5' of the T-Residue at a D(Gt) Step in Oligonucleotides - Shuttling between Deoxyribose Attack Sites Based on Isotope Selection Effects.* Biochemistry, 1991. **30**(8): p. 2034-2042.

87. Saito, I., et al., *A Novel Ribose C-4' Hydroxylation Pathway in Neocarzinostatin-Mediated Degradation of Oligonucleotides.* Journal of the American Chemical Society, 1989. **111**(21): p. 8302-8303.

88. Frank, B.L., et al., *Isotope Effects on the Sequence-Specific Cleavage of DNA by Neocarzinostatin - Kinetic Partitioning between 4'-Hydrogen and 5'-Hydrogen Abstraction at Unique Thymidine Sites.* Journal of the American Chemical Society, 1991. **113**(6): p. 2271-2275.

89. Kappen, L.S. and I.H. Goldberg, *Activation and inactivation of neocarzinostatin-induced cleavage of DNA.* Nucleic Acids Res, 1978. **5**(8): p. 2959-67.

90. Zein, N., et al., *Calicheamicin-Gamma-1-I - an Antitumor Antibiotic That Cleaves Double-Stranded DNA Site Specifically.* Science, 1988. **240**(4856): p. 1198-1201.

91. Epstein, J.L., et al., *Interplay of hydrogen abstraction and radical repair in the generation of single- and double-strand DNA damage by the esperamicins.* Journal of the American Chemical Society, 1997. **119**(29): p. 6731-6738.

92. Isildar, M., et al., *Gamma-Radiolysis of DNA in Oxygenated Aqueous-Solutions - Alterations at the Sugar Moiety.* International Journal of Radiation Biology, 1981. **40**(4): p. 347-354.

93. Kappen, L.S., I.H. Goldberg, and J.M. Liesch, *Identification of Thymidine-5'-Aldehyde at DNA Strand Breaks Induced by Neocarzinostatin Chromophore.* Proceedings of the National Academy of Sciences of the United States of America-Biological Sciences, 1982. **79**(3): p. 744-748.

94. Chen, B.Z., et al., *5 '-(2-phosphoryl-1,4-dioxobutane) as a product of 5 '-oxidation of deoxyribose in DNA: Elimination as trans-1,4-dioxo-2-butene and approaches to analysis.* Chemical Research in Toxicology, 2004. **17**(11): p. 1406-1413.

95. Pratviel, G., et al., *Furfural as a Marker of DNA Cleavage by Hydroxylation at the 5' Carbon of Deoxyribose.* Angewandte Chemie-International Edition in English, 1991. **30**(6): p. 702-704.

96. Dedon, P.C. and I.H. Goldberg, *Free-radical mechanisms involved in the formation of sequence-dependent bistranded DNA lesions by the antitumor antibiotics bleomycin, neocarzinostatin, and calicheamicin.* Chem Res Toxicol, 1992. **5**(3): p. 311-32.

97. Jackson, S.P., *Sensing and repairing DNA double-strand breaks - Commentary.* Carcinogenesis, 2002. **23**(5): p. 687-696.

98. Rich, T., R.L. Allen, and A.H. Wyllie, *Defying death after DNA damage.* Nature, 2000. **407**(6805): p. 777-783.

99. Khanna, K.K. and S.P. Jackson, *DNA double-strand breaks: signaling, repair and the cancer connection.* Nature Genetics, 2001. **27**(3): p. 247-254.

100. Richardson, C. and M. Jasin, *Frequent chromosomal translocations induced by DNA double-strand breaks.* Nature, 2000. **405**(6787): p. 697-700.

101. Box, H.C., J.B. Dawidzik, and E.E. Budzinski, *Free radical-induced double lesions in DNA.* Free Radical Biology and Medicine, 2001. **31**(7): p. 856-868.

102. Cadet, J. and M. Berger, *Radiation-Induced Decomposition of the Purine-Bases within DNA and Related Model Compounds.* International Journal of Radiation Biology, 1985. **47**(2): p. 127-143.

103. Dizdaroglu, M., P. Jaruga, and H. Rodriguez, *Identification and quantification of 8,5 '-cycle-2 '-deoxyadenosine in DNA by liquid chromatography/mass spectrometry.* Free Radical Biology and Medicine, 2001. **30**(7): p. 774-784.

104. Jaruga, P., et al., *Mass spectrometric assays for the tandem lesion 8,5 '-cyclo-2 '-deoxyguanosine in mammalian DNA.* Biochemistry, 2002. **41**(11): p. 3703-3711.

105. Kroeger, K.M., et al., *Cross-linking of 2-deoxyribonolactone and its beta-elimination product by base excision repair enzymes.* Biochemistry, 2003. **42**(8): p. 2449-2455.

106. Hashimoto, M., et al., *The 2-deoxyribonolactone lesion produced in DNA by neocarzinostatin and other damaging agents forms cross-links with the base-excision repair enzyme endonuclease III.* Journal of the American Chemical Society, 2001. **123**(13): p. 3161-3162.

107. DeMott, M.S., et al., *Covalent trapping of human DNA polymerase beta by the oxidative DNA lesion 2-deoxyribonolactone.* J Biol Chem, 2002. **277**(10): p. 7637-40.

108. Zheng, Y. and T.L. Sheppard, *Half-life and DNA strand scission products of 2-deoxyribonolactone oxidative DNA damage lesions.* Chem Res Toxicol, 2004. **17**(2): p. 197-207.

109. Bohnert, T., L. Gingipalli, and P.C. Dedon, *Reaction of 2 '-deoxyribonucleosides with cis- and trans-1,4-dioxo-2-butene.* Biochemical and Biophysical Research Communications, 2004. **323**(3): p. 838-844.

110. Johnson, A.W. and B. Demple, *Yeast DNA diesterase for 3'-fragments of deoxyribose: purification and physical properties of a repair enzyme for oxidative DNA damage.* J Biol Chem, 1988. **263**(34): p. 18009-16.

111. Izumi, T., et al., *Requirement for human AP endonuclease 1 for repair of 3'-blocking damage at DNA single-strand breaks induced by reactive oxygen species.* Carcinogenesis, 2000. **21**(7): p. 1329-34.

112. Johnson, A.W. and B. Demple, *Yeast DNA 3'-repair diesterase is the major cellular apurinic/apyrimidinic endonuclease: substrate specificity and kinetics.* J Biol Chem, 1988. **263**(34): p. 18017-22.

113. Xu, Y.J., E.Y. Kim, and B. Demple, *Excision of C-4 '-oxidized deoxyribose lesions from double-stranded DNA by human Apurinic/Apyrimidinic endonuclease (Ape1 protein) and DNA polymerase beta.* Journal of Biological Chemistry, 1998. **273**(44): p. 28837-28844.

114. Greenberg, M.M., et al., *In vitro effects of a C4 '-oxidized abasic site on DNA polymerases.* Biochemistry, 2004. **43**(9): p. 2656-2663.

115. Greenberg, M.M., et al., *In vitro replication and repair of DNA containing a C2 '-oxidized abasic site.* Biochemistry, 2004. **43**(48): p. 15217-15222.

116. Dix, T.A. and J. Aikens, *Mechanisms and biological relevance of lipid peroxidation initiation.* Chem Res Toxicol, 1993. **6**(1): p. 2-18.

117. Pryor, W.A., *Oxy-radicals and related species: their formation, lifetimes, and reactions.* Annu Rev Physiol, 1986. **48**: p. 657-67.

118. Waldeck, A.R. and R. Stocker, *Radical-initiated lipid peroxidation in low density lipoproteins: insights obtained from kinetic modeling.* Chem Res Toxicol, 1996. **9**(6): p. 954-64.

119. Barclay, L.R.C., et al., *Autoxidation of Micelles and Model Membranes - Quantitative Kinetic Measurements Can Be Made by Using Either Water-Soluble or Lipid-Soluble*

Initiators with Water-Soluble or Lipid-Soluble Chain-Breaking Antioxidants. Journal of the American Chemical Society, 1984. **106**(8): p. 2479-2481.

120. Marnett, L.J., *Lipid peroxidation-DNA damage by malondialdehyde.* Mutat Res, 1999. **424**(1-2): p. 83-95.

121. Porter, N.A., S.E. Caldwell, and K.A. Mills, *Mechanisms of free radical oxidation of unsaturated lipids.* Lipids, 1995. **30**(4): p. 277-90.

122. Meagher, E.A. and G.A. Fitzgerald, *Indices of lipid peroxidation in vivo: Strengths and limitations.* Free Radical Biology and Medicine, 2000. **28**(12): p. 1745-1750.

123. Kaneko, T., et al., *Lethal Effects of a Linoleic-Acid Hydroperoxide and Its Autoxidation Products, Unsaturated Aliphatic-Aldehydes, on Human-Diploid Fibroblasts.* Chemico-Biological Interactions, 1987. **63**(2): p. 127-137.

124. Esterbauer, H., H. Zollner, and R.J. Schaur, *Hydroxyalkenals - Cyto-Toxic Products of Lipid-Peroxidation.* Isi Atlas of Science-Biochemistry, 1988. **1**(4): p. 311-317.

125. Ichihashi, K., et al., *Endogenous formation of protein adducts with carcinogenic aldehydes - Implications for oxidative stress.* Journal of Biological Chemistry, 2001. **276**(26): p. 23903-23913.

126. Uchida, K., et al., *Acrolein is a product of lipid peroxidation reaction - Formation of free acrolein and its conjugate with lysine residues in oxidized low density lipoproteins.* Journal of Biological Chemistry, 1998. **273**(26): p. 16058-16066.

127. Uchida, K., et al., *Protein-bound acrolein: Potential markers for oxidative stress.* Proceedings of the National Academy of Sciences of the United States of America, 1998. **95**(9): p. 4882-4887.

128. Esterbauer, H., R.J. Schaur, and H. Zollner, *Chemistry and Biochemistry of 4-Hydroxynonenal, Malonaldehyde and Related Aldehydes.* Free Radical Biology and Medicine, 1991. **11**(1): p. 81-128.

129. Basu, A.K., P. Weller, and L.J. Marnett, *Modification of Purine Nucleosides by Malondialdehyde and Beta-Substituted Acroleins.* Proceedings of the American Association for Cancer Research, 1984. **25**(Mar): p. 88-88.

130. Marnett, L.J., et al., *Reaction of Malondialdehyde with Guanine Nucleosides - Formation of Adducts Containing Oxadiazabicyclononene Residues in the Base-Pairing Region.* Journal of the American Chemical Society, 1986. **108**(6): p. 1348-1350.

131. Seto, H., et al., *Reaction of Malonaldehyde with Nucleic-Acid .1. Formation of Fluorescent "Pyrimido[1,2-Alpha]Purin-10(3H)-One Nucleosides.* Bulletin of the Chemical Society of Japan, 1983. **56**(6): p. 1799-1802.

132. Stone, K., M.B. Ksebati, and L.J. Marnett, *Investigation of the Adducts Formed by Reaction of Malondialdehyde with Adenosine.* Chemical Research in Toxicology, 1990. **3**(1): p. 33-38.

133. Stone, K., A. Uzieblo, and L.J. Marnett, *Studies of the Reaction of Malondialdehyde with Cytosine Nucleosides.* Chemical Research in Toxicology, 1990. **3**(5): p. 467-472.

134. Esterbauer, H., H. Zollner, and N. Scholz, *Reaction of Glutathione with Conjugated Carbonyls.* Zeitschrift Fur Naturforschung C-a Journal of Biosciences, 1975. **30**(7-8): p. 466-473.

135. Foiles, P.G., S.A. Akerkar, and F.L. Chung, *Application of an Immunoassay for Cyclic Acrolein Deoxyguanosine Adducts to Assess Their Formation in DNA of Salmonella-Typhimurium under Conditions of Mutation-Induction by Acrolein.* Carcinogenesis, 1989. **10**(1): p. 87-90.

136. Rindgen, D., et al., *Covalent modifications to 2 '-deoxyguanosine by 4-oxo-2-nonenal, a novel product of lipid peroxidation.* Chemical Research in Toxicology, 1999. **12**(12): p. 1195-1204.

137. Kawai, Y., et al., *Immunohistochemical detection of a substituted 1,N-2-ethenodeoxyguanosine adduct by omega-6 polyunsaturated fatty acid hydroperoxides in the liver of rats fed a choline-deficient, L-amino acid-defined diet.* Carcinogenesis, 2002. **23**(3): p. 485-489.

138. Kawai, Y., K. Uchida, and T. Osawa, *2 '-deoxycytidine in free nucleosides and double-stranded DNA, as the major target of lipid peroxidation products.* Free Radical Biology and Medicine, 2004. **36**(5): p. 529-541.

139. Jian, W.Y., et al., *Unexpected formation of etheno-2 '-deoxyguano sine adducts from 5(S)-hydroperoxyeicosatetraenoic acid: Evidence for a bis-hydroperoxide intermediate.* Chemical Research in Toxicology, 2005. **18**(3): p. 599-610.

140. Yocum, A.K., et al., *Novel lipid hydroperoxide-derived hemoglobin histidine adducts as biomarkers of oxidative stress.* Journal of Mass Spectrometry, 2005. **40**(6): p. 754-764.

141. Nappez, C., S. Battu, and J.L. Beneytout, *trans,trans-2,4-decadienal: Cytotoxicity and effect on glutathione level in human erythroleukemia (HEL) cells.* Cancer Letters, 1996. **99**(1): p. 115-119.

142. Carvalho, V.M., et al., *Novel 1,N(6)-etheno-2'-deoxyadenosine adducts from lipid peroxidation products.* Chem Res Toxicol, 2000. **13**(5): p. 397-405.

143. Schoneich, C., *Methionine oxidation by reactive oxygen species: reaction mechanisms and relevance to Alzheimer's disease.* Biochim Biophys Acta, 2005. **1703**(2): p. 111-9.

144. Droge, W., *Oxidative stress and aging.* Adv Exp Med Biol, 2003. **543**: p. 191-200.

145. Stadtman, E.R. and R.L. Levine, *Free radical-mediated oxidation of free amino acids and amino acid residues in proteins.* Amino Acids, 2003. **25**(3-4): p. 207-18.

146. Linton, S., M.J. Davies, and R.T. Dean, *Protein oxidation and ageing.* Exp Gerontol, 2001. **36**(9): p. 1503-18.

147. Stadtman, E.R. and B.S. Berlett, *Reactive oxygen-mediated protein oxidation in aging and disease.* Chemical Research in Toxicology, 1997. **10**(5): p. 485-494.

148. Dean, R.T., et al., *Biochemistry and pathology of radical-mediated protein oxidation.* Biochemical Journal, 1997. **324**: p. 1-18.

149. Giasson, B.I., et al., *Oxidative damage linked to neurodegeneration by selective alpha-synuclein nitration in synucleinopathy lesions.* Science, 2000. **290**(5493): p. 985-989.

150. Berlett, B.S. and E.R. Stadtman, *Protein oxidation in aging, disease, and oxidative stress.* Journal of Biological Chemistry, 1997. **272**(33): p. 20313-20316.

151. Abuja, P.M. and R. Albertini, *Methods for monitoring oxidative stress, lipid peroxidation and oxidation resistance of lipoproteins.* Clin Chim Acta, 2001. **306**(1-2): p. 1-17.

152. Betteridge, D.J., *What is oxidative stress?* Metabolism, 2000. **49**(2 Suppl 1): p. 3-8.

153. Sies, H., *Strategies of antioxidant defense.* Eur J Biochem, 1993. **215**(2): p. 213-9.

154. Gros, L., M.K. Saparbaev, and J. Laval, *Enzymology of the repair of free radicals-induced DNA damage.* Oncogene, 2002. **21**(58): p. 8905-25.

155. Ide, H. and M. Kotera, *Human DNA glycosylases involved in the repair of oxidatively damaged DNA.* Biol Pharm Bull, 2004. **27**(4): p. 480-5.

156. Izumi, T., et al., *Mammalian DNA base excision repair proteins: their interactions and role in repair of oxidative DNA damage.* Toxicology, 2003. **193**(1-2): p. 43-65.

157. Hoeijmakers, J.H.J., *Genome maintenance mechanisms for preventing cancer.* Nature, 2001. **411**(6835): p. 366-374.

158. Gros, L., A.A. Ishchenko, and M. Saparbaev, *Enzymology of repair of etheno-adducts.* Mutation Research-Fundamental and Molecular Mechanisms of Mutagenesis, 2003. **531**(1-2): p. 219-229.

159. Boiteux, S., et al., *Substrate specificity of the Escherichia coli Fpg protein (formamidopyrimidine-DNA glycosylase): excision of purine lesions in DNA produced by ionizing radiation or photosensitization.* Biochemistry, 1992. **31**(1): p. 106-10.

160. Hatahet, Z., et al., *New substrates for old enzymes. 5-Hydroxy-2'-deoxycytidine and 5-hydroxy-2'-deoxyuridine are substrates for Escherichia coli endonuclease III and formamidopyrimidine DNA N-glycosylase, while 5-hydroxy-2'-deoxyuridine is a substrate for uracil DNA N-glycosylase.* J Biol Chem, 1994. **269**(29): p. 18814-20.

161. Jiang, D., et al., *Characterization of Escherichia coli endonuclease VIII.* J Biol Chem, 1997. **272**(51): p. 32230-9.

162. Melamede, R.J., et al., *Isolation and characterization of endonuclease VIII from Escherichia coli.* Biochemistry, 1994. **33**(5): p. 1255-64.

163. Krokan, H.E., F. Drablos, and G. Slupphaug, *Uracil in DNA - occurrence, consequences and repair.* Oncogene, 2002. **21**(58): p. 8935-8948.

164. Saparbaev, M., K. Kleibl, and J. Laval, *Escherichia-Coli, Saccharomyces-Cerevisiae, Rat and Human 3-Methyladenine DNA Glycosylases Repair 1,N-6-Ethenoadenine When Present in DNA.* Nucleic Acids Research, 1995. **23**(18): p. 3750-3755.

165. Saparbaev, M. and J. Laval, *Excision of Hypoxanthine from DNA Containing Dimp Residues by the Escherichia-Coli, Yeast, Rat, and Human Alkylpurine DNA Glycosylases.* Proceedings of the National Academy of Sciences of the United States of America, 1994. **91**(13): p. 5873-5877.

166. Gallinari, P. and J. Jiricny, *A new class of uracil-DNA glycosylases related to human thymine-DNA glycosylase.* Nature, 1996. **383**(6602): p. 735-738.

167. Saparbaev, M. and J. Laval, *3,N-4-ethenocytosine, a highly mutagenic adduct, is a primary substrate for Escherichia coli double-stranded uracil-DNA glycosylase and human mismatch-specific thymine-DNA glycosylase.* Proceedings of the National Academy of Sciences of the United States of America, 1998. **95**(15): p. 8508-8513.

168. Tsaiwu, J.Y.Y.J., J.P. Radicella, and A.L. Lu, *Nucleotide-Sequence of the Escherichia-Coli Mica Gene Required for a/G-Specific Mismatch Repair - Identity of Mica and Muty.* Journal of Bacteriology, 1991. **173**(6): p. 1902-1910.

169. Zharkov, D.O. and A.P. Grollman, *MutY DNA glycosylase: Base release and intermediate complex formation.* Biochemistry, 1998. **37**(36): p. 12384-12394.

170. Bjoras, M., et al., *Opposite base-dependent reactions of a human base excision repair enzyme on DNA containing 7,8-dihydro-8-oxoguanine and abasic sites.* Embo J, 1997. **16**(20): p. 6314-22.

171. Bruner, S.D., D.P. Norman, and G.L. Verdine, *Structural basis for recognition and repair of the endogenous mutagen 8-oxoguanine in DNA.* Nature, 2000. **403**(6772): p. 859-66.

172. Hazra, T.K., et al., *Identification and characterization of a novel human DNA glycosylase for repair of cytosine-derived lesions.* J Biol Chem, 2002. **277**(34): p. 30417-20.

173. Hazra, T.K., et al., *Identification and characterization of a human DNA glycosylase for repair of modified bases in oxidatively damaged DNA.* Proc Natl Acad Sci U S A, 2002. **99**(6): p. 3523-8.

174. Takao, M., et al., *A back-up glycosylase in Nth1 knock-out mice is a functional Nei (endonuclease VIII) homologue.* J Biol Chem, 2002. **277**(44): p. 42205-13.

175. Takao, M., et al., *Novel nuclear and mitochondrial glycosylases revealed by disruption of the mouse Nth1 gene encoding an endonuclease III homolog for repair of thymine glycols.* Embo J, 2002. **21**(13): p. 3486-93.

176. Boorstein, R.J., et al., *Definitive identification of mammalian 5-hydroxymethyluracil DNA N-glycosylase activity as SMUG1.* J Biol Chem, 2001. **276**(45): p. 41991-7.

177. Matsubara, M., et al., *Identification and characterization of mammalian 5-formyluracil-DNA glycosylase.* Nucleic Acids Res Suppl, 2003(3): p. 233-4.

178. Oconnor, T.R. and J. Laval, *Human Cdna Expressing a Functional DNA Glycosylase Excising 3-Methyladenine and 7-Methylguanine.* Biochemical and Biophysical Research Communications, 1991. **176**(3): p. 1170-1177.

179. Cooper, P.K., T. Nouspikel, and S.G. Clarkson, *Defective transcription coupled repair of oxidative base damage in Cockayne syndrome patients from XP group G (vol 275, pg 990, 1997).* Science, 2005. **308**(5729): p. 1740-1740.

180. Cooper, P.K., et al., *Defective transcription-coupled repair of oxidative base damage in Cockayne syndrome patients from XP group G.* Science, 1997. **275**(5302): p. 990-993.

181. Dianov, G., et al., *Repair pathways for processing of 8-oxoguanine in DNA by mammalian cell extracts.* Journal of Biological Chemistry, 1998. **273**(50): p. 33811-33816.

182. Karran, P., *DNA double strand break repair in mammalian cells.* Current Opinion in Genetics & Development, 2000. **10**(2): p. 144-150.

183. Haber, J.E., *Partners and pathways - repairing a double-strand break.* Trends in Genetics, 2000. **16**(6): p. 259-264.

Chapter 2

Quantification of DNA strand breaks and abasic sites

Most of the work in this chapter has been published in "Zhou, X., Liberman, R. G., Skipper, P. L., Margolin, Y., Tannenbaum, S. R., and Dedon, P. C. (2005) Quantification of DNA strand breaks and abasic sites by oxime derivatization and accelerator mass spectrometry: Application to gamma-radiation and peroxynitrite. *Analytical Biochemistry 343*, 84-92."

Abstract

We report a highly sensitive method to quantify abasic sites and deoxyribose oxidation products arising in damaged DNA. The method exploits the reaction of aldehyde- and ketone-containing deoxyribose oxidation products and abasic sites with [^{14}C]-methoxyamine to form stable oxime derivatives, as originally described by Talpaert-Borle and coworkers (*Biochim Biophys Acta* 740: 410-6, 1983). The sensitivity of the method was dramatically improved by the application of accelerator mass spectrometry (AMS) to quantify the ^{14}C, with a limit of detection of <1 lesion in 10^6 nucleotides (nt) in 1 μg of DNA. The method was validated using DNA containing a defined quantity of abasic sites, with a >0.95 correlation between the quantities of abasic sites and methoxyamine labels. To assess the utility of methoxyamine labeling for quantifying strand breaks as well as abasic sites, the method was applied to plasmid DNA treated with γ-radiation and peroxynitrite. For γ-radiation, there was a 0.99 correlation between the quantity of methoxyamine labels and the quantity of strand breaks and abasic sites determined by a plasmid nicking assay; the abasic sites comprised less than 10% of the radiation-induced DNA damage. Studies with peroxynitrite demonstrate that the method, in conjunction with DNA repair enzymes that remove damaged bases to produce aldehydic sugar residues or abasic sites, is also applicable to quantifying nucleobase lesions in addition to strand break products. Finally [^{14}C]-methoxyamine labeling method was shown to be a valuable tool to study cellular DNA strand breaks and abasic sites induced by oxidative agents such as hydrogen peroxide. Compared to other abasic site quantification techniques, the modified method offers the advantage of providing a straightforward and direct measurement of aldehyde and ketone-containing strand breaks and abasic sites.

2.1. Introduction

2.1.1 Formation of strand breaks and abasic sites

Genomic DNA is continuously exposed to endogenous and exogenous DNA damaging agents, such as oxidizing, alkylating and nitrosating chemicals [1, 2]. These species react with both the nucleobase and deoxyribose moieties of DNA to produce base adducts, strand breaks and damaged abasic sites. The bulk of DNA strand breaks arise from oxidative processes involving radical attack at each of the five carbon atoms in the sugar. As illustrated in Figure 2-1, the resulting damages consist of a unique set of lesions for each position, including sugar fragments and oxidized abasic sites [3, 4].

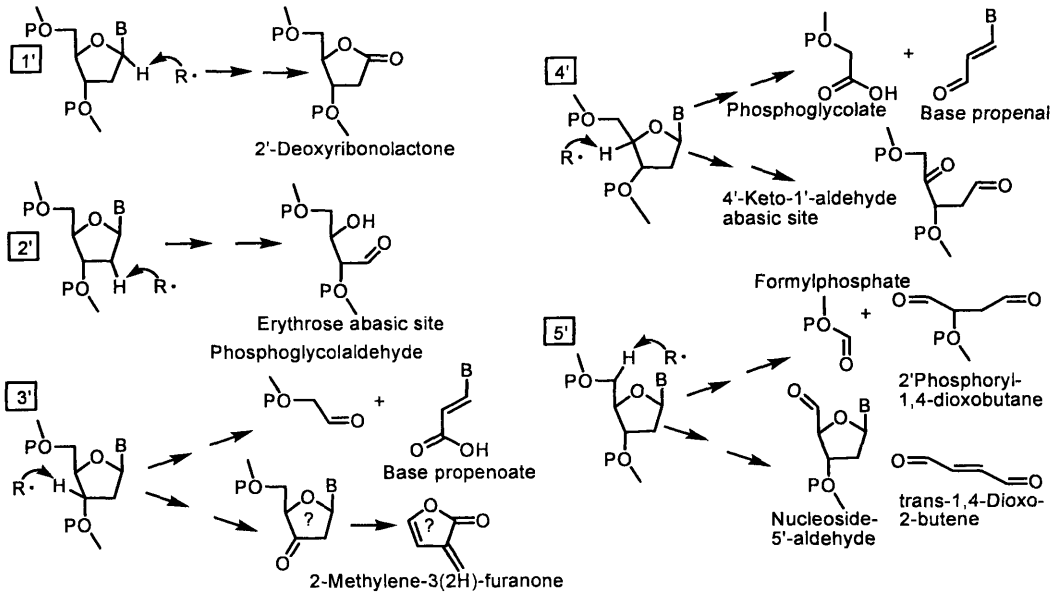

Figure 2-1. Overview of deoxyribose oxidation products

Abasic sites can also be formed by simple hydrolysis of the glycosidic bond [1] and secondarily as a result of the process of base excision DNA repair in which removal of damaged

nucleobases leaves an intact or partially cleaved abasic site [5, 6]. As a result, strand breaks and abasic sites are considered to be important lesions in cellular DNA.

2.1.2 Quantification of strand breaks and abasic sites

Several methods have been developed to quantify strand breaks and abasic sites in an effort to gain insights into the DNA damage processes occurring in cells. These procedures usually involve the estimation of single-strand breaks formed as a result of alkali treatment of apurinic/apyrimidinic (AP) site-containing DNA. Using a ^{32}P-postlabeling assay, Weinfeld et al. were able to quantify AP sites in DNA at the femtomole level [7, 8]. However, the procedure involves gel electrophoresis and HPLC separation of the end-labeled radioactive dinucleotides.

Although the original source was unknown, our research group has been using a plasmid nicking assay to quantify the strand breaks and abasic sites *in vitro*. The assay uses negatively supercoiled circular DNA (form I) as a substrate. Oxidative damage introduces strand breaks or abasic sites (which can be cleaved to strand breaks by putrescine treatment) in the plasmid DNA and coverts the plasmid from supercoiled to a nicked form (form II). These two forms of plasmid can be separated on gel electrophoresis and the amount of strand breaks and abasic sites can be quantified based on their relative ratio. One restriction is that the method only applies to supercoiled plasmid. Since gel electrophoresis cannot separate plasmid containing multiple nicks from containing one nick, the method requires single-hit conditions. This generally indicates that the number of nicked plasmid should account for less than 20% of the total plasmid molecules. We have adopted a mathematical adjustment based on Poisson distribution that helps mitigate the problem. Nevertheless, the method has a limited dynamic range in general.

While the plasmid nicking assay is useful and sensitive for *in vitro* DNA damage studies (*e.g.*, see ref. [9]), the most useful methods for measuring strand breaks and putative abasic sites in cells involve the comet assay [10, 11] and the aldehyde-reactive probe [12, 13], respectively. The comet assay entails microscopic quantification of changes in the electrophoretic mobility of nuclear DNA when the strands are broken. The method requires analysis of hundreds of individual cells to achieve statistical validity and the individual cells must be embedded in agarose prior to processing and analysis.

Aldehyde-reactive probe (ARP) method takes advantage of the fact that most strand breaks and abasic sites in the ring opening form contains an aldehyde or ketone group [14, 15], which enables them to react with oxyamine to form stable oxime derivatives. Chen *et al.* demonstrated that O-(4-nitro-benzyl) hydroxylamine reacts with AP sites to produce O-(nitrobenzyl) hydroxylamine residues at the AP sites. The ARP bound to DNA can easily be separated from free probes by ethanol precipitation or membrane filtration and quantified by ELISA using monoclonal antibody against a 5'-phosphodeoxyribosyl O-4-nitrobenzyl hydroxylamine-BSA conjugate. Another well-developed method for detection of abasic sites uses a biotin-containing ARP [12, 13]. The method again takes advantage of the fact that simple abasic sites as well as many strand break products and oxidized abasic sites, contain aldehyde or ketone groups that react with biotin-containing oxyamine reagents to form stable oxime derivatives. Following reaction with damaged DNA, the DNA-bound ARP molecule is quantified by ELISA *via* the linked biotin. Atamna *et al.* also applied the it to living cells and nuclei and found that the number of AP sites after a 1-hour incubation in old IMR90 cells was about two to three times higher than that in young cells, and the number in human leukocytes from old donors was about seven times that in young donors [14]. While useful for quantification

of aldehyde- and ketone-containing DNA lesions, the method is hampered by several limitations. First, like most methods, it is a relative measure of abasic sites and an internal standard containing defined quantities of abasic sites is required for lesion quantification by fluorescence or chemiluminescence methods. Second, ARP is a fairly bulky and polar compound, so it is unlikely to diffuse into intact cells. Finally, the ARP assay is a lengthy, multi-step process.

A less sensitive alternative to ARP, and indeed the basis for ARP, was developed two decades ago by Talpaert-Borle and coworkers [7, 16]. As with ARP, this approach was developed to exploit the aldehyde moieties of strand breaks and abasic sites by oximation with ^{14}C-labeled methoxyamine, as shown in Figure 2-2.

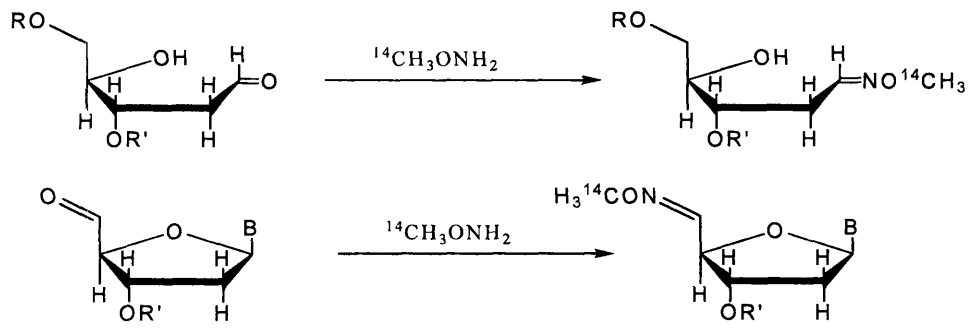

Figure 2-2. Derivatization of aldehydes and ketones in native abasic sites and deoxyribose oxidation products as stable oximes of oxyamine

2.1.3 Accelerator mass spectrometry

The major drawback to the [^{14}C]-methoxyamine technique was the limited sensitivity of the assay. For more than 50 years, ^{14}C has been measured by decay counting, primarily liquid scintillation counting (LSC) by virtue of the fact that this isotope is a low energy β-emitter. Due

to the long half-life of ^{14}C (5740 years), the current detection limit by LSC is about 10 dpm (72 fmol), which does not offer enough sensitivity to detect strands breaks/abasic sites to the background level (1-10/10^6 nt). We have modified the [^{14}C]-methoxyamine method to provide the greatest sensitivity possible by quantifying the ^{14}C using an accelerator mass spectrometer (AMS).

AMS was originally developed to quantify ^{14}C for radiocarbon dating 30 years ago, but has been applied to biological research since early 1990s [17-19]. As shown in Figure 2-3, the three isotopic species ^{14}C, ^{13}C and ^{12}C are evaporated to CO_2, ionized, accelerated, separated and quantified by virtue of their differing energies and mass/charge ratios through magnetic fields. Since the AMS method does not depend on radioactive decay, it is far more sensitive than LSC for ^{14}C detection. A detection limit lower than one amol (10^{-18} mol) has been achieve at the MIT Biological Engineering AMS laboratory [20]. Instead of high purity ^{14}C-methoxyamine, it is now possible to use 0.5-1% ^{14}C methoxyamine (diluted with 99% -99.5% ^{12}C methoxyamine) for most of the assays.

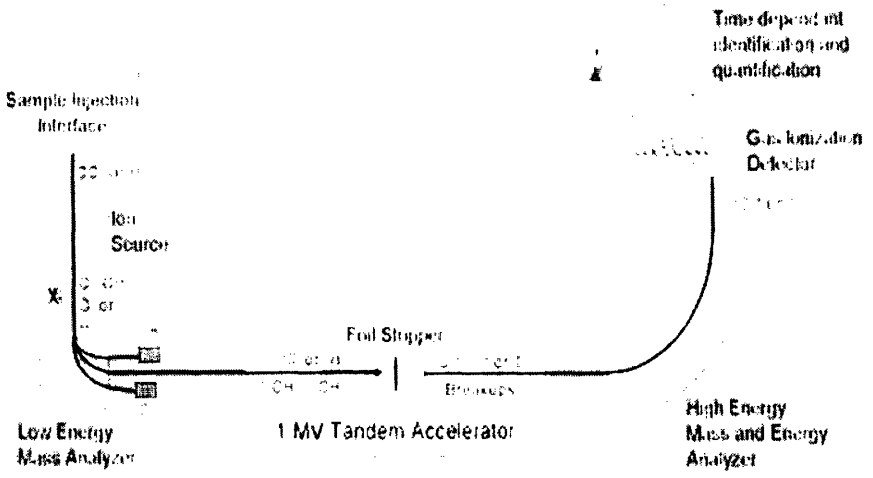

Figure 2-3. Outline of AMS system at MIT Biological Engineering AMS laboratory

This method was found to be highly sensitive and straightforward in applications with DNA damaged by γ-radiation and the endogenous oxidant peroxynitrite, and we demonstrate the involvement of deoxyribose oxidation products, in addition to abasic sites, in the assay signal. We also demonstrate that the method can be applied to study DNA base damage and cellular DNA damage induced by different oxidative species.

2.2. Materials and methods

2.2.1 Materials

All chemicals and reagents were of the highest purity available and were used without further purification unless otherwise noted. [^{14}C]-Methoxyamine (55 Ci/mmol) was obtained from Moravek Biochemicals (Brea, CA). N'-Aminooxymethylcarbonylhydrazino-D-biotin (Aldehyde Reactive Probe) was purchased from Dojindo Laboratories (Kumamoto, Japan). Ion-exchange based genomic DNA kit was from Qiagen (Valencia, CA). Protein-precipitation based genomic DNA purification kit was from Puregene (Minneapolis, MN). Peroxynitrite ($ONOO^-$) was prepared by reaction of ozone with sodium azide as described by Pryor *et al.* [21] and quantified spectrophotometrically in 0.1 M sodium hydroxide (ε_{302} = 1670 $M^{-1}cm^{-1}$). DNA glycosylase (hOGG1) was purchased from New England Biolabs (Beverly, MA) and endonuclease III (Endo III) was purchased from Trevigen (Gaithersburg, MD). Fetal calf serum, glutamine, and penicillin/streptomycin were purchased from Calibiochem (San Diego, CA). Deionized water was further purified with a Milli-Q system (Millipore Corporation, Bedford, MA) for use in all experiments.

2.2.2 DNA treatment

Irradiation of DNA. For the γ-irradiation studies, 20 μg of pUC19 plasmid (325 μg/ml in Chelex-treated 50 mM potassium phosphate buffer, pH 7.4) was irradiated in a ^{60}Co source at ambient temperature with a dose of 0-0.3 Gy. Following treatment, samples were incubated at ambient temperature for 30 min before subsequent quantification of strand breaks and abasic sites.

Peroxynitrite treatment of DNA. Plasmid pUC19 (final concentration 325 μg/ml) was treated with $ONOO^-$ in a buffer (pH 7.4) consisting of 50 mM potassium phosphate and sodium bicarbonate at concentrations of 0, 10, 100 mM. The concentration of the $ONOO^-$ stock solution was measured by UV prior to treatment and was immediately diluted with cold 0.1 M sodium hydroxide for the working stock solutions. $ONOO^-$ was added to the DNA solution by placing an aliquot of the $ONOO^-$ solution on the sidewall of a microcentrifuge tube followed by careful capping of the tube and rapid vortexing for 15 s to mix the contents. Following treatment, samples were incubated at ambient temperature for 30 min before dividing them into two equal portions for subsequent analysis. As described shortly, the first portion was labeled with [^{14}C]-methoxyamine (10 mM final methoxyamine concentration, containing 1% [^{14}C]-methoxyamine) for AMS analysis directly. The other portion was incubated with a mixture of HOGG1 and Endo III repair enzyme in a reaction buffer (10 mM Tris–HCl, pH 7.9, 50 mM NaCl, 1 mM DTT and 2 mM EDTA) at 37 °C for 2 h. Proteins were removed by phenol-chloroform extraction [22] and the DNA was labeled with [^{14}C]-methoxyamine for AMS analysis.

2.2.3 Methoxyamine labeling & AMS analysis

[^{14}C]-Methoxyamine labeling. The general strategy for methoxyamine labeling involves addition of an aliquot of methoxyamine solution (1% [^{14}C]-methoxyamine) to 60 μL of plasmid pUC19 (325 μg/ml) followed by incubation at 37 °C. The unbound methoxyamine was quickly removed by Microcon YM-30 filtration and 6-8 successive washes with the same buffer system. Alternatively, the DNA was precipitated by adding 0.1 volume of sodium acetate (3 M, pH 5.6) and 3 volumes of ethanol, followed by centrifugation at 16,000xg for 30 min at 4 °C. The precipitated DNA was washed three times with 70% ethanol. The DNA was resuspended in potassium phosphate (50 mM, pH 7.4) buffer and the concentration was determined by UV absorbance. AMS analysis was performed on aliquots containing 0.1-1 μg of DNA.

The methoxyamine reaction conditions were optimized for pH and reaction time to ensure the quantitative reaction of the [^{14}C]-methoxyamine with reactive sites in the DNA and to reduce non-specific binding of methoxyamine. The total methoxyamine concentration was varied from 1 to 20 mM; the pH varied from 2 to 10 using 50 mM concentrations of sodium borate or potassium phosphate; and the incubation time varied from 0 to 60 min. All subsequent processing and AMS analysis was as described. To assess the stability of the methoxyamine adducts, γ-irradiated DNA was treated with 10 mM methoxyamine (containing 1% [^{14}C]-methoxyamine) in 50 mM potassium phosphate buffer (pH 7.4) and an aliquot of the oxime-containing DNA (200 μL) was dialyzed against 50 mM potassium phosphate buffer (pH 7.4) in a Pierce Slide-a-Lyzer Mini Dialysis Unit at 37 °C for 0 to 12 h with constant stirring. Aliquots (20 μL) of the solution were removed at 0, 0.5, 1, 2, 3, 6 and 12 h, and the amount of the oxime in each DNA sample was quantified using AMS and compared with the initial level of labeling.

Accelerator mass spectrometry. AMS analyses were conducted by the BEAMS Lab at MIT as described in detail elsewhere [20]. The interface used to generate CO_2 from liquid

samples and its operation have also been described in detail [20]. With no AMS-specific sample preparation necessary, solutions of plasmid DNA were applied directly to the CuO matrix (used for sample combustion) using a 0–2.5 μL adjustable pipette set to deliver 1.00 μL. Typically, 15–18 samples were analyzed successively in one run (10 min), using the full capacity of a CuO holder. The first and last samples were always a standard consisting of a solution of [^{14}C-methyl]-bovine serum albumin. Sample concentrations were calculated from the peak area ratio of the sample to standard. All samples were analyzed at least twice.

2.2.4 Plasmid nicking assay

To convert all types of abasic sites to strand breaks, aliquots of plasmid solution containing 2 μg of DNA were treated with 100 mM putrescine dihydrochloride for 0.5 h at 37 °C [3, 23]. The plasmid topoisomers present in the DNA sample were resolved on a 1% agarose gel at 2.5 V/cm for 2 h in Tris-borate-EDTA buffer [22]. The gel was stained in a 0.5 μg/ml ethidium bromide solution for 0.5 h and then destained for 30 min in water, followed by acquisition of a digital image of the fluorescent DNA bands in the gel subjected to UV illumination (315 nm). The quantity of strand breaks caused by γ-radiation was calculated from the net increase in the percentage of nicked (form II) plasmid, with a correction factor of 1.4 applied to the signal from the supercoiled (form I) plasmid due to its lower affinity for binding of ethidium bromide [24]. The calculation below demonstrates the conversion from fraction of nicked plasmid, which is equal to the number of strand breaks per 100 plasmid molecules, to strand breaks per 10^6 nucleotides, keeping in mind that each pUC19 plasmid molecule has 5372 nucleotides (or 2686 bp): $\frac{strand\ breaks}{100\ plasmid\ molecules} \times \frac{1\ plasmid\ molecule}{5372\ nucleotides} \times 10^6 = \frac{strand\ breaks}{10^6\ nucleotides}$.

When the relative percentage of nicked plasmid is more than 15%, the nicked plasmid may contain more than one damage site. An adjustment was made to account for multiple lesions: $Adjusted\ nicked\% = -\ln(1 - nicked\%)$ using a Poisson distribution assumption for the number of nicks in each plasmid.

2.2.5 Aldehyde reactive probe assay

DNA with strand breaks and abasic sites was treated with 1 mM biotin-containing ARP in TE (10 mM Tris-HCl, 1 mM EDTA, pH 7.4) or phosphate buffer at 37°C for 45 min. After precipitation and washes with 70% cold ethanol, DNA was dissolved in TE and the concentration was adjusted to give 3.3 μg of DNA in 150 μL of solution. The amount of ARP on DNA was analyzed using Pierce chemiluminescent nucleic acid detection module (Pierce Biotechnology, Rockford, IL). DNA was heat-denatured at 100 °C for 15 min, and cooled in ice water immediately for 10 min. The solution was then diluted by addition of 150 μL of 2 M cold ammonium acetate and 91 μL aliquots (1 μg DNA) were blotted in triplicate onto a nitrocellulose membrane using a BioRad BioDot Microfiltration System (Hercules, CA). The wells were washed twice with ammonium acetate (200 μL, 1 M) and the membrane was baked (85 °C, 90 min) and then blocked at ambient temperature for 40 min with 30 ml of blocking buffer. The membrane was then incubated with a 1:250 dilution of stabilized streptavidin-horseradish peroxidase conjugate in 30 ml of blocking solution for 30 min, washed 5 times for 7 min in 40 ml of washing solution at ambient temperature and once for 7 min in 40 ml of substrate equilibration buffer. The membrane was incubated in 12 ml of enhanced chemiluminescent Substrate for 5 min. The chemiluminescence signal on the membrane was

quantified using an Alpha Innotech Fluorochem CCD camera system (San Leandro, CA). Standard curves were prepared by plotting the ARP level (using standards containing 0 – 60/10^6nt ARP) against the enhanced chemiluminescence signal. The strand breaks and abasic site levels of unknown samples were based on standard curves analyzed in parallel on the same blot.

2.2.6 Method validation using uracil-enriched DNA

An *E. coli* mutant lacking uracil DNA glycosylase (ung$^-$) was used to prepare pUC19 plasmid containing a high level of uracil. The uracil content of the DNA was quantified to be 1.0% by a gas chromatography-mass spectrometry (GC/MS) method using [1,3-$^{15}N_2$]-uracil (Cambridge Isotope, Andover, MA) as the internal standard, as described elsewhere [25]. The uracil-enriched plasmid was diluted with unlabeled pUC19 to prepare standards containing ~0.005-0.1% uracil. The DNA (5 μg) was incubated for 60 min with 2 units of uracil-DNA N-glycosylase (UNG; New England Biolabs, Beverley, MA) at 37 °C in a buffer containing 20 mM Tris-HCl (pH 8.0), 1 mM EDTA and 1 mM dithiothreitol. Following filtration of the solution on a YM-3 filter apparatus (MWCO 3,000; Millipore Corp., Medford, MA), the filtrate was spiked with 5 pmol of [1,3-$^{15}N_2$]-uracil and the amount of released uracil was quantified by GC/MS. The plasmid DNA retained on the YM-3 filter was resuspended in 60 μL potassium phosphate buffer (pH 7.4) and extracted with 60 μL phenol-chloroform twice to remove the uracil glycosylase. The strand breaks and abasic sites were quantified using [^{14}C]-methoxyamine labeling with AMS quantification.

2.2.7 Cell culture and exposure

Cell Culture. TK6 cells were maintained in exponentially growing suspension cultures at 37°C in a humidified atmosphere of 95% air and 5% CO_2 in RPMI-1640 medium supplemented with 10% heat-inactivated donor calf serum, 100 units/mL penicillin, 100 μg/mL streptomycin, and 2 mM L-glutamine. Stock cells were subcultured and routinely passaged to maintain an optimal growth density ((0.6-1.0) × 10^6/ml) in 150-mm dishes during experiments. The cell stock used in the present studies was treated with CHAT (10 μM 2'-deoxycytidine, 200 μM hypoxanthine, 0.1 M μaminopterin, and 17.5 μM thymidine) to remove mutant cells, as described by Wang et al. [26].

H_2O_2 Exposure. Cells were grown to a density of 1 × 10^6 cells/ml of fresh RPMI 1640 medium containing 10% heat-inactivated calf serum. 1M H_2O_2 stock solution was directly added to the cell culture to yield a final concentration 0 -- 25 mM. Cells were further incubated at 37°C for 3 hrs. After incubation, the cells were pelleted at 700 g for 4 minutes and washed with cold PBS four times. Each experiment was performed in duplicate.

2.2.8 Genomic DNA isolation

Genomic DNA isolation using ion-exchange column (Qiagen). Following centrifugation at 500g, the supernatant was decanted and the cell pellet (5-10×10^6 cells) was resuspended in 0.5 ml of PBS and lysed by addition of 1 ml cold cell lysis buffer C1 (1.28 M sucrose, 40 mM Tris-HCl, pH 7.5, 20 mM $MgCl_2$, 4% Triton X-100, 5 μg/ml coformycin, 50 μg/ml tetrahydrouridine, and 0.1 mM desferrioxamine) plus 3 ml of H_2O. The sample was incubated on ice for 10 min. The released nuclei were pelleted at 1300g for 10 min and washed

again in 1 ml C1 and 3 ml of H_2O. The nuclei pellet was resuspended in 3 ml of buffer G2 (800 mM guanidine HCl, 30 mM Tris-HCl, pH 8.0, 30 mM EDTA, 5% Tween-20, 0.5% Triton X-100, 5 μg/ml coformycin, 50 μg/ml tetrahydrouridine, and 0.1 mM desferrioxamine) and digested with 30 μl of proteinase K solution (20 mg/ml, Roche Applied Bioscience) and 15 μl RNase A (100 mg/ml, 7000 units/ml, Qiagen) at 37 °C for 1 hr and then at 50 °C for 45 min. The mixture was loaded onto an equilibrated Qiagen 100/G Genomic-tip. The RNA and protein fragments were removed using 2 x 7.5 ml of buffer QC (1.0 M NaCl, 50 mM MOPS, pH 7.0, 15% isopropanol) followed by DNA elution with 5 ml buffer QF (1.25 M NaCl, 40 mM Tris-HCl, pH 8.5, 15% isopropanol). DNA was precipitated with 5 ml of 100% isopropanol and pelleted via centrifugation at 12,000*g* for 12 min. The recovered DNA was washed with 0.9 ml of cold 70% ethanol three times, air-dried at ambient temperature and dissolved in TE buffer. DNA concentration was measured by absorption at 260 nm and samples were stored at −80°C until further analysis.

Genomic DNA isolation using protein precipitation kit. The cell pellet (5- 10 × 10^6 cells) was lysed in 1 ml of cold cell lysis buffer (Puregene) containing 5 μg/ml coformycin, 50 μg/ml tetrahydrouridine, and 0.1 mM desferrioxamine. The cell lysate was incubated with 15 μl RNase A (100 mg/ml, 7000 units/ml, Qiagen) at 37°C for 1 hr to digest the RNA. After cooling to room temperature on ice, the protein was precipitated by addition of 1 ml protein precipitation solution, 30-second vortex at maximum speed and then centrifugation at 2000 g for 10 min at 4°C. The supernatant was carefully transferred to a new tube and DNA was precipitated by adding 4 ml of 100% isopropanol, pelleted, washed, dried and resupsended as described in Genomic DNA isolation using ion-exchange column.

NaI chaotropic DNA extraction (*15*). The cell pellet was resuspended in 500 µl of cold cell lysis buffer (320 mM Sucrose, 5 mM $MgCl_2$, 10 mM Tris-HCl, 5 µg/ml coformycin, 50 µg/ml tetrahydrouridine, and 0.1 mM desferrioxamine, pH 7.5, 1% (v/v) Triton X-100), vortexed at moderate speed for 1 min and incubated on ice for 5 min. After centrifugation at 1300 *g* for 4 min at 4 °C, the nuclei pellets were resuspended in 500 µl lysis buffer and vortexed for 1 min. The nuclei were pelleted again at 1300*g* for 10 min and resuspended in 210 µl Proteinase K Reaction Buffer (12.5 mM Tris, pH 8.0, 0.5 mM EDTA, 5 µg/ml coformycin, 50 µg/ml tetrahydrouridine, and 0.1 mM desferrioxamine, pH 7.5). The cell suspension was mixed with 20 µl of 10% SDS, 10 µl of proteinase K solution (20 mg/ml) and RNase µg/ml. The mixture was incubated at 37 °C for 1 hr and then at 50 °C for 45 min. DNA was precipitated by adding 750 µl of isopropanol and then 500 µl of NaI solution (40 mM Tris, 20 mM EDTA, 7.6 M NaI, pH 8.0). DNA was then pelleted, washed, dried and resupsended as described earlier.

2.2.9 Genomic DNA purification

To eliminate the small amount of protein in the isolated DNA, a fraction of the isolated DNA was further purified after ARP or ^{14}C-methoxyamine labeling by successive extraction with buffer-equilibrated phenol (0.1 M Tris-HCl, pH 8.0, 0.1% 8-hydroxyquinoline [w/v]), phenol/chloroform (1:1), and chloroform. DNA was recovered by precipitation in 200 mM NaCl with 2 volume of 100% ethanol, washed and resuspended in TE buffer.

2.3. Results

2.3.1 Optimization and validation of [^{14}C]-methoxyamine labeling

To ensure a quantitative reaction of the [^{14}C]-methoxyamine with strand breaks and abasic sites and to reduce the non-specific binding under the conditions employed in the present studies, optimization experiments were performed with untreated or γ-irradiated plasmid pUC19 incubated with [^{14}C]-methoxyamine. γ-Radiation induces a variety of aldehyde- and ketone-containing strand breaks and oxidized abasic sites in DNA [4], so it was used as positive control to optimize [^{14}C]-methoxyamine incorporation. The buffer systems tested (phosphate-buffered saline, 50 mM potassium phosphate or borate buffers) were found to produce consistent results for specific [^{14}C]-methoxyamine binding at 37 °C and at pH ranging from 6 to 8 (data not shown), so we chose potassium phosphate buffer at pH 7.4 for our studies. As shown in Figure 2-4, the labeling reaction was complete within 15 min with the irradiated DNA. The undamaged DNA incorporated 4.4 methoxyamine labels per 10^6 nt, which is consistent with the background of plasmid nicking determined by plasmid nicking assay (*vide infra*).

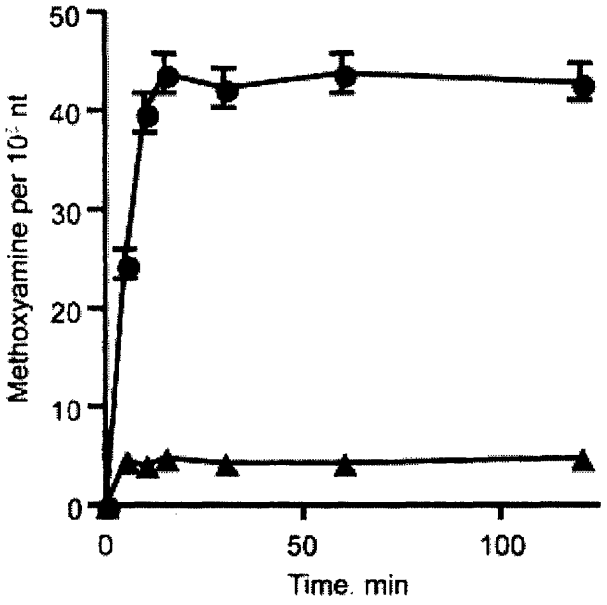

Figure 2-4. Time course for the incorporation of [^{14}C]methoxyamine into damaged DNA. Undamaged plasmid pUC19 (▲) or γ-irradiated plasmid (•) was incubated with 10 mM methoxyamine containing 1% [^{14}C]methoxyamine. At various times, the DNA was washed and the [^{14}C]methoxyamine quantified by AMS as described under Materials and methods. Data represent mean ± SD for n = 3; in some cases, error bars are smaller than the symbol.

Any method involving chemical derivatization of the analyte relies on the stability of the derivative. With respect to the oximation reaction in the methoxyamine method, DNA purification, especially separation of genomic DNA from cells or tissues, involves enzyme digestion steps with mild heating (37-50 °C), while removal of free [^{14}C]-methoxyamine from DNA requires extensive washing. To this end, the stability of oxime was assessed by incubating [^{14}C]-methoxyamine-derivatized, γ-irradiated DNA and quantified radioactivity as a function of time. As shown in Figure 2-5, there was essentially no loss of the [^{14}C]-methoxyamine bound to DNA after 12 h of exhaustive dialysis at 37 °C.

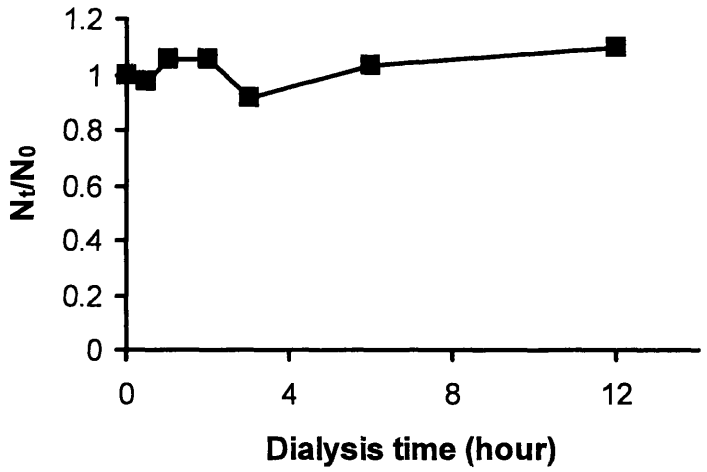

Figure 2-5. Stability of oxmine adduct. ^{14}C-oximine containing DNA was dialyzed in 5,000 volume of 50mM phosphate buffer at 37°C with constant stirring for up to 12 hours. At the indicated times, the amount of ^{14}C-methoxamine still bound to DNA (N_t) was measured against the initial adduct level (N_0).

To validate the [^{14}C]-methoxyamine labeling method, a uracil-containing DNA standard was treated with uracil DNA N-glycosylase to create a defined quantity of abasic sites. As shown in Figure 2-5, a comparison of released uracil bases and [^{14}C]-methoxyamine label reveals a nearly one-to-one correlation (Correlation coefficient = 0.98) between the two indices, thereby confirming the accuracy of the method.

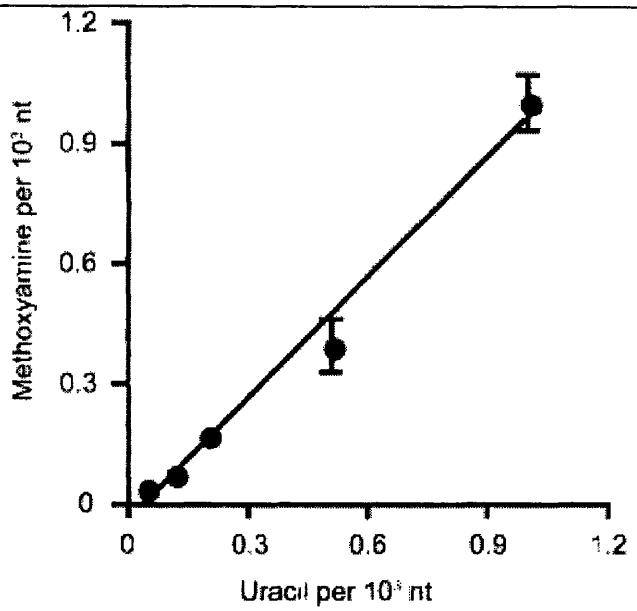

Figure 2-6. Methoxyamine labeling of DNA containing defined quantities of abasic sites. Plasmid DNA containing a defined quantity of uracil was treated with uracil glycosylase followed by [^{14}C]methoxyamine labeling. The quantity of label was determined by AMS as described under Materials and methods. Data represent mean ± SD for $n = 3$; in some cases, error bars are smaller than the symbol. Linear regression of the data yielded a line with $y = 0.95x + 0$, $r^2 = 0.98$.

2.3.2 Quantification of strand breaks and abasic sites in γ-irradiated DNA

To assess the utility of the [^{14}C]-methoxyamine labeling method for quantifying strand breaks and oxidized abasic sites in oxidized DNA, we compared the quantity of [^{14}C]-methoxyamine labels in γ-irradiated DNA to the number of deoxyribose oxidation events quantified by plasmid nicking assay. The latter assay exploits the change in electrophoretic migration of plasmid DNA when a strand break relieves the negative supercoiling of a substrate plasmid molecule. Abasic sites created by deoxyribose oxidation were converted to strand

breaks by treatment of the irradiated DNA with putrescine dihydrochloride, which has been shown to cleave all types of oxidized abasic sites without apparent conversion of base lesions to strand breaks [3, 9, 23, 28]. As shown in Figure 2-7A, the number of [^{14}C]-methoxyamine labels increased linearly with radiation doses over the range of 0 to 0.3 Gy ($R^2 = 0.95$), with a slope of 120 labels per 10^6 nt per Gy. As shown in Figure 2-7B, there was a one-to-one relationship between [^{14}C]-methoxyamine labels and the number of deoxyribose oxidation events measured by plasmid nicking assay.

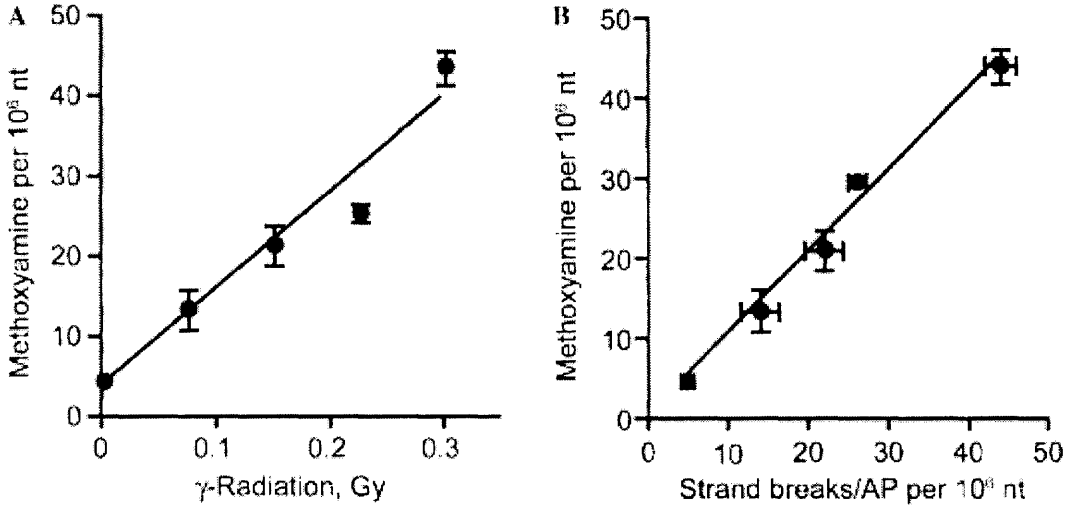

Figure 2-7. [^{14}C]Methoxyamine labeling of γ-radiation-induced DNA damage. (A) γ-Radiation dose–response for [^{14}C]methoxyamine labeling. Irradiated plasmid pUC19 DNA was labeled as described under Materials and methods. Linear regression of the data yielded a line with $y = 120x + 4$, $r^2 = 0.95$. (B) Correlation between [^{14}C]methoxyamine labeling and deoxyribose oxidation events (strand breaks + abasic sites) in γ-irradiated DNA. A portion of the irradiated plasmid DNA from samples used for methoxyamine labeling (A) was subjected to plasmid nicking assay to quantify strand breaks and abasic sites, as described under Materials and methods. Linear regression of the data yielded a line with $y = 1.0x + 0.5$, $r^2 = 0.99$. Data represent mean ± SD for $n = 3$; in some cases, error bars are smaller than the symbol.

2.3.3 [^{14}C]-Methoxyamine labeling of DNA damage induced by $ONOO^-$

$ONOO^-$ is a powerful oxidizing and nitrating agent that is formed in inflamed tissues by a diffusion-limited reaction of nitric oxide with superoxide anion and that exhibits high reactivity with DNA at physiological pH [2]. Previous studies indicate that the presence of CO_2 suppresses deoxyribose oxidation chemistry and enhances base oxidation and nitration reactions due to the formation of $ONOOCO_2^-$ as the reactive intermediate [29].

As a test of the utility of the methoxyamine labeling method, we varied the bicarbonate concentration in the buffer (and thus the CO_2 concentration) to modulate the proportions of base and deoxyribose lesions in the oxidized DNA. The quantity of base damage in ONOO-treated DNA was quantified using two *E. coli* base excision repair enzymes: hOGG1 and EndoIII. HOGG1 recognizes a variety of oxidized purines while Endo III recognizes mainly oxidized pyrimidines [6]. Both enzymes also possess DNA lyase activity for cleavage of resulting abasic sites, which produces an aldehyde-containing sugar residue attached to the 3'-end of the resulting strand break [6]. Treatment of the damaged DNA with a mixture of hOGG1 and Endo III before [^{14}C]-methoxyamine labeling provides a means to quantify the base lesions in addition to the direct deoxyribose oxidation events that are measured by [^{14}C]-methoxyamine labeling in the absence of enzyme reactions.

As shown in Figure 2-8A, an increase in the concentration of bicarbonate from 0 to 10 mM caused a 3-fold decrease in the deoxyribose damage events (*i.e.*, strand breaks and oxidized abasic sites) resulting in [^{14}C]-methoxyamine adducts. Treatment of the oxidized DNA with HOGG1 and Endo III prior to methoxylamine derivatization resulted in nearly the same quantity of ^{14}C labeling for $ONOO^-$ reactions run in the presence or absence of 10 mM bicarbonate

(Figure 2-8B). These results are entirely consistent with previous studies of ONOO-induced DNA damage and indicate a switch in the chemistry of the damage from deoxyribose to guanine bases when the damaging species is converted from $ONOO^-$ to $ONOOCO_2^-$ [2].

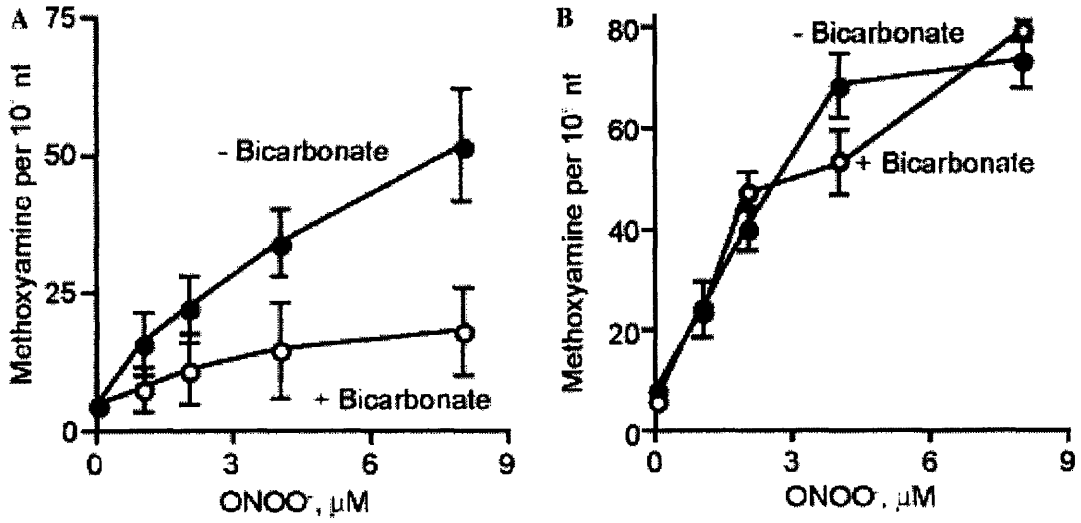

Figure 2-8. $ONOO^-$ dose–response for [^{14}C]methoxyamine labeling. Plasmid pUC19 DNA was treated with $ONOO^-$ in the absence (•) and presence (○) of 10 mM sodium bicarbonate. One portion of the treated DNA was analyzed directly by [^{14}C]methoxyamine labeling (A) and the other portion was reacted with hOGG1 and EndoIII to convert base lesions to strand breaks possessing an abasic site residue attached to the 3′ end of the break, followed by [^{14}C]methoxyamine labeling (B). Data represent mean ± SD for $n = 3$; in some cases, error bars are smaller than the symbol.

Figure 2-9 shows the correlation between methoxyamine labeling and the total quantity of ONOO-induced deoxyribose oxidation as determined by plasmid nicking assay. In the absence of bicarbonate, there are 0.7 methoxyamine adducts per deoxyribose oxidation event (Figure 2-9A). The addition of 10 mM bicarbonate to the $ONOO^-$ reaction reduces the ratio of methoxyamine labels to deoxyribose lesions to 0.5 (Figure 2-9B). These results suggest that

$ONOO^-$ produces deoxyribose oxidation with a lower level of aldehyde- and ketone-containing deoxyribose oxidation products than does γ-radiation.

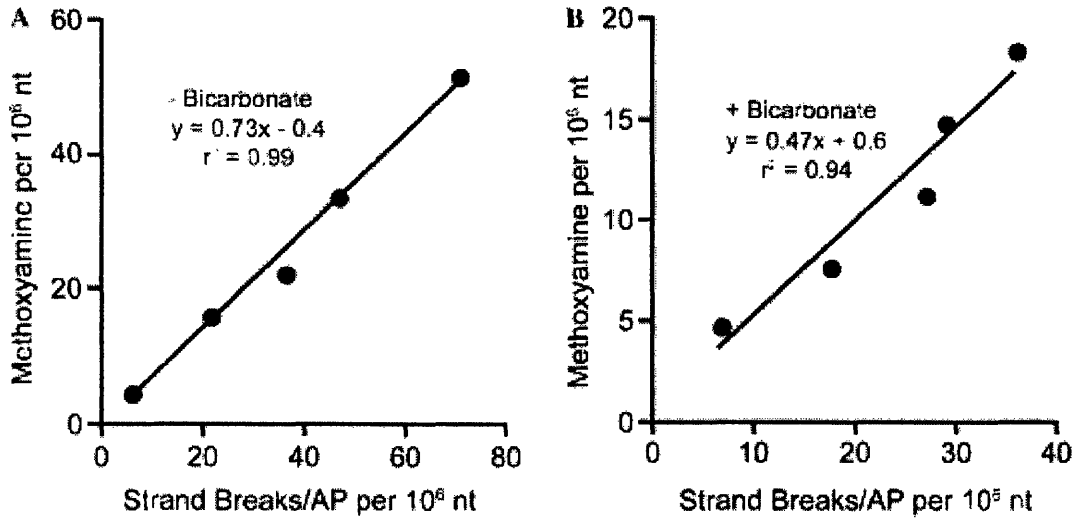

Figure 2-9. [^{14}C]Methoxyamine labeling of ONOO-induced DNA damage. Correlation between [^{14}C]methoxyamine labeling and deoxyribose oxidation events (strand breaks + oxidized abasic sites; no hOGG1 treatment) in DNA treated with $ONOO^-$ in the absence (A) or presence (B) of 10 mM bicarbonate. Data were fitted by linear regression, with equations noted in the graphs.

2.3.4 H_2O_2-induced cellular DNA damage

Studies showed that a significant amount of oxidative damage can occur during the isolation of DNA, especially in the presence of phenol [30]. Phenol is able to reduce metal ions (e.g. Fe^{3+}) present in biological extracts. Considering the relatively high amounts of iron in cellular extract (2-5nmol/mg protein), the Fe^{2+} generated by phenol reduction may induce oxidative damage during DNA isolation [31]. As a result, oxidative damage introduced by transition-metal-mediated oxidation during DNA purification often results in overestimation. So

we investigated three phenol-free methods for DNA purification from cells. For the Qiagen Genomic DNA isolation kit, genomic DNA is bound to anion-exchange resin under appropriate low-salt and pH conditions. RNA, proteins, and low molecular weight impurities are removed by a medium-salt wash and DNA is then eluted in a high-salt buffer. The Puregene kit directly precipitates the protein using the proprietary protein precipitation solution and then precipitates the DNA. For the 8-oxodG study, the combined use of chelating agents and NaI in the chaotropic DNA extraction method was found to be the best method to reduce spurious oxidation [27], [32]. Therefore three DNA extraction methods were compared to identify one with consistently high DNA yield and least amount of artificial oxidative damage during the DNA isolation.

For each method, DNA was isolated from 10^7 of TK6 cells in quadruplets and then labeled with biotin-containing ARP to investigate the background level of strand breaks and abasic sites. As shown in table 2-1, the Qiagen ion-exchange columns yields the least amount of DNA (42 μg vs.>60 μg) on average and has a high variance from sample to sample. This method also has the highest background level for strand breaks and abasic sites as measured by biotin-containing ARP. On the other hand, the protein precipitation method yields similar amounts of DNA as the NaI chaotropic DNA precipitation method, and slightly higher background strand break/basic sites. This method has a lower A_{260}/A_{280} than the other two methods, yet well within the expected 1.8-2 range. Overall, the NaI precipitation proved to be the best method to consistently reduce oxidative damage during the DNA isolation, so it was chosen as our method for cellular DNA damage analysis.

Table 2-1. Comparison of three genomic DNA isolation methods

Method	DNA form 10^7 cells	A_{260}/A_{280}	ARP sites/10^6 nt
Ion-exchange	42 ± 17	1.93 ± 0.06	9.7 ± 3.2
Protein precipitation	64 ± 7	1.85 ± 0.05	5.4 ± 1.3
NaI chaotropic	61 ± 3	1.92 ± 0.05	4.3 ± 0.9

To study cellular DNA damage using [^{14}C]-methoxyamine, we treated TK6 cells with 0 – 25 mM H_2O_2, isolated the DNA using NaI chaotropic DNA precipitation, labeled DNA with [^{14}C]-methoxyamine and then removed the free [^{14}C]-methoxyamine through extensive membrane filtration washes. However, the isolated DNA contained a relatively high amount of [^{14}C]-methoxyamine labels, which is believed to come mainly from the protein impurities present in the isolated DNA. Since proteins are more easily oxidized to form carbonyl groups and as a result contain more aldehyde lesions, a small amount of protein contamination might result in a large number of [^{14}C]-methoxyamine labels. As shown in Figure 2-10, even extra phenol-chloroform extraction steps failed to completely remove protein contamination. Nuclease P1 digestion of DNA converted DNA to nucleotides, which were then separated from any protein contaminants through a YM-10 size-exclusion column, resulting in a reduction of the background level of calculated strand breaks/abasic sites from 33/10^6 to 8/10^6 nt in untreated cells. Treatment with H_2O_2 increased the strand breaks/abasic sites levels to ~ 20/10^6 nt. These results indicate that extensive cleanup steps to remove protein are crucial to measure the real strand breaks and abasic sites in genomic DNA.

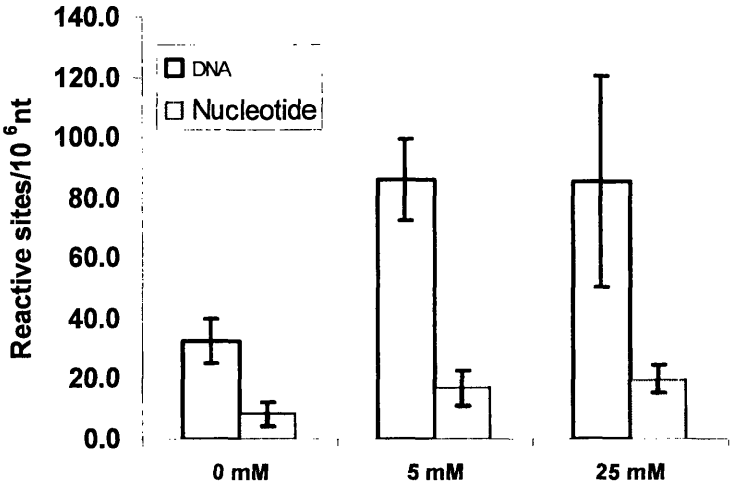

Figure 2-10. H_2O_2 induced ^{14}C-methoxyammine reactive sites in TK6 cellular DNA. DNA was extracted with phenol-chloroform to remove protein (□) or DNA was further digested to nucleotides and filtrated to remove protein ( ). Cells were treated with 0 mM, 5 mM and 25 mM H_2O_2 for 3 hours. Data represent mean ± SD for n = 3.

Fractions from the H_2O_2 treated TK6 cells were also used for biotin-containing ARP labeling. Besides labeling DNA with biotin-containing ARP after isolation, we also directly treated the TK6 cells with 5 mM ARP. Our results in Figure 2-11 show that biotin-contain ARP was unable to diffuse into intact cells, and as a result no DNA was labeled with ARP in control cells. When the cell membrane was broken using a high concentration of hydrogen peroxide, the probe was able to bind to a percentage of the DNA strand break and abasic site lesions. Both ^{14}C-methoxyammine labeling and biotin-containing ARP yielded similar results except in control cells, in which the biotin-containing methods yielded a slightly lower result. It again confirmed that ^{14}C-methoxyammine labeling is a valid method for cellular DNA damage quantification.

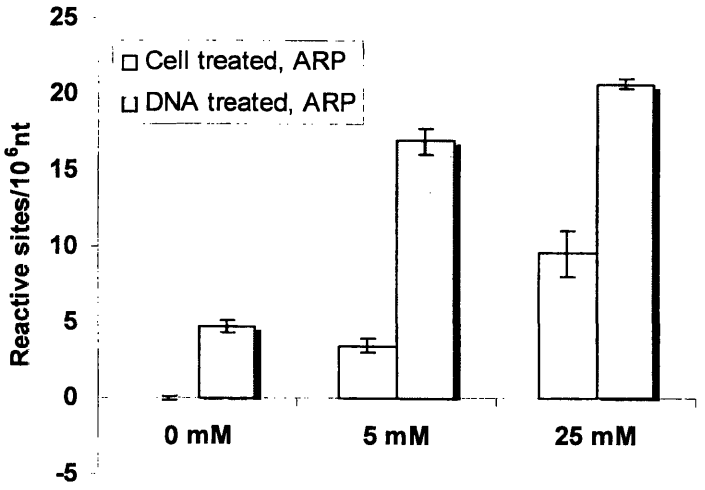

Figure 2-11. H_2O_2 induced ARP reactive sites in cellular DNA. H_2O_2-treated cells were directly treated with 10 mM ARP before DNA isolation (□) or DNA was isolated from H_2O_2-treated cells before labeling with 1 mM ARP ( ). Cells were treated with 0 mM, 5 mM and 25 mM H_2O_2 for 3 hours. Data represent mean ± SD for n = 3.

2.4. Discussion

Neither the ARP approach nor the [^{14}C]-methoxyamine approach offers the specificity required for unequivocal identification of abasic sites. Roberts *et al.* developed an accurate method based on mass spectrometry detection of AP sites from AP DNA that have been prelabeled with O-4-nitrobenzylhydroxylamine (NBHA). Once labeled and the excess labeling agent has been removed, enzymatic digestion of DNA to monomeric subunits can be accomplished, followed by isolation and detection with high-performance liquid chromatography coupled to electrospray ionization tandem mass spectrometry (HPLC-ESI-MS/MS) [34]. Initial results show a quantification limit with 100 μg of DNA to be 100 fmol ($3/10^7$ nt).

The methoxyamine derivatization method studied here represents an enhancement of the basic technique developed two decades ago by Talpaert-Borle and coworkers [16]. The major modifications include a significant enhancement of sensitivity as a result of the use of AMS for quantifying the ^{14}C and a reduction in cost due to the dilution of the [^{14}C]-methoxyamine reagent. The results point to several important misinterpretations of the formation and repair of abasic sites in DNA and to novel differences in the chemistry of deoxyribose oxidations produced by different biologically-relevant oxidants.

As described earlier, the problem of sensitivity has been solved with AMS, which is fundamentally a mass spectrometric technique that counts ^{14}C atoms as particles, and does so rapidly and with relatively high efficiency (typically ~0.2% of the ^{14}C atoms in the CO_2 entering the ion source, with the instrumentation described here). Using AMS, attomole quantities of ^{14}C can be measured with good precision, a sensitivity that is currently 10^5-fold higher than conventional decay counting techniques. Scintillation counting of ^{14}C involves detection of the low energy β-particles produced by nuclear decay. Because of the long half-life of ^{14}C (5740 yr), the scintillation counting detection limit is on the order of 100 fmol of ^{14}C (14 disintegrations per minute), which translates to a methoxyamine labeling assay limit of detection of 1 lesion per 10^6 nucleotides using carrier-free [^{14}C]-methoxyamine and 30 μg of DNA for analysis. With AMS, we achieved a limit of detection equal to 1 lesion in 10^6 nucleotides using 1 μg of DNA and 100-fold dilution of the methoxyamine label, so the method described here uses substantially less DNA and [^{14}C]-methoxyamine and still has much greater sensitivity than the original methoxyamine labeling technique [16]. The sensitivity achieved does not represent an ultimate limit: modifications to both the combustion interface and the particle detector made since these analyses were conducted have improved the detection limit by two orders of magnitude.

The major advantages of the methoxyamine labeling method over the ARP method are convenience, the lack of a requirement for a standard curve, and the potential applicability to studies performed in living cells. While the underlying principle of oxime derivatization is the same for both the methoxyamine and ARP methods, the ARP method requires purification of the DNA prior to derivatization and a lengthy ELISA process to quantify the DNA-bound ARP. The methoxyamine method is likely to be applicable to *in situ* labeling of DNA lesions in cells given the observations of Ames and coworkers [14]. They treated cells with methoxyamine to block ARP-reactive sites prior to DNA isolation, this in an effort to quantify processing-induced ARP binding sites in the isolated DNA, and they observed quantitative blocking of aldehydes and ketones in the DNA [14]. This suggests that strand breaks and abasic sites can be labeled with [^{14}C]-methoxyamine *in situ* to avoid deoxyribose oxidation artifacts during DNA isolation and to provide a means to measure fast repair kinetics for abasic sites and deoxyribose oxidation products.

Several pieces of evidence are consistent with a general lack of reaction of oxyamine with products of nucleobase oxidation. First, the most obviously reactive products, such as the formyl residue of 5-formyl-dU, arise at relatively low frequencies in oxidized DNA compared to other unreactive products [35], such that they represent an insignificant fraction of the total methoxyamine reactive species in DNA. Second, chemical arguments suggest that most base damage products, such as the formamide residue in adenine and guanine formamidopyrimidines, will be unreactive with methoxyamine. Finally, the fact that neither γ-radiation nor $ONOO^-$ produced more methoxyamine labeling than deoxyribose oxidation events (Figures 5 and 7) is consistent with the relative non-reactivity of base oxidation products.

A second advantage of the methoxyamine labeling method is the lack of need for a DNA standard containing a known amount of abasic sites. In our approach, the number of [^{14}C]-methoxyamine labels is directly measured by AMS, thus obviating the need for a standard curve though still requiring a ^{14}C AMS calibration standard ([^{14}C]-albumin in the studies performed here). Also, because of the sensitivity offered by AMS, a very low specific activity of [^{14}C]-methoxyamine can be employed, which greatly reduces the cost of the assay.

The ARP and original [^{14}C]-methoxyamine labeling methods have been promoted for the quantification of abasic sites in DNA. An assessment of the chemistry of deoxyribose oxidation indicates that this interpretation of the labeling results is inaccurate, since an oxyamine reacts with any aldehyde or ketone and many products of deoxyribose oxidation, including strand breaks, contain these reactive functional groups, as illustrated in Figure 1. Oxidation of some positions in deoxyribose produce more than one ketone or aldehyde, such as the 4'-oxidation that partitions to form an abasic site containing a 4′-ketone and a 1′-aldehyde [3]. Other oxidation products at some sites, or oxidation of other sites, produces sugar residues that are unreactive toward oxyamines, such as the 3'-phosphoglycolate of 4'-oxidation and the 2-deoxyribonolactone arising from 1'-oxidation of deoxyribose [3]. Indeed, most of the methoxyamine reactive sites in γ-irradiated DNA studied by Talpaert-Borley and coworkers were probably not, as claimed, abasic sites, such as those that arise from deoxyribose oxidation or the native abasic sites that arise from base excision repair. Oxidized and native abasic sites represent less than 10% of the deoxyribose lesions produced by γ-radiation in isolated DNA [9, 36]. Similar problems confound the interpretation of ARP results [13, 14].

This discussion of deoxyribose oxidation chemistry suggests that our observation of a one-to-one correspondence of methoxyamine labeling and plasmid nicking events in DNA

damaged by γ-radiation is somewhat fortuitous. The results with $ONOO^-$ illustrate an oxidizing agent for which the correlation is not one-to-one. It is now well established that when the concentration of carbon dioxide increases, there is a shift in the chemistry of ONOO-induced DNA damage from deoxyribose oxidation to base oxidation and nitration [2]. This shift in chemistry is accompanied by a shift in the chemistry of deoxyribose oxidation, as suggested by the drop in the frequency of methoxyamine labeling from 70% to 50% of the deoxyribose oxidation events (Figure 2-7). One possible explanation is that the proportion of deoxyribose oxidation products that are reactive toward methoxyamine decreases as the proportion of $ONOOCO_2^-$ increases. Shifts in the chemistry of deoxyribose oxidation with similar agents are not uncommon as we demonstrated in comparisons of α- and γ-radiations [36]. The variable nature of the correspondence of methoxyamine labeling with deoxyribose oxidation frequency suggests caution in the interpretation of [^{14}C]-methoxyamine labeling results unless empirical studies have been performed to define the relationship between labeling frequency and total deoxyribose oxidation frequency. For example, bleomycin specifically performs 4'-oxidation of deoxyribose and produces mainly 3'-phosphoglycolate-ended strand breaks under normal oxygenated solutions [3]. If the methoxyamine or ARP method were used to quantify total DNA deoxyribose oxidation events, the number would be an underestimate.

In summary, we have used AMS to greatly improve the sensitivity of the methoxyamine labeling method as a means to quantify abasic sites and deoxyribose oxidation product in damaged DNA *in vitro*, with the potential to apply the method to *in situ* labeling studies in cells. The method has provided novel insights into differences in the chemistries of deoxyribose oxidation caused by different oxidizing agents.

References

1. Lindahl, T., *Instability and decay of the primary structure of DNA.* Nature, 1993. **362**: p. 709-714.
2. Dedon, P.C. and S.R. Tannenbaum, *Reactive nitrogen species in the chemical biology of inflammation.* Arch Biochem Biophys, 2004. **423**(1): p. 12-22.
3. Dedon, P.C. and I.H. Goldberg, *Free-radical mechanisms involved in the formation of sequence-dependent bistranded DNA lesions by the antitumor antibiotics bleomycin, neocarzinostatin, and calicheamicin.* Chem Res Toxicol, 1992. **5**(3): p. 311-32.
4. Pogozelski, W.K. and T.D. Tullius, *Oxidative strand scission of nucleic acids: Routes initiated by hydrogen atom abstraction from the sugar moiety.* Chem. Rev., 1998. **98**: p. 1089-1107.
5. Sancar, A., et al., *Molecular Mechanisms of Mammalian DNA Repair and the DNA Damage Checkpoints.* Annu Rev Biochem, 2004. **73**: p. 39-85.
6. Demple, B. and L. Harrison, *Repair of oxidative damage to DNA: Enzymology and biology.* Annu. Rev. Biochem., 1994. **63**: p. 915-948.
7. Weinfeld, M., M. Liuzzi, and M.C. Paterson, *Response of phage T4 polynucleotide kinase toward dinucleotides containing apurinic sites: design of a 32P-postlabeling assay for apurinic sites in DNA.* Biochemistry, 1990. **29**(7): p. 1737-43.
8. Esterbauer, H., H. Zollner, and N. Scholz, *Reaction of Glutathione with Conjugated Carbonyls.* Zeitschrift Fur Naturforschung C-a Journal of Biosciences, 1975. **30**(7-8): p. 466-473.
9. Collins, C., et al., *Analysis of 3'-phosphoglycolaldehyde residues in oxidized DNA by gas chromatography/negative chemical ionization/mass spectrometry.* Chem Res Toxicol, 2003. **16**(12): p. 1560-6.
10. Collins, A.R., *The comet assay for DNA damage and repair: principles, applications, and limitations.* Mol Biotechnol, 2004. **26**(3): p. 249-61.
11. Cadet, J., et al., *Hydroxyl radicals and DNA base damage.* Mutation Research-Fundamental and Molecular Mechanisms of Mutagenesis, 1999. **424**(1-2): p. 9-21.
12. Chen, B.X., et al., *Properties of a monoclonal antibody for the detection of abasic sites, a common DNA lesion.* Mutat Res, 1992. **273**(3): p. 253-61.
13. Nakamura, J., et al., *Highly sensitive apurinic/apyrimidinic site assay can detect spontaneous and chemically induced depurination under physiological conditions.* Cancer Res, 1998. **58**(2): p. 222-5.
14. Atamna, H., I. Cheung, and B.N. Ames, *A method for detecting abasic sites in living cells: age-dependent changes in base excision repair.* Proc Natl Acad Sci U S A, 2000. **97**(2): p. 686-91.

15. Nakamura, J., D.K. La, and J.A. Swenberg, *5'-nicked apurinic/apyrimidinic sites are resistant to beta-elimination by beta-polymerase and are persistent in human cultured cells after oxidative stress.* J Biol Chem, 2000. **275**(8): p. 5323-8.

16. Talpaert-Borle, M. and M. Liuzzi, *Reaction of apurinic/apyrimidinic sites with [14C]methoxyamine. A method for the quantitative assay of AP sites in DNA.* Biochim Biophys Acta, 1983. **740**(4): p. 410-6.

17. Barker, J. and R.C. Garner, *Biomedical applications of accelerator mass spectrometry isotope measurements at the level of the atom.* Rapid Communications in Mass Spectrometry, 1999. **13**(4): p. 285-293.

18. Hellborg, R., et al., *Accelerator mass spectrometry - an overview.* Vacuum, 2003. **70**(2-3): p. 365-372.

19. Garner, R.C., et al., *A validation study comparing accelerator MS and liquid scintillation counting for analysis of C-14-labelled drugs in plasma, urine and faecal extracts.* Journal of Pharmaceutical and Biomedical Analysis, 2000. **24**(2): p. 197-209.

20. Liberman, R.G., et al., *An interface for direct analysis of C-14 in nonvolatile samples by accelerator mass spectrometry.* Analytical Chemistry, 2004. **76**(2): p. 328-334.

21. Pryor, W.A., et al., *A practical method for preparing peroxynitrite solutions of low ionic strength and free of hydrogen peroxide.* Free Rad. Biol. Med., 1995. **18**: p. 75-83.

22. Ausubel, F.M., et al., *Current Protocols in Molecular Biology.* 1989, New York: John Wiley and Sons.

23. Povirk, L.F. and C.W. Houlgrave, *Effect of apurinic/apyrimidinic endonucleases and polyamines on DNA treated with bleomycin and neocarzinostatin: Specific formation and cleavage of closely opposed lesions in complementary strands.* Biochemistry, 1988. **27**: p. 3850-3857.

24. Milligan, J.R., J.A. Aguilera, and J.F. Ward, *Variation of single-strand break yield with scavenger concentration for plasmid DNA irradiated in aqueous solution.* Radiat. Res., 1993. **133**(2): p. 151-7.

25. Blount, B.C. and B.N. Ames, *Analysis of uracil in DNA by gas chromatography-mass spectrometry.* Anal Biochem, 1994. **219**(2): p. 195-200.

26. Wang, Z.Y., *A shrinkage approach to model uncertainty and asset allocation.* Review of Financial Studies, 2005. **18**(2): p. 673-705.

27. Nakae, D., et al., *Improved Genomic Nuclear-DNA Extraction for 8-Hydroxydeoxyguanosine Analysis of Small Amounts of Rat-Liver Tissue.* Cancer Letters, 1995. **97**(2): p. 233-239.

28. Tretyakova, N.Y., et al., *Peroxynitrite-induced reactions of synthetic oligonucleotides containing 8-oxoguanine.* Chem Res Toxicol, 1999. **12**(5): p. 459-66.

29. Tretyakova, N.Y., et al., *Peroxynitrite-induced DNA damage in the supF gene: correlation with the mutational spectrum.* Mutat Res, 2000. **447**(2): p. 287-303.

30. Claycamp, H.G., *Phenol Sensitization of DNA to Subsequent Oxidative Damage in 8-Hydroxyguanine Assays.* Carcinogenesis, 1992. **13**(7): p. 1289-1292.

31. Sohal, R.S., et al., *Effect of age and caloric restriction on bleomycin-chelatable and nonheme iron in different tissues of C57BL/6 mice.* Free Radical Biology and Medicine, 1999. **27**(3-4): p. 287-293.

32. Helbock, H.J., et al., *DNA oxidation matters: The HPLC-electrochemical detection assay of 8-oxo-deoxyguanosine and 8-oxo-guanine.* Proceedings of the National Academy of Sciences of the United States of America, 1998. **95**(1): p. 288-293.

33. Pouget, J.P., et al., *Measurement of DNA base damage in cells exposed to low doses of gamma-radiation: comparison between the HPLC-EC and comet assays.* International Journal of Radiation Biology, 1999. **75**(1): p. 51-58.

34. Roberts, K.P., et al., *Determination of apurinic/apyrimidinic lesions in DNA with high-performance liquid chromatography and tandem mass spectrometry.* Chem Res Toxicol, 2006. **19**(2): p. 300-9.

35. Frelon, S., et al., *High-performance liquid chromatography--tandem mass spectrometry measurement of radiation-induced base damage to isolated and cellular DNA.* Chem Res Toxicol, 2000. **13**(10): p. 1002-10.

36. Collins, C., et al., *Differential oxidation of deoxyribose in DNA by gamma and alpha-particle radiation.* Radiat Res, 2005. **163**(6): p. 654-62.

Chapter 3

Quantification of C4′ deoxyribose lesions 3'-Phosphoglycolate and 4′-ketoaldehyde abasic sites

This work is done in collaboration with Dr. Bingzi Chen, who developed the method to quantify 4′-ketoaldehyde abasic sites. The paper 'Quantification of C4′ Deoxyribose Lesions Induced by Bleomycin and γ-radiation Using Gas Chromatography/Mass Spectrometry Method' by Chen, B., Zhou, X., and Dedon, P. C. is in preparation.

For completeness, the chapter incorporates the results of 4′-ketoaldehyde abasic sites quantification wherever appropriate and briefly covers the relevant information about quantification methods of 4′-ketoaldehyde abasic sites.

Abstract

Oxidation of deoxyribose in DNA produces a wide range of lesions, with a different spectrum of products resulting from oxidation of each position of the deoxyribose moeity. Due to both solvent accessibility and issues of site-specificity, oxidation of the C4′ position of deoxyribose is common with many DNA damaging agents, including ionizing radiation and the antitumor antibiotic bleomycin. The chemistry of C4'-oxidation by a variety of agents partitions along either of two pathways to form an abasic site lesion, 2-deoxypentos-4-ulose (4′-keto-1′-aldehyde), or a strand break comprised of a 3'-phosphoglycolate residue with the release of malondialdehyde and a free base with ionizing radiation or base propenals with bleomycin. 3′-Phosphoglycolate is a major 3'- terminal blocking group that must be removed prior to polymerase-mediated gap-filling reactions, while the 4′-keto-1′-aldehyde abasic site is a strong electrophile that has the potential to react with a variety of nucleophiles (*e.g.*, protein, DNA bases) to form adducts. To provide direct and definitive chemical evidence for the formation of deoxyribose oxidation products *in vivo* and to better understand the chemical mechanisms of deoxyribose oxidation related to genotoxin chemistry, we have developed highly sensitive gas chromatography-mass spectrometry (GC/MS) methods to quantify 3′-phosphoglycolate residues and 4′-keto-1′-aldehyde abasic sites and we have applied these methods to quantify 4'-chemistry caused by γ-radiation and Fe(II)·bleomycin. The method used to quantify abasic sites entails conversion of the 2-deoxypentos-4-ulose to a 3-hydroxymethylpyridazine (HMP) residue by reaction with hydrazine, which, together with the 3'-phosphoglycolate, is released by enzymatic hydrolysis and quantified by isotope dilution GC/MS. The detection limits are ~200 fmol for 3'-phosphoglycolate and ~100 fmol for the 4′-keto-1′-aldehyde abasic site. These methods provide a means to define the determinants of deoxyribose oxidation in isolated DNA subjected to oxidative stress.

3.1. Introduction

3.1.1 DNA deoxyrobise oxidation

Genomic DNA is continuously exposed to endogenous and exogenous DNA damaging agents, such as oxidizing, alkylating and nitrosating chemicals [1, 2]. These species react with both the nucleobase and deoxyribose moieties of DNA to produce adducts, strand breaks and abasic sites. While the chemistry of nucleobase oxidation has dominated studies of DNA damage, there is growing evidence that oxidation of DNA deoxyribose plays a critical role in the genetic toxicology of oxidative stress, including involvement in complex DNA lesions, cross-linking with DNA repair proteins and the formation of endogenous DNA adducts. As shown in Figure 3-1, oxidation of deoxyribose in DNA produces a wide range of lesions, with a different spectrum of products arising from oxidation of each position of the sugar.

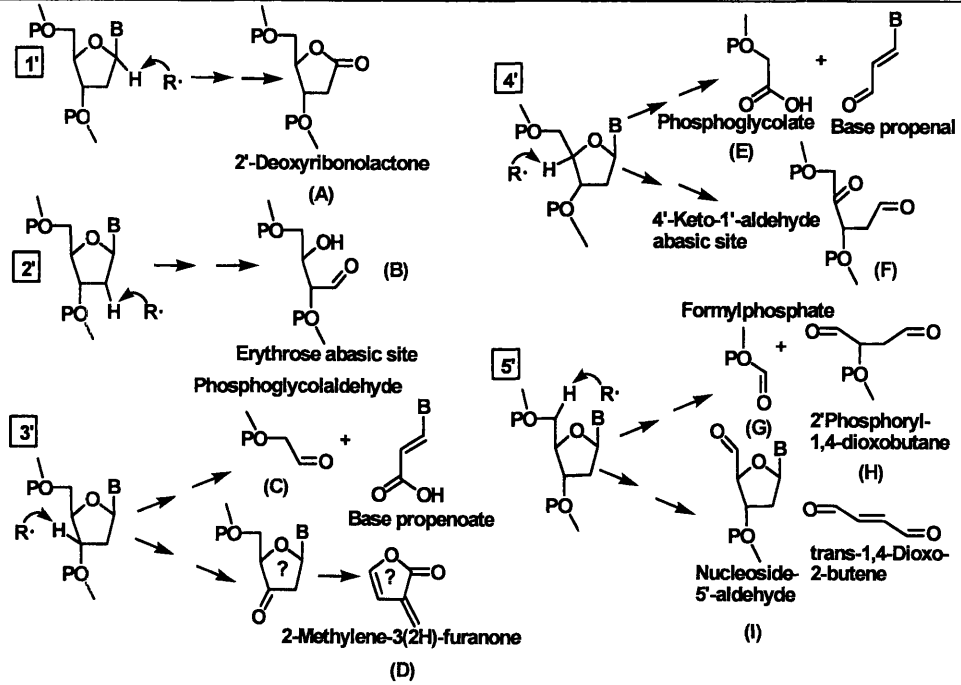

Figure 3-1. Overview of deoxyribose oxidation products

3.1.2 C4'-oxidation products

As discussed in Chapter 1, the general accessibility of different carbon-bound hydrogens in deoxyribose demonstrates the following order: 5' > 4' > 2' ≈ 3' > 1'. Located on the outer edge of the minor groove in DNA, the C4'-hydrogen atom is solvent accessible and has a relatively low bond dissociation energy, which makes the C4'-hydrogen atom a major target of radical species and many minor groove-binding oxidants. The focus of this study is DNA deoxyribose 4'-oxidation because it is an inherent part of the deoxyribose oxidation and one of the products, base propenal, structural analogs of the enol tautomer of MDA, reacts with DNA to form secondary adduct M_1dG. It has been proposed that DNA damage initiated by 4'-hydrogen abstraction can be caused by a number of species, from ionizing radiation, Fe^{2+}/EDTA, Fenton-generated hydroxyl radicals to drugs such as bleomycin, calicheamicin, neocarzinostatin, elsamicin. At least two degradation pathways are proposed for deoxyribose C4'-carbon oxidation, the first including strand breaks terminated by 5'-phosphate and 3'-phosphoglycolate moieties and a release of base propenal or malondialdehyde and the free base. The second degradation pathway includes free base and the abasic site lesion 2-deoxypentos-4-ulose (4′-keto-1′-aldehyde). 3′-Phosphoglycolate (PGL) is a major 3′- terminal blocking group, which must be removed to create a single nucleotide gap before base excision repair (BER). With two free aldehyde/ketone groups, the 4′-ketoaldehyde abasic site is a strong electrophile that can react with a variety of nucleophiles (protein, DNA bases) to form crosslink products.

3.1.3 Quantification of deoxyribose oxidation products

In contrast to the extensive effort to study DNA base lesions, relatively little work has been successful in defining the chemistry of dR oxidation; quantification of DNA deoxyribose oxidation products and the investigation into the formation of secondary DNA adducts formed from doxyribose oxidation products. The Dedon laboratory has been developing sensitive analytical techniques to quantify the deoxyribose oxidation products to provide direct and definitive chemical evidence for deoxyribose oxidation products formed under biological conditions and the chemical mechanisms of deoxyribose oxidation.

5'-(2-Phosphoryl-1,4-dioxobutane)

The Dedon research group has developed two approaches to quantify the formation of 5'-oxidation product, 5'-(2-phosphoryl-1,4-dioxobutane) [3]. The first approach uses O-benzylhydroxylamine to form stable dioxime derivatives of the putative 5'-(2-phosphoryl-1,4-dioxobutane) residues. The β-elimination product of this dioxime proved to be the expected *trans*-1,4-dioxo-2-butene, which can be identified and quantified using benzylhydroxylamine dioxime derivative of [D_4]-labeled *cis*-1,4-dioxo-2-butene as an internal standard, as shown in Figure 3-2. A second approach to identify and quantify the sugar residue involved derivatization with hydrazine and β-elimination to form pyridazine followed by quantification of the pyridazine by GC/MS.

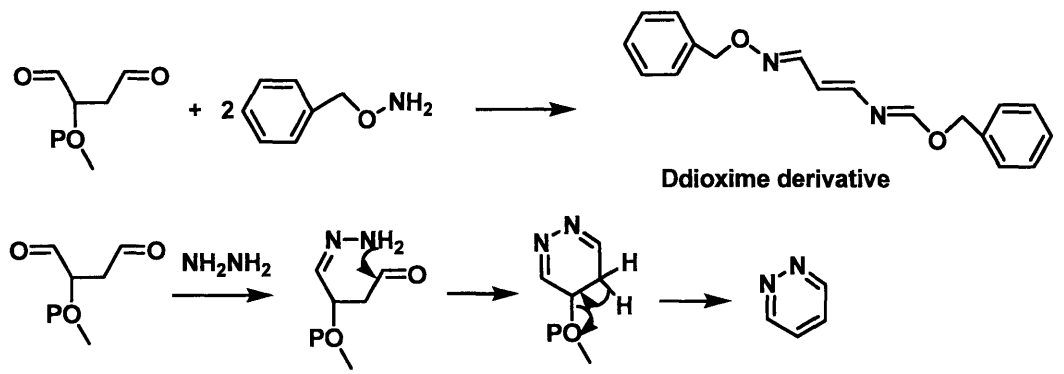

Figure 3-2. Reaction of 5'-(2-phosphoryl-1,4-dioxobutane) residues with O-benzylhydroxyl amine and hydrazine to form oxime and pyridazine derivative

As a positive control for 5'-oxidation of deoxyribose, the enediyne calicheamicin was observed to produce 5'-(2-phosphoryl-1,4-dioxobutane) at the rate of ~9 lesions/10^6 nt/μM measured by these approaches. It was also observed that the enediyne neocarzinostatin produced a linear dose-response for pyridazine formation as expected given the ability of this oxidant to cause 1'-, 4'-, and 5'-oxidation of deoxyribose in DNA. The antitumor antibiotic bleomycin, on the other hand, produced pyridazine at a 10-fold lower rate, which is consistent with 4'-chemistry as the predominant mode of deoxyribose oxidation by this agent.

C5'-aldehyde

The intrinsic reactivity of the 5'-aldehyde terminus with nucleophiles (*e.g.*, formation of hydrate with water or a Tris adduct with Tris buffer) or its ability to spontaneously undergo β-elimination reaction made the direct measure of the 5'-aldehyde difficult [4]. Upon heating, two consecutive β-elimination reactions result in the formation of furfural, free base, and a 5'-phosphate terminus. Pratviel *et al.* developed a GC/MS method to quantify furfural and showed

that it could be used as a convenient marker of C5' hydroxylation of deoxyribose [5]. Angeloff *et al.* found that the formation of a O-carboxymethyl oxime derivative from the 5'-aldehyde terminus avoids β-scission reaction and the formation of adducts with nucleophilic species present in the reaction medium. They subsequently developed an LC/ESI-MS analysis to quantify O-carboxymethyl oxime derivatives, thereby characterizing 5'-aldehyde moiety of DNA strand breaks directly [4].

3'-phosphoglycoaldehyde

There have been few studies of the 3'-oxidation product 3'-phosphoglycoaldehyde (PGA). Barton and co-workers used a sequencing gel technique to tentatively identify DNA fragments with PGA termini attached to their 3'-ends as a result of deoxyribose oxidation by rhodium(III) complexes in 1992 [6]. In recent years, Collins *et al.* in the Dedon research group developed a method for the quantification of PGA residues. This method exploits the aldehyde moiety in PGA by oxime derivatization with pentafluorobenzylhydroxylamine, followed by solvent extraction, O-Bis-(trimethylsilyl)trifluoroacetamide (BSTFA) derivatization and GC/NCI-MS [7, 8]. A stable isotopically labeled [$^{13}C_2$]-PGA was synthesized and used as an internal standard.

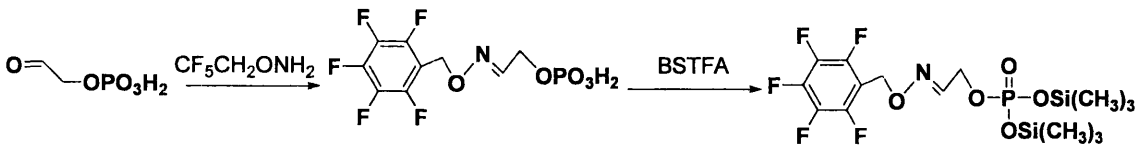

Figure 3-3. Derivitization of phosphoglycoaldehyde by pentafluorobenzyl-hydroxylamine and O-Bis-(trimethylsilyl)trifluoroacetamide (BSTFA).

These studies showed that ^{60}Co γ-radiation induced 1.5 PGA residues/10^6 nt/Gy, which accounted for 1% of deoxyribose oxidation events. This small fraction is consistent with models

of limited solvent accessibility of the 3'-position of deoxyribose [7]. In contrast, PGA formation occurred in 7% of deoxyribose oxidation events produced by α-particle radiation, which indicates a shift in the chemistry of deoxyribose oxidation, possibly as a result of the different track structures of two types of ionizing radiation [8]. Studies with gamma radiation were extended to TK6 cells; γ-radiation produced a linear dose response of 0.0019 PGA residues/10^6nt/Gy. This is consistent with an approximately 1000-fold quenching effect in cells, similar to the results of other published studies of oxidative DNA damage *in vivo* [9].

3.1.4 Quantification of 3'-phosphoglycolate and 4'-ketoaldehyde abasic sites

To our knowledge, no direct measurement of 3'-phosphoglycolate (3'-PGL) or 4'-keto-1'-aldehyde abasic sites have been reported. A ^{32}P-postlabeling assay has been developed for 3'-PGL detection [10]. This technique is based on the inability of DNase I and snake venom phosphodiesterase to cleave the internucleotide phosphodiester bond immediately 5' to the site of the 3'-PGL residue, so that complete digestion of irradiated DNA with these nucleases and alkaline phosphatase yields lesion-bearing "dinucleoside" monophosphates. These monophosphates can be separated from mononucleoside monophosphates by HPLC and subsequently quantified. Alternatively, 3'-PGL has been detected indirectly after acid or enzymatic hydrolysis of the 3'-DNA precursor to glycolic acid. Glycolic acid has long been analyzed using thin layer chromatography (TLC) purification and derivatized by trimethylsilylation, and quantified by GC-MS [11]. Glycolate was also derivatized to 3,5-bis(trifluoromethyl)benzylglycolate and O^2-pivalyl-3',5'-bis(trifluoromethyl)benzylglycolate

using bis(trifluoromethyl)benzyl bromide and pivalic anhydride respectively [12]. 4′-ketoaldehyde abasic sites were indirectly quantified by reduction to **compound A** as shown in Figure 3-4A [13]. **A** was subsequently purified by HPLC, digested by nuclease P1 and phosphatase, and derivatized using trimethylchlorosilane for GC/MS analysis.

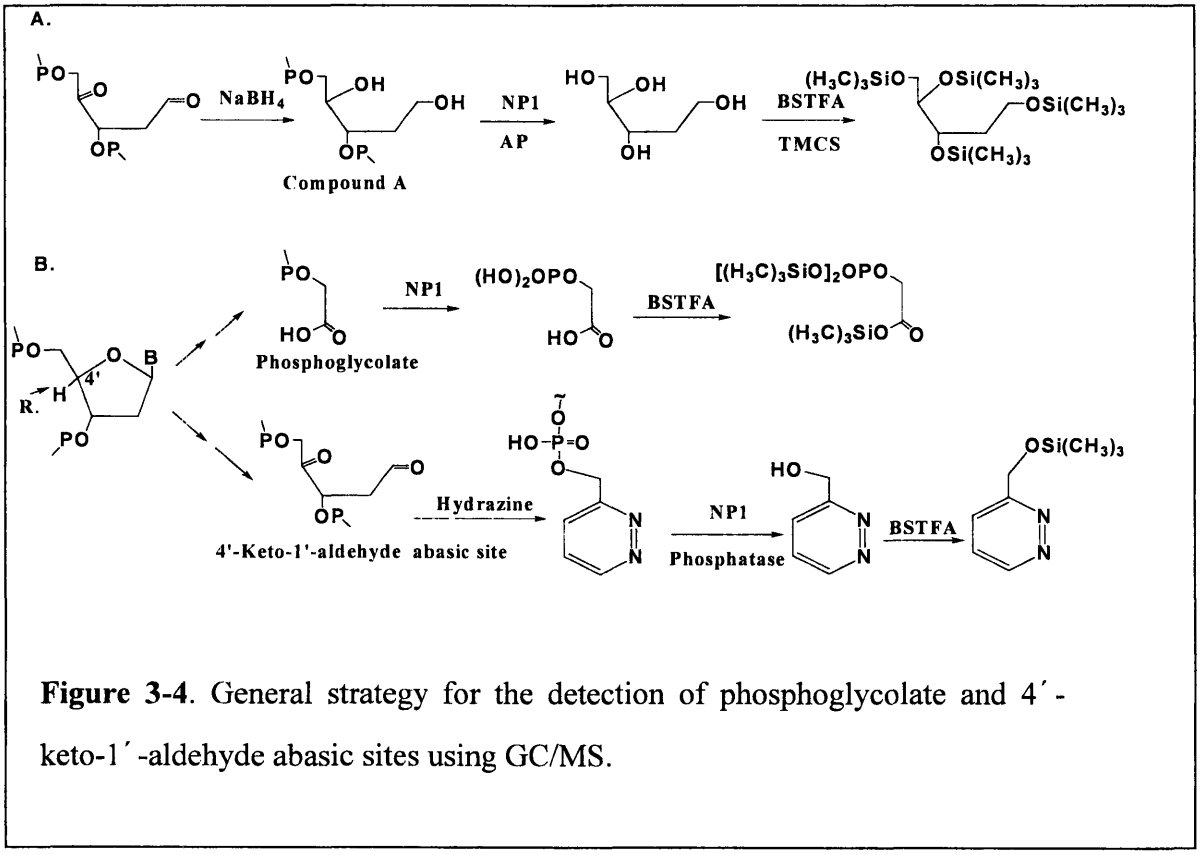

Figure 3-4. General strategy for the detection of phosphoglycolate and 4′-keto-1′-aldehyde abasic sites using GC/MS.

As part of a larger effort to systematically quantify deoxyribose lesions and investigate the secondary lesions arising from them, we present new GC/MS methods to quantify 3′-phosphoglycolate residues and 4′-ketoaldehyde abasic sites in this chapter. The general approach to quantify both the ketoaldehyde abasic sites and phosphoglycolate residues is shown in Figure 3-4B. Since the 4′-ketoaldehyde abasic site is an unstable electrophile, it is stabilized by conversion to a 3′-pyridazine moiety by derivatization with hydrazine immediately after

oxidative DNA damage to capture all the lesions [14]. Nuclease digestion releases the phosphoro-3′-pyridazinylmethylate (alkaline phosphatase may be used to further remove the phosphate to produce 3-hydroxymethylpyridazine product), which is purified by extraction with ethyl acetate. Both the hydroxymethylpyridazine and the phosphoglycolate were quantified by GC/MS after silylation with BSTFA.

With a limit of detection of 100 fmol for hydroxymethylpyridazine and 200 fmol for PGL, the technique is illustrated with DNA damaged by Fe(II)·bleomycin and γ-radiation. The results provide a new approach to study DNA deoxyribose oxidation in biological systems.

3.2. Materials and methods

3.2.1 Materials

All chemicals and reagents were of the highest purity available and were used without further purification unless noted otherwise. Calf thymus DNA, alkaline phosphatase, nuclease P1, and hydrazine were purchased from Sigma-Aldrich Chemical Co (St. Louis, MO). Unlabeled and [1,2-$^{15}N_2$]-hydroxymethylpyridazines were prepared through two steps of chemical synthesis. Silica gel-60 (pore size, 0.040-0.063 mm) was used for flash chromatography. Samples were irradiated in a Gammacell-220 with an annular Cobalt-60 source at room temperature with 1.35 Gy/min intensity. Deionized water was further purified with a Milli-Q system (Millipore Corporation, Bedford, MA) for use in all experiments.

3.2.2 Instrumental analyses

All HPLC analyses were performed on a Hewlett-Packard model 1100, equipped with a G1315A diode array detector. UV spectra were obtained using a Beckman DU640 UV-visible spectrophotometer. GC/MS analyses were performed with a Hewlett-Packard 6890 series GC system equipped with a Hewlett-Packard 5973 mass selective detector using electron impact ionization at 70 ev. The carrier gas was He and the column used was DB-35MS, mid-polar capillary column (30 m x 0.25 mm x 0.25 μm film thickness, crosslinked 35% phenyl-methylpolysiloxane); oven temperature ramp of 10°C/min from 100 to 310°C; the injector temperature was 250°C. The MS was operated in selective ion monitoring mode with an m/z 357 for PGL (PGL -CH_3 fragment, the base peak), 182 for silylated 3-hydroxymethylpyridazine (HMP), 359 and 184 for their corresponding deuterium-labeled internal standards.

3.2.3 Synthesis of PGL standard

To a solution of phosphoryl chloride (PCl_3, 0.28 ml, 3.05 mmoles) in 2 ml of trimethyl phosphate cooled to 0°C, glycolic acid (1 mmol, 76 mg for unlabeled, 78 mg for D_2-labeled) was added. The mixture was stirred at 0°C for 3 hours and then at ambient temperature for 1 hour. The clear solution was poured into 10 ml of ice water and adjusted to pH 4 with cold 2N sodium hydroxide. The reaction is shown in Figure 3-5. Similarly [D_2]-PGL was synthesized using D_2-glycolic acid. Since it was difficult to remove all the salt in PGL, the amount of PGL was quantified using ^{1}H NMR with a known amount of DMSO as the internal standard. ^{1}H NMR (D_2O): δ 4.50 (d, 2H). GC/EI-MS: M 372; M-CH_3 357 (base peak).

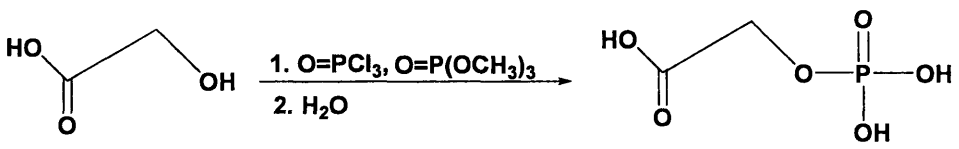

Figure 3-5. Synthesis of PGL

3.2.4 DNA damage by γ-irradiation and Fe(II)·bleomycin

Calf thymus DNA was dissolved in Chelex-treated 50 mM potassium phosphate buffer (pH 7.4; see ref. [7]), dialyzed and aliquots were stored at -80°C. For γ-irradiation, DNA was exposed to 0-100 Gy in a ^{60}Co source at 1.35 Gy/min. For bleomycin treatment, 5 μL aliquots of an aqueous bleomycin solution (0-5 mM) were added to the DNA solution (490 μL) followed by addition of 5 μL aliquots of freshly prepared $Fe(NH_4)_2(SO_4)_2$ solution (0-5 mM) to initiate the DNA damage reaction. All DNA damage reactions were conducted at ambient temperature for 0.5 h.

3.2.5 PGL quantification

Following DNA oxidation, the solutions were filtered by YM-30 columns and washed with 30 mM of ammonium acetate three times to remove non-volatile salts. Samples were re-dissolved in 450 μl water, followed by the addition of ammonium acetate buffer (5 μl, 3 M, pH 5.3) and zinc chloride (20 μl, 10 mM). The damaged DNA was digested by addition of nuclease

P1 (10 units, MP Biomedicals Inc., Irvine CA) and incubation at 37°C for 3 hours. 500 pmol D_2-PGL internal standard was added before digestion. The resulting solution was filtered by Microcon YM-30 column to remove the enzyme. The filtrate was dried and resuspended in 30 μl of 0.1% TFA solution and pre-purified by HPLC. Samples were resolved with the following gradient of acetonitrile in H_2O (both containing 0.1% TFA): 0–20 min, 1-5%; 20-21 min, 5–100%; 21–30 min, 100%. Retention time: PGL 8.0 min; GMP 9.3 min; AMP 11.4 min; TMP 13.7 min; TMP 15.9 min.

The collected fractions were dried under vacuum. The sample residues were taken up with 20 μl of BSTFA (containing 1% of trimethylchlorosilane) and mixed at ambient temperature. 1 μl of the final solution was injected on the GC/MS and analyzed with scanning for m/z 357 and 359 simultaneously. GC retention times: 13.99 min. Quantities of phosphoglycolate formed in Fe(II)·bleomycin or γ-radiation damage of calf thymus DNA were determined from the ratio of the areas of the PGL(from Fe(II)·bleomycin or γ-radiation damage of DNA) peak to the known labeled PGL peak as related to a calibration curve derive from samples containing from 0 pmole to 500 pmoles of PGL (m/z 359) plus 500 pmoles of labeled PGL (m/z 357) described as above.

3.2.6 Total deoxyribose oxidation and keto-1′-aldehyde quantification

Both total deoxyribose oxidation and 4′-ketoaldehyde abasic site were quantified by Dr. Bingzi Chen. PUC19 plasmid DNA (2686 bp) was also treated with γ-irradiation and Fe(II)•bleomycin under the same conditions and the total deoxyribose oxidation was quantified

using the plasmid nicking assay as detailed in Chapter 2. 4′-ketoaldehyde abasic sites were quantified as briefly discussed in the introduction section, with one difference present in the extra derivatization step for 4′-ketoaldehyde abasic site. Due to its instability, 4′-ketoaldehyde abasic sites were first derivatized using hydrazine to form a stable hydrazine derivative, and the derivative was extracted using ethyl acetate following DNA digestion.

3.3. Results

3.3.1 GC/MS analysis of PGL

PGL silylation derivative measured by GC/EI-MS was shown to be more sensitive than PGL directly measured by LC/ESI-MS. The GC/MS peak was well defined at the retention time of 13.99 minutes (Figure 3-6). The m/z results matched the PGL silyation derivative in the standard EI spectrum library. The molecular ion was shown to be 372. For quantification, the fragment with the loss of one methyl group (m/z = 357) and the corresponding D_2-PGL derivative fragement (m/z = 359) were used. Since the internal standard has the same structure as PGL, it compensates any variability caused by potential PGL loss during the purification. Both inorganic salts and normal nucleotides were shown to interfere with the BSTFA derivatization of PGL and the final GC/MS quantification. As a result, the procedures were optimized to eliminate any interference due to these salts. Ammonium acetate buffer was used in place of sodium acetate buffer for enzyme digestion, since it can be removed by evaporation. The small amount of $ZnCl_2$ and large quantity of normal nucleotides were separated from PGL through HPLC under acidic conditions. To reduce artifact formation during the BSTFA derivatization, we tested

silylation reactions at different temperatures 25°C, 37°C, 50°C, 70°C and 95 °C and finally found on-line derivatization (the sample was derivatized in the GC/MS inlet directly) yielded the best and most consistent results (recommended by Dr. Koli Taghizadeh).

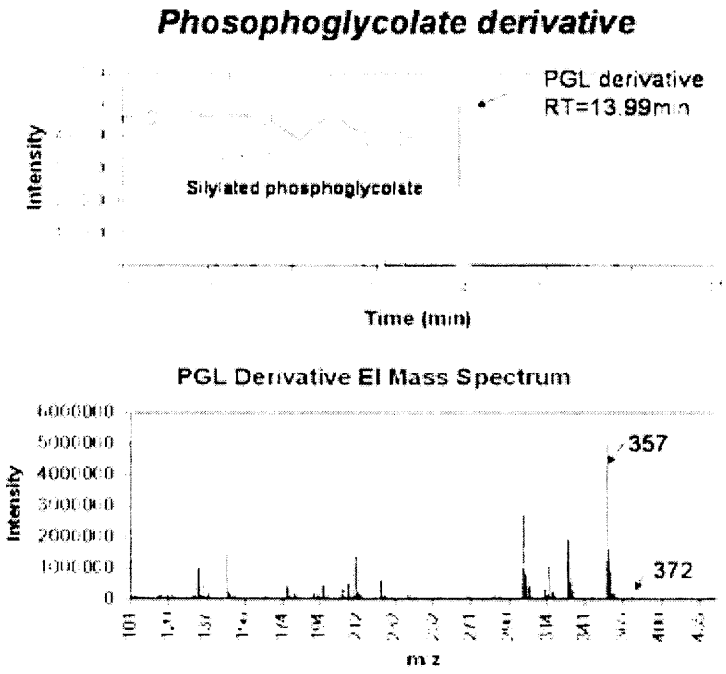

Figure 3-6. Chromatogram and mass spectrum of PGL using positive EI of GC/MS.

Samples containing 500 pmol of D_2-PGL and 0-500 pmol of PGL and 250 μg of calf thymus DNA were used to construct the standard curve. Excellent linearity was observed (Figure 3-7, $r^2 = 0.99$) in the relationship between the quantity of PGL added and the ratio of the area of the PGL signal (*m/z* 357) to the area of the D_2-PGL signal (*m/z* 359). The calibration curve does not pass through the origin due to background level of PGL in calf-thymus DNA. A slope of 0.0021 ± 0.0002 indicated that there was little difference between the signal of PGL and D_2-PGL, which suggests there is no bio-matrix related isotope effect as we observed in C3'-oxidation product phosphoglycoaldehyde GC/CI-MS quantification [7].

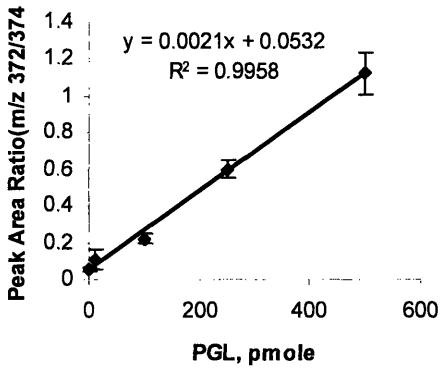

Figure 3-7. Standard curve for the GC/EI-MS analysis of PGL. Samples were prepared containing varying amounts (0 – 500 pmoles) of PGL standard added to a fixed amount (500 pmoles) of [D_2]-PGL internal standard. The aqueous samples were subjected to enzymatic digestions, followed by extraction, silylation and GC/MS analysis as described in Experimental Procedures. The data are combined results of six separate experiments.

3.3.2 PGL induced by Fe(II)·bleomycin and γ-radiation

Approximately 32 PGL molecules per 10^6 nucleotides of calf thymus DNA was formed for each μM of bleomycin and 13 PGL molecules per 10^6 nucleotides was formed for each Gray of γ-radiation. Fe(II)·bleomycin/γ-radiation dose response curves with the number of PGL molecules formed per 10^6 nucleotides are shown as Figure 3-8.

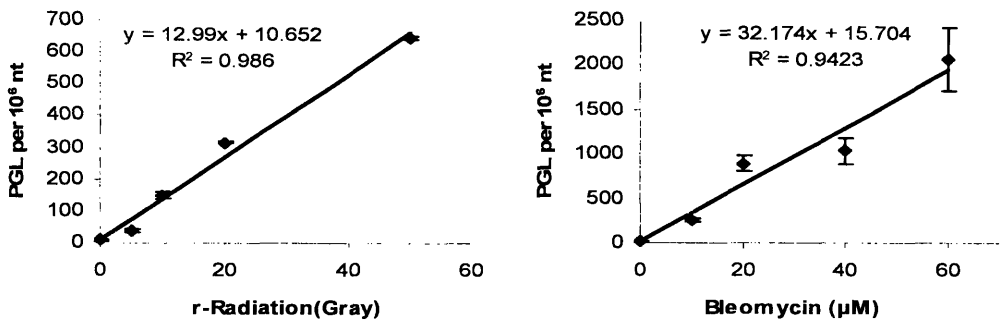

Figure 3-8. Phosphoglycolate dose response curves. PGL levels in bleomycin-mediated and γ-irradiated calf thymus DNA. PGL levels were determined in 250 μg of calf thymus DNA in potassium phosphate buffer (50 mM, pH = 7.4). DNA was subjected to various concentrations of bleomycin or 0 – 60 Gray of γ-radiation. The data are combined results of three separate experiments.

3.3.3 PGL vs. total deoxyribose oxidation (by Bingzi Chen)

The total amount of deoxyribose damage in PUC19 was determined using a plasmid-nicking assay. Plasmid was irradiated with 0 – 0.4 Gray or treated with 0 – 1.2 μM of bleomycin and then treated with putresceine to convert abasic sites into strand breaks. Bleomycin induced 42 strand breaks/10^6 nt/uM and γ-radiation induced 130 strand breaks and abasic sites/10^6 nt/gray as measured by the plasmid nicking assay. Figure 3-9 shows the correlation between PGL and strand breaks/abasic sites. Overall PGL accounts for 78% of the strand breaks and abasic sites induced by bleomycin and 10% by γ-radiation.

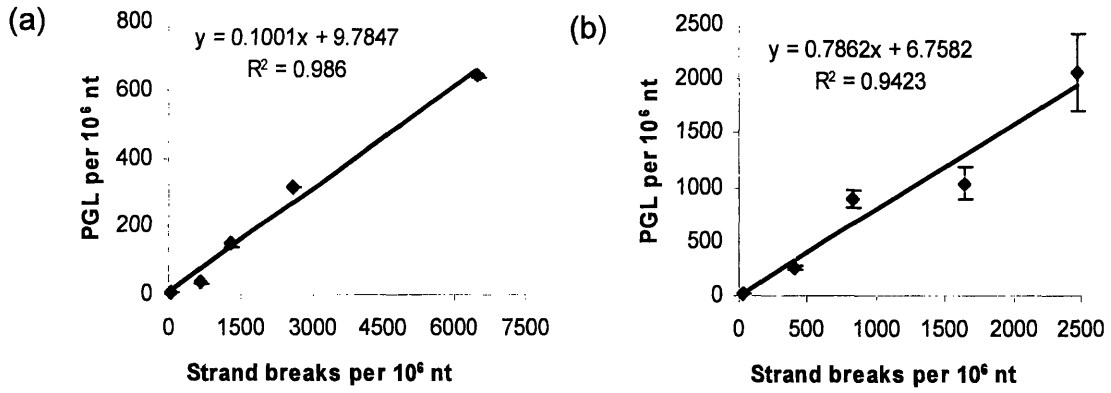

Figure 3-9. Correlation between PGL and deoxyribose oxidation events in DNA treated with (a) γ-radiation and (b) Fe(II) ·bleomycin.

3.3.4 4′-ketoaldehyde induced by Fe(II)·bleomycin and γ-radiation

(by Bingzi Chen)

Approximately 32 4′-ketoaldehyde abasic sites per 10^6 nucleotides of calf thymus DNA was formed for each μM of bleomycin and 13 4′-ketoaldehyde abasic sites per 10^6 nucleotides was formed for each Gray of γ-radiation. Fe(II)·bleomycin and γ-radiation dose response curves with the number of PGL molecules formed per 10^6 nucleotides are shown as Figure 3-10. upon correlation between 4′-ketoaldehyde abasic sites and strand breaks/abasic sites as measured by plasmid nicking assay, 4′-ketoaldehyde abasic sites account for 29% of the strand break and abasic sites induced by bleomycin, and 3.1% by γ-radiation.

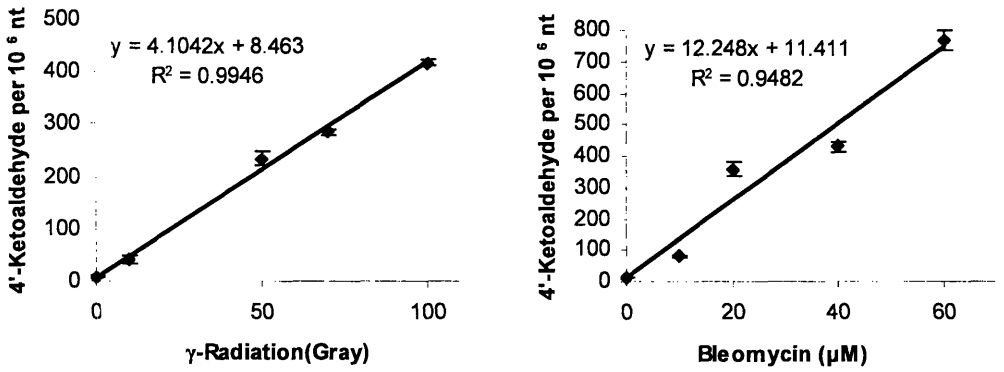

Figure 3-10. 4′-Ketoaldehyde abasic site dose response curves. HMP levels in bleomycin-mediated and γ-irradiated calf thymus DNA. HMP levels were determined in 250 μg of calf thymus DNA in potassium phosphate buffer (50 mM, pH = 7.4). DNA was subjected to various concentrations of bleomycin or 0 – 60 Gray of γ-radiation. The data are combined results of three separate experiments.

3.4. Discussion

In addition to the direct toxicity posed by strand breaks and abasic sites formed by DNA deoxyribose oxidation, there is growing evidence that electrophilic deoxyribose oxidation products react with DNA bases to form secondary adducts. One of the 4'-oxidation pathways produces PGL and base propenal (or MDA and base), which react with DNA to form M_1dG. The other identified 4'-oxidation pathway induces a formation of an unstable electrophile 4'-ketoaldehyde abasic site, which can react with a variety of nucleophiles (protein, DNA bases) to form crosslink products. In this chapter we have developed a sensitive and quantitative GC/MS

method to identify and quantify oxidation products from the 4′ sugar position of DNA, and have successfully defined the levels of 4'-oxidation relative to total DNA deoxyribose oxidation events.

Although the use of GC/MS for measurement of oxidative DNA damage has raised some questions due to the potential over-estimation of base and sugar damage caused by oxidation during derivatization, special care can be taken to minimize artifacts. For PGL analysis, our method circumvents the problem of artifact formation by separating the PGL from normal nucleotides using HPLC before derivatization. Online derivatization further eliminates the artifacts during silylation. Derivatization of 4′-keto-1′-aldehyde abasic sites using hydrazine was undertaken at ambient temperature. The assay is linear with regard to ketoaldehyde quantities from 0.5 pmoles to 10 nmoles and can detect as little as 100 fmoles of ketoaldehyde in a DNA sample.

γ-Radiation has been shown to induce oxidation at almost all deoxyribose positions with a variety of deoxyribose oxidation products. PGL has so far only been observed by ^{32}P-postlabeling assay [10]. Our studies show that ^{60}Co γ-radiation induced 13 PGL residues and 4.1 4'-ketoaldehyde abasic sites per 10^6 nucleotides per Gray. When compared to the total quantity of deoxyribose oxidation occurring under the same conditions (132 oxidation events per 10^6 nucleotides per Gray; determined by plasmid topoisomer analysis), PGL formation occurred in 10% of deoxyribose oxidation events. Using ^{32}P postlabeling assay, Weinfeld et al. showed that the 351 3'-phosphoglycolate residues per 10^6 nucleotides were induced by 50 Gray of r-radiation ($7/10^6$ nt/Gray), which is comparable to our GC/MS measurements resulting in $13/10^6$ nt/Gray [10]. We also developed a method to quantify MDA from DNA deoxyribose oxidation, which

will be discussed in detail in the next chapter. The results showed that γ-radiation induced free MDA formation at a rate of $10/10^6$ nt/Gray. Using a ^{137}Cs source, Rashid *et al.* showed that released MDA only accounts for ~70% for the total TBA reactive species generated by γ-radiation [15], while the other 30% is still DNA bound. This could explain why the free MDA level we measured as a thiobarbituric acid (TBA) derivative was slightly lower than the PGL detected. Although the relative ratio of PGL to 4'-ketoaldehyde abasic sites was never quantified, it is believed the PGL was the major product from C4'-oxidation under oxygen-rich environment. Our results are consistent with this belief with PGL formed at a rate 3 times faster than 4'-ketoaldehyde abasic sites.

Overall two C4'-oxidation pathways account for only 13% of the total deoxyribose oxidation damages. The dose-response for the formation of 5'-oxidative DNA minor damage, 5'-(2-phosphoryl-1,4-dioxobutane) was determined by Dr. Bingzi Chen *et al.* to be linear for γ-radiation, with ~6 lesions/10^6 nt/Gy, and nonlinear for Fe^{2+}-EDTA. A comparison of 5'-(2-phosphoryl-1,4-dioxobutane) formation to total deoxyribose oxidation suggests that γ-radiation produces ~0.04 lesions per deoxyribose oxidation event [3]. Goldberg and co-workers determined that approximately 10% of the 5'-oxidation chemistry produced by neocarzinostatin and calicheamicin partitions along the pathway leading to formyl phosphate and 5'-(2-phosphoryl-1,4-dioxobutane); the other ~90% of 5'-chemistry is comprised of the 5'-nucleoside-5'-aldehyde residue [16, 17]. This value suggests that 40% of the deoxyribose oxidation produced by γ-radiation arises from 5'-chemistry if the same ratio applies to γ-radiation. Our studies also show that ^{60}Co γ-radiation induced 1.5 PGA residues per 10^6 nucleotides per Gy. When compared to the total quantity of deoxyribose oxidation occurring under the same conditions, 3'-oxidation product PGA formation occured in 1% of total deoxyribose oxidation

events. This small fraction is consistent with models of limited solvent accessibility of the 3'-position of deoxyribose [7]. In a recent study, Roginskaya *et al.* showed that the C1'-oxidation lesion 5-methylene-2-furanone accounts for more than 30% of γ-radiation induced sugar damage, which is far more significant than predicted by the solvent exposure model [18, 19]. Interestinly, if the methylene-2-furanone indeed accounts for >30% of γ-radiation induced sugar damage, while 4'-oxidation accounts for 13%, the solvent exposure model alone may not explain the partition of DNA deoxyribose oxidation for γ-radiation as Tulius *et al.* proposed based on Fe(II)/EDTA results [20].

Bleomycin specifically targets the 4′ position of deoxyribose in DNA and induces the formation of both 3′-phosphoglycolate and 4′-ketoaldehyde abasic sites. To the best of our knowledge, no direct studies were conducted to study the partition between ketoaldehyde and phosphoglycolate pathways for beleomycin-induced damage, although 3′-phosphoglycolate is expected to be the major product under aerobic conditions in bleomycin-mediated damage under aerobic conditions. Our results clearly show that the relative amount of 3′-phosphoglycolate to 4′-ketoaldehyde abasic sites is 3:1, which is consistent with former estimation that PGL was the major product from C4'-oxidation in oxygen-rich environment [21].

3.5. Conclusion

In conclusion, our results corroborate the proposed 4′-position oxidation product formation pathways. We have developed novel and highly sensitive methods to quantify two 4′-deoxyribose (dR) oxidation products, 4′-ketoaldehyde abasic sites and 3′-phosphoglycolate, and

have successfully applied these methods to study DNA damage induced by γ-radiation, and Fe(II)· bleomycin. The results verify the hypothesis related to 4′- chemistry of dR oxidation in DNA. Combining these methods with quantification of total DNA deoxyribose oxidation events and quantification of products from other deoxyribose positions, they will offer valuable insights into the spectrum of DNA deoxyribose oxidation products and the chemical mechanisms behind the partitioning.

References

1. Lindahl, T., *Instability and decay of the primary structure of DNA.* Nature, 1993. **362**: p. 709-714.

2. Dedon, P.C. and S.R. Tannenbaum, *Reactive nitrogen species in the chemical biology of inflammation.* Arch Biochem Biophys, 2004. **423**(1): p. 12-22.

3. Chen, B.Z., et al., *5 '-(2-phosphoryl-1,4-dioxobutane) as a product of 5 '-oxidation of deoxyribose in DNA: Elimination as trans-1,4-dioxo-2-butene and approaches to analysis.* Chemical Research in Toxicology, 2004. **17**(11): p. 1406-1413.

4. Angeloff, A., et al., *Characterization of a 5 '-aldehyde terminus resulting from the oxidative attack at C5 ' of a 2-deoxyribose on DNA.* Chemical Research in Toxicology, 2001. **14**(10): p. 1413-1420.

5. Pratviel, G., et al., *Furfural as a Marker of DNA Cleavage by Hydroxylation at the 5' Carbon of Deoxyribose.* Angewandte Chemie-International Edition in English, 1991. **30**(6): p. 702-704.

6. Sitlani, A., et al., *DNA Photocleavage by Phenanthrenequinone Diimine Complexes of Rhodium(Iii) - Shape-Selective Recognition and Reaction.* Journal of the American Chemical Society, 1992. **114**(7): p. 2303-2312.

7. Collins, C., et al., *Analysis of 3'-phosphoglycolaldehyde residues in oxidized DNA by gas chromatography/negative chemical ionization/mass spectrometry.* Chem Res Toxicol, 2003. **16**(12): p. 1560-6.

8. Collins, C., et al., *Differential oxidation of deoxyribose in DNA by gamma and alpha-particle radiation.* Radiat Res, 2005. **163**(6): p. 654-62.

9. Frelon, S., et al., *High-performance liquid chromatography--tandem mass spectrometry measurement of radiation-induced base damage to isolated and cellular DNA.* Chem Res Toxicol, 2000. **13**(10): p. 1002-10.

10. Weinfeld, M. and K.J. Soderlind, *32P-postlabeling detection of radiation-induced DNA damage: identification and estimation of thymine glycols and phosphoglycolate termini.* Biochemistry, 1991. **30**(4): p. 1091-7.

11. Giloni, L., et al., *Bleomycin-Induced Strand-Scission of DNA - Mechanism of Deoxyribose Cleavage.* Journal of Biological Chemistry, 1981. **256**(16): p. 8608-8615.

12. Wang, P.G., et al., *2-Phosphoglycolate and glycolate-electrophore detection, including detection of 87 zeptomoles of the latter by gas chromatography electron-capture mass spectrometry.* Journal of Chromatography A, 1996. **721**(2): p. 289-296.

13. Chen, J.Y. and J. Stubbe, *Synthesis and characterization of oligonucleotides containing a 4 '-keto abasic site.* Biochemistry, 2004. **43**(18): p. 5278-5286.

14. Lopez-Larraza, D.M., K. Moore, and P.C. Dedon, *Thiols alter the partitioning of calicheamicin-induced deoxyribose 4 '-oxidation reactions in the absence of DNA radical repair.* Chemical Research in Toxicology, 2001. **14**(5): p. 528-535.

15. Rashid, R., et al., *Bleomycin versus OH-radical-induced malonaldehydic-product formation in DNA.* Int J Radiat Biol, 1999. **75**(1): p. 101-9.

16. Chin, D.H., L.S. Kappen, and I.H. Goldberg, *3'-Formyl Phosphate-Ended DNA - High-Energy Intermediate in Antibiotic-Induced DNA Sugar Damage.* Proceedings of the National Academy of Sciences of the United States of America, 1987. **84**(20): p. 7070-7074.

17. Dedon, P.C., Z.W. Jiang, and I.H. Goldberg, *Neocarzinostatin-Mediated DNA Damage in a Model Agt-Act Site - Mechanistic Studies of Thiol-Sensitive Partitioning of C4' DNA Damage Products.* Biochemistry, 1992. **31**(7): p. 1917-1927.

18. Roginskaya, M., et al., *The release of 5-methylene-2-furanone from irradiated DNA catalyzed by cationic polyamines and divalent metal cations.* Radiation Research, 2005. **163**(1): p. 85-89.

19. Roginskaya, M., Y. Razskazovskiy, and W.A. Bernhard, *2-Deoxyribonolactone lesions in X-ray-irradiated DNA: Quantitative determination by catalytic 5-methylene-2-furanone release.* Angewandte Chemie-International Edition, 2005. **44**(38): p. 6210-6213.

20. Pogozelski, W.K. and T.D. Tullius, *Oxidative Strand Scission of Nucleic Acids: Routes Initiated by Hydrogen Abstraction from the Sugar Moiety.* Chem Rev, 1998. **98**(3): p. 1089-1108.

21. Worth, L., et al., *Isotope Effects on the Cleavage of DNA by Bleomycin - Mechanism and Modulation.* Biochemistry, 1993. **32**(10): p. 2601-2609.

Chapter 4

Chemical and biological evidence for base propenals as the major source of M_1dG adducts in cellular DNA

The work in this chapter has been published in 'Zhou, X. F., Taghizadeh, K., and Dedon, P. C. (2005) Chemical and biological evidence for base propenals as the major source of the endogenous M(1)dG adduct in cellular DNA. *Journal of Biological Chemistry 280*, 25377-25382.'

Abstract

The endogenous DNA adduct, M_1dG, has been shown to arise *in vitro* in reactions of dG with malondialdehyde (MDA), a product of both lipid peroxidation and 4'-oxidation of deoxyribose in DNA, and with base propenals also derived from deoxyribose 4'-oxidation. We now report the results of cellular studies consistent with base propenals, not MDA, as the major source of M_1dG under biological conditions. As a foundation for cellular studies, M_1dG, base propenals and MDA were quantified in purified DNA treated with oxidizing agents known to produce deoxyribose 4'-oxidation. The results revealed a consistent pattern: Fe^{+2}-EDTA and γ-radiation generated MDA but not base propenals or M_1dG, while bleomycin and peroxynitrite ($ONOO^-$) both produced M_1dG as well as base propenals with no detectable MDA. These observations were then assessed in *E. coli* with controlled membrane levels of polyunsaturated fatty acids (PUFA). $ONOO^-$ treatment (2 mM) of cells containing no detectable PUFA (defined medium with 18:0/stearic acid) produced 6.5 M_1dG per 10^7 nt and no detectable lipid peroxidation products, including MDA, as compared to 3.8 M_1dG per 10^7 nt and 0.07 μg/mL lipid peroxidation products with control cells grown in a mixture of fatty acids (0.5% PUFA) mimicking Luria-Bertani medium. In cells grown with linoleic acid (18:2), the level of PUFA rose to 54% and the level of MDA rose to 0.14 μg/mL, while M_1dG fell to 1.4 per 10^7 nt. Parallel studies with γ-radiation revealed levels of MDA similar to those produced by $ONOO^-$ but no detectable M_1dG. These results are consistent with base propenals as the major source of M_1dG in this model cell system, and with a protective role for PUFA in cells exposed to oxidants.

4.1. Introduction

4.1.1 Sources of M_1dG

There is now substantial evidence linking reactive oxygen and nitrogen species to aging and chronic diseases [1], as illustrated by the epidemiological evidence associating chronic inflammation and increased cancer risk [2-5]. A variety of endogenous and exogenous oxidants react directly with bases in DNA to produce mutagenic lesions such as 8-oxo-dG and thymine glycol. The oxidants also react with lipids, carbohydrates and proteins to generate electrophilic species capable of reacting with DNA bases to form adducts. This is illustrated by the reaction of a metabolite of hydroxynonenal, a product of polyunsaturated fatty acid (PUFA) peroxidation, with dG, dA, and dC to form etheno adducts [6]. A similar argument has been made for the PUFA peroxidation product, malondialdehyde (MDA), which reacts *in vitro* with dG to form M_1dG, the exocyclic pyrimido[1,2-α]purin-10-(3H)-one adduct (Figure 4-1). Evidence has shown that over a range of MDA concentrations from 10 to 40 mM, the level of M_1G residues in bacterial *Salmonella typhimurium* DNA increased from 0.2 to $2.5/10^6$ base pairs [7].

Recent studies suggest that deoxyribose oxidation may be an alternative to lipid peroxidation as a source of DNA-reactive electrophiles. Oxidation of deoxyribose in DNA produces a variety of oxidized abasic sites and strand breaks with different sugar residues, many of which are electrophilic and thus capable of reacting with local nucleophiles to form adducts. For example, the β-elimination product of the 5'-(2-phosphoryl-1,4-dioxobutane) residue arising from 5'-oxidation of deoxyribose (*trans*-1,4-dioxo-2-butene) reacts with dG, dA and dC to form stable bicyclic adducts [8, 9]. Similarly, we demonstrated that the base propenal products of

deoxyribose 4'-oxidation, structural analogs of the enol tautomer of MDA (Figure 4-1), also react with DNA to form M_1dG [10], though with significantly greater efficiency than MDA [10, 11]. This may explain the 30- to 60-fold greater mutagenicity of base propenals than MDA [11].

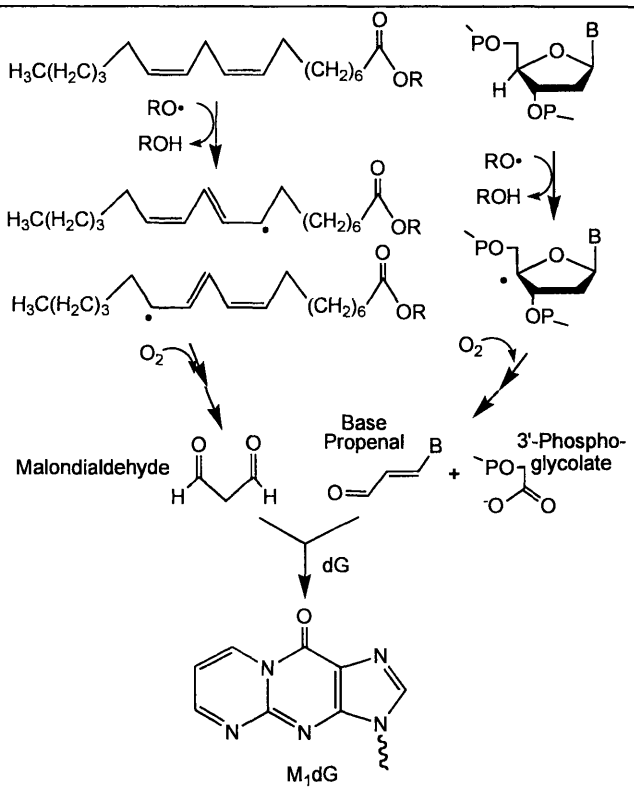

Figure 4-1. MDA from lipid peroxidation and base propenals from deoxyribose oxidation react with dG to form M_1dG.

4.1.2 Mutagenesis and repair of M_1dG

M_1dG is present in normal human tissues (liver, white blood cells, pancreas, and breast) at levels of 1-120 adducts per 10^8 nt [12]. Solution structures have shown that M_1dG maintains stacking interactions with neighboring bases but does not form Watson–Crick hydrogen bonds

[13]. When placed opposite to cytosine in duplex DNA, M_1dG spontaneously and quantitatively converts to the ring-opened derivative N^2-(3-oxo-1-propenyl)-dG, which is reversible upon thermal denaturation of the duplexes. M_1G has been shown to be highly mutagenic in bacteria and mammalian cells [14, 15] causing base pair substitutions, frameshift mutations and large insertions and deletions, as well as arresting transcription [16, 17]. For example, modified genomes containing a cytosine opposite M_1G resulted in roughly equal numbers of M_1G→A and M_1G→T mutations with few M_1G→C mutations [14]. M_1G induced frameshift mutations when positioned in a reiterated $(CpG)_4$ sequence but not when positioned in a nonreiterated sequence in Escherichia coli and in COS-7 cells [15].

Studies of site-specific mutagenesis indicate that M_1G is repaired by the nucleotide excision repair (NER) pathway in bacteria [14, 18]. Transformation of M13MB102 phase containing M_1G was introduced into *E. coli* strains deficient in individual genes of DNA repair. No effect on mutation frequency was observed when cells were defective in base excision repair enzyme formamidopyrimidine glycosylase or 3-methyladenine glycosylase. On the contrary, approximately a four-fold increase in mutation frequency was observed when M_1G-containing genomes were transformed into cells deficient in nucleotide excision repair (either *uvrA*$^-$ or *uvrB*$^-$) into NER deficient *E. coli* strains. These results indicate the importance of NER in the removal of M_1G relative to BER. Nevertheless, it has been proposed that *E. coli* MUG and human full-length ANPG proteins may play a role in the repair of six-membered exocyclic DNA adducts such as propano-dG [19], although their potential role in M_1G repair is not well studied. Therefore, M_1G repair mechanisms deserve further investigation.

4.1.3 M_1G/M_1dG Quantification

Because of the mutagenic nature of M_1G, major efforts have been devoted to quantify this exocyclic DNA adduct. Due to the low M_1G adduct level in cells, the quantification of M_1G had encountered some difficulty. In 1997, a sensitive immunoassay to detect MDA-DNA and MDA-RNA adducts was developed by Marnett and coworkers. Murine monoclonal antibodies reactive with the MDA-deoxyguanosine adduct 3-β-D-erythro-pentofuranosylpyrimido[1,2-a]purin-10(3H)-one (M_1dG) were prepared and characterized. A slot/dot blot assay using this antibody was developed and applied to quantify multiple samples with a sensitivity of less than 1 fmol [4]. A ^{32}P-postlabeling/HPLC assay was also developed for sensitive detection and quantification of M_1G in 1998 as well [14]. In 2004, Sun *et al.* further improved them method using monoclonal antibody (MAb D10A1) enrichment and O^4-ethylthymidine 3'-monophosphate as an internal standard [17, 20]. The detection limit in biological samples was ~200 amol of M_1G from 10 μg of DNA, corresponding to 6 adducts/10^9 nucleotides.

Gas chromatography/mass spectrometry with electron capture negative chemical ionization detection (GC/EC NCI/MS) has also been employed for the quantification of M_1G [21]. After DNA digestion, M_1dG was isolated from unmodified nucleosides using immunoaffinity column purification. The deoxyribose residue was then removed by acid hydrolysis; the M_1G base was derivatized with pentafluorobenzyl (PFB) bromide and subsequently quantified using GC/EC NCI/MS. This method has a detection limit of approximately $1/10^8$ nucleotides using 1 mg of DNA. Immunoaffinity purification in combination with tandem mass spectrometry (LC-MS/MS) provides specific identification with

limited sensitivity [22]. Upon reducing the double bond in the exocyclic ring of M_1dG to yield 5,6-dihydro derivative, Hoberg *et al.* was able to increase the sensitivity by 10 fold [23].

In the past few years, new LC-MS/MS methods were developed by quantifying M_1G as its oximine or hydrazone derivatives [24-26]. M_1G is a reactive electrophile that can react with hydroxylamine to form stable oximines at neutral pH, with amines to form unstable enaminoimine conjugates at basic pH, and with hydroxide to form N^2-(3-oxopropenyl)-G. Pentafluorophenylhydrazine was also shown to react rapidly with M_1G to form stable hydrazone, which can be purified and analyzed by LC-MS/MS. Such derivatization dramatically increases the sensitivity of LC-MS/MS analysis, giving it the potential to become a more standard method for M_1G quantification since it is more specific than slot blot assay/^{32}P post-labeling and is less prone to artifact than GC-MS analysis.

We now report the results of studies aimed at defining the source of M_1dG under biologically relevant conditions. We first performed studies with purified DNA and oxidants known to cause 4'-oxidation of deoxyribose to define the relationship between generation of base propenals and M_1dG formation. These observations were then assessed in *E. coli* cells in which the membrane content of PUFA was varied by growth in defined media. This model system provided an opportunity to compare MDA and M_1dG formation caused by exposure of the cells to different oxidants.

4.2. Materials and methods

4.2.1 Materials

All chemicals and reagents were of the highest purity available and were used without further purification unless noted otherwise. Adenine propenal was purchased from Salford Ultrafine Chemicals (Manchester, U.K.). Thymine propenal and cytosine propenal were synthesized using a published method [27]. Fatty acids, Bleomycin and calf thymus DNA were all purchased from Sigma Chemical Co. (St. Louis, MO). Nitrocellulose membrane was obtained from Schleicher and Schuell (Keene, NH). M_1dG monoclonal antibody and a lipid peroxidation kit were purchased from Oxford Biomedical Research (Oxford, MI Ion-exchange based genomic DNA kit was from Qiagen (Valencia, CA). Peroxynitrite ($ONOO^-$) was prepared by reaction of ozone with sodium azide as described by Pryor *et al.* and quantified spectrophotometrically in 0.1 M sodium hydroxide ($\varepsilon_{302} = 1670\ M^{-1}cm^{-1}$) (*27*).

4.2.2 Instrumental analyses

All HPLC analyses were performed on a Hewlett-Packard model 1100 HPLC system, equipped with a Vydac C18 reversed phase column (250 x 4.6 mm) and a 1040A diode array detector. Samples were resolved with the following gradient of acetonitrile in 10 mM sodium acetate buffer (pH 6.9): 0–18 min, 1-30%; 18-22 min, 30–50%; 22–30 min, 50–100%; 30–40 min, 100%. Gas chromatography (GC)/mass spectrometry [28] analyses of fatty acid methyl esters were performed on a Hewlett-Packard 5890 Series II Plus gas chromatograph equipped with a Hewlett-Packard 5872 mass selective detector. The operating parameters were as follows:

250 °C inlet (splitless mode); ionizing voltage, 70 eV; HP-5MS (cross-linked 5% Ph-Me Silicone) capillary column (0.25 mm x 30 m x 0.25 μm film thickness); oven temperature ramp of 10 °C/min from 100 to 310 °C.

4.2.3 Reaction of DNA with oxidizing agents

Calf thymus DNA was dissolved in Chelex-treated 50 mM potassium phosphate buffer (pH 7.4; see ref. [29] and aliquots were stored at -80 °C. For γ-irradiation, DNA was exposed to 0-200 Gy in a ^{60}Co source at 2 Gy/min. For Fe^{2+}/EDTA treatment, a freshly prepared $FeSO_4$/EDTA solution (20 mM) was diluted with water and 4 μL aliquots were added to the DNA solution (196 μL) to yield a final Fe^{2+}-EDTA concentration of 0-300 μM. For bleomycin treatment, 2 μL aliquots of an aqueous bleomycin solution (0-5 mM) were added to the DNA solution (196 μL) followed by addition of 2 μL aliquots of freshly prepared $Fe(NH_4)_2(SO_4)_2$ solution (0-5 mM) to initiate the DNA damage reaction. $ONOO^-$ damage reactions (0 to 300 μM) were carried out by adding 4 μL aliquots of the oxidant in 0.1 M NaOH to DNA dissolved in 100 mM potassium phosphate buffer (pH 6; higher buffer concentration and lower pH to compensate for the addition of 0.1 N NaOH). All DNA damage reactions were conducted at ambient temperature for 0.5 h followed by ultrafiltration using Microcon YM10 Centrifugal filters to separate MDA and base propenals from the DNA fragments.

4.2.4 Quantification of MDA and base propenals

The ultra-filtrate prepared from the *in vitro* reactions above or from cell suspensions exposed to $ONOO^-$ (*vide infra*) were resolved by HPLC and MDA and base propenals were isolated by collection of fractions bracketing their retention times: MDA, 6.4 min; C-propenal, 9.3 min; T-propenal, 13.0 min; A-propenal, 20.0 min. Following combination of the base propenal fractions, 1/25 volume of a thiobarbituric acid (TBA) suspension (10 mg/mL in 0.2 M HCl) was added to each MDA and base propenal solution, followed by heating to 90 °C for 30 min. The quantities of the identical MDA and base propenal derivatives of TBA were then determined by absorbance at 532 nm ($\varepsilon = 1.53 \times 10^5\ M^{-1}cm^{-1}$); if necessary, the TBA reaction solutions were concentrated under vacuum to increase the final concentration of the 532 nm-absorbing species.

As an alternative to the HPLC method for the cell studies (*vide infra*), MDA (free and bound to proteins or other biological molecules) and other analogous lipid peroxidation products were quantified using a lipid peroxidation kit from Oxford Biomedical Research (Oxford, MI). Cells were washed twice (2050xg, 15 min, 4 °C) with phosphate buffered saline (PBS; 10 mM potassium phosphate, 137 mM NaCl) and resuspended in 200 μL of water, followed by sequential addition of 50 μL of butylated hydroxytoluene (40 mM in ethanol), 600 μL of diluted R1 reagent (3:1 N-methyl-2-phenylindole in acetonitrile:ferrous iron in methanol), and 150 μL of 12 N HCl. The mixture was mixed by vortexing and incubated at 60 °C for 1 h, followed by centrifugation (16,100xg, 20 min) and removal of the supernatant for measurement of absorbance at 586 nm. A standard curve was prepared with solutions of 1,1,3,3-tetramethoxypropane (MDA precursor) in 200 μL of water.

4.2.5 Quantification of M_1dG

The M_1dG content of all DNA samples was measured by an immunoblot assay [11]. To construct standard curves, MDA-modified DNA (calibrated against a standard provided by Prof. Lawrence Marnett, Vanderbilt University) was diluted with calf thymus DNA to give 6.6 μg of DNA in 150 μL of PBS followed by sonication for 15 min at 4 °C, heating at 100 °C for 15 min, and cooling in ice water for 10 min. The solution was then immediately diluted by addition of 150 μL of 2 M cold ammonium acetate and 90 μL aliquots (2 μg DNA) were blotted in triplicate onto a nitrocellulose membrane using a BioRad BioDot Microfiltration System (Hercules, CA). The wells were washed twice with ammonium acetate (200 μL, 1 M) and the membrane was baked (80 °C, 90 min) and then blocked at ambient temperature for 1.5 h with PBS containing 0.1% Tween-20 and 5% nonfat dry milk. The membrane was washed twice for 5 min in blocking solution and then incubated with a 1:30000 dilution of anti-M_1dG monoclonal antibody (0.3 mg/mL stock) in blocking solution containing 0.5% milk. Following agitation for 30 min at ambient temperature and overnight at 4 °C, the membrane was washed with blocking solution (4 times, 5 min) and incubated at ambient temperature for 2 h with a 1:3000 dilution of goat anti-mouse IgG horseradish peroxidase conjugate in blocking solution containing 0.5% milk. The membrane was again washed (4 times, 5 min) with blocking solution followed by incubation in 10 mL of Super Signal West Dura substrate (Pierce Biotechnology, Rockford, IL) for 5 min. The chemiluminescence signal on the membrane was quantified using an Alpha Innotech Fluorochem CCD camera system (San Leandro, CA). The membrane was then washed in PBS overnight and stained with 5 μg/mL propidium iodide in PBS (3 h, ambient temperature, dark)

followed by washing in PBS and quantification of the fluorescence using the Alpha Innotech Fluorochem CCD camera system. Standard curves were prepared by plotting the adduct level against the enhanced chemiluminescence signal following normalization of the latter to the propidium iodide staining intensity. The M_1dG levels of unknown samples were based on standard curves analyzed in parallel on the same blot.

4.2.6 Modulation of the PUFA content of *E. coli*

E. coli strain DH5α was grown at 37 °C in medium E [30] supplemented with 0.5% glucose, 0.5% casamino acids, 0.0015% thiamine and fatty acids to a final, total concentration of 0.05 g/L. Fatty acids were added from stock solutions (100 mL, ethanol) with the following compositions: **Solution A**, 0.1 g each of lauric acid (12:0), myristic acid (14:0), palmitic acid (16:0), stearic acid (18:0), and oleic acid (18:1); **Solution B**, 0.5 g of stearic acid (18:0); **Solution C**, 0.5 g of linoleic acid (18:2). Cells cultured in media with the three different fatty acid compositions grew at the same rate (data not shown; OD_{600} doubling time ~1.8 h) and oxidant treatments were performed at a cell density of ~5 x 10^8 cells/mL (OD_{600} = 0.6).

The fatty acid composition of *E. coli* membranes was quantified by a modification of the method of Harley [31]. Following three washes in PBS (5000xg, 15 min, 4 °C), the cells were resuspended in 1 N KOH in 90% ethanol and heated for 1 h at 75 °C. The solution was filtered and 6 N HCl was added to the filtrate followed by two extractions with chloroform. The organic layers were combined and dried under a stream of N_2. To the white residue was added methanol and 12 N HCl (2:1 V/V) and the solution was refluxed at 75 °C for 1 h. The fatty acid methyl esters were extracted with petroleum ether, dried over anhydrous Na_2SO_4, concentrated under

vacuum and the fatty acid methyl ester composition was analyzed by GC/MS following injection of 1 μL samples. Fatty acids were identified by retention time and mass using standards and by matching data against a standard EI spectrum library. GC retention times: 14:0, 11.3 min; 16:1, 13.5 min; 16.0 13.8 min; Cy17:0 14.3 min; 18:2, 15:0 min; 18:1 15.1 min; 18:0 15.3 min.

4.2.7. γ-Radiation and ONOO- treatment of *E. coli*

Cells grown to a density of ~5 x 10^8/mL were washed three times in PBS and then resuspended (OD_{600} = 3) in 100 mM potassium phosphate buffer (pH 7). For γ-radiation, the cell suspension (5 mL) was irradiated (0-300 Gy) in a ^{60}Co-source at 2 Gy/min at ambient temperature. For $ONOO^-$, 4.5 mL of cell suspension was mixed with 170 μL of 0.2 M HCl (to neutralize the 0.1 M NaOH added with the ONOO-). This was followed quickly by addition of 0.33 mL of $ONOO^-$ solution (0-30 mM in 0.1 M NaOH; final $ONOO^-$ 0-2.2 mM) that was carefully transferred to the sidewall of a 15 mL conical tube wall and rapidly mixed with cell suspension by vortexing. The mixture was incubated at ambient temperature for 1 h. The treated *E. coli* suspensions were then washed once with PBS (2050xg, 15 min, 4 °C) and DNA was purified using a Qiagen Cell Culture DNA Midi Kit (Valencia, CA), precipitated with isopropanol, and washed with 70% cold ethanol. The DNA pellet was air-dried, resuspended in 200 μL of PBS and stored at -80 °C until used for the M_1dG immunoblot assay. For several samples of ONOO-treated *E. coli*, the exposed cells were pelleted by centrifugation and the supernatant subjected to YM-10 ultrafiltration as described earlier followed by quantification of MDA in the ultra-filtrate.

4.3. Results

4.3.1. Correlation of M1dG formation with MDA or base propenal in DNA

We first undertook experiments to define the deoxyribose 4'-oxidation chemistry for several oxidizing agents and to correlate these products with the formation of M_1dG. These studies are based on disparate reports that: (1) γ-radiation produces MDA rather than base propenals as the product of 4'-oxidation of deoxyribose that accompanies the 3'-phosphoglycolate residue [32]; (2) γ-radiation did not cause formation of M_1dG in DNA [10]; (3) Fe^{+2}-EDTA caused lower levels of M_1dG to form in DNA than did Fe^{+2}/H_2O_2 [33]; and (4) $ONOO^-$ caused formation of base propenals [34]. The goal was to define the relationship between M_1dG formation and the generation of MDA or base propenals by deoxyribose 4'-oxidants.

As shown in Figure 4-2, HPLC resolution provided a means to separate MDA and the base propenals for subsequent quantification by TBA derivatization. This method was used to quantify these species in the various DNA oxidation reactions, as shown in Figure 4-3. While G-propenal was not quantified in these studies due to the lack of a synthetic standard, quantification of the other three base propenals represents a rigorous metric since γ-radiation, Fe^{+2}-EDTA and $ONOO^-$ are sequence non-selective deoxyribose oxidants [35, 36] and bleomycin causes formation mainly of C- and T-propenals and some A-propenal [32]. The graphs in Figure 4-3 reveal that the various oxidizing agents produced either MDA or base propenals but did not simultaneously produce detectable levels of both products. It is also apparent that agents

producing base propenals also caused M_1dG formation and those agents that produced MDA did not.

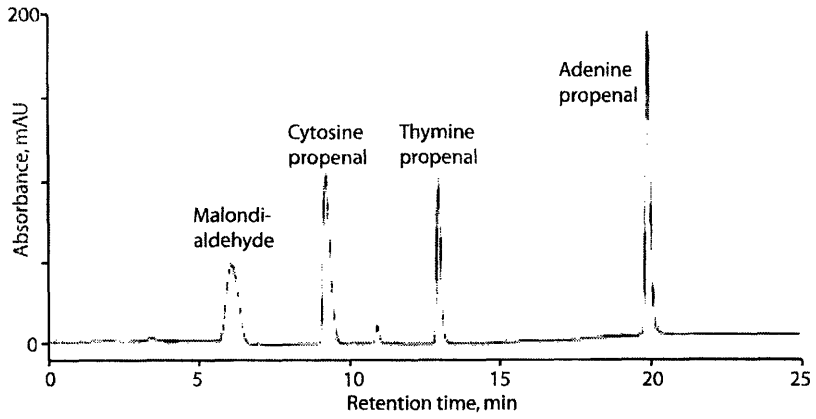

Figure 4-2. HPLC resolution of MDA and base propenals for post-column detection. This chromatograph was prepared by injection of chemical standards. See Materials and Methods for details.

For unknown reasons, we were unable to detect base propenals in the $ONOO^-$ reactions, in spite of the literature evidence for their formation [34]. That MDA was also not detected and that M_1dG formation occurred in the ONOO-treated DNA are both consistent with base propenal formation in light of definitive evidence for formation of the 3'-phosphoglycolate residue, the 4'-oxidation partner to base propenals and MDA [36]. One possible explanation for this discrepancy involves nucleophilic destruction of the base propenals by high concentrations of nitrite, which is more nucleophilic than imidazole and pyridine [37] and, along with nitrate, is a major degradation product of $ONOO^-$ at millimolar concentrations [38]. Alternatively, high

concentrations of $ONOO^-$ could oxidize base propenals arising from initial deoxyribose oxidation, a conclusion supported by the non-linear formation of M_1dG apparent in Figure 4-3D.

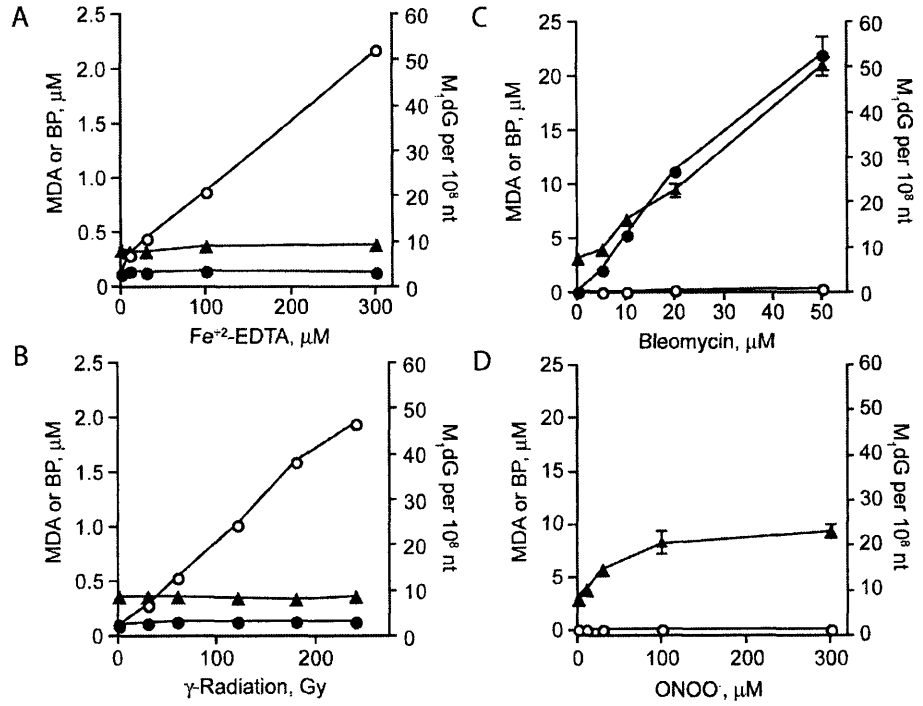

Figure 4-3. Correlation between M_1dG and the generation of either MDA or base propenals in purified DNA treated with different oxidants. (A) Fe^{+2}-EDTA; (B) γ-radiation; (C) Fe^{+2}-bleomycin; and (D) $ONOO^-$. Reactions were performed as described in Materials and Methods.

4.3.2 Control of the fatty acid composition of *E. coli* membranes

As a model system to define the role of PUFA-derived MDA in M_1dG formation, DH5α *E. coli* was cultured in defined media containing different fatty acids. As shown in Table 1, GC-MS analysis of *E. coli* extracts revealed a PUFA content consistent with the growth conditions.

While cells grown in the 18:0-enriched medium did not contain detectable PUFA, the level of PUFA increased to 53.9% of fatty acid content for cells grown in the 18:2-medium (Table 1). This level of linoleic acid incorporation is similar to that reported by Harley *et al.* (45%) for experiments performed with an unsaturated fatty acid auxotroph of *E. coli* [39]. As expected, an intermediate level of PUFA was present in the medium containing a mixture of fatty acids.

Table 4-1. Fatty acid composition (mole %) of *E. coli* cells grown in defined media.

	Fatty Acid Supplement[1]		
Component	Mixture	18:0	18:2
14:0	4.1	3.0	1.5
16:1	13	9.1	3.3
16:0	52	28	24
Cy17:0[2]	3.9	3.3	5.7
18:2	0.5	n.d.[2]	54
18:1	20	3.4	9.5
18:0	6.2	53	1.6
Total % UFA[2]	33	12	67
% PUFA[2]	0.5	n.d.[2]	54

[1] Sole fatty acid source in defined culture media (see Materials and Methods)

[2] Abbreviations: n.d., not detected; Cy17:0, *cis*-9,10-methylene hexadecanoic acid; UFA, unsaturated fatty acid..

Attempts to grow *E. coli* DH5α in minimal media containing linolenate (18:3) or arachidonate (20:4) were unsuccessful in that the membrane levels of both fatty acids fell below the detection limit of the GC/MS assay. One possible explanation for this result is that, unlike the unsaturated fatty acid auxotrophs used in the studies of Harley *et al.* [39] for example, *E. coli* DH5α is able to metabolize PUFA and thus possibly maintained low levels of 18:3 and 20:4.

4.3.3 Correlation of M1dG formation with oxidant-induced lipid peroxidation in *E. coli*

To assess the role of MDA in the formation of M_1dG in living cells, *E. coli* grown in the three defined media were treated with γ-radiation or $ONOO^-$ and the level of M_1dG quantified by an immunoblot assay. As shown in Figure 4-4, $ONOO^-$ treatment of *E. coli* grown in the absence of PUFA led to a dose-dependent increase in M_1dG, which is consistent with the results obtained with purified DNA (Figure 4-3D). It is also apparent that there is an inverse correlation between PUFA content and M_1dG formation (Figure 4-4D), while there is a direct correlation between PUFA content and MDA formation, as expected (Figure 4-4C).

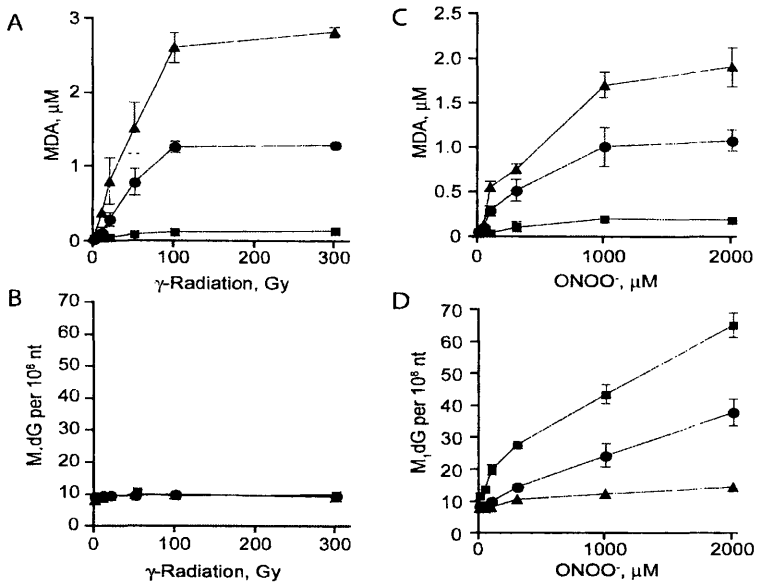

Figure 4-4. Correlation between M_1dG (B,D) and lipid peroxidation (A,C) in *E. coli* with controlled levels of PUFA and treated with either (A,B) γ-radiation or (C,D) $ONOO^-$. *E. coli* grown in defined medium containing a mixture of fatty acids (●), stearic acid (■; 18:0) or linoleic acid (▲; 18:2) were treated with oxidants. M_1dG, MDA and lipid peroxidation products were quantified as described in Materials and Methods.

Exposure to γ-radiation did not induce detectable levels of M_1dG in *E. coli* grown in any of the fatty acid conditions (Figure 4-4B), which is again consistent with the *in vitro* results (Figure 4-3). However, γ-radiation did produce MDA, as a result of lipid peroxidation, in amounts directly proportional to the PUFA content of the cells (Figure 4-4A). Similar results were obtained by treating the three cell types with hydrogen peroxide with or without added Fe^{+2}.

4.4. Discussion

There is strong evidence for the existence of a host of endogenous DNA adducts (reviewed in ref. [40]), yet the mechanisms of their formation have not been rigorously defined. The goal of the present studies was to address this problem for M_1dG. The chemical species known to form M_1dG *in vitro*, namely MDA and base propenals, arise from different sources. Lipids represent a major target for free radicals [41] and peroxidation of PUFA generates a host of reactive electrophiles, many of which have been implicated in the formation of DNA adducts, such as the etheno adducts of dG, dA, and dC [42]. In a similar manner, MDA is ubiquitously present in cells and tissues and has been demonstrated to react with dG to form M_1dG *in vitro* [43-45], hence the proposal that it is involved in M_1dG formation *in vivo* [12, 46, 47]. However, the enol form of MDA, β-hydroxyacrolein is a weak acid with pKa 4.6, so most MDA exists in the form of negative charged salt at physiological PH, which not only has poor access to negatively-charged DNA backbone, but only diminishes its capacity as an electrophile We previously demonstrated that base propenals derived from deoxyribose 4'-oxidation in DNA served as an alternative source of M_1dG [10, 48]. The higher reactivity of base propenals than MDA toward dG (>100-fold; refs. [10, 48]) and their proximity to guanine bases in DNA suggested that base propenals might be a significant source of M_1dG formation *in vivo*. The results of the present studies support this conclusion.

As a foundation for interpretation of results obtained *in vivo*, a systematic comparison of the DNA 4'-oxidation chemistry caused by bleomycin, γ-radiation, Fe^{+2}-EDTA and $ONOO^-$ confirmed fragmentary observations in the literature and revealed a trend that amounts to a third pathway for 4'-oxidation chemistry in DNA. Treatment of DNA with bleomycin and $ONOO^-$

gives rise to base propenals (Figure 4-3; ref. [49]) in addition to 3'-phosphoglycolate residues [36, 50], but did not yield detectable amounts of MDA. On the other hand, γ-radiation and Fe^{+2}-EDTA produce damage consisting of 3'-phosphoglycolate residues (reviewed in ref. [51]) and MDA but no detectable base propenals (Figure 4-3). The results with γ-radiation confirm the observations of von Sonntag and coworkers [32], with the Fe^{+2}-EDTA results extending this novel partitioning of 4'-oxidation of deoxyribose to another commonly used DNA oxidant. At least with this small set of oxidizing agents, the partitioning between base propenals and MDA appears to be complete, with no detectable amount of the other species being formed.

The chemical basis for the two phosphoglycolate-generating pathways is not known and is not apparent from the currently proposed mechanisms for 4'-oxidation chemistry [50, 52]. However, there is one mechanistic distinction between the two sets of oxidants used in the present studies. Current evidence suggests that DNA-bound bleomycin participates in the subsequent chemistry of the deoxyribose oxidation it initiates [53, 54], while degradation of $ONOO^-$ simultaneously produces both hydroxyl radical and nitrogen dioxide radical (reviewed in ref. [55]). In both cases, secondary reactions with the oxidants, or degradation products of the oxidants, could alter the chemistry subsequent to formation of the 4'-carbon radical. On the other hand, the negative charge of Fe^{+2}-EDTA likely precludes any binding interaction with DNA, and thus any chemical cycling of oxidant or its derivatives. Furthermore, neither the sparsely ionizing γ-radiation nor Fe^{+2}-EDTA simultaneously produces significant amounts of other DNA-proximate radical species that could participate in the deoxyribose degradation. This model can be tested by comparing other soluble and DNA-binding oxidants capable of 4'-oxidation of deoxyribose.

Kadlubar et al. studied DNA adduct levels associated with oxidative stress in human pancreases. They found no correlation in adduct levels between εdC or εdA and M_1dG. However, there was a significant correlation between the levels of 8-oxodG and M_1dG. These results indicate that the MDA derived from lipid peroxidation may not contribute significantly to M_1dG formation and are consistent with the hypothesis that M_1dG is formed primarily through DNA damage [12].

Whatever the basis for the different DNA oxidation chemistries, the results from purified DNA serve as a benchmark for interpreting the studies in *E. coli*. The fatty acid requirements of *E. coli* and *S. cerevisiae* differ from those of mammalian cells in that they do not require PUFA for growth and their membranes normally contain mainly saturated and monounsaturated fatty acids [56, 57]. (The observation by Fridovich and coworkers that *E. coli* synthesize linoleic acid during late stationary phase [58] has been shown to be an artifact of contamination [59]). However, these organisms readily incorporate PUFA into cell membranes when the fatty acids are supplied in the growth medium [39, 60]. Upon challenge with oxidizing agents, the PUFA undergo peroxidation that results in the formation of thiobarbiturate-reactive species (*e.g.*, MDA) [39, 60], products that are not generated when PUFA are not provided [58, 60]. We were able control the levels of PUFA as indicated by the GC/MS analysis presented in Table 4-1, which confirmed an absence of PUFA in the stearate-containing medium, intermediate levels in the fatty acid mixture and high levels in the linoleate-containing medium. The choice of linoleic acid is based on the fact that it is the major PUFA in mammalian cell membranes (*e.g.*, ref. [61]). While it has been claimed that linoleate peroxidation does not produce MDA [62, 63], recent studies using more rigorous analytical methods proved that MDA formation does occur [64, 65].

In a similar manner, we used HPLC with post-column detection to quantify MDA in suspensions of linoleic acid-labeled *E. coli*.

This well characterized model cell system was used to assess the role of MDA in the formation of M_1dG, with two important observations. The first involves an inverse relationship between the level of lipid peroxidation, as measured by both MDA formation and generation of thiobarbiturate-reactive species, and the level of M_1dG in DNA from $ONOO^-$ exposed cells (Figure 4-4). If MDA were responsible for the bulk of M_1dG formation, then a direct relationship would be expected. A lack of correlation between M_1dG and lipid peroxidation, however, is consistent with deoxyribose oxidation and base propenals as the source of M_1dG in the *E. coli* cells. The results with γ-irradiation further strengthen this argument. There was a high level of MDA produced upon irradiation of the 18:2-labeled cells yet no increase in M_1dG in any of the three cell cultures. This is entirely consistent with the results obtained with purified DNA (Figure 4-3; refs. [10, 32], in which γ-irradiation caused MDA formation but not base propenals or M_1dG. The results suggest that lipid peroxidation alone is insufficient to induce M_1dG formation if the oxidizing reagent cannot generate base propenals by direct oxidation of deoxyribose in DNA.

It is important to point out that our results do not rule out MDA as a source of M_1dG in human cells. Indeed, we have observed that exposure of *E. coli* to 10 mM MDA (37 °C, 24 hr) caused a doubling of the M_1dG adduct level to 2 lesions per 10^7 nt (Zhou and Dedon, unpublished observations), which is similar to the trebling of the M_1dG level (1.2 to 3.9 per 10^7 nt) observed by Marnett and coworkers in studies of *S. typhimurium* exposed to 10 mM MDA [7]. However, given the small increases in M_1dG occurring with these highly non-physiological

MDA concentrations, we argue that base propenals arising from oxidative DNA damage make the major contribution to the cellular burden of M_1dG. This model is supported by the lack of a correlation between M_1dG and lipid peroxidation-derived etheno adducts and by the positive correlation between M_1dG and 8-oxodG, a DNA oxidation product, in human pancreas [12]. Similar results have been obtained in the SJL/RcsX mouse model of nitric oxide overproduction, in which it was observed that εdA adducts increase several-fold in inflamed spleens [66]; while M_1dG levels were unchanged from values obtained in non-inflamed mice (as detailed in chapter 5).

The second notable observation was the apparent protective effect of PUFA with regard to M_1dG formation. There are several possible explanations for the observed inverse correlation between PUFA content and M_1dG formation. One involves differences in the rate of uptake of $ONOO^-$ into cells containing different levels of PUFA. Increases in membrane fluidity caused by incorporation of PUFA into *E. coli* membranes have been shown to increase the rate of diffusion of glycerol into the cells. However, if $ONOO^-$ behaved in a similar manner, we would have expected an increase in M_1dG formation in the 18:2-labeled cells due to an increase in the quantity of intracellular $ONOO^-$; this assumes that M_1dG is derived from DNA oxidation. The most likely explanation for the results with $ONOO^-$ involves preferential reaction of $ONOO^-$ with the PUFA either as a result of a first-encounter phenomenon as the $ONOO^-$ diffuses into the cells or as a result of a thermodynamic preference for reaction of $ONOO^-$ with PUFA compared to deoxyribose in DNA. The greater reactivity of PUFA can be rationalized by the stability conferred to the initial oxidant-induced radical by the conjugated system carbon-carbon double-bonds that define PUFA. Such electron delocalization is not possible with a radical centered at the 4'-position in deoxyribose.

A recent paper from Swenberg research group yielded similar results for in *vitro* studies [26]. They showed that the addition of PUFAs to CF-DNA inhibits the M_1dG induction by oxidant mixture NAD(P)H/$CuCl_2$/H_2O_2 . The number of M_1dG in the DNA was decreased by 75, 64 and 40%, respectively, when the methyl esters of linoleic, linolenic, or arachidonic acid were added to the reaction mixtures. The results also showed that M_1dG from lipid peroxidation accounted for less than 10% of total M_1dG in an oxidant-induced linoleic/DNA mixture, which indicates both DNA deoxyribose oxidation as a major source and MDA from lipid peroxidation as a possible minor source for M_1dG formation.

4.5. Conclusion

In conclusion, the results from studies in purified DNA and an *E. coli* model suggest that base propenals, and not MDA, are the major source of M_1dG in biological systems. Furthermore, PUFA appear to protect from M_1dG formation, possibly by virtue of their location in cells relative to DNA or their higher reactivity with oxidants than deoxyribose in DNA.

References

1. Klaunig, J.E. and L.M. Kamendulis, *The role of oxidative stress in carcinogenesis.* Annu Rev Pharmacol Toxicol, 2004. **44**: p. 239-67.
2. Ohshima, H., M. Tatemichi, and T. Sawa, *Chemical basis of inflammation-induced carcinogenesis.* Arch Biochem Biophys, 2003. **417**(1): p. 3-11.
3. Ohshima, H., *Genetic and epigenetic damage induced by reactive nitrogen species: implications in carcinogenesis.* Toxicol Lett, 2003. **140-141**: p. 99-104.
4. Balkwill, F. and A. Mantovani, *Inflammation and cancer: back to Virchow?* Lancet, 2001. **357**(9255): p. 539-45.
5. Shacter, E. and S.A. Weitzman, *Chronic inflammation and cancer.* Oncology (Huntingt), 2002. **16**(2): p. 217-26, 229; discussion 230-2.
6. Chung, F.-L., H.-J.C. Chen, and R.G. Nath, *Lipid peroxidation as a potential endogenous source for the formation of exocyclic DNA adducts.* Carcinogenesis, 1996. **17**(10): p. 2105-2111.
7. Sevilla, C.L., et al., *Development of monoclonal antibodies to the malondialdehyde-deoxyguanosine adduct, pyrimidopurinone.* Chem Res Toxicol, 1997. **10**(2): p. 172-80.
8. Gingipalli, L. and P.C. Dedon, *Reaction of cis- and trans-2-butene-1,4-dial with 2 '-deoxycytidine to form stable oxadiazabicyclooctaimine adducts.* Journal of the American Chemical Society, 2001. **123**(11): p. 2664-2665.
9. Byrns, M.C., D.P. Predecki, and L.A. Peterson, *Characterization of nucleoside adducts of cis-2-butene-1,4-dial, a reactive metabolite of furan.* Chemical Research in Toxicology, 2002. **15**(3): p. 373-379.
10. Dedon, P.C., et al., *Indirect mutagenesis by oxidative DNA damage: formation of the pyrimidopurinone adduct of deoxyguanosine by base propenal.* Proc Natl Acad Sci U S A, 1998. **95**(19): p. 11113-6.
11. Plastaras, J.P., et al., *Reactivity and mutagenicity of endogenous DNA oxopropenylating agents: base propenals, malondialdehyde, and N(epsilon)-oxopropenyllysine.* Chem Res Toxicol, 2000. **13**(12): p. 1235-42.
12. Kadlubar, F.F., et al., *Comparison of DNA adduct levels associated with oxidative stress in human pancreas.* Mutat Res, 1998. **405**(2): p. 125-33.
13. Mao, H., et al., *Solution structure of an oligodeoxynucleotide containing the malondialdehyde deoxyguanosine adduct N-2-(3-oxo-1-propenyl)-dG (ring-opened M(1)G) positioned in a (CpG)(3) frameshift hotspot of the Salmonella typhimurium hisD3052 gene.* Biochemistry, 1999. **38**(41): p. 13491-13501.
14. Fink, S.P., G.R. Reddy, and L.J. Marnett, *Mutagenicity in Escherichia coli of the major DNA adduct derived from the endogenous mutagen malondialdehyde.* Proc Natl Acad Sci U S A, 1997. **94**(16): p. 8652-7.

15. VanderVeen, L.A., et al., *Induction of frameshift and base pair substitution mutations by the major DNA adduct of the endogenous carcinogen malondialdehyde.* Proceedings of the National Academy of Sciences of the United States of America, 2003. **100**(24): p. 14247-14252.

16. Niedernhofer, L.J., et al., *Malondialdehyde, a product of lipid peroxidation, is mutagenic in human cells.* Journal of Biological Chemistry, 2003. **278**(33): p. 31426-31433.

17. Cline, S.D., et al., *Malondialdehyde adducts in DNA arrest transcription by T7 RNA polymerase and mammalian RNA polymerase II.* Proceedings of the National Academy of Sciences of the United States of America, 2004. **101**(19): p. 7275-7280.

18. Johnson, K.A., S.P. Fink, and L.J. Marnett, *Repair of propanodeoxyguanosine by nucleotide excision repair in vivo and in vitro.* J Biol Chem, 1997. **272**(17): p. 11434-8.

19. Saparbaev, M., et al., *1,N-2-ethenoguanine, a mutagenic DNA adduct, is a primary substrate of Escherichia coli mismatch-specific uracil-DNA glycosylase and human alkylpurine-DNA-N-glycosylase.* Journal of Biological Chemistry, 2002. **277**(30): p. 26987-26993.

20. Sun, X., J. Nair, and H. Bartsch, *A modified immuno-enriched P-32-postlabeling method for analyzing the malondialdehyde-deoxyguanosine adduct, 3-(2-deoxy-beta-D-erythro-pentofuranosyl)-pyrimido [1,2-alpha]purin-10(3H)one in human tissue samples.* Chemical Research in Toxicology, 2004. **17**(2): p. 268-272.

21. Rouzer, C.A., et al., *Analysis of the malondialdehyde-2'-deoxyguanosine adduct pyrimidopurinone in human leukocyte DNA by gas chromatography/electron capture/negative chemical ionization/mass spectrometry.* Chem Res Toxicol, 1997. **10**(2): p. 181-8.

22. Otteneder, M., et al., *Development of a method for determination of the malondialdehyde-deoxyguanosine adduct in urine using liquid chromatography-tandem mass spectrometry.* Analytical Biochemistry, 2003. **315**(2): p. 147-151.

23. Hoberg, A.M., et al., *Measurement of the malondialdehyde-2 '-deoxyguanosine adduct in human urine by immunoextraction and liquid chromatography/atmospheric pressure chemical ionization tandem mass spectrometry.* Journal of Mass Spectrometry, 2004. **39**(1): p. 38-42.

24. Jeong, Y.C., et al., *Pyrimido[1,2-a]-purin-10(3H)-one, M1G, is less prone to artifact than base oxidation.* Nucleic Acids Res, 2005. **33**(19): p. 6426-34.

25. Jeong, Y.C., et al., *Analysis of M(1)G-dR in DNA by aldehyde reactive probe labeling and liquid chromatography tandem mass spectrometry.* Chemical Research in Toxicology, 2005. **18**(1): p. 51-60.

26. Jeong, Y.C. and J.A. Swenberg, *Formation of M1G-dR from endogenous and exogenous ROS-inducing chemicals.* Free Radic Biol Med, 2005. **39**(8): p. 1021-9.

27. Johnson, F., et al., *Synthesis and biological activity of a new class of cytotoxic agents: N-(3-oxoprop-1-enyl)-substituted pyrimidines and purines.* J Med Chem, 1984. **27**(8): p. 954-8.

28. Delaney, J.C., et al., *AlkB reverses etheno DNA lesions caused by lipid oxidation in vitro and in vivo.* Nature Structural & Molecular Biology, 2005. **12**(10): p. 855-860.

29. Collins, C., et al., *Analysis of 3'-phosphoglycolaldehyde residues in oxidized DNA by gas chromatography/negative chemical ionization/mass spectrometry.* Chem Res Toxicol, 2003. **16**(12): p. 1560-6.

30. Vogel, H.J. and D.M. Bonner, *Acetylornithinase of Escherichia coli: partial purification and some properties.* J Biol Chem, 1956. **218**(1): p. 97-106.

31. Harley, J.B., et al., *Dependence of Escherichia coli hyperbaric oxygen toxicity on the lipid acyl chain composition.* J Bacteriol, 1978. **134**(3): p. 808-20.

32. Rashid, R., et al., *Bleomycin versus OH-radical-induced malonaldehydic-product formation in DNA.* Int J Radiat Biol, 1999. **75**(1): p. 101-9.

33. Frelon, S., et al., *High-performance liquid chromatography--tandem mass spectrometry measurement of radiation-induced base damage to isolated and cellular DNA.* Chem Res Toxicol, 2000. **13**(10): p. 1002-10.

34. Yermilov, V., et al., *Effects of carbon dioxide/bicarbonate on induction of DNA single-strand breaks and formation of 8-nitroguanine, 8-oxoguanine and base propenal mediated by peroxynitrite.* FEBS Lett., 1996. **399**: p. 67-70.

35. Tullius, T.D., *Chemical snapshots of DNA: using hydroxyl radical to study the structure of DNA and DNA-protein complexes.* Trends Biochem Sci., 1987. **12**: p. 297-300.

36. Tretyakova, N.Y., et al., *Peroxynitrite-induced reactions of synthetic oligonucleotides containing 8-oxoguanine.* Chem Res Toxicol, 1999. **12**(5): p. 459-66.

37. Pearson, R.G., H. Sobel, and J. Songstad, *Nucleophilic reactivity constants toward methyl iodide and trans-[Pt(py)$_2$Cl$_2$].* J Am Chem Soc, 1968. **90**: p. 319.

38. Kissner, R. and W.H. Koppenol, *Product distribution of peroxynitrite decay as a function of pH, temperature, and concentration.* J Am Chem Soc, 2002. **124**(2): p. 234-9.

39. Harley, J.B., et al., *Dependence of Escherichia coli hyperbaric oxygen toxicity on the lipid acyl chain composition.* J. Bacteriol., 1978. **134**(5): p. 808-820.

40. De Bont, R. and N. van Larebeke, *Endogenous DNA damage in humans: a review of quantitative data.* Mutagenesis, 2004. **19**(3): p. 169-85.

41. Dix, T.A. and J. Aikens, *Mechanisms and biological relevance of lipid peroxidation initiation.* Chem Res Toxicol, 1993. **6**(1): p. 2-18.

42. Marnett, L.J. and P.C. Burcham, *Endogenous DNA adducts: Potential and paradox.* Chem. Res. Tox., 1993. **6**: p. 771-785.

43. Basu, A.K., P. Weller, and L.J. Marnett, *Modification of Purine Nucleosides by Malondialdehyde and Beta-Substituted Acroleins.* Proceedings of the American Association for Cancer Research, 1984. **25**(Mar): p. 88-88.

44. Singer, B., et al., *Both Purified Human 1,N(6)-Ethenoadenine-Binding Protein and Purified Human 3-Methyladenine-DNA Glycosylase Act on 1,N(6)-Ethenoadenine and 3-Methyladenine.* Proceedings of the National Academy of Sciences of the United States of America, 1992. **89**(20): p. 9386-9390.

45. Chaudhary, A.K., et al., *Detection of endogenous malondialdehyde-deoxyguaninosine adducts in human liver.* Science, 1994. **265**(September 9): p. 1580-1582.

46. Rouzer, C.A., et al., *Analysis of malondialdehyde-2'-deoxyguanosine adduct pyrimidopurinone in human leukocyte DNA by gas chromatography/electron capture/negative chemical ionization/mass spectrometry.* Chem. Res. Toxicol., 1997. **10**(2): p. 181-188.

47. Sharma, R.A., et al., *Cyclooxygenase-2, malondialdehyde and pyrimidopurinone adducts of deoxyguanosine in human colon cells.* Carcinogenesis, 2001. **22**(9): p. 1557-60.

48. Plastaras, J.P., P.C. Dedon, and L.J. Marnett, *Effects of DNA structure on oxopropenylation by the endogenous mutagens malondialdehyde and base propenal.* Biochemistry, 2002. **41**(15): p. 5033-42.

49. Rubio, J., V. Yermilov, and H. Ohshima, *DNA damage induced by peroxynitrite: Formation of 8-nitroguanine and base propenals.*, in *The Biology of Nitric Oxide*, S. Moncada, et al., Editors. 1996, Portland Press: London. p. 34.

50. Dedon, P.C. and I.H. Goldberg, *Free-radical mechanisms involved in the formation of sequence-dependent bistranded DNA lesions by the antitumor antibiotics bleomycin, neocarzinostatin, and calicheamicin.* Chem Res Toxicol, 1992. **5**(3): p. 311-32.

51. Pogozelski, W.K. and T.D. Tullius, *Oxidative strand scission of nucleic acids: Routes initiated by hydrogen atom abstraction from the sugar moiety.* Chem. Rev., 1998. **98**: p. 1089-1107.

52. Stubbe, J. and J.W. Kozarich, *Mechanisms of bleomycin-induced DNA degradation.* Chem. Rev., 1987. **87**: p. 1107-1136.

53. Steighner, R.J. and L.F. Povirk, *Bleomycin-induced DNA lesions at mutational hot spots: Implications for the mechanism of double-strand cleavage.* Proc. Natl. Acad. Sci. USA, 1990. **87**: p. 8350-8354.

54. Wu, W., et al., *Interaction of Co-Center-Dot-Bleomycin a2 (Green) with D(Ccaggcctgg)(2) - Evidence for Intercalation Using 2D Nmr.* Journal of the American Chemical Society, 1994. **116**(23): p. 10843-10844.

55. Dedon, P.C. and S.R. Tannenbaum, *Reactive nitrogen species in the chemical biology of inflammation.* Archives of Biochemistry and Biophysics, 2004. **423**(1): p. 12-22.

56. Avery, S.V., N.G. Howlett, and S. Radice, *Copper toxicity towards Saccharomyces cerevisiae: Dependence on plasma membrane fatty acid composition.* Appl. Environ. Microbiol., 1996. **62**(11): p. 3960-3966.

57. Raetz, C.R.H. and W. Dowhan, *Biosynthesis and function of phospholipids of Escherichia coli.* J. Biol.Chem., 1990. **265**: p. 1235-1238.

58. Rabinowitch, H.D., et al., *Escherichia coli produces linoleic acid during late stationary phase.* J. Bacteriol., 1993. **175**(17): p. 5342-5328.

59. Cronan, J.E. and C.O. Rock, *The presence of linoleic acid in Escherichia coli cannot be confirmed.* J. Bacteriol., 1994. **176**(10): p. 3069-3071.

60. Howlett, N.G. and S.V. Avery, *Induction of lipid peroxidation during heavy metal stress in Saccharomyces cerevisiae and influence of plasma membrane fatty acid unsaturation.* Appl. Environ. Microbiol., 1997. **63**(8): p. 2971-2976.

61. Esterbauer, H., et al., *The role of lipid peroxidation and antioxidants in oxidative modification of LDL.* Free Radic Biol Med, 1992. **13**(4): p. 341-90.

62. Pryor, W.A., J.P. Stanley, and E. Blair, *Autoxidation of polyunsaturated fatty acids: II. A suggested mechanism for the formation of TBA-reactive materials from prostaglandin-like endoperoxides.* Lipids, 1976. **11**(5): p. 370-9.

63. Esterbauer, H. and K.H. Cheeseman, *Determination of aldehydic lipid peroxidation products: malonaldehyde and 4-hydroxynonenal.* Methods Enzymol, 1990. **186**: p. 407-21.

64. Sheu, J.Y., et al., *Determination of thiobarbituric acid adduct of malondialdehyde using on-line microdialysis coupled with high-performance liquid chromatography.* Anal Sci, 2003. **19**(4): p. 621-4.

65. Liu, J., et al., *Assay of aldehydes from lipid peroxidation: gas chromatography-mass spectrometry compared to thiobarbituric acid.* Anal Biochem, 1997. **245**(2): p. 161-6.

66. Nair, J., et al., *Etheno adducts in spleen DNA of SJL mice stimulated to overproduce nitric oxide.* Carcinogenesis, 1998. **19**(12): p. 2081-4.

Chapter 5
A survey of DNA biomarkers from a SJL mouse model of nitric oxide overproduction

This work is done in collaboration with Professor Steven R. Tannenbaum's research group. Dr. Bo Pang analyzed the deamination products; Dr. Hongbin Yu analyzed the guanosine oxidation products; I contributed to the analysis of etheno adducts and M_1dG. The paper "A survey of DNA biomarkers from a SJL mouse model of nitric oxide overproduction" by Bo Pang, Xinfeng Zhou, Hongbin Yu, Steven R. Tannenbaum and Peter C. Dedon (2006) is in preparation.

For completeness, this chapter incorporates the results of the collaborators wherever appropriate and briefly covers the corresponding methods.

Abstract

A SJL mouse model in conjunction with RcsX tumor has been used to evaluate the genotoxicity of nitric oxide (NO•). NO• and its derivatives are able to cause broad damages on cellular components and result in various direct and indirect DNA damage adducts. Here we present a DNA biomarker survey in SJL mouse model to systematically study the DNA damage spectrum induced by NO• overproduction. An LC/MS/MS coupled with an HPLC pre-purification method was successfully developed to measure low levels of DNA damage adducts with high sensitivity and specificity. In our measurements, nucleobase deamination products (deoxyinosine, deoxyxanthosine and deoxyuridine) and the oxidation product (8-oxodeoxyguanosine), which are produced by direct DNA damage, showed small increases (<30%) in the spleen, liver and kidney of the SJL/RcsX mice relative to the controls. The levels of deoxyoxanosine, guanidinohydantoin, oxazolone, 5-guanidino-4-nitroimidazole, and spiroiminodihydantoin were all below detection limit of $1/10^7$ bases. The formation of the secondary DNA damage adduct-M_1dG follows a similar trend, with <50% increase compared with the controls. The relatively large (2~3 fold) and statistically significant increases were only observed on the levels of etheno adducts ($1,N^6$-etheno-deoxyadenosine and $1,N^2$-etheno-deoxyguanosine), which are believed to be secondary DNA adducts derived from electrophiles generated by lipid peroxidation. These results reveal the complexity of NO• chemistry *in vivo* in terms of DNA damage, and indicate that the etheno adducts might serve as useful DNA biomarkers to study the genotoxicity of NO• mediated inflammation.

5.1. Introduction

5.1.1 Potential RNS induced DNA damage in inflammatory tissues

In the past twenty years there has been a growing body of evidence supporting the causative role of inflammation in cancer development [1-3]. It has been suggested that approximately one in four of all cancers are associated with chronic infection and inflammation [4]. Although the detailed mechanism through which persisted infection/inflammation increases cancer risks is not completely elucidated, the bridge between inflammatory processes and human diseases is directed toward persistent oxidative and nitrosative stress and excess lipid peroxidation (LPO). Current studies strongly support that nitric oxide (NO•), acting as an inflammatory mediator, displays cytotoxic and mutagenic properties that contributes to the carcinogenic process [3, 5].

While nitric oxide is essential as an endogenous regulator of the cardiovascular, nervous, and immune systems, a long-term overproduction of NO• and its derivatives stimulated by inducible NO• synthase (iNOS) during chronic inflammation causes unwanted adverse effect *in vivo*. Interaction of NO• with oxygen (O_2) or superoxide ($O_2^{\bullet-}$) form a variety of reactive species, including NO_2, N_2O_3, N_2O_4 and $ONOO^-$, which are collectively referred to as reactive nitrogen species (RNS) [5, 6]. RNS have been shown to induce the oxidation of DNA, RNA, proteins, carbohydrates, and lipids [7]. Since the concentrations of most RNS are low and their half-lives are very short, it is very difficult to study them directly under biologically relevant conditions. The difficulty in making direct measurements motivates the complementary development of biomarkers as surrogates for RNS, for example, DNA biomarkers.

DNA is one of the most important biological targets for oxidative attack, and DNA lesions formed by RNS have the potential to lead to mutation, hence, an increased cancer risk. RNS are capable of causing direct DNA damage by deamination or oxidation of the nucleobases. Nitrosation of DNA nucleobases by N_2O_3 lead to the conversion of cytosine to uracil (dU as 2'-deoxyuridine), guanine to xanthine (dX as 2'-deoxyxanthosine) and oxanine (dO as 2'-deoxyoxanosine), and adenine to hypoxanthine (dI as 2'-deoxyinosine) as shown in Figure 5-1 [8, 9]. Evidence has shown that exposure of calf thymus DNA, plasmid DNA, yeast RNA and bovine liver transfer RNA to NO• and O_2 gas *in vitro* result in substantial formation of uracil, xanthine and hypoxanthine [10]. The DNA oxidation chemistry associated with RNS involves $ONOO^-$, which can be generated by the reaction of NO• and $O_2^{\bullet-}$ *in vivo*. In addition to DNA strand break, $ONOO^-$ and its CO_2 adduct, nitrosoperoxycarbonate ($ONOOCO_2^-$), react preferentially with dG and produce several primary oxidation products such as 8-oxo-7,8-dihydro-2'-deoxyguanosine (8-oxodG) and 5-guanidino-4-nitroimidazole (NitroIm) [11, 12]. 8-oxodG is has often been used as a biomarker for oxidative stress; nevertheless the steady state levels of 8-oxodG in cellular DNA is difficult to determine due to DNA repair and artifactual oxidation during DNA isolation and digestion [13].

In addition to causing direct DNA damage, RNS are able to react with lipids, especially polyunsaturated fatty acids, to generate reactive electrophiles, which subsequently attack DNA bases to form exocyclic DNA adducts. For example, lipid peroxidation induces the formation of a variety of α, β-unsaturated aldehydes such as *trans*-4-hydroxy-2-nonenal (HNE), acrolein and 4-oxo-2-nonenal. These reactive electrophiles can react with DNA bases to form exocyclic propano adducts directly or substituted/unsubstituted etheno adducts through epoxide intermediates [14]. These promutagenic, chemically stable markers appear to be useful for

assessing oxidative stress-derived DNA damage. Among these markers, unsubstituted promutagenic etheno adducts (Figure 5-1) 1,N^6-etheno-2'-deoxyadenosine (εdA), 3,N^4-etheno-2'-deoxycytidine (εdC), and 1,N^2-etheno-2'-deoxyguanosine (1,N^2-εdG) have been extensively studied. Another major reactive electrophile from lipid peroxidation is malondialdehyde (MDA) that has the potential to react with guanosine to form the exocyclic adduct pyrimido ppurine-10(3H)-one-2'deoxyribose (M_1dG) [15]. Additionally there is evidence suggests that the base propenal products of deoxyribose 4'-oxidation (structural analogs of the enol tautomer of MDA) also react with DNA to form M_1dG [16], though with significantly greater efficiency than MDA [15, 16].

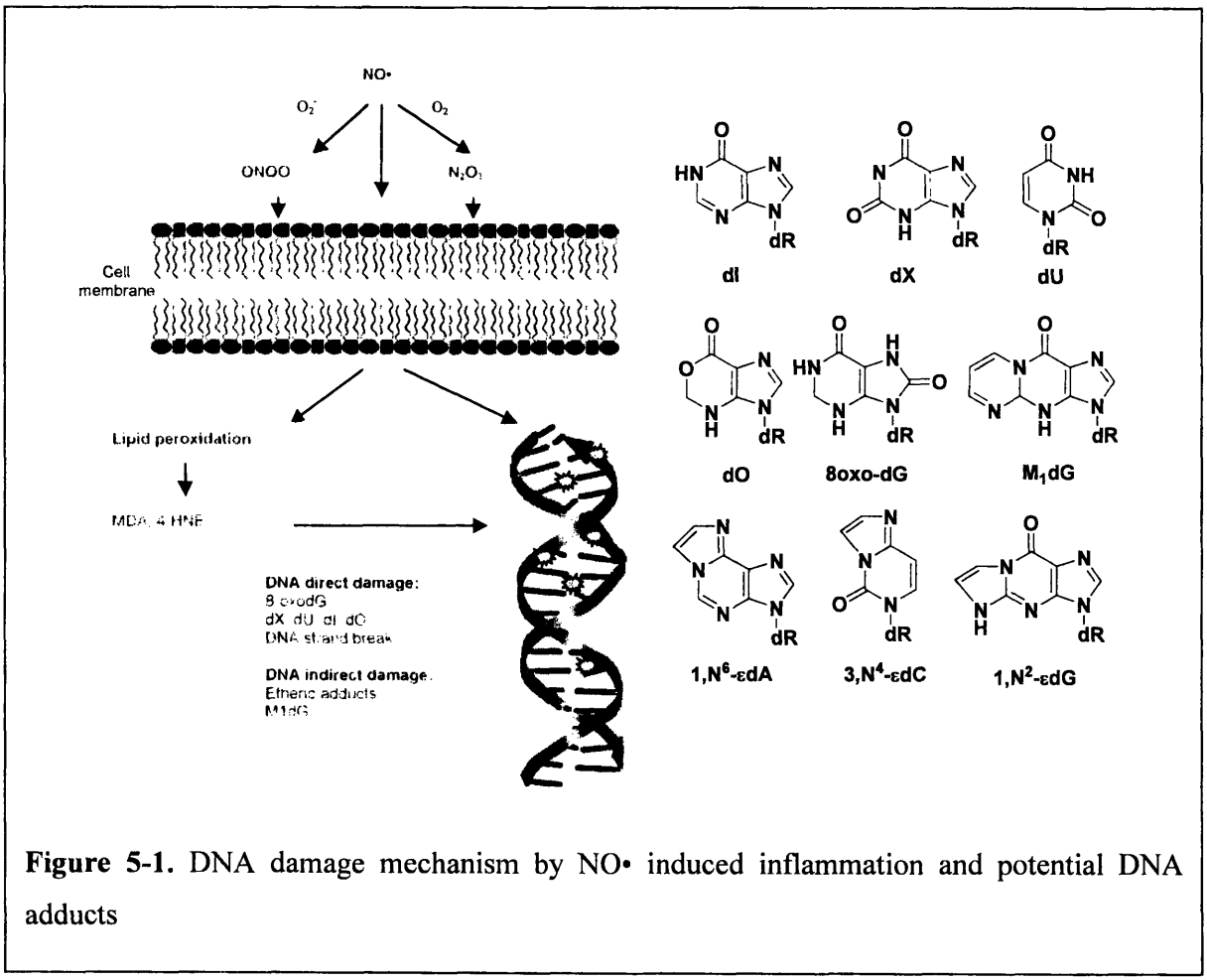

Figure 5-1. DNA damage mechanism by NO• induced inflammation and potential DNA adducts

One of the key questions involving inflammation-related chemical biology is whether direct DNA base deamination/oxidation or indirect DNA damages change the steady-state DNA adduct levels. Despite huge efforts in developing oxidative DNA biomarkers of inflammation, little is known about the relative quantities of different DNA damage products arising under inflammation. Systematic studies to define the DNA damage spectrum produced by RNS will assist in understanding pathophysiological changes during the inflammatory process [3].

5.1.2 Mutagenesis and repair of etheno adducts

Our research group has developed LC-MS/MS method to quantify εdA, 1,N^2-εdG and εdC. Currently we are working on similar methods to include the last member of the unsubstituted etheno adducts, N^2,3-εdG. Plans to develop LC-MS/MS methods for substituted etheno adducts and propano adducts are also under way. The substantial effort put into investigating these adducts is largely a result of their high mutagenicity in mammalian cells, and their potential as biomarkers for a variety of diseases.

Etheno adducts induce base pair substitutions, deletions and rearrangements. For example, in *E. coli* and simian kidney cells, εC produces mostly εC ·G to A·T transversions and εC ·G to T·A transitions [17]. Both εA and εC were shown to be weak mutagens in *E. coli* and strong mutagens in mammalian cells. For example, εC induces mutations at a frequency of 1.5-2% in *E. coli* cells and 81% in simian kidney cells [17, 18]. Since all etheno adducts are potentially mutagenic *in vivo*, the mechanisms to remove these lesions have also been extensively studied. Etheno adducts are eliminated mainly by the base excision repair (BER) pathway, with DNA glycosylases being the key enzymes of this pathway [19]. In *E. coli*, Saccharomyces cerevisiae,

and human cells, the glycosylase that cleaves εA have been identified as the AlkA, MAG and ANPG proteins respectively [20, 21]. Recently Delaney *et al.* showed that AlkB, an α-ketoglutarate dioxygenase, repairs εdA and εdC [22-24]. The potent toxicity and mutagenicity of εdA and εdC in *E. coli* lacking AlkB were reversed or mitigated in AlkB+ cells. Based on biochemical studies, the authors proposed the following direct reversal mechanism shown in Figure 5-2):

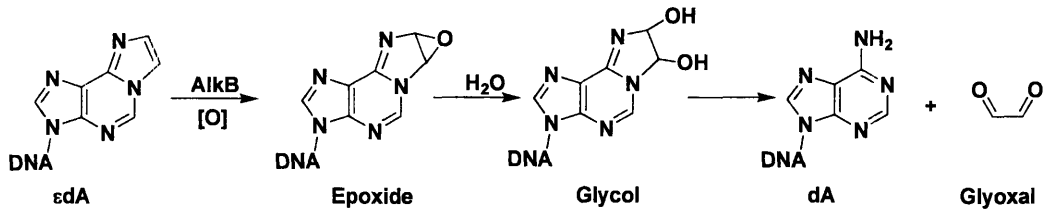

Figure 5-2. Proposed AlkB reaction mechanism for repair of etheno adducts

According to the work, the etheno bond is epoxidized and subsequently hydrolyzed to form a glycol. Finally the glycol moiety is released as glyoxal and the etheno adduct is reverted to the corresponding normal nucleobase. The authors believe that AlkA probably predominantly repairs duplex DNA. In situations where repair by AlkA is not feasible or would result in toxic single-strand break (single-stranded regions in promoters, transcription bubbles, replication forks and loop structure), the direct reversal by AlkB can prevent the lethality and mutagenicity of such lesions.

E. coli mismatch-specific uracil-DNA glycosylase (MUG protein) and its human homologue mismatch-specific thymine-DNA glycosylase (hTDG protein) were identified as the glycosylases that excise εC [25, 26]. More recently, two human enzymes methyl-CpG binding domain protein (MBD4/MED1) and single-stranded mono-functional uracil-DNA glycosylase

(SMUG1) were also shown to cleave εC, although at a much slower rate compared with hTDG [27, 28]. *E. coli* MUG protein also cleaves εG, whereas in human cells a structurally unrelated protein alkyl-N-purine-DNA glycosylase (ANPG) cleaves 1,N^2-εG [29]. Both MUG and ANPG proteins preferentially excise 1,N^2-εG when it is opposite C.

5.1.3 Etheno adduct quantification

Because of their potential as biomarkers for oxidative stress and related diseases, a variety of methods were developed to quantify ehteno adducts. The ^{32}P-postlabeling technique, in conjunction with immunoaffinity purification, is a major analytical method used for assessment of εdA and εdC [30-32]. Nucleotides 3'-εdAMP and 3'-εdACMP were purfied on specific immunogels and postlabeled on the 5'-position with [γ-^{32}P]ATP and T4 polnucleotide kinase. The labeled nucleotides were separated by two-dimensional thin-layer chromatography on polyethyleneimine cellulose and quantified with a PhosphorImager [33]. This method could reach a detection limit of $1/10^9$ nt using 10-50 μg of DNA. Using monoclonal antibodies with a high binding affinity and specificity for εdA, semi-quantitative immunohistochemical staining methods were also developed to analyze mammalian tissue sections directly. LC-MS/MS based methods have also been extensively studied [34, 35]. A typical LC-MS/MS method can detect 1 εdA in 10^8 nt from 100 μg of DNA. Although LC-MS/MS appears to be less sensitive than ^{32}P-postlabeling method, it offers a much higher specificity.

Relative to εdA and εdC, there have been few studies of 1,N^2-εdG. An immunoaffinity/gas chromatography/electron capture negative chemical ionization high-resolution mass spectrometry (IA/GC/ECNCI-HRMS) assay were developed to quantify 1,N^2-

εdG and N^2,3-εdG simultaneously [36]. The demonstrated limits of quantitation in hydrolyzed DNA were 7.6 fmol of N^2,3- εdG and 15 fmol of 1,N^2-εdG in 250 μg of DNA, which corresponded to 1.3 N^2,3-εdG Gua and 2.1 1,N^2-εdG/10^8 nt respectively. In 2002, Loureiro *et al.* developed an on-line HPLC/ESI-MS/MS method to analyze 1,N^2- εdG. The methodology can quantify 20 fmol (2 adducts/10^8 nt) of the etheno adduct from approximately 350 μg of crude DNA hydrolysate [35]. These HPLC purification and MS/MS quantification methods laid the foundation for our simultaneous analysis of DNA deamination and etheno adducts.

5.1.4 SJL mouse model for NO• induced inflammation study

In order to test the hypothesis that genotoxic damage contributes to NO• mediated inflammatory process *in vivo*, a SJL mouse model in conjunction with RcsX cells from a reticulum cell sacroma has been developed [37]. With the implantation of RcsX cell, SJL mice rapidly develop tumor and exhibit large production of NO• as reflected in urinary nitrate excretion. It has been demonstrated that elevated NO• production is generated by activated macrophages in spleen, lymph nodes and liver [38]. A "reverse immune surveillance" mechanism was proposed to illustrate the interaction between macrophage and injected RcsX tumor cells, as shown in Figure 5-3. In brief, the superantigen expressed on the surface of the RcsX cells stimulates a subset of Th2 cells and Vβ-16^+ T cells, which stimulate the proliferation of B cells and Th1 cytokines that activate macrophages. Activated macrophages initiate the inflammation response along with over-production of NO•, which in turn leads to oxidative stress, mutagenesis and apoptosis [39, 40]. SJL/RcsX mice were developed as model for *in vivo* toxicological studies of NO•; and in the previous experiments the amount of 8-oxodG and etheno

adducts were assessed separately. Despite a lack of increase in 8-oxodG, etheno adducts $1,N^6$-ethenodoxyadenosine (ε-dA) and $3,N^4$-ethenodeoxycytidine (ε-dC) were both found elevated in spleen DNA of SJL/RcsX mice [38, 41].

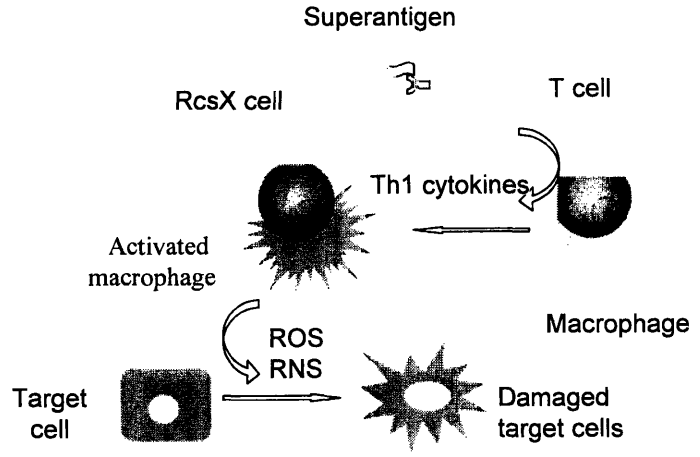

Figure 5-3. Macrophage-mediated cytoxicity by RcsX cells.

In this chapter, we systematically study the *in vivo* formation of endogenous DNA adducts, which includes nucleobase deamination products (dU, dX, dO and dI), oxidation products (8-oxodG, spiroiminodihydantoin, guanidinohydantoin, nitroimidazole and oxazolone) and other secondary DNA damage adducts (etheno products and M_1dG) to provide a better understanding of the role of chronic inflammation induced DNA damage. Analysis of low levels of endogenous DNA adducts is a challenging task that requires high specificity and sensitivity for unequivocal identification and quantification. We resolved this problem by combining HPLC pre-purification with LC/MS/MS method to remove unmodified deoxynucleosides and bases that increases specificity. Deaminase inhibitors and an antioxidant were added during DNA isolation and digestion to minimize artifacts. DNA deamination products, oxidation product and etheno adducts from spleen, liver and kidney of SJL/RcsX mice have been successfully quantified by

this method. M_1dG was quantified by the previously established immunoblot assay [42]. Collectively, this study can provide us information to determine whether one or more of these lesions could be used as potential biomarkers of the inflammatory process.

5.2. Materials and methods

5.2.1 Materials

Ng-methyl L-arginine acetate (NMA), sodium pyruvate, and insulin (bovine) were purchased from Bhem Biochem Research (Salt Lake City, UT) and Qiagen (Valencia, CA). Nuclease P1 and genomic DNA isolation kit were obtained from Roche Diagnostic Corporation (Indianapolis, IL). Phosphodiesterase I was purchased from USB (Cleveland, Ohio). Alkaline phosphatase and desferrioxamine were purchased from Sigma Chemical (St. Louis, MO). Iscove's modified Dulbecco's medium, fetal calf serum, glutamine, and penicillin/streptomycin were purchased from Calbiochem (San Diego, CA). Acetonitrile and HPLC-grade water were purchased from Mallinckrodt Baker (Phillipsburg, NJ). Water purified through a Milli-Q system (Millipore Corporation, Bedford, MA) was used for all applications.

5.2.2 Isotopic-labeled internal standards

^{15}N-labeled etheno adducts εdA, εdC and $1,N^2$-εdG were synthesized from the reactions of ^{15}N-labeled dA, dC and dG respectively with chloroacetaldehyde at 37 °C in 100 mM potassium phosphate buffer (pH = 6) in the dark for 16 hr and then purified by HPLC [43]. The synthesis of uniformly ^{15}N-labeled dX, dU, dI and dO was performed as described [9]. The

uniformly ^{13}C, ^{15}N labeled 8-oxodG, ^{13}C, ^{15}N labeled oxazolone, ^{13}C, ^{15}N labeled Spiroiminodihydantoin, ^{13}C, ^{15}N labeled 5-guanidino-4-nitroimisazole, 1,2,7-$^{15}N_3$-8-oxodG and 3,7,8-$^{15}N_3$-N^1-(β-D-erythro-pentofuranosyl)-5-guanidinohydantoin were synthesized (by Dr. Hongbin Yu) according to the protocols which were previously published [12, 44]. 7-^{15}N-dG was a generous gift from Dr. T. M. Harris of Vanderbilt University.

5.2.3 Instrumental analyses

HPLC analyses were performed on a Hewlett-Packard model 1100, equipped with a Phenomenex Synergi C18 reversed-phase column (250 mm 4.6 mm, 4 μm particle size, 80 Å pore size, Torrance, CA) and a 1100A diode array detector. Deoxyribose nucleoside samples were resolved with the following gradient of acetonitrile in 8 mM sodium acetate buffer (pH 6.9) a flow rate of 0.5 ml/min: 0–42 min, 1-6%; 42-55 min, 6–8%; 44–59 min, 8%; 55-60min, 8–100%; 60–65 min, 100%.

5.2.4 RcsX cell line and animal experiments (by Laura Trudel)

The RcsX cell line was kindly supplied by Dr. N. Ponzio (University of New Jersey Medical Center, Newark NJ). Cells were passaged through mice and harvested from lymph nodes 14 days after inoculation. Cells were manually dissociated from lymph nodes by teasing the tissues, followed by washing in PBS and freezing in aliquots of 5 x 10^7 cells in 10% DMSO/FBS. Of a group of 18 male SJL mice (5-6) weeks old (Jackson Labs, Bar Harbor, ME), 8 were each injected intraperitoneally with 10^7 RcsX cells in 200 μl of PBS. 10 kept as the

controls by injecting with 200 µl of PBS. 5 treated and 3 control mice were killed 12 days after injection. Spleens, livers, and kidneys were removed, weighed and snap frozen in liquid nitrogen for DNA damage analysis.

5.2.5 DNA isolation from tissues

DNA from spleen, liver and kidneys was isolated using a Roche (Indianapolis, IN) DNA isolation kit following the manufacturer's instructions with additional precautions taken to reduce artifactual oxidative and nitrosative damage during the isolation. Briefly, 400 mg samples of frozen tissue were homogenized in 10 ml of cellular lysis buffer containing a combination of deaminase inhibitors and an antioxidant (5 µg/ml coformycin, 50 µg/ml tetrahydrouridine, and 0.1 mM desferrioxamine) for 20-30 s using a Brinkman (Westbury, NY) Polytron homogenizer on a medium setting. The homogenate was digested with proteinase K (33 µl, 20 mg/ml) at 65 °C for 1 hr. DNase-free RNase A was then added (400 µl, 25 mg/ml) for additional 30 min incubation at 37 °C. Proteins were removed by adding 4.2 ml of protein precipitation solution followed by a 5 min incubation on ice and centrifugation at 26,900g for 20 min at 4 °C. The supernatant was carefully transferred to a fresh tube and DNA was recovered by precipitation in 200 mM NaCl and 2.5 volumes of absolute ethanol. The floating DNA filament was recovered with a micropipette tip followed by two washes with 70% cold ethanol, air-drying at ambient temperature and resuspended in Milli-Q-purified water. DNA concentration was then determined by UV spectroscopy and stored at -80 °C until further analysis.

5.2.6 Quantification of deamination products and etheno adducts

100 μg DNA was dissolved in 200 μl of sodium acetate buffer (30 mM, pH 5.6, 0.2 mM zinc chloride, 10 pmol labeled ^{15}N-dX, dI and dU internal standards, 33.3 fmol of ^{15}N- εdA, εdC and 1,N^2- εdG strandards, coformycin, tetrahydrouridine and 0.1 mM desferoxamine). The DNA was digested to deoxynucleoside monophosphates by incubation with 4 units of nuclease P1 at 37 °C for 3 h. Following addition of 200 μl of sodium acetate buffer (30 mM, pH 8.1), phosphate groups were removed with 20 units alkaline phosphatase and 1 unit of phosphodiesterase I by incubation at 37 °C for 6 h. The enzymes were subsequently removed by passing the reaction mixture over a Microcon YM-10 column, and were concentrated and separated by collection of HPLC fractions bracketing empirically determined elution times for each product: dX, 12.1min; dU, 18.5 min; dI, 25.3 min; dO, 36.2 min; 1,N^2- εdG, 48.6 min; εdC, 54.8 min; εdA, 55.7 min.

An API 3000 triple quadrupole mass spectrometer (Applied Biosystems, Foster City, CA, USA) was coupled to an Agilent (Palo Alto, CA) 1100 HPLC system for the sample analysis. The turbo ion-spray was used as an ion source, and the temperature was set at 380°C. The mass spectrometer was operated in a positive ion mode, and the resolution of Q1 and Q3 were fixed to unit. The voltages and source gas were optimized for maximal sensitivity, and the parameters were as followed: IS source voltage: 4.0 kV; nebulizer gas: 8; curtain gas: 8; collision gas (nitrogen): 4; declustering potential: 20; focusing potential: 100; entrance potential: 5; collision energy: 10 for deamination adducts and 20 for etheno adducts; collision cell exit potential: 10. Multiple reaction monitoring (MRM) mode was used for detection of deamination samples with a dwell time to 200 ms. The first quadrupole (Q1) was set to transmit the precursor ions MH$^+$ at m/z 273, 257, , 231, 297, 255 and 281 for U-^{15}N-dX/dO, dI , dU 1,N^2- εdG, εdC, and εdA, and,

which were used as internal standards; at m/z 269, 253, 229, 292, 252, and 276 for dX/dO, dI and dU. The product ions were monitored in the third quadrupole (Q3) at m/z 157, 141, 115, 181, 139, 165 for U-^{15}N-X/O, I, U 1,N^2- εG, εC, and εA; at m/z 153, 137, 111, 176, 136, 160 for X/O, I, U, 1,N^2- εG, εC, and εA respectively. Reversed-phased HPLC was carried out using a Phenomenex C18 column (150 mm x 1.0 mm, 5 μm) and the injection volume was 20 μl. The column was eluted isocratically at a flow rate of 100 μl /min with a mobile phase consisting of permanganate-treated H_2O (0.1% acetic acid): acetonitrile (0.1% acetic acid) at 97:3 for dX/dO, dI and dU or at 98:2 for 1,N^2- εdG, εdC, and εdA.

(8-oxodG and its secondary oxidation products were quantified by Dr. Hongbin Yu as described by Yu *et al.* [12]. M_1dG was quantified using immunoslot blot assay as described in Chapter 4.)

5.3. Results

Here we present the development and validation of a method involved HPLC pre-purification followed by LC/MS/MS assay for systematic quantification of deamination products and etheno adducts in genomic DNA. As shown in Figure 5-4, HPLC resolution provided a means to separate DNA deamination adducts and etheno adducts from normal nucleotides. For each endogenous DNA adduct measured in our system, its corresponding uniform ^{15}N-labeled standard was synthesized and added into genomic DNA before the enzymatic digestion as internal standards. The advantage of using ^{15}N-labeled internal standards in the experiment is that sample loss during analysis can be compensated with the loss of the corresponding internal standards. From the calculation of ^{15}N-labeled standards, we validated that the recovery yields of

DNA adducts (through size exclusion filtration and HPLC pre-purification) were excellent: more than 80% of DNA damage products were recovered.

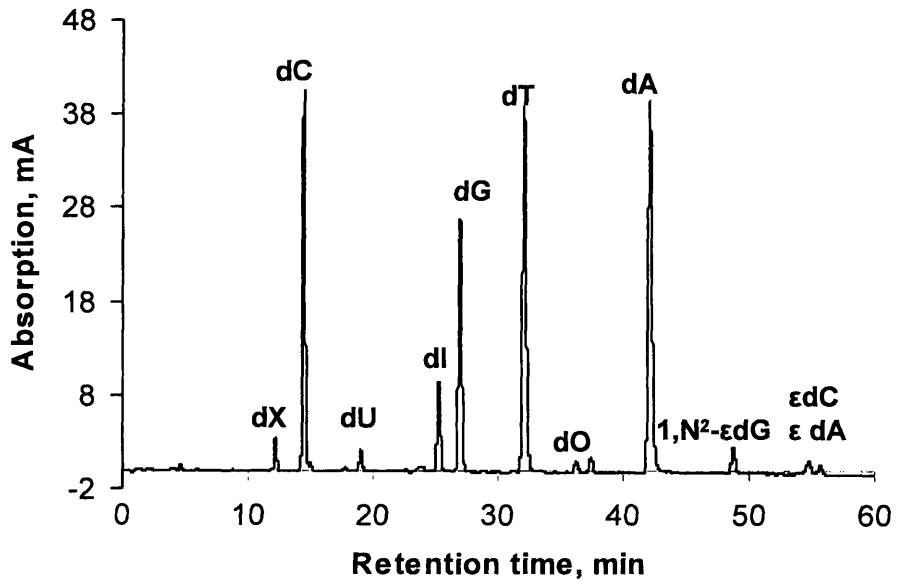

Figure 5-4. Example of HPLC resolution of normal deoxynucleosides and various DNA damage adducts prior to LC/MS/MS analysis. This chromatograph was prepared by injection of chemical standards.

The tandem mass spectrometric detection was done in the multiple reaction monitoring (MRM) mode, and the mass spectrometry parameters were optimized using standards. The MRM mode was chosen due to a shared fragmentation pattern of the nucleosides during glycosidic bond breakage. For example, MRM transition of dI was m/z 253 to 137, dU 229 to 113, and $1,N^2$- εdG 292 to 176. The detection limits in MS varied depending on the chemical structure of each sample, and ranged from 6 per 10^9 for εdA and 1 per 10^7 nt for dU in 100 μg DNA.

One of the important features in our system is that we introduce an HPLC pre-purification step for nucleoside separation prior to LC/MS/MS analysis. The nucleosides of DNA

damage adducts were collected separately according to the HPLC retention time of adduct standard. This step not only increases sample specificity in detection, but also removes potential interfering signals from normal nucleosides. For example, the difference in molecular weight between dI and dA (252/136) is only one unit. This is also the case for dC (228/112) and dU, and dG(268/152) and dX/dO. Since the amounts of normal nucleosides are 10^6 to 10^8 times higher than the endogenously modified adducts, the isotopic effects of dA, dC and dG would interfere significantly with the mass spectroscopy analysis for modified nucleosides. Therefore, the HPLC pre-purification was performed as the sample clean up step and each desired fractions were collected separately.

5.3.1 Isolation of genomic DNA from mouse tissues

An important problem in bioanalytical studies of DNA adducts is artifactual nucleobase damage occurring during isolation, digestion and further processing of DNA for LC-MS/MS analysis [45, 46]. Previous studies in our group show that adventitious formation of dI and dU in DNA isolation, and hydrolysis as a result of cellular nucleobase deaminases [9, 47]. The deaminase activities were completely eliminated by the addition of the deaminase inhibitors coformycin and tetrahydrouridine. Desferrioxamine was also included in the DNA isolation step as an antioxidant in the following work-up to minimize the formation of iron catalyzed oxidation products. Despite the presence of desferrioxamine, the artifactual formation of 8-oxodG in the experimental procedure cannot be completely eliminated [12]. Therefore appropriate corrections were applied in the calculation to obtain the amount of authentic 8-oxodG.

Two groups of male SJL mice were housed in an ALAC certified facility. One group of mice was injected intraperitoneally with RcsX cells in 200 μl PBS, and another group was

treated with PBS buffer only as the control. Treated mice showed a time-dependent increase in urinate nitrate excretion (average 0.4 μmol/g/day in RcsX lymphoma-bearing SJL mice vs 0.02 μmol/g/day in control SJL mice) which is considered as an index of NO• production. Animals were sacrificed 12 days after injection of tumor cells, and the size of spleens in RcsX treated mice expand 10 times due to tumor formation. Genomic DNA was isolated from the tissues in the presence of coformycin, tetrahydrouridine and desferrioxamine, which were also added in the following enzymatic digestion cocktails. After HPLC pre-purification, the recovered deamination products and etheno adducts were subject to LC/MS/MS quantification.

5.3.2 Analysis of deamination products (by Dr. Bo Pang)

The inducible NO• synthase (iNOS) from activated macrophages was localized in spleen, lymph nodes and liver of the SJL/RcsX mice, but not in kidney [37, 38]. Therefore, the DNA from kidney was digested as a control in this experiment. NO• reacts rapidly with O_2 to form N_2O_3, a potent nitrosative reagent that causes the deaminated nucleobases dX, dI, dU and dO [9, 48]. The levels of dX, dI and dU in mouse genomic DNA were quantified in LC/MS/MS measurement by using ^{15}N-labeled internal standards. To ensure the deaminase activities were completely controlled, all reaction enzymes and buffers in the experiment had been carefully tested. As shown in Figure 5-5, only slight increases in dX, dI and dU were observed in the spleen and liver of the RcsX treated mice compared to the control, in which spleen tissues contained dI at 1.6 ± 0.2 per 10^6 nt vs. 1.4 ± 0.1 per 10^6 nt; dX increase to 0.8 ± 0.1 per 10^6 nt compared to 0.6 ± 0.1 per 10^6 nt in the control; dU 57 ± 7 per 10^6 nt vs. 48 ± 7 per 10^6 nt. In the kidney samples of treated mice, dU also showed small increases compared to the controls from

51.9±0.3 per 10^6 nt to 55.1±1.9 per 10^6 nt (<10%), but dI and dX levels even decrease a little. In all DNA samples, dO was not detectable, consistent with our previous data which shows dO is not a major deamination product under the physiological condition (<1 per 10^8 nt) [9, 47]. The lack of dO can be explained by a model proposed by Glaser and co-workers , in which the dG base-pairing cytosine constrain the conversion of dO in the double-stranded DNA [49]. Among these three major deamination products measured here, the dU levels are relatively high (50~60 per 10^6). This may result from the AID (activation-induced cytidine deaminase) activities within the cells.

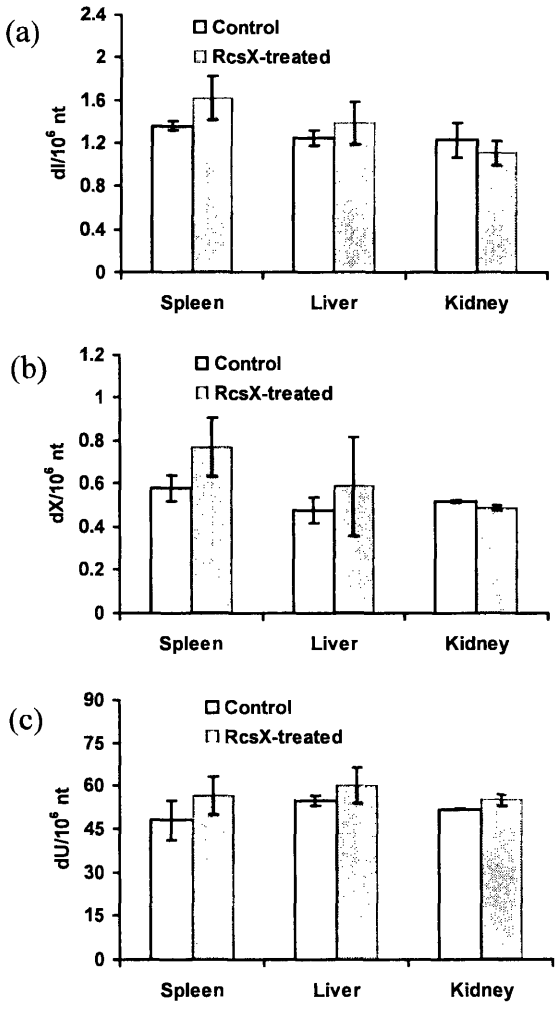

Figure 5-5. Formation of nucleobase deamination products in spleen and liver DNA of SJL mice bearing the RcsX tumor. Following isolation and processing of DNA from tissues, dI (a), dX (b) and dU (c) were quantified by HPLC purification and LC-MS/MS analysis. Each control group sample was pooled from six mice. Data represent mean ± SD for three measures of mice from three different cages. Values for treated mice represent mean ± SD of n=5 per group.

5.3.3 Analysis of guanosine oxidation products (by Dr. Hongbin Yu)

The reactive $ONOO^-$ is formed by the diffusion control reaction of nitric oxide with superoxide. It has been suggested that guanine, with the lowest oxidation potential among four DNA bases, is the most reactive substrate in the reaction with $ONOO^-$ [11, 50]. 8-oxodG is the major oxidation product from the reaction of dG with $ONOO^-$ [50]. Since 8-oxodG is at least 1000 times more reactive than dG upon reacting with $ONOO^-$, hence, 8-oxodG is further react with $ONOO^-$ to generate secondary oxidation products including 2,2-diamino-4[(2-deoxy-β-D-*erythro*-pentafuranosyl)-5(2H)-oxazolone (Ox), spiroiminodihydantoin (Sp), nitroimidazolone (NI) and N^1-(-β-D-*erythro*-pentafuranosyl)-5-guanidinohydantoin (Gh) [12, 51]. In order to achieve best sensitivity and specificity, 8-oxo-dG and its serial secondary oxidation products were measured separately from the deamination products and etheno adducts as describe in method section. The artifact of 8-oxodG induced from sample preparation has been taken into account. The result shown in Figure 5-6 represents the authentic level of 8-oxodG from spleen and liver DNA. For the RcsX cell treated mice, the 8-oxodG level increase slightly from 1.2 ± 0.2 per 10^6 nt to 1.4 ± 0.4 per 10^6 nt in spleen DNA, and it even show a small decrease from 1.4 ± 0.2 per 10^6 nt to 1.2 ± 0.6 per 10^6 nt in liver. The secondary oxidation products Sp, Gh and Ox were also subject to the LC/MS/MS analysis, but the signals were under the detection limit. It indicates that their quantities are less than 1 per 10^7 from 50 μg DNA.

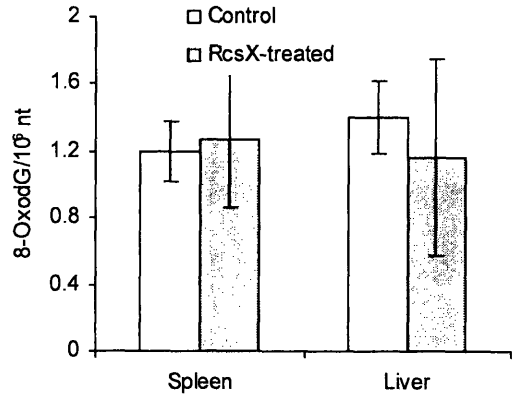

Figure 5-6. Formation of 8-oxodG in spleen and liver DNA of SJL mice bearing the RcsX tumor. Values represent mean ± SD of n=5 per group.

5.3.4 Analysis of etheno adducts in SJL mice

RNS/ROS-induced lipid peroxidation is believed to be the main source of etheno adduct formation [52]. Therefore we measured the formation of εdA and 1,N^2-εdG adducts in tissues of the SJL mouse. In spleen, liver and kidney DNA from SJL mice bearing RcsX cells, the level of ε-dA and ε-dG show ~3 fold increase relative to the controls. For example, ε-dA increased from 2.4±0.9 per 10^8 nt to 6.5±1.7 per 10^8 nt, from 3.9±3.8 per 10^8 nt to 10.2±2.2 per 10^8 nt and from 2±0.7 per 10^8 nt to 7.7±3.1 per 10^8 nt in spleen, liver and kidney, respectively; ε-dG increased from 1.2±0.4 per 10^8 nt to 4.5±1.0 per 10^8 nt, from 2±0.9 per 10^8 nt to 3.3±0.9 per 10^8 nt and from 1.5±0.5 per 10^8 nt to 4.2±1.3 per 10^8 nt, respectively, in spleen, liver and kidney DNA [Figure 5-7 (a) & (b)]. Statistically significant increases in etheno adduct levels

were found in the target tissues of RcsX cell treated mice ($p<0.05$) except ε-dG in liver (p = 0.13). Although spleen and liver contain inducible NO• synthnase (iNOS) and kidney was considered to be as a control organ with no iNOS activity, elevation of etheno adduct level was also detected in kidney, with no significant difference to spleen and liver. These results indicate that the oxidative stress induced by RNS may not be restricted to the locations where iNOS is generated.

5.3.5 Analysis of M_1dG adduct

M_1dG is a secondary DNA damage lesion arises from primary oxidative damage to lipid membrane or deoxyribose. Considering the insensitivity of M_1dG under LC-MS/MS detection, M_1dG was often quantified by reducing the double bond in the exocyclic ring of M_1dG to yield 5,6-dihydro derivative or as its oximine or hydrazone derivatives. As an alternative to LC-MS/MS, we used a previously established slot/dot blot assay to quantify multiple samples with a sensitivity of less than 1 fmol [15]. As shown in Figure 5-6, in spleen tissues, M_1dG elevated to 2.5 ± 1.4 per 10^7 nt compared to 1.5 ± 0.1 in the control; 2.2 ± 1.6 per 10^7 vs. 1.7 ± 0.5 per 10^7 in liver; 1.9 ± 0.5 per 10^7 vs. 1.6 ± 0.2 per 10^7 in kidney [Figure 5-7 (c)].

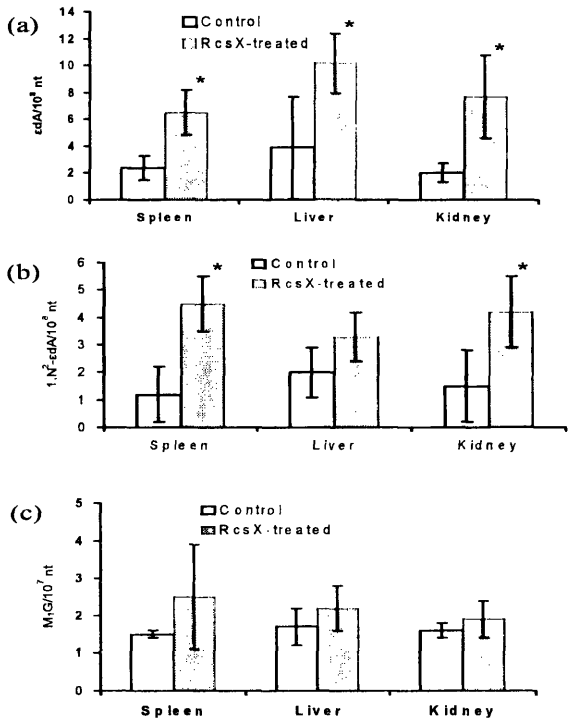

Figure 5-7. Formation of εdA and εdG and M_1dG in spleen and liver DNA of SJL mice bearing the RcsX tumor. Each control group sample was pooled from six mice. Values for control mice represent mean ± SD for three measures of mice from three different cages. Values for treated mice represent mean ± SD of n=5 per group. * means the difference is statistically significant ($p<0.05$).

5.4. Discussion

The association between chronic inflammation and its induced cancer risk has long been recognized by epidemiological studies [3, 53]. One of the strongest evidence for a mechanistic link between inflammation and cancer involves the generation of NO• and other reactive species by macrophage and neutrophils that respond to cytokines and other signaling processes arising at sites of inflammation. These chemical mediators of inflammation can also damage surrounding host tissues causing oxidation, nitration, halogenation and deamination of biomolecules of all types, including lipids, proteins, carbohydrates, and nucleic acids, with the formation of toxic and mutagenic products. NO• and its derivative species have been shown to produce a wide variety of lesions by direct or indirect DNA damage mechanism *in vitro* [5]. However it is unclear whether the steady-state level of DNA adducts increase in the tumor progression associated with NO• overproduction in this animal model. Therefore we quantified a range of DNA deamination products, oxidation products and some secondary DNA adducts to provide us more insights into inflammation induced DNA damage.

The most widely used methods for the detection of DNA adducts including ^{32}P-postlabeling, GC/MS, and LC/MS/MS. The postlabeling assay involves gel electrophoresis or HPLC separation of the end-labeled radioactive nucleotides [30, 54]. Despite its high sensitivity, this method lacks specificity in comparison with the MS methods. GC/MS and LC/MS/MS can provide more rigorous quantification by adding an appropriate amount of isotope-labeled internal standard into DNA samples. However, the propensity to artifactual oxidation during sample preparation limits the application of GC/MS [55]. In contrast, the LC/MS/MS methods measure DNA base damage products in the form of nucleosides that exhibit excellent separation on C18

chromatography and easy fragmentation into daughter ions with the loss of deoxyribose, which provide both sensitivity and specificity [55]. Compared with other LC/MS/MS analyses coupling with immunoaffinity purification, our method is able to identify a wide spectrum of lesions from genomic DNA. For example, the adducts of interest could be separated and collected by a single run on the HPLC, instead of only one single adduct recognized by an immunoaffinity column [56]. However the results need to be interpreted with caution because of the huge amounts of normal nucleosides relative to adducts. For example, the molecular weight and principal MRM transition (loss of sugar) of dA are identical to those of εdC (252/136), the presence of unmodified dA in DNA hydrolysates can interfere with εdC detection. Due to the overwhelming amount of dA relative to εdC, even a 12-minute retention time difference between dA and εdC failed to eliminate all the dA in the εdC fraction and dA yielded a huge MRM peak in the order of 2 pmol, relatively to 10-100 fmol of εdC.

The genotoxicity of NO• likely arises from its derivatives, such as N_2O_3 and $ONOO^-$, which are formed in the reaction with O_2 and $O_2^{\bullet-}$, respectively. N_2O_3 and $ONOO^-$ are able to cause direct damage on DNA molecules, resulting in the formation of DNA deamination and oxidation products. In particular, 8-oxodG has been considered as the major product resulted from $ONOO^-$ oxidation due to the low oxidation potential of guanosine. A direct correlation between 8-oxodG formation and carcinogenesis *in vivo* were demonstrated in many studies, and it has shown that 8-oxodG is a suitable biomarker of oxidative stress [57, 58]. Nevertheless, our results showed that the level of 8-oxodG remain constant in spleen and liver DNA from SJL/RcsX mice (Figure 5-4), which is consistent with a previous study [38]. Since 8-oxodG has lower redox potential 8-oxodG (E^0 = 0.74V vs. NHE) than dG (E^0 = 1.29V vs. NHE), it can be readily oxidized to form a variety of secondary lesions. The conversion of 8-oxodG to these

secondary lesions offers a possible explanation why we did not observe an increase in 8-oxodG level. However, the unaltered level of 8-oxodG did not lead to accumulation of secondary oxidation products as expected. None of such secondary lesions Sp, Gh and Ox, was detectable in both treated and control mice. Therefore, unlike the *in vitro* experiment on calf thymus DNA exposed to $ONOO^-$, NO• overproduction in spleen and liver does not enhance the formation of these DNA primary oxidation products.

Current evidence suggests that N_2O_3 is a more stable species compared with $ONOO^-$, and can lead to the formation of DNA deamination products by nitrosative chemistry. Our previous studies of nucleobase deamination in purified DNA exposed to NO• and O_2 indicated that the nucleobase deamination products form at nearly identical rate. After 12h exposure to 1.3 μM NO• and 190 μM O_2 (936 μM•min dose), 8-10 fold increase of dX, dU and dI levels in DNA were observed [9]. However, we observed only moderate increases (3 -- 4 fold) of the dX, dU and dI level in DNA from human TK6 cells, while the cells were exposed to the similar dose of NO• and O_2 [47]. It is worth noting that this highly toxic NO• dose is a non-physiological dose to the TK6 cells, which cause a 90% loss of viability. When the cells were treated with smaller dose of NO•, which enable cells maintain normal viability, the levels of deamination products dX, dI and dU did not increase, in contrast to the *in vitro* data on purified plasmid DNA [59]. In this study, a large increase of N_2O_3 concentration were expected in spleen and liver of treated mice due to the observation of NO• overproduction in these tissues, thus, commensurate increases in the deamination products. However, only small increase in the formation of dX, dU and dI were detected as shown in Table 5-1, which is consistent with our observation from TK6 cells in the NO• exposure experiment. Taken together, the DNA oxidation and deamination data *in vivo*

differ substantially from the previous in vitro studies performed on purified DNA, which highlights the complexity of NO• chemistry *in vivo*.

Table 5-1. DNA adducts derived from direct damage and indirect damage mechanism in SJL mouse spleen. * means $p < 0.05$.

Adducts	DNA oxidation		DNA nitrosation		Lipid peroxidation		DNA oxidation
	8-oxodG/10^6	dX/10^7	dI/10^6	dU/10^6	ε-dA/10^9	ε-dG/10^9	M_1dG/10^7
Control	1.2±0. 2	5.8±0. 6	1.4±0. 04	48±7	12±4	24±9	1.5±0. 1
RcsX	1.3±0. 4	7.7±1. 4	1.6±0. 2	57±7	45±10	65±17	2.1±1. 4
Ratio	1.1	1.3	1.1	1.2	3.8*	2.7*	1.4
	Direct DNA damage				Indirect DNA damage		

One possible factor that might contribute to this complexity is DNA repair. The DNA damage products measured here reflect a steady-state level equilibrated by both damage formation and damage repair. It is possible that substantial levels of deamination or oxidation products are formed in the tissues with NO• overproduction, but significant repair of those lesions might occur simultaneously. Another possible explanation for the lack of significant increase of deamination and oxidation products is a lesion dilution effect. In this assay, a whole organ has been used for the DNA isolation and the subsequent DNA lesion analysis, but only a small fraction of cell was actually affected by NO• that depends on its proximity to the NO• generator cells. Given the hypothesis that DNA direct damage products in the SJL/RcsX mice arise as a result of NO• overproduction, the formation of DNA oxidative and deaminated lesions are unlikely to be uniformly distributed in the whole organ. Therefore, it might not be appropriate to use the whole organ to evaluate the NO• damage effect on DNA. The third possible explanation is that only a small fraction of NO• or its derivatives are able to access the

nucleus DNA, thus, little damage occurs. For example, NO• can first react with protein, carbohydrates, lipids, and other nucleophilic species present in the cells or NO• derivatives are quenched by some radical scavengers. These possible phenomena might limit the accessibility of RNS to DNA. All these possible explanations are not mutually exclusively and they may collectively contribute to the lack of significant increases in direct oxidation and deamination adducts.

Contrary to direct oxidation and deamination adducts, the DNA etheno adducts (ε-dA and ε-dG) in spleen, liver and kidney of SJL/RcsX mice showed ~3-fold increases by our LC/MS/MS method compared to the controls, which confirms 6-fold increases in ε-dA and ε-dC in the spleen DNA of the SJL/RcsX mice measured by post-labeling assay [41]. The small variation between these two studies might be ascribed to different batches of mice or different detection methods. The mechanism of DNA etheno adduct formation is considered as indirect DNA damage related to lipid peroxidation mediated by $ONOO^-$ and other RNS/ROS. It is different from the formation of 8-oxodG as oxidation product or deamination products that are direct damages caused by RNS. It has been suggested that polyunsaturated fatty acids (PUFAs) in lipids are extremely sensitive to oxidation. NO• and its derivatives show better solubility in lipid membrane and hydrophobic cellular regions then in aqueous cytosol [60, 61]. These properties enable lipids to be potential primary targets for oxidized reagents, such as OH• and $ONOO^-$, leading to a complex series of reactions that ultimately generate a range of electrophilic derivatives (e.g., epoxides, aldehydes, etc.) [62]. For example, peroxidation of ω-6-polyunsaturated fatty acids have been shown to produce intermediates that further react with dA or dG to form etheno-dA (ε-dA) or etheno-dG (ε-dG) *in vitro*. So it is generally believed that the etheno DNA damage adducts could be introduced from lipid peroxidation related to NO•

overproduction. In fact, etheno adducts have been associated with are several oxidative stress induced clinical disorders [17, 63, 64]. For example, levels of ε-dA and ε-dC are elevated 3-fold in liver DNA from patients with Wilson's disease [65]. A similar increase is found in colonic polyps of familial adenomatous polyposis patients [66]. In addition, the Long-Evans Cinnamon rats which have abnormal copper metabolism show significant increases of etheno adducts in liver DNA relative to Long Evans Agouti rats [67]. These evidences indicate that lipid peroxidation appears to be one of the major sources of endogenous DNA damage in humans which makes etheno DNA adducts useful biomarkers in determining the extent of genetic damage from pathological process of inflammation. The lipid bilayer also limits the NO• diffusion into the nuclei and allows little direct DNA damage. So that it could partially explain why no significant increase is found of deamination and oxidation product levels. PUFAs, as well as protein and anti-oxidant small molecules can react with RNS/ROS, which may result in insufficient $ONOO^-$ and N_2O_3 concentration in nuclei. Our experiment results presented here, combined with previous observations [41, 47], imply this possible mechanism.

It is of particular interest to see that the etheno adducts level were enhanced in parallel in all three tested organs, including kidney which is not a target organ for NO• overproduction in tumor bearing SJL mice, although it was shown that the rate of apoptosis, iNOS expression and mutant frequency were not affected in the RcsX kidney [37, 38, 68]. Nevertheless, a recent publication revealed that, in this SJL mouse model, NO• induced glutathione (GSH) upregulated in the kidney and spleen in the RcsX tumor-bearing mice [59]. GSH is the most abundant intracellular antioxidant with multifaceted and complex biological function, and it might play a significant role in protecting cells against toxic level of NO• during inflammation. Those results suggest that the kidney and spleen might experience similar oxidative stress mediated by NO•,

although the kidney is not a direct NO• exposure target. Therefore, it is rational to detect the elevation of etheno adduct in kidney, given the assumption that etheno adducts are formed as secondary DNA damage lesions from lipid peroxidation respond to oxidative stress. Collectively, the results from our etheno adduct assay provide us a new aspect in understanding the complex physiological and pathophysiological functions of NO•.

As mentioned earlier, MDA is another major product result from lipid peroxidation, and it can further react with DNA strands and cause secondary DNA lesions, for example M_1dG [69]. The formation of M_1dG can be induced from an alternative more efficient pathway via base propenal, a product from DNA backbone breaks attacked by free radical [15, 16]. Although which pathway is the primary source to cause M_1dG formation is still under debate, some of our recent results indicated that base propenal from DNA damage plays a major role in M_1dG formation in cellular DNA [42]. Since LC-MS/MS was not a sensitive method for M_1dG quantification, we quantified the M_1dG adducts using an immunoblot assay which is very sensitive and required only very small amount of DNA (1 μg). Similar to deamination data, our results showed small increases of M_1dG formation in the RcsX cell-treated mice compared to the controls, which is consistent with the hypothesis that base propenal as the major source of M_1dG. If the direct damage on DNA is not a major event, the amount of base propenal formed is small, which in turn induces few M_1dG adducts.

A LC/MS/MS method coupled with aldehyde reactive probe labeling was recently developed in the Swenberg group, and they revealed the background level of M_1dG in mice DNA of 0.8-4.2 per 10^8 nt depending on the tissue type [70, 71], which is about 5-fold lower than our observation in the SJL/RcsX mice DNA. We cannot rule out the possibility that artifacts were introduced in the immuno-blot assay due to unspecific binding of M_1dG antibody to DNA.

So that the amounts of authentic M_1dG adduct inherent from the samples only contribute a small portion to the overall M_1dG measurement. It is possible that the difference of M_1dG levels between treated mice and controls was more significant than what we observed here. Therefore it is important to point out that our results do not rule out MDA as a source of M_1dG in SJL mice. However, the *in vitro* study also by the Swenberg group also showed that the existence of PUFA reduced direct DNA damage by diverting the oxidative species, and suggested that base propenal was the major source of M_1dG. Kadlubar *et al.* studied DNA adduct levels associated with oxidative stress in human pancreases. They found no correlation in adduct levels between εdC or εdA and M_1dG. On the contrary, there was a significant correlation between the levels of 8-oxodG and M_1dG. Kadiiska *et al.* also showed that injection of CCl_4 into Fisher 344 rats induced significant increases in lipid peroxidation products MDA and isprostanes, yet it failed to elevate strand breaks and M_1G formation in leukocyte [72]. All these results again indicate that DNA deoxyribose oxidation, instead of lipid peroxidation, is the major source of M_1dG. As a result, we only observed the relative small increase (<50%) of M_1dG formation in the samples compared with 2~3 increases in etheno adducts from lipid peroxidation (Table V-1).

In summary, in this SJL/RcsX mouse model, activation of inflammatory cells leads to the overproduction of NO• and a variety of NO• derivatives, which cause broad damages on the cellular components, such as nucleic acids, proteins, carbohydrates, phospholipids etc., and alter cell function. In the DNA biomarker survey presented here, we study the nucleus DNA damage adducts in response to oxidative and nitrosative insults induced by NO•. Statistically significant increases only occur in the levels of etheno adducts, as secondary DNA damage lesions induced from the lipid peroxidation pathway. The DNA damage adducts being measured here represent a steady state level of products balanced by both adduct formation and DNA repair. DNA damage

in inflammation is predominantly repaired by BER enzymes. There is a growing body of evidence suggesting that some key DNA repair enzymes in BER pathway are inhibited by NO•-mediated nitrosylation at the active sites, including 6-O-alkyl DNA transferase, foramidopyrimidine glycosylase, human 8-oxodG glycosylase and poly(ADP-ribose) polymerase [73-76]. It is also recognized that NO•-dependent nitration of the protein tyrosine is a significant and prevalent post-translational protein modification that reflects the extent of oxidant production during both physiological and pathological conditions [77]. Therefore, these results imply that, in addition to DNA damage, protein damage can be considered as another choice for searching suitable biomarkers of NO• mediated inflammation.

5.5. Conclusions

We take advantage of SJL/RcsX mouse model to study the DNA damage under pathological condition associated with NO• and inflammation. We apply a new LC/MS/MS method coupled with HPLC pre-purification to systematically quantify the formation of DNA damage adducts, including deamination products, oxidation products and etheno adducts, in NO• overproduction tissue. Our results suggest that direct reaction of RNS with DNA in SJL/RcsX mice only produce small increase (<30%) of DNA deamination and oxidation products, but the etheno DNA adducts presumably derived from lipid peroxidation show a more significant increase (~3 fold) with an indirect DNA damage mechanism. M_1dG as another secondary DNA damage adducts is also measured using an immunoblot assay, and no significant increase is observed, most likely because it is a secondary adduct of DNA deoxyribose oxidation instead of lipid peroxidation. This study provides us an opportunity to define the predominant DNA damage products in a mouse model of inflammation.

Reference

1. Coussens, L.M. and Z. Werb, *Inflammation and cancer.* Nature, 2002. **420**(6917): p. 860-7.
2. Klaunig, J.E. and L.M. Kamendulis, *The role of oxidative stress in carcinogenesis.* Annu Rev Pharmacol Toxicol, 2004. **44**: p. 239-67.
3. Yermilov, V., et al., *Effects of carbon dioxide/bicarbonate on induction of DNA single-strand breaks and formation of 8-nitroguanine, 8-oxoguanine and base-propenal mediated by peroxynitrite.* Febs Letters, 1996. **399**(1-2): p. 67-70.
4. Ames, B.N., L.S. Gold, and W.C. Willett, *The Causes and Prevention of Cancer.* Proceedings of the National Academy of Sciences of the United States of America, 1995. **92**(12): p. 5258-5265.
5. Dedon, P.C. and S.R. Tannenbaum, *Reactive nitrogen species in the chemical biology of inflammation.* Arch Biochem Biophys, 2004. **423**(1): p. 12-22.
6. Tamir, S., S. Burney, and S.R. Tannenbaum, *DNA damage by nitric oxide.* Chem Res Toxicol, 1996. **9**(5): p. 821-7.
7. Hussain, S.P., L.J. Hofseth, and C.C. Harris, *Radical causes of cancer.* Nat Rev Cancer, 2003. **3**(4): p. 276-85.
8. Lewis, R.S., et al., *Kinetic analysis of the fate of nitric oxide synthesized by macrophages in vitro.* J Biol Chem, 1995. **270**(49): p. 29350-5.
9. Dong, M., et al., *Absence of 2'-deoxyoxanosine and presence of abasic sites in DNA exposed to nitric oxide at controlled physiological concentrations.* Chem Res Toxicol, 2003. **16**(9): p. 1044-55.
10. Day, B.W., et al., *Molecular dosimetry of polycyclic aromatic hydrocarbon epoxides and diol epoxides via hemoglobin adducts.* Cancer Res, 1990. **50**(15): p. 4611-8.
11. Burney, S., et al., *DNA damage in deoxynucleosides and oligonucleotides treated with peroxynitrite.* Chem Res Toxicol, 1999. **12**(6): p. 513-20.
12. Yu, H., et al., *Quantitation of four Guanine oxidation products from reaction of DNA with varying doses of peroxynitrite.* Chem Res Toxicol, 2005. **18**(12): p. 1849-57.
13. Marnett, L.J., *Oxy radicals, lipid peroxidation and DNA damage.* Toxicology, 2002. **181-182**: p. 219-22.
14. Chen, H.J., et al., *2,3-epoxy-4-hydroxynonanal, a potential lipid peroxidation product for etheno adduct formation, is not a substrate of human epoxide hydrolase.* Carcinogenesis, 1998. **19**(5): p. 939-43.
15. Plastaras, J.P., et al., *Reactivity and mutagenicity of endogenous DNA oxopropenylating agents: base propenals, malondialdehyde, and N(epsilon)-oxopropenyllysine.* Chem Res Toxicol, 2000. **13**(12): p. 1235-42.

16. Dedon, P.C., et al., *Indirect mutagenesis by oxidative DNA damage: formation of the pyrimidopurinone adduct of deoxyguanosine by base propenal.* Proc Natl Acad Sci U S A, 1998. **95**(19): p. 11113-6.

17. Basu, A.K., et al., *Mutagenic and Genotoxic Effects of 3 Vinyl Chloride-Induced DNA Lesions - 1,N(6)-Ethenoadenine, 3,N(4)-Ethenocytosine, and 4-Amino-5-(Imidazol-2-Yl)Imidazole.* Biochemistry, 1993. **32**(47): p. 12793-12801.

18. Moriya, M., et al., *Mutagenic Potency of Exocyclic DNA-Adducts - Marked Differences between Escherichia-Coli and Simian Kidney-Cells.* Proceedings of the National Academy of Sciences of the United States of America, 1994. **91**(25): p. 11899-11903.

19. Gros, L., A.A. Ishchenko, and M. Saparbaev, *Enzymology of repair of etheno-adducts.* Mutation Research-Fundamental and Molecular Mechanisms of Mutagenesis, 2003. **531**(1-2): p. 219-229.

20. Saparbaev, M., K. Kleibl, and J. Laval, *Escherichia-Coli, Saccharomyces-Cerevisiae, Rat and Human 3-Methyladenine DNA Glycosylases Repair 1,N-6-Ethenoadenine When Present in DNA.* Nucleic Acids Research, 1995. **23**(18): p. 3750-3755.

21. Singer, B., et al., *Both Purified Human 1,N(6)-Ethenoadenine-Binding Protein and Purified Human 3-Methyladenine-DNA Glycosylase Act on 1,N(6)-Ethenoadenine and 3-Methyladenine.* Proceedings of the National Academy of Sciences of the United States of America, 1992. **89**(20): p. 9386-9390.

22. Delaney, J.C. and J.M. Essigmann, *Mutagenesis, cytotoxicity and repair of 1-methyladenine, 3-alkylcytosines, 1-methylguanine and 3-methylthymine in AlkB Escherichia coli.* Environmental and Molecular Mutagenesis, 2004. **44**(3): p. 195-195.

23. Delaney, J.C. and J.M. Essigmann, *Mutagenesis, genotoxicity, and repair of 1-methyladenine, 3-alkylcytosines, 1-methylguanine and 3-methylthymine, in alkB Escherichia coli.* Proceedings of the National Academy of Sciences of the United States of America, 2004. **101**(39): p. 14051-14056.

24. Delaney, J.C., et al., *AlkB reverses etheno DNA lesions caused by lipid oxidation in vitro and in vivo.* Nature Structural & Molecular Biology, 2005. **12**(10): p. 855-860.

25. Saparbaev, M. and J. Laval, *3,N-4-ethenocytosine, a highly mutagenic adduct, is a primary substrate for Escherichia coli double-stranded uracil-DNA glycosylase and human mismatch-specific thymine-DNA glycosylase.* Proceedings of the National Academy of Sciences of the United States of America, 1998. **95**(15): p. 8508-8513.

26. Gallinari, P. and J. Jiricny, *A new class of uracil-DNA glycosylases related to human thymine-DNA glycosylase.* Nature, 1996. **383**(6602): p. 735-738.

27. Petronzelli, F., et al., *Investigation of the substrate spectrum of the human mismatch-specific DNA N-glycosylase MED1 (MBD4): Fundamental role of the catalytic domain.* Journal of Cellular Physiology, 2000. **185**(3): p. 473-480.

28. Kavli, B., et al., *HUNG2 is the major repair enzyme for removal of uracil from U : A matches, U : G mismatches, and U in single-stranded DNA, with hSMUG1 as a broad specificity backup.* Journal of Biological Chemistry, 2002. **277**(42): p. 39926-39936.

29. Saparbaev, M., et al., *1,N-2-ethenoguanine, a mutagenic DNA adduct, is a primary substrate of Escherichia coli mismatch-specific uracil-DNA glycosylase and human alkylpurine-DNA-N-glycosylase.* Journal of Biological Chemistry, 2002. **277**(30): p. 26987-26993.

30. Fernando, R.C., et al., *Detection of 1,N-6-ethenodeoxyadenosine and 3,N-4-ethenodeoxycytidine by immunoaffinity/P-32-postlabelling in liver and lung DNA of mice treated with ethyl carbamate (urethane) or its metabolites.* Carcinogenesis, 1996. **17**(8): p. 1711-1718.

31. Nair, J., et al., *1,N-6-Ethenodeoxyadenosine and 3,N-4-Ethenodeoxycytidine in Liver DNA from Humans and Untreated Rodents Detected by Immunoaffinity P-32 Postlabeling.* Carcinogenesis, 1995. **16**(3): p. 613-617.

32. Yang, Y., et al., *Immunohistochemical detection of 1,N-6-ethenodeoxyadenosine, a promutagenic DNA adduct, in liver of rats exposed to vinyl chloride or an iron overload.* Carcinogenesis, 2000. **21**(4): p. 777-781.

33. Barbin, A., et al., *Endogenous deoxyribonucleic acid (DNA) damage in human tissues: A comparison of ethenobases with aldehydic DNA lesions.* Cancer Epidemiology Biomarkers & Prevention, 2003. **12**(11): p. 1241-1247.

34. Doerge, D.R., et al., *Quantification of Etheno-DNA adducts using liquid chromatography, on-line sample processing, and electrospray tandem mass spectrometry.* Chemical Research in Toxicology, 2000. **13**(12): p. 1259-1264.

35. Loureiro, A.P.M., et al., *Development of an on-line liquid chromatography-electrospray tandem mass spectrometry assay to quantitatively determine 1,N-2-etheno-2'-deoxyguanosine in DNA.* Chemical Research in Toxicology, 2002. **15**(10): p. 1302-1308.

36. Morinello, E.J., et al., *Simultaneous quantitation of N-2,3-ethenoguanine and 1,N-2-ethenoguanine with an immunoaffinity/gas chromatography/high-resolution mass spectrometry assay.* Chemical Research in Toxicology, 2001. **14**(3): p. 327-334.

37. Gal, A., et al., *Nitric oxide production in SJL mice bearing the RcsX lymphoma: a model for in vivo toxicological evaluation of NO.* Proc Natl Acad Sci U S A, 1996. **93**(21): p. 11499-503.

38. Gal, A., et al., *Nitrotyrosine formation, apoptosis, and oxidative damage: relationships to nitric oxide production in SJL mice bearing the RcsX tumor.* Cancer Res, 1997. **57**(10): p. 1823-8.

39. Ponzio, N.M. and G.J. Thorbecke, *Requirement for reverse immune surveillance for the growth of germinal center-derived murine lymphomas.* Semin Cancer Biol, 2000. **10**(5): p. 331-40.

40. Thorbecke, G.J. and N.M. Ponzio, *Reverse immune surveillance: an adaptive mechanism used by tumor cells to facilitate their survival and growth.* Semin Cancer Biol, 2000. **10**(5): p. 327-30.

41. Nair, J., et al., *Etheno adducts in spleen DNA of SJL mice stimulated to overproduce nitric oxide.* Carcinogenesis, 1998. **19**(12): p. 2081-4.

42. Zhou, X., K. Taghizadeh, and P.C. Dedon, *Chemical and biological evidence for base propenals as the major source of the endogenous M1dG adduct in cellular DNA.* J Biol Chem, 2005. **280**(27): p. 25377-82.

43. Lee, S.H., T. Oe, and I.A. Blair, *4,5-Epoxy-2(E)-decenal-induced formation of 1,N(6)-etheno-2'-deoxyadenosine and 1,N(2)-etheno-2'-deoxyguanosine adducts.* Chem Res Toxicol, 2002. **15**(3): p. 300-4.

44. Gu, F., et al., *Peroxynitrite-induced reactions of synthetic oligo 2'-deoxynucleotides and DNA containing guanine: formation and stability of a 5-guanidino-4-nitroimidazole lesion.* Biochemistry, 2002. **41**(23): p. 7508-18.

45. Kasai, H., *Analysis of a form of oxidative DNA damage, 8-hydroxy-2'-deoxyguanosine, as a marker of cellular oxidative stress during carcinogenesis.* Mutat Res, 1997. **387**(3): p. 147-63.

46. Helbock, H.J., et al., *DNA oxidation matters: The HPLC-electrochemical detection assay of 8-oxo-deoxyguanosine and 8-oxo-guanine.* Proceedings of the National Academy of Sciences of the United States of America, 1998. **95**(1): p. 288-293.

47. Jiang, T., et al., *Histone Protein Formylation Caused by Deoxyribose Oxidation in DNA.* 2006.

48. Vongchampa, V., et al., *Stability of 2'-deoxyxanthosine in DNA.* Nucleic Acids Res, 2003. **31**(3): p. 1045-51.

49. Glaser, R., H. Wu, and M. Lewis, *Cytosine catalysis of nitrosative guanine deamination and interstrand cross-link formation.* J Am Chem Soc, 2005. **127**(20): p. 7346-58.

50. Douki, T. and J. Cadet, *Peroxynitrite mediated oxidation of purine bases of nucleosides and isolated DNA.* Free Radic Res, 1996. **24**(5): p. 369-80.

51. Niles, J.C., J.S. Wishnok, and S.R. Tannenbaum, *Spiroiminodihydantoin and guanidinohydantoin are the dominant products of 8-oxoguanosine oxidation at low fluxes of peroxynitrite: mechanistic studies with 18O.* Chem Res Toxicol, 2004. **17**(11): p. 1510-9.

52. Chung, F.L., H.J. Chen, and R.G. Nath, *Lipid peroxidation as a potential endogenous source for the formation of exocyclic DNA adducts.* Carcinogenesis, 1996. **17**(10): p. 2105-11.

53. Shacter, E. and S.A. Weitzman, *Chronic inflammation and cancer.* Oncology (Williston Park), 2002. **16**(2): p. 217-26, 229; discussion 230-2.

54. Zeisig, M. and L. Moller, *32P-HPLC suitable for characterization of DNA adducts formed in vitro by polycyclic aromatic hydrocarbons and derivatives.* Carcinogenesis, 1995. **16**(1): p. 1-9.

55. Frelon, S., et al., *Comparative study of base damage induced by gamma radiation and Fenton reaction in isolated DNA.* Journal of the Chemical Society-Perkin Transactions 1, 2002(24): p. 2866-2870.

56. Ham, A.J., et al., *New immunoaffinity-LC-MS/MS methodology reveals that Aag null mice are deficient in their ability to clear 1,N6-etheno-deoxyadenosine DNA lesions from lung and liver in vivo.* DNA Repair (Amst), 2004. **3**(3): p. 257-65.

57. Feig, D.I., T.M. Reid, and L.A. Loeb, *Reactive oxygen species in tumorigenesis.* Cancer Res, 1994. **54**(7 Suppl): p. 1890s-1894s.

58. Frelon, S., et al., *High-performance liquid chromatography--tandem mass spectrometry measurement of radiation-induced base damage to isolated and cellular DNA.* Chem Res Toxicol, 2000. **13**(10): p. 1002-10.

59. Li, C.Q., et al., *Biological role of glutathione in nitric oxide-induced toxicity in cell culture and animal models.* Free Radic Biol Med, 2005. **39**(11): p. 1489-98.

60. Dix, T.A. and J. Aikens, *Mechanisms and biological relevance of lipid peroxidation initiation.* Chem Res Toxicol, 1993. **6**(1): p. 2-18.

61. Liu, X., et al., *Accelerated reaction of nitric oxide with O2 within the hydrophobic interior of biological membranes.* Proc Natl Acad Sci U S A, 1998. **95**(5): p. 2175-9.

62. Hogg, N., et al., *The oxidation of alpha-tocopherol in human low-density lipoprotein by the simultaneous generation of superoxide and nitric oxide.* FEBS Lett, 1993. **326**(1-3): p. 199-203.

63. Pandya, G.A. and M. Moriya, *1,N6-ethenodeoxyadenosine, a DNA adduct highly mutagenic in mammalian cells.* Biochemistry, 1996. **35**(35): p. 11487-92.

64. Bartsch, H., et al., *Formation, detection, and role in carcinogenesis of ethenobases in DNA.* Drug Metab Rev, 1994. **26**(1-2): p. 349-71.

65. Nair, J., et al., *Lipid peroxidation-induced etheno-DNA adducts in the liver of patients with the genetic metal storage disorders Wilson's disease and primary hemochromatosis.* Cancer Epidemiol Biomarkers Prev, 1998. **7**(5): p. 435-40.

66. Schmid, K., et al., *Increased levels of promutagenic etheno-DNA adducts in colonic polyps of FAP patients.* Int J Cancer, 2000. **87**(1): p. 1-4.

67. Nair, J., et al., *Copper-dependent formation of miscoding etheno-DNA adducts in the liver of Long Evans cinnamon (LEC) rats developing hereditary hepatitis and hepatocellular carcinoma.* Cancer Res, 1996. **56**(6): p. 1267-71.

68. Gal, A. and G.N. Wogan, *Mutagenesis associated with nitric oxide production in transgenic SJL mice.* Proc Natl Acad Sci U S A, 1996. **93**(26): p. 15102-7.

69. Marnett, L.J., *Lipid peroxidation-DNA damage by malondialdehyde.* Mutat Res, 1999. **424**(1-2): p. 83-95.

70. Jeong, Y.C., et al., *Pyrimido[1,2-a]-purin-10(3H)-one, M1G, is less prone to artifact than base oxidation.* Nucleic Acids Res, 2005. **33**(19): p. 6426-34.

71. Jeong, Y.C. and J.A. Swenberg, *Formation of M1G-dR from endogenous and exogenous ROS-inducing chemicals.* Free Radic Biol Med, 2005. **39**(8): p. 1021-9.

72. Kadiiska, M.B., et al., *Biomarkers of oxidative stress study II: are oxidation products of lipids, proteins, and DNA markers of CCl4 poisoning?* Free Radic Biol Med, 2005. **38**(6): p. 698-710.

73. Jaiswal, M., et al., *Human Ogg1, a protein involved in the repair of 8-oxoguanine, is inhibited by nitric oxide.* Cancer Res, 2001. **61**(17): p. 6388-93.

74. Saparbaev, M. and J. Laval, *Excision of Hypoxanthine from DNA Containing Dimp Residues by the Escherichia-Coli, Yeast, Rat, and Human Alkylpurine DNA Glycosylases.* Proceedings of the National Academy of Sciences of the United States of America, 1994. **91**(13): p. 5873-5877.

75. Miles, A.M., et al., *Modulation of superoxide-dependent oxidation and hydroxylation reactions by nitric oxide.* J Biol Chem, 1996. **271**(1): p. 40-7.

76. Sidorkina, O., et al., *Inhibition of poly(ADP-RIBOSE) polymerase (PARP) by nitric oxide and reactive nitrogen oxide species.* Free Radic Biol Med, 2003. **35**(11): p. 1431-8.

77. Greenacre, S.A. and H. Ischiropoulos, *Tyrosine nitration: localisation, quantification, consequences for protein function and signal transduction.* Free Radic Res, 2001. **34**(6): p. 541-81.

Chapter 6

Conclusions and Future Studies

6.1. Conclusions

The major goal of this thesis is to better define deoxyribose oxidation products and the role of these products in the formation of DNA and protein adducts. Much of the progress is related to establishing the existence of deoxyribose oxidation products, quantification of these products and defining the relative importance of intermediate electrophiles from lipid peroxidation and deoxyribose oxidation in the formation of secondary adducts.

First we developed an index of total deoxyribose oxidation that provides a means to compare different oxidizing agents (*1*). The method exploits the reaction of aldehyde- and ketone-containing deoxyribose oxidation products with ^{14}C-methoxyamine to form stable oxime derivatives that are quantified by accelerator mass spectrometry (AMS). The method was optimized to ensure the quantitative incorporation of the ^{14}C-methoxyamine to reactive strand breaks/abasic sites and reduce the non-specific binding. DNA containing a defined quantity of abasic sites (generated from uracil-containing DNA) was used to validate the methods. The developed method was applied to *in vitro* and *in vivo* DNA damage studies, which offered an index of total deoxyribose oxidation that allows comparison of different oxidants. In conjunction with DNA repair enzymes that remove damaged bases to produce aldehydic sugar residues or abasic sites, the method was also shown to be able to study nucleobase lesions in addition to strand break products.

Since 4'-carbon is a major DNA deoxyribose oxidation target and one of its potential product base propenal was proposed to be the major source of secondary DNA adduct M_1dG, we defined the spectrum of deoxyribose 4'-oxidation products associated with different oxidizing agents (*2*). Oxidation of the 4'-position of deoxyribose results in the formation of either a 3'-

phosphoglycolate-ended fragment with release of base propenal (or malondialdehyde and free base), or a 4′-keto-1′-aldehyde without strand break. We first developed an analytical method to quantify base propenals and malondialdehyde. The approach is to use HPLC to resolve products released following DNA oxidation, followed by chemical derivatization and spectroscopic (*e.g.*, TBA reaction with malondialdehyde) quantification. We also developed a method to quantify the 4'-oxidation products 3'-phosphoglycolate and 4′-keto-1′-aldehyde abasic site (part of collaboration with Dr. Bingzi Chen) using GC-MS analysis after derivatization by BSTFA and hydrazine respectively. When the results for 4'-oxidation products were combined with quantification of total deoxyribose oxidation site under the same conditions, these results offered direct insights into the partitioning of 4-oxidation chemistry and thus into the chemical mechanism at work in the cellular environment.

With a foundation of deoxyribose oxidation chemistry in general and 4'-oxidation in particular, we defined the roles of base propenals and malondialdehyde in the formation of M_1dG *in vitro* and in cultured *E. coli* cells (*3*). The *in vitro* DNA oxidative damage induced by γ-irradiation, Fe^{2+}/EDTA, bleomycin and peroxynitrite showed that MDA was neither sufficient nor necessary to induce M_1dG formation, while induced base propenal was effective in generating M_1dG. To test the hypothesis that MDA derived from peroxidation of polyunsaturated fatty acids does not play a major role in M_1dG formation, we varied the quantity of polyunsaturated fatty acids present in the membranes of *E. coli* and subjected the cells to oxidative stress followed by measurement of M_1dG levels as well as for the formation of MDA and base propenals. γ-Irradiation results showed that the MDA produced by lipid peroxidation was insufficient to induce M_1dG formation in cells. The level of M_1dG adduct was inversely correlated with the quantity of membrane polyunsaturated fatty acid and hence with the level of

lipid peroxidation when E. coli cells were treated with the oxidant, peroxynitrite. These results indicate that base propenal is the major source of M_1dG in this model cell system.

We also undertook quantification of M_1dG in a comparative study of various types of DNA damage associated with inflammation (*4*). To this end, Dr. Koli Taghizadeh and I developed an analytical method to quantify the unsubstituted etheno adducts thought to arise from reaction of lipid peroxidation products with DNA. The M_1dG and etheno adducts methods were than applied to the measurement of DNA lesions in the SJL mouse model of nitric oxide overproduction as part of a collaboration with Dr. Bo Pang (nucleobase deamination products) and Dr. Hongbin Yu (guanine oxidation products). The results revealed that the etheno adducts of dA and dG were the only DNA lesions significantly elevated in the inflamed spleen tissues from the Rcs-X-bearing mice. The four nucleobase deamination products, M_1dG and 8-oxodG were not elevated, which suggests that lipid peroxidation products play an important role in the genetic toxicology of nitric oxide overproduction such as occurs at sites of inflammation. The results are also consistent with base propenals from deoxyribose oxidation, and not malondialdehyde from lipid peroxidation, are the major source of M_1dG in biological systems.

Aside from secondary DNA damage, we also began to investigate protein adducts from reactions between DNA deoxyribose oxidation products and protein. The study by Dr. Jiang Tao, Dr. Min Dong and I established the formation of N^6-formylation of lysines caused by 3'-formylphosphate residues in histones arising from 5'-oxidation of DNA deoxyribose (*5*). Using a sensitive LC/MS/MS analytical method to quantify N^6-formyl-lysine phenylisothiocyanate (PITC) derivative, we also showed that there is a direct relationship between NCS treatment and the level of N^6-formyl-lysine in histones.

6.2. Future Studies

One of the remarkable results of the studies is the observation of different sets of 4'-oxidation products for various oxidizing agents. In particular, bleomycin and peroxynitrite induce the formation of bases propenals from deoxyribose C4'-oxidation, which is consistent with previous studies of enediyne antibiotics, while γ-radiation and Fe^{+2}-EDTA exclusively induce formation of malondialdehyde and free base.

There are several mechanisms that could account for these observations, perhaps the most appealing of which is the simple idea that agents that leave a reactive species at the site of initial deoxyribose oxidation will drive the 4'-oxidation reaction pathway toward base propenals, while agents that produce only a single oxidant species that does not bind to DNA, or react with the carbon-centered radical on deoxyribose, will lead to formation of the base and malondialdehyde. Support for this model comes from previous studies of bleomycin, an agent that remains bound to DNA near the C4' radical after hydrogen atom abstraction and decisively governs formation of final products (*6, 7*). Similar arguments could be made for the enediyne antibioics that remain bound to DNA after the formation of the sugar radical.

The formation of base propenals from $ONOO^-$ induced 4'-oxidation is more complicated. Evidence indicates that hydroxyl radical-like activity of peroxynitrous acid (ONOOH) dominates in the absence of CO_2/HCO_3^-, while the presence of CO_2/HCO_3^- converts $ONOO^-$ to $ONOOCO_2^-$, a potent oxidizing and nitrating agent, and diminishes the hydroxyl radical-like activity of ONOOH (*8*). Nevertheless, the kinetics and thermodynamics of the reaction of $ONOO^-$ with CO_2 indicate that a small percentage of $ONOO^-$ exists under the biological conditions of CO_2 concentration in blood and tissues (~1mM). This species can still induce DNA deoxyribose

damage, presumably by generating •OH and the products from 4'-oxidation have been shown to generate base propenals instead of MDA (*3, 8*). One possible explanation for the formation of base propenals is that the $•NO_2$ radical (the partner of hydroxyl radical arising by homolysis of ONOO-) stabilizes the C4'-oxyl radical and influences the subsequent chemistry. If this mechanism is correct, then one would expect to find nitrosation of DNA deoxyribose as well. Quantification of possible deoxyribose nitrosation products can thus be applied to test the validity of the hypothesis that $•NO_2$ facilitates the formation of base propenals.

Although the formation of M_1dG was mainly demonstrated from exposure to exogenous sources such as radiomimetic anticancer drugs (*e.g.,* bleomycin and calicheamicin) (*9, 10*) or high concentrations of $ONOO^-$ (μM levels compared with nM concentrations predicted for inflamed tissues) (*3*), the origin of endogenous sources of base propenals and M_1dG were also investigated (*11, 12*). For example, Frelon *et al.* showed that the DNA subjected to the Fenton reaction (Fe^{2+}/H_2O_2) induces M_1dG formation (*12*), though in low yield, which is different from the γ-radiation results. The exact identity of the oxidizing species produced by Fe^{2+} and H_2O_2 through Fenton chemistry, in particular the formation of •OH, has been a matter of debate. A growing body of evidence indicates that •OH alone cannot explain the DNA damages caused by Fenton chemistry (*13-16*). The difference between products formed by Fenton oxidants versus ionizing radiation could be the participation of iron ions directly in the product formation (*15, 16*). The binding of free Fe^{2+} to exocyclic nitrogens on the DNA bases or to the anionic phosphate oxygens on DNA may lead to C4'-oxidation and subsequent formation of base propenals in the context of the binding model. Interestingly, when EDTA was added to the Fenton reaction mixture (Fe^{2+}/H_2O_2), a significant decrease in the yield of M_1dG was observed (*12*). A logic explanation is that $Fe(EDTA)^{2-}$ complex cannot bind to DNA backbone, and is

indeed repulsed by the anionic sugar-phosphate backbone, and the damage to deoxyribose is caused by •OH that yields malondialdehyde instead of base propenals. This is consistent with our observation that $Fe(EDTA)^{2-}$ only generates malondialdehyde. Jeong *et al.* also showed that $Cu^{2+}/H_2O_2/NAD(P)H$ and estrogen metabolites could both induce M_1dG formation through DNA deoxyribose oxidation, presumably by generation of base propenals. Considering that copper can also bind to bases and the phosphate oxygens in DNA, the formation of base propenals in $Cu^{2+}/H_2O_2/NAD(P)H$-induced DNA damage is likely because of the facilitation of the copper as well. To test this hypothesis, one can apply the HPLC/post-column derivatization (TBA assay) to confirm the production of base propenals from Fe^{2+}/H_2O_2 and $Cu^{2+}/H_2O_2/NAD(P)H$. Contrary to this model, however is the observation that (3-Clip-phen)$CuCl_2$ (a 3-Clip-Phen-distamycin Copper complex) treatment of DNA does not lead to detectable formation ofbase propenals , although malondialdehyde was formed (*17*). In cells, deoxyribose in DNA and more abundantly in the nucleotide and nucleoside pool can be oxidized by endogenous ROS such as Fe^{2+}/H_2O_2 to produce base propenals and induce M_1dG formation.

It is important to point out that our results do not rule out MDA as a source of M_1dG in human cells. Indeed, Marnett and coworkers showed that the level of M_1dG increased from 1.2 per 10^7 nt to 3.9 per 10^7 nt in studies of *S. typhimurium* exposed to 10 mM MDA (*18*) . Recently, *in vitro* studies also showed that the peroxidation of polyunsaturated fatty acids such as linoleic acid (18:2) and linolenic acid (18:3) could also induce M_1dG formation (*11*). Although both our *E. coli* results and the *in vitro* results of Swenberg and coworkers (*11*) indicated that base propenals played a major role in M_1dG formation compared with lipid peroxidation products, all of these studies were conducted under strongly oxidizing and unphysiological conditions, and no systematic study has been conducted on M_1dG formation at background levels in human cells or

tissues. We will continue studies of M_1dG formation, with emphasis on moving the studies into human cells, which has higher percentage of PUFA in cell membrane compared with *E. coli* cells. The goal will be to use isotopically-labeled PUFA and deoxyribose to quantify the relative contributions of malondialdehyde and base propenals to M_1dG formation at background level and under oxidative stress. For example, as shown in Figure 6-1, if the cell membrane PUFA are replaced with uniformly labeled PUFA such as U-[^{13}C]-linoleic acid (18:2) and U-[^{13}C]-Linolenic acid (18:3), the MDA produced from lipid peroxidation are uniformly ^{13}C labeled as well, which if is indeed the major source of M_1dG will yield M_1dG containing three ^{13}C labels. On the contrary, the base propenal from DNA deoxyribose oxidation contains no ^{13}C labels and the M_1dG from base propenal does not contain ^{13}C labels either.

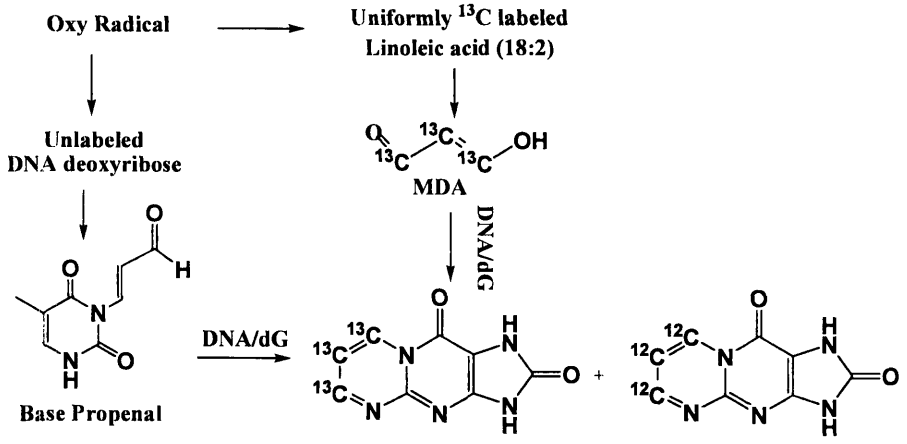

Figure 6-1. $^{13}C_3$-M_1dG formed from peroxidation of uniform -[^{13}C]- labeled lipids vs. unlabled M_1dG formed from deoxyribose oxidation product base propenal.

The relative ratio of unlabeled M_1dG as deoxyribose oxidation products and ^{13}C-containing M_1dG from lipid peroxidation will be quantified in cellular DNA by LC/MS/MS, as described by Swenberg and coworkers following oxime derivatization and enzymatic hydrolysis. Our preliminary results have shown that, unlike *E. coli* cells, human cell lines such as TK6 and

HCT116 are able to incorporate high percentage of linolenic acid (18:3) and arachidonic acid (20:4) in medium containing either acid. The method for M_1dG quantification as its oxime derivatization has also been under development in our research group.

In this thesis, we focus on DNA deoxyribose as a source of reactive electrophiles and DNA bases as targets for reactive electrophile from lipid peroxidation and deoxyribose oxidation. Besides DNA, RNA is a potential target for reactive electrophiles as well. The Dedon research group has expanded the studies to include RNA as a potential target for reactive electrophiles, as a control for defining chemical mechanisms and as a potential participant in the pathophysiology of oxidative stress. We can also test the base propenal hypothesis by quantifying M_1G in RNA. As far as we know, oxidation of ribose in RNA does not lead to formation of base propenals to any significant extent, so we expect little if any M_1G to form in RNA if base propenals are the sole source of M_1G. However, the wider cellular distribution of RNA species and the greater solvent exposure of nucleobases in RNA could cause RNA molecules to be greater targets for malondialdehyde reactions than DNA.

Given the potential for this adduct to interfere with the physiologically important N^6-acetylation of lysine in chromatin proteins, we also propose to continue to characterize the chemistry and biology of protein formylation in several sets of studies. These include proteomic mapping of the formyllysines in histone tails, LC/MS/MS quantification of the adducts in cells and tissues subjected to oxidative stress and biochemical assessment of the reactivity of histone deactylases with formyllysines in peptides.

Altogether, the proposed studies should provide new insights into the chemical basis for endogenous nucleic acid and protein adducts that could be useful as biomarkers of exposure and disease.

References

(1) Zhou, X. F., Liberman, R. G., Skipper, P. L., Margolin, Y., Tannenbaum, S. R., and Dedon, P. C. (2005) Quantification of DNA strand breaks and abasic sites by oxime derivatization and accelerator mass spectrometry: Application to gamma-radiation and peroxynitrite. *Analytical Biochemistry 343*, 84-92.

(2) Chen, B., Zhou, X., and Dedon, P. C. (2006) Quantification C4′ deoxyribose lesions induced by bleomycin and ♈-radiation using Gas Chromatography/Mass Spectrometry Method.

(3) Zhou, X. F., Taghizadeh, K., and Dedon, P. C. (2005) Chemical and biological evidence for base propenals as the major source of the endogenous M(1)dG adduct in cellular DNA. *Journal of Biological Chemistry 280*, 25377-25382.

(4) Pang, B., Zhou, X., Yu, H., Tannenbaum, S. R., and Dedon, P. C. (2006) A survey of DNA biomarkers from a SJL mouse model of nitric oxide overproduction.

(5) Jiang, T., Zhou, X., Dong, M., and Dedon, P. C. (2006) Histone Protein Formylation Caused by Deoxyribose Oxidation in DNA.

(6) Rashid, R., Langfinger, D., Wagner, R., Schuchmann, H. P., and von Sonntag, C. (1999) Bleomycin versus OH-radical-induced malonaldehydic-product formation in DNA. *Int J Radiat Biol 75*, 101-9.

(7) Breen, A. P., and Murphy, J. A. (1995) Reactions of Oxyl Radicals with DNA. *Free Radical Biology and Medicine 18*, 1033-1077.

(8) Yermilov, V., Yoshie, Y., Rubio, J., and Ohshima, H. (1996) Effects of carbon dioxide/bicarbonate on induction of DNA single-strand breaks and formation of 8-nitroguanine, 8-oxoguanine and base-propenal mediated by peroxynitrite. *Febs Letters 399*, 67-70.

(9) Dedon, P. C., Plastaras, J. P., Rouzer, C. A., and Marnett, L. J. (1998) Indirect mutagenesis by oxidative DNA damage: formation of the pyrimidopurinone adduct of deoxyguanosine by base propenal. *Proc Natl Acad Sci U S A 95*, 11113-6.

(10) Plastaras, J. P., Riggins, J. N., Otteneder, M., and Marnett, L. J. (2000) Reactivity and mutagenicity of endogenous DNA oxopropenylating agents: base propenals, malondialdehyde, and N(epsilon)-oxopropenyllysine. *Chem Res Toxicol 13*, 1235-42.

(11) Jeong, Y. C., and Swenberg, J. A. (2005) Formation of M1G-dR from endogenous and exogenous ROS-inducing chemicals. *Free Radic Biol Med 39*, 1021-9.

(12) Frelon, S., Douki, T., Favier, A., and Cadet, J. (2002) Comparative study of base damage induced by gamma radiation and Fenton reaction in isolated DNA. *Journal of the Chemical Society-Perkin Transactions 1*, 2866-2870.

(13) Collins, C., Awada, M. M., Zhou, X., and Dedon, P. C. (2003) Analysis of 3'-phosphoglycolaldehyde residues in oxidized DNA by gas chromatography/negative chemical ionization/mass spectrometry. *Chem Res Toxicol 16*, 1560-6.

(14) Goldstein, S., Meyerstein, D., and Czapski, G. (1993) The Fenton Reagents. *Free Radical Biology and Medicine 15*, 435-445.

(15) Henle, E. S., and Linn, S. (1997) Formation, prevention, and repair of DNA damage by iron hydrogen peroxide. *Journal of Biological Chemistry 272*, 19095-19098.

(16) Henle, E. S., Luo, Y. Z., and Linn, S. (1996) Fe2+, Fe3+, and oxygen react with DNA-derived radicals formed during iron-mediated fenton reactions. *Biochemistry 35*, 12212-12219.

(17) Pitie, M., Burrows, C., and Meunier, B. (2000) Mechanism of DNA cleavage by copper complexes of 3-Clip-Phen and of its conjugate with a distamycin analogue. *Nucleic Acids Res. 28*, 4856-4864.

(18) Sevilla, C. L., Mahle, N. H., Eliezer, N., Uzieblo, A., O'Hara, S. M., Nokubo, M., Miller, R., Rouzer, C. A., and Marnett, L. J. (1997) Development of monoclonal antibodies to the malondialdehyde-deoxyguanosine adduct, pyrimidopurinone. *Chem Res Toxicol 10*, 172-80.